Modulation of the progesterone receptor by progestogens, antiretroviral drugs and the glucocorticoid receptor

Kim Enfield

Thesis presented for the degree of

DOCTOR OF PHILOSOPHY

Department of Molecular and Cell Biology

Faculty of Science

UNIVERSITY OF CAPE TOWN

Supervisor: Janet P. Hapgood

Co-supervisor: Chanel Avenant

March 2021

Declaration

I, **Kim Enfield**, hereby declare that the work on which this thesis is based is my original work (except where acknowledgements indicate otherwise) and that neither the whole work nor any part of it has been, is being, or is to be submitted for another degree in this or any other university. I authorise the University to reproduce for the purpose of research either the whole or any portion of the contents in any manner whatsoever.

Signature: Signed by candidate Date: _____

Acknowledgements

I wish to convey my deepest gratitude to the following people for their constant support and love without which I doubt I would've survived the challenge of this PhD.

To my supervisor, Prof. Janet Hapgood. Thank you for always pushing me to my limit and for always wanting nothing but the best from and for me. Your knowledge of the field leaves me in awe, and I will forever strive to leave that same impression on others throughout my scientific journey.

To my co-supervisor, Dr. Chanel Avenant. You are the only person I know who is as patient as they are brutally honest. This balance has made you someone I will always admire on and off the bench. Thank you for always being 'just a WhatsApp away' whenever I needed you.

To all my funders without whom I would not have been able to undertake my PhD. These include The National Research Foundation, the Poliomyelitis Research Foundation, the University of Cape Town as well as through grants from my supervisor; the National Institute of Health and Advancing Womxn for Womxn.

Thank you to the crew from Stellenbosch University: Assoc. Prof. Donita Africander, Dr. Renate Louw-Du Toit, Meghan Cartwright and Dr. Karl Storbeck for opening up your labs to me whenever I needed assistance. A huge thank you to Jonathan Quason for your patience when you were teaching me the MTBE steroid extraction method during the early days of this degree.

Thank you to the MCB CCS, Unis, aunty Priscilla and aunty Jenny; and the departmental assistants, Mario and Maureen for always cheering me up when lab work wasn't working out for me. Just a friendly greeting and a chat made me forget where I was and helped me regroup to tackle the next task. I will be eternally grateful to you all. Thank you to the MCB scientific officers for always ensuring that the tissue culture labs and all departmental equipment were always up to par. Bronwyn, Faezah and Shakiera, you guys are an unmatched trio.

A huge thank you to the ‘OG’ lab mates who have taught me more than they could ever imagine! Dr. Alexis Bick, Dr. Mosoko Moliki, Sigcinile Dlamini and Calvin Kemp. Your wealth of knowledge continues to leave me speechless. To the recently joined lab members, Carole Capitaine and Nxalati Mkhombo, trust me, you are in great hands.

To Karen Van der Merwe for not only running the lab like it’s never been run before but for also being a mother away from home! Your loving and nurturing ways always made the lab feel so much warmer.

To the M.K.B crew: Maleshigo Komane (Mali) and Salndave Skosana (Bobs) I can guarantee that I would never have made it through this PhD without you two struggling beside me all the way. The respect and gratitude that I have for you both is immense and I can only hope that I have been even just slightly as helpful as you two have been to me throughout this journey.

Lastly a huge thank you to my parents, Leon and Glynis for recognising the importance of education and for choosing to invest in me. I am eternally grateful to you two for giving me this head start in life. Another thanks to my siblings Lee, Luke, Yaseen and Charvan for putting up with my moods and ever-loafing behaviour. I guess I can no longer use the “but I’m a student” line anymore. Thank you for bringing normality back to me whenever I started to feel completely overwhelmed by my life choices. Also, a big thank you to my little niece Luna for always putting a smile on my face!

Abstract

Hormonal contraceptives (HCs) and hormonal replacement therapies (HRTs) are widely used globally by women. However, the relative activity of some of the progestogens used in HCs and HRT has not been determined via their target steroid receptor (SR), the progesterone receptors and its isoforms (PR-A and PR-B). This thesis involves an *in vitro* investigation of some of the factors that affect PR activity and that may thus impact progestogen responses in women on HC or HRT. These include progestogen-specific effects via PR-A and PR-B, progestogen metabolism, the role of antiretroviral drugs (ARVs) and crosstalk with the glucocorticoid receptor (GR).

The PR isoforms play important roles in multiple physiological processes, including cognition, regulation of inflammation, mitochondrial function, neurogenesis, female reproduction and disease. Due to the gender disparity of higher prevalence of HIV infection among women compared to same-aged men, there is increased interest in developing treatments designed to protect women from HIV infection. These include HIV pre-exposure prophylactics (PrEPs) and multipurpose prevention technologies (MPTs). Furthermore, many HIV -infected women are using combined antiretroviral therapy (cART) to treat AIDS as well as an HC to prevent unwanted pregnancy. Importantly, the effects of the combination of a progestogen with ARVs on the activity of the PR is unexplored. In addition, there are many studies which provide evidence that SRs interact and influence each other's activity. Therefore, the presence of the ubiquitously GR may also influence PR activity.

To characterise the progestogen-induced activity of the PRs, dose-response analysis was performed using promoter-reporter genes and varying doses of progesterone (P4) and five widely-used progestogens namely; norethisterone (NET), etonogestrel (ETG), levonorgestrel (LNG), medroxyprogesterone acetate (MPA) and nestorone (NES), in parallel relative to the reference progestogen promegestone (R5020). The effects of experimental conditions and progestogen metabolism on PR activity were investigated in U2OS cells using two different transient transfection conditions to express PR-B. The effect of model system on PR activity was investigated by comparing the

progestogen-induced PR-B responses obtained in U2OS cells to those obtained in MDA-MB-231 cells stably transfected with expression vectors for PR-A or PR-B. Progestogen-induced PR activity was also investigated on endogenous genes by quantitative real-time PCR (real-time qPCR) in the MDA-MB-231 PR-B-stably expressing (MDA-PR-B+) cells. Once the progestogen responses via the PR were characterised, PR-B activity in the presence of three ARVs namely; tenofovir disoproxil fumarate (TDF), dapivirine (DPV) and maraviroc (MVC), was investigated next using promoter-reporter assays and real-time qPCR in MDA-PR-B+ cells. The mechanism of ARV action on PR-B activity was investigated by competitive binding assays, as well as by determination of PR phosphorylation levels. The effect of the GR on progestogen-induced PR-B activity in terms of potency, efficacy and biocharacter was investigated using promoter-reporter assays, real-time qPCR on select endogenous genes and efficacy on multiple genes in a PCR array. Using GR-specific siRNA knockdown in MDA-PR-B+ cells, the progestogen-induced PR responses were compared for higher and lower GR levels. The mechanism of the effect of the GR on PR activity was further investigated by co-immunoprecipitation studies and the degree of PR phosphorylation in the presence of higher and lower GR levels was also compared.

Results show that in the presence of the progestogens investigated, *in vitro* biological responses via PR-B can vary significantly in biocharacter and absolute values for efficacies and potencies. Progestogen-specific responses were found on the same synthetic promoter, as well as on the same endogenous gene in the same cell. These progestogen-specific responses negatively correlated with progestogen-specific metabolism in U2OS cells. Furthermore, the progestogen-specific responses also varied in a gene- and model system-specific manner. The majority of the progestogen-induced responses via PR-B were significantly more efficacious, but less potent that the progestogen-induced responses via PR-A, highlighting the importance of the relative expression of PR-B vs PR-A protein levels in determining the resultant progestogen-specific response. It was shown for the first time that the ARVs, MVC and TDF activated PR-B transcription in the absence of progestogens to result in increased transcription in promoter-reporter assays and increased mRNA for endogenous genes. MVC and TDF exhibited no direct binding to PR-B; however, novel data from this thesis showed increased PR-B phosphorylation at Ser294 with TDF but

not MVC. DPV activated two PR-regulated genes in the absence of progestogens and competed for binding of P4 to PR-B, while resulting in no effect on PR-B phosphorylation. Using GR-specific siRNA, it was determined by promoter-reporter assays that the presence of the GR had an inhibitory effect on PR-B efficacy. This surprising observation was supported by the global and promoter-specific gene expression changes observed for some genes using a PCR array with and without GR knockdown. The mechanism by which the GR affects the PR-B activity was determined to be most likely by association with PR-B in the same protein complex, probably resulting in a significant decrease in PR-B phosphorylation.

Taken together, the *in vitro* differences between progestogen actions via the PR suggest that the absolute values of the progestogen-induced efficacies and potencies are likely to vary *in vivo* in a progestogen-, promoter-, model system- and isoform-specific manner. While obtaining such data *in vivo* is not possible, the *in vitro* data from the present study show proof-of-concept of potential significant cell-, gene- and progestogen-specific PR-B effects, as well as PR isoform-specific effects. Additionally, this study shows that potential novel off-target immunomodulatory effects of MVC, TDF and DPV occur *in vitro* and these are most likely mediated by different mechanisms of PR-B activation. Lastly, this study shows that in cells where both the GR and PR-B are co-expressed, the resultant PR response is likely to be inhibited on select genes as a result of reduced PR-B phosphorylation. The extent to which the presence of the GR affected the determination of progestogen-, model system-, promoter- and isoform-specific responses of progestogens via the PR in this study was not investigated for all models and genes, but is likely to be an unavoidable confounding factor. However, since all cells that express the PR also express the GR *in vivo* to the best of the author's knowledge, characterising PR activity in the absence of detectable GR expression is unlikely to be physiologically relevant. Collectively these data suggest that multiple factors influence PR activity and these need to be taken into account, especially given the treatments available and under investigation, which are designed to specifically target the PR.

Table of contents

Abbreviations

AIDS	acquired immunodeficiency syndrome
AF	activation function
AKR1C1	aldo-keto reductase 1
AP-1	activator protein 1
AR	androgen receptor
ARV	antiretroviral
ATP1A1	ATPase NA+/K+ transporting subunit alpha
cAMP	cyclic adenosine monophosphate
cART	combined antiretroviral therapy
CCR5	C-C chemokine receptor 5
ChIP-seq	chromatin immunoprecipitation sequencing
Co-IP	co-immunoprecipitation
CPGR	Centre for Proteomic and Genomic Research
CREB	cyclic AMP response element binding protein
cs-FCS	charcoal-stripped foetal calf serum
Ct	cycle threshold
ctrl	control
CXCL1	C-X-C motif chemokine ligand 1
DBD	DNA binding domain
DEPC	diethyl pyrocarbonate
Dex	dexamethasone
DMSO	dimethyl sulfoxide
DNPN	dinitrodiphenylamine
DPV	dapivirine
EC_{50}	potency
ER	estrogen receptor
ETG	etonogestrel
EtOH	absolute ethanol
ezh2	zeste homolog 2
FCS	foetal calf serum
GAPDH	glyceraldehyde 3-phosphate dehydrogenase
gata2	GATA binding protein 2
GC	glucocorticoid
GILZ	glucocorticoid induced leucine zipper

GR	glucocorticoid receptor
GR-KD	glucocorticoid receptor knockdown
GREs	glucocorticoid receptor response element
H/SRE	hormone/ steroid receptor element
HC	hormonal contraceptive
HDAC	histone deacetylase
HIV	human immunodeficiency virus
HP1	heterochromatin protein 1
HRT	hormone replacement therapy
HSP	heat shock protein
IL-6	interleukin-6
K_d	equilibrium dissociation constant
LBD	ligand binding domain
LLOQ	lower limit of quantification
LNG	levonogestrel
LOD	limit of detection
LSD1	lysine specific demethylase 1
LXR	liver X receptor
MAPK	mitogen-activated protein kinase
MPA	medroxyprogesterone acetate
MPT	multipurpose prevention technology
MR	mineralocorticoid receptor
MRM	multiple reaction monitoring
MTBE	methyl-tert-butyl-ether
MVC	maraviroc
NCoR	nuclear receptor corepressor
NES	nestorone
NET	norethisterone
NET-EN	norethisterone-enanthate
NFκB	nuclear factor kappa-light-chain-enhancer of activated B cells
NP	not predicted
NSC	non-silencing control
NTD	amino-terminal domain
P4	progesterone
PBS	phosphate-buffered saline
PGE2	prostaglandin E2 synthesis

PI3K	phosphoinositide 3-kinase
PR	progesterone receptor
PR-B-KD	progesterone receptor B knockdown
PRE	progesterone receptor response element
PrEP	pre-exposure prophylactic
PTGS2	prostaglandin-endoperoxide synthase 2
R5020	promegestone
RBA	relative binding affinity
real-time qPCR	quantitative real-time RT-PCR
RIN	RNA integrity number
RNA-seq	RNA sequencing
RPL7/ SPA	ribosomal protein L7
RU486	mifepristone
RUNX1	Runt-Related Transcription Factor 1
S/N	signal-to-noise
SDS	sodium dodecyl sulfate
SEM	standard error of the mean
Ser	serine
SERM	selective ER modulator
SF	serum-free
SMRT	silencing mediator of retinoid and thyroid receptor
sox17	SRY-Box transcription factor 17
Sp-1	specificity protein 1 transcription factor
SP100	SP100 nuclear antigen
SR	steroid receptor
STAT5	signal transducer and activator of transcription 5
Sumo	sumoylation
TBS	TRIS-buffered saline
TBST	TRIS-buffered saline tween
TC	transfection condition
TDF	tenofovir disoproxil fumarate
TF	transcription factor
TFV	tenofovir
TLR4	toll like receptor 4
UHPSFC-MS/MS	ultra-high performance supercritical fluid chromatography– tandem mass spectrometry

Thesis outline

This thesis comprises of eight chapters and two appendices. There are four results chapters and supplementary results are included in the appendix.

Chapter 1: Literature review. This chapter outlines the current literature on the different factors that influence SR activity and the strategies used for investigating SR activity. Additionally, functions of the PR and the GR are discussed as well as the cross talk between SRs. The available literature on the activity of progestogen metabolism and the progestogen-induced activity via the PR and GR are summarised and discussed. ARV-induced activity via nuclear receptors is discussed. Lastly, the rationale behind the research and the aims and hypotheses are stated.

Chapter 2: Materials and methods. This chapter describes in detail the methods used to obtain the results in the subsequent chapters.

Chapter 3: Results: The progestogens exhibit progestogen-, model system-, promoter- and isoform-specific effects. This chapter investigates four aims: To determine whether the progestogens exhibit 1) progestogen-, 2) model system-, 3) promoter-, and 4) isoform-specific transcriptional effects via the PR.

Chapter 4: Results: Progestogens are differentially metabolised in extra-hepatic cells and potency via PR-B is negatively correlated to progestogen metabolism. This chapter investigates 1) progestogen metabolism in a model cell line and 2) the effect of progestogen metabolism on the progestogen-induced activity via PR-B.

Chapter 5: Results: Maraviroc, Tenofovir disoproxil fumarate and Dapivirine, activate the PR-B in the absence of progestogens. This chapter investigates the ARV-induced activity via PR-B and analyses potential biological mechanisms behind the ARV-induced activation of PR-B.

Chapter 6: Results: GR inhibits PR-B activity. This chapter investigates the modulation of PR-B activity by the GR. The potential mechanism behind the modulation of PR-B transcriptional responses by the GR is investigated in this chapter.

Chapter 7: Discussion. This chapter critically discusses the results presented in the previous chapters and contextualises the data within the field of progestogen-induced activity via the PR, as well as the mechanisms behind the ARV-induced and GR-modulated activity of PR-B.

Chapter 8: Conclusions and future perspectives. This chapter draws concluding remarks from the observations presented in this thesis and proposes new avenues for future research.

References: This is an alphabetic list including all the publications referred to in this thesis.

Appendix A: Supporting information for chapter 2. The supporting information for chapter 2 is presented in this appendix.

Appendix B: Supporting information for chapters 3 – 6. This appendix shows the supplementary data referred to in chapters 3 – 6.

Appendix C: Publications, conference presentations and statements by the candidate. This appendix shows the list of the publications and conference presentations that the current author has presented. It also contains statements of the work done by the candidate towards the publications and conference presentations.

Appendix D: Research articles. This appendix contains PDF versions of the research articles co-authored by the candidate.

Chapter 1

Literature Review

1.1 Steroid receptors (SRs)

SRs are ligand-activated transcription factors (TFs) that regulate a wide variety of responses in the human body (Agbo & Lambert, 2019). All SRs belong to the nuclear receptor superfamily and share the same structure which is comprised of a highly conserved DNA-binding domain (DBD), hinge-region, moderately conserved ligand-binding domain (LBD) and a variable amino terminal domain (Agbo & Lambert, 2019, McEwan et al., 2007) (Fig. 1.1.1). The variable amino terminal domain is suggested to be responsible for the ligand-specific SR interaction (McEwan et al., 2007).

As shown in Figure 1.1.1, the SRs are the androgen receptor (AR), estrogen receptor(s) (ER-α and ER-β), GR, PR-A and PR-B and the mineralocorticoid receptor (MR) (Africander et al., 2011, Agbo & Lambert, 2019, Helmreich & Huseby, Perissi & Rosenfeld, 2005) (Fig. 1.1.1). Once the cognate ligand has bound the respective SR, the liganded-SR carries out an array of different functions. For example, the GR regulates physiological functions relating to metabolism, immune function, reproduction, cognition and cardiovascular function (Agbo & Lambert, 2019, Oakley & Cidlowski, 2013). Progesterone (P4), the endogenous hormone of the PR, regulates the female reproductive cycle, maintenance of pregnancy, regulation of inflammation and bone density as well as the development of female reproductive organs (Bunma et al., 2020, Daniel, A. R.; et al., 2011, Gadsby et al., 2020, Polikarpova et al., 2019).

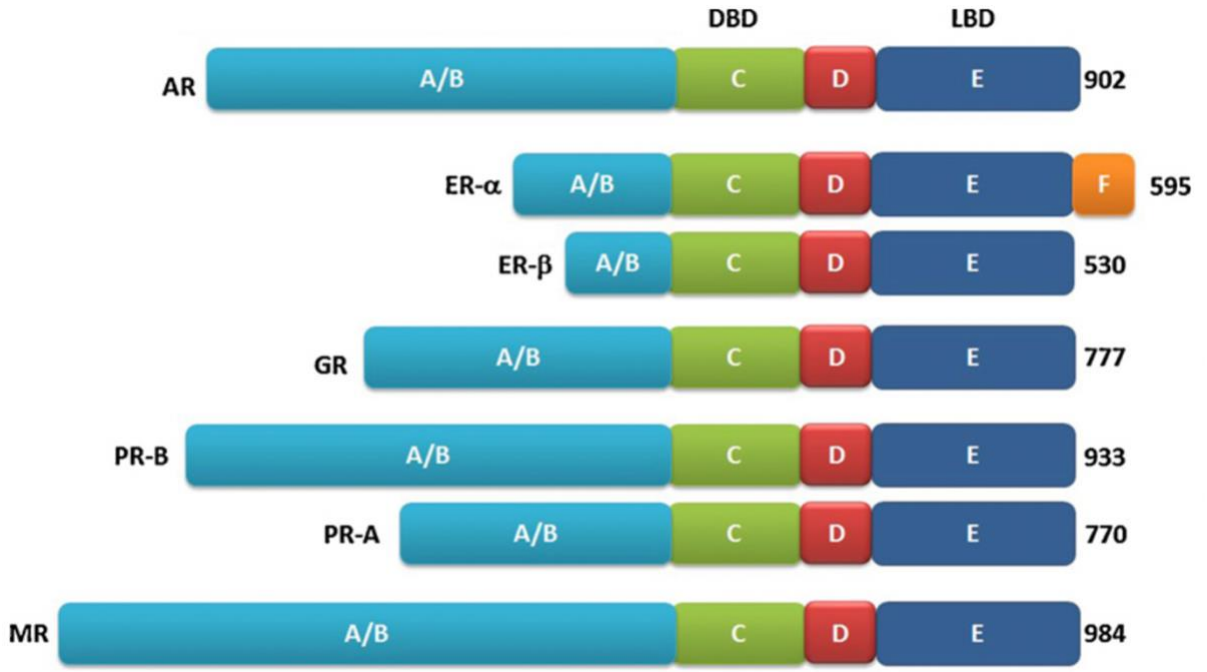

Figure 1.1.1: Schematic presentation showing the receptor domains present in different SRs. SRs are composed of the amino terminal domain (A/B), DNA-binding domain (DBD) (C), hinge region (D), ligand-binding domain (LBD) (E). The ERα contains an additional unique carboxy-terminal F domain. The numbers on the right show the number of amino acids that make up each SR. The image shown above is adapted from Africander *et al.,* 2011.

1.1.1 Mechanisms by which SRs elicit physiological responses

SRs can elicit physiological responses via different mechanisms which can be genomic (classical) or non-genomic (non-classical). Genomic effects (summarised in Fig. 1.1.1.1) either involve the direct interaction of SRs with DNA or SR interaction with other TFs to directly interact with DNA while non-genomic effects do not.

During classical activation a ligand binds a SR which causes the SR to undergo a conformational change. This allows the SR to dissociate from heat shock proteins (Lu et al., 2006), become phosphorylated, and to migrate to the nucleus (Agbo & Lambert, 2019, Griekspoor et al., 2007, Zhou & Cidlowski, 2005). However, some SRs are primarily nuclear even in the absence of ligand and therefore do not undergo nuclear translocation (Henríquez et al., 2017, Scarpin et al., 2009). Depending on the SR, two ligand-bound SR monomers either dimerise in the cytoplasm, before nuclear translocation, or in the nucleus (Sever & Glass, 2013) and bind to the respective SR response element within the promoter of a gene where they interact with coregulators

and other proteins involved in the transcription machinery to regulate the transcription of genes (Agbo & Lambert, 2019, Beato & Klug, 2000, Griekspoor et al., 2007, Perissi & Rosenfeld, 2005, Tanenbaum et al., 1998) (Fig. 1.1.1.1a). These proteins include other TFs such as the specificity protein 1 transcription factor (Sp-1) to initiate transcription (Fig. 1.1.1.1b). A SR can also affect gene transcription as a ligand-bound monomer (Fig. 1.1.1.1c). Genes can also be modulated by SRs without binding directly to the SR response element in a process known as 'tethering', by targeting other TFs such as activator protein 1 (AP-1) or nuclear factor kappa-light-chain-enhancer of activated B cells (NFκB) as a monomer or SR dimer (Africander et al., 2011, De Bosscher & Haegeman, 2009, Kassel & Herrlich, 2007, Lu et al., 2006) (Fig. 1.1.1.1c and d).

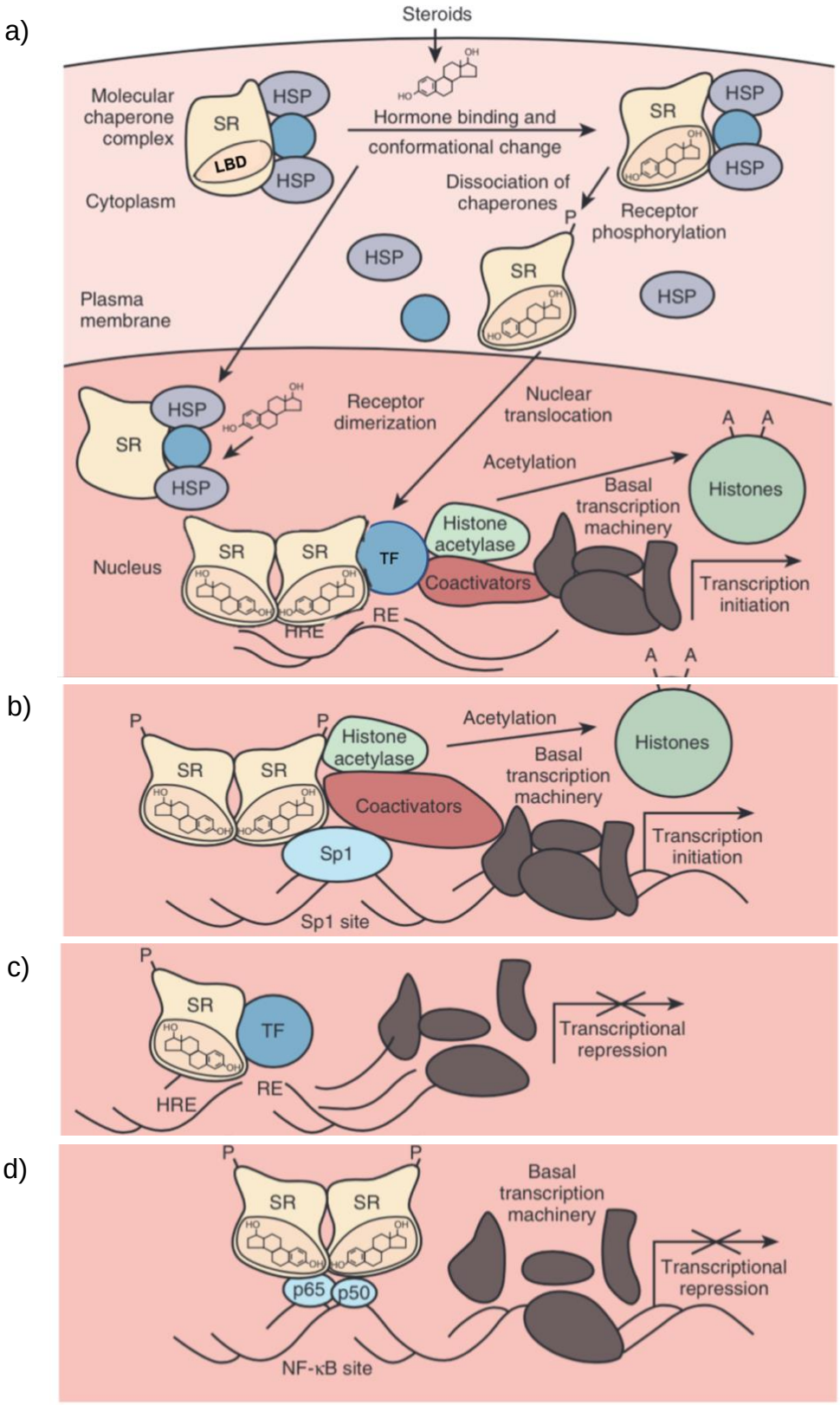

Figure 1.1.1.1: Schematic showing the classical (genomic) mechanisms by which steroid receptors regulate transcription. a) In the absence of ligand, the ligand binding domain (LBD) of a SR remains unbound and the SR remains associated with heat shock proteins (HSP) in the cytoplasm. In the presence of ligand, the ligand-bound SR

dimerises in the nucleus or cytoplasm (not shown). The SR dimer interacts with other transcriptional machinery to initiate transcription by associating with coactivators and binding to the SR hormone/ response element (H/RE) within the genome. b) Ligand-bound SR dimer interacts with another transcription factor (TF), specificity protein 1 (SP-1) and binds to that TFs RE within the DNA to initiate transcription. c) Ligand-bound SR monomer interacts with another TF to repress transcription and d) ligand-bound SR dimer interacts with another TF (example shows the two subunits of nuclear factor kappa-light-chain-enhancer of activated B cells, NFκB namely; p65 and p50) to repress transcription by preventing the transcriptional machinery from interacting with the NFκB-bound DNA. The image shown is adapted from Whirledge & Cidlowski, 2019.

SRs can also elicit biological responses via non-classical (non-genomic) signalling. This is brought about by the activation of secondary messenger pathways by SRs such as extracellular-signal-regulated kinase (Louw-du Toit et al., 2017), phosphatidylinositol 3-kinase (Akt) or mitogen-activated protein kinase (MAPK) (Africander et al., 2011, Diep et al., 2016, Estrada et al., 2003, Kang et al., 2004).

1.1.2 Factors that influence SR activity

The simplified mechanisms of how SRs regulate transcription summarised in Figure 1.1.1.1 and in section 1.1.1, do not convey the complexity of gene-, cell- and tissue-specific activity of ligands. The ultimate cell response, in terms of magnitude, and whether the ligand-bound SR response will repress, or enhance transcription also depends on a number of other factors (Whirledge & Cidlowski, 2019, Zhou & Cidlowski, 2005) which are discussed in this section.

1.1.2.1 Hormone availability

The concentration of hormone or ligand available intracellularly is dependent on specific enzymes which can either increase or reduce the expression of hormones. The activity of these enzymes therefore controls the cell-specific and tissue-specific patterns of hormone responsiveness via SRs (Whirledge & Cidlowski, 2019). For example, the enzyme aromatase P450 converts androgens to estrogens and is expressed in the ovaries, testes, skin and placenta (Kamat et al., 2002). In women, the concentration of estrogen fluctuates during the menstrual cycle. Specifically, circulating estrogen levels are too low to activate the ER at the lowest concentration during the menstrual cycle; however, at peak estrogen concentrations, the ER is

activated. Therefore, the activity of the ER is controlled by circulating estrogen concentrations. A similar relationship is seen with the GR and glucocorticoids (GCs). There are two enzymes which regulate the circulating levels of GCs namely; 11β-HSD type 1 and 11β-HSD type 2, where the former converts weak GCs (cortisone) into potent GCs (cortisol and corticosterone), and the latter reverses the reaction to inactivate the potent GCs (Chapman et al., 2013). The expression and activity of these enzymes in cells play an important role in the physiological actions of GCs. In general, the steroid-synthesising and -metabolising enzymes therefore determine the circulating hormone levels which ultimately affect the resultant activity of SRs.

1.1.2.2 Receptor expression

The intracellular expression level of a particular SR determines the responsiveness and sensitivity of that SR to ligand. One of the best-characterised mechanisms of sensitisation to the presence of ligand is the increased expression of the PR during the menstrual cycle. During the menstrual cycle, there is a rapid increase in circulating estrogen before ovulation occurs which is followed by a surge of P4 (Lauber et al., 1991, Pfaff et al., 1994). In a study by Mangal *et al.,* using endometrial tissue samples from women, it was discovered that the level of PR-B increased in the presence of high levels of estrogen. On the contrary, in the presence of high levels of P4, the level of PR-B decreased (Mangal et al., 1997). Thus, the rapid increase in estrogen activates the ER which targets the PR gene and initiates transcription. In addition, the increase in PR expression allows for a timely increase in sensitivity to P4.

For the PR which exists as two isoforms (PR-A and PR-B) (Fig. 1.1.1), the effect of PR-A and PR-B expression greatly influences the resultant PR response to ligand treatment. There is evidence which suggests that PR-A inhibits the activity of PR-B. For example, in the study by Vegeto *et al.,* the group showed that when two different cell lines, CV-1 (monkey kidney fibroblast cell line) and HeLa cells (a human cervical cell line), were co-transfected to express both PR-A and PR-B, PR-A had a repressive effect on the PR-B activity in the presence of 10 nM P4. In another study which highlighted the importance of PR isoform expression, it was discovered that the PR-B response to ligand treatment was more potent than the PR-A response (Lim, C. S.; et al., 1999). In addition to PR-A influencing PR-B activity, some studies have suggested

that other SRs also exhibit cross-reactivity primarily due to the shared homology in structure (Fig. 1.1.1) (Ballaré et al., 2002, Mohammed et al., 2015, Mueller et al., 2014, Ogara et al., 2019, Pooley et al., 2020, Rivers et al., 2019). Thus, the ability of SRs to form heterodimers and interact with other SRs has been an area of interest for many years (see section 1.1.6 for more detail). In summary, the expression of the PR isoforms and the resultant PR ratio, as well as the expression of other SRs therefore greatly influences the final PR response to ligand treatment.

The expression of SRs can also be regulated by changes in SR mRNA stability. It is well-documented that SR mRNA and/or protein stability are regulated by its cognate ligand (Ing, 2005)(Fuller et al., 1991, Skowron et al., 2019). Additionally, SR mRNA stability can also be regulated by microRNAs (Orang et al., 2014) which are small single-stranded non-coding RNA molecules which reduce the stability of SR mRNA. In addition, SR expression is regulated at the protein level by post-translational modifications such as ubiquitination or phosphorylation (discussed in more detail in section 1.1.2.4 of this chapter). Treatment with a ligand results in a time-dependent decrease in the level of its cognate SR in a process called homologous downregulation. As a result, there is desensitisation to the ligand treatment. After the SR has performed its function, the SR is ubiquitinated resulting in its degradation by the ubiquitin–proteasome pathway (Helzer et al., 2015).

1.1.2.3 Changes in SR conformation upon ligand binding

Some studies investigated the crystal structure of the LBDs of the AR, ER, PR and GR alone or in complex with different types of ligands (Bledsoe et al., 2002, Matias et al., 2002, Tanenbaum et al., 1998). A ligand can either act as an agonist or antagonist via an SR. The definition of a full agonist for an SR is a ligand which induces a high maximal response (efficacy) relative to the chosen reference ligand while occupying a relatively low proportion of receptors. The strategies for investigating the transcriptional effects of an SR are discussed in section 1.1.3 of this chapter.

The effect of the different SR conformations formed upon ligand binding on SR activity is the most well-studied for the ER. Some postmenopausal women choose to undergo hormone replacement therapy (HRT) to alleviate the symptoms of menopause. HRT

makes use of a progestin (synthetic progestogenic ligand designed to target the PR) and a selective ER modulator (SERM) (designed to target the ER) to replace the estrogen no longer being synthesised in postmenopausal women. Raloxifene and tamoxifen, having been crystalised in complex with ER, are two of the best-characterised SERMs (Brzozowski et al., 1997, Shiau et al., 1998, Thiebaud & Secrest, 2001). Raloxifene acts as an ER agonist in bone tissue to increase bone mineral density. In contrast, raloxifene acts as an ER antagonist in breast and uterus tissues. Tamoxifen antagonises ER action in the breast but acts as an agonist in the uterus. Studies suggest that differences in ER conformation induced by different SERMs are responsible for the tissue-specific effects of these SERMs (Brzozowski et al., 1997, Shiau et al., 1998).

Generally, the ligand-selectivity appears to be affected by the complementarity of shape and hydrogen bonding between the SR and a ligand (Huang et al., 2010). Although SRs share some homology in terms of the three-dimension structure, the subtle differences in secondary structure and topology of the LBDs of SRs could explain the ligand-selective responses via SRs (Wan et al., 2001). Ultimately, these differences in secondary structure of SRs result in differences in co-factor recruitment which contribute to differential activity in the presence of ligands (Ronacher et al., 2009).

1.1.2.4 SR phosphorylation

In the absence of ligand SRs can be basally phosphorylated. Alternatively, the phosphorylation of SRs can be ligand-induced. SRs can also be phosphorylated as a result of the activation of other signaling pathways such as cyclin-dependent kinases, or MAPKs (Whirledge & Cidlowski, 2019). While phosphorylation in general is well-understood for SR function, the effect of site-specific phosphorylation of SRs is becoming more appreciated.

For example, phosphorylation occurs at multiple sites within the PR. These include Serine (Ser) 190, Ser81, Ser162, Ser400 (Clemm et al., 2000, Pierson-Mullany & Lange, 2004) (Fig. 1.1.2.4.1). These sites are all basally phosphorylated and reach maximum phosphorylation after 2 hours of ligand treatment (Clemm et al., 2000). The

following sites are, however, exclusively ligand-inducible; Ser294, Ser102 and Ser345. Of the phosphorylation sites that have been identified, only Ser190, Ser294, Ser345 and Ser400 are common to PR-A and PR-B (Clemm et al., 2000) (Fig. 1.1.2.4.1). The other sites are located in the N-terminal domain unique to PR-B. In the study by the Clemm group, it was discovered that Ser294 is preferentially phosphorylated in response to ligands in PR-B which contributes to the specificity of the distinct functional roles of PR-A and PR-B (Clemm et al., 2000). In another study, although believed to be ligand-inducible, the Ser294 residue was also shown to be phosphorylated in the absence of ligand by MAPKs (Lange et al., 2000). More detail on the differences between the PR isoforms is discussed in section 1.1.4.

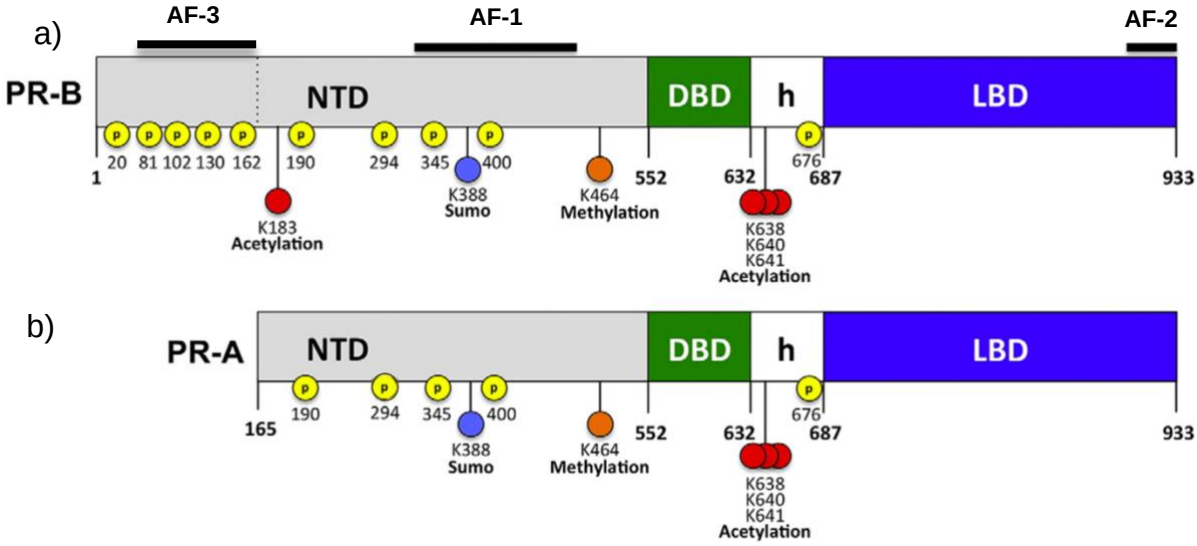

Figure 1.1.2.4.1: Schematic showing the structural domains of human PR-B and PR-A as well as the post-translation modification sites. The amino-terminal domain (NTD), DNA-binding domain (DBD), hinge region (h) and ligand binding domain (LBD) are present in both PR-B and PR-A. a) shows PR-B containing an additional 164 amino acids at the N-terminal housing the transcriptional activation function 3 (AF-3) which is unique to PR-B while AF-1 and AF-2 are present in both PR isoforms. b) Shows the structure of the PR-A isoform which contains a truncated NTD. The post-translational modification sites present in PR-B and PR-A are shown by yellow, red, blue and orange circles indicating phosphorylation, acetylation, sumoylation (Sumo) and methylation, respectively. The image shown is adapted from Grimm *et al.*, 2016.

Phosphorylation of the GR also plays an important role in determining the final GR response in the presence or absence of ligand (Avenant et al., 2010, Hapgood, J. P.; et al., 2016). In a study by Avenant *et al.* it was shown that the extent of phosphorylation at Ser226 and Ser211 of the GR in the presence of ligand affected GR half-life and transcriptional response in a ligand-dependent manner (Avenant et

al., 2010). Phosphorylation of the GR at Ser404 is ligand-dependent and expands the transcriptional profile of the GR compared to unphosphorylated GR (Galliher-Beckley et al., 2008, Panettieri et al., 2018, Præstholm et al., 2020). In contrast, phosphorylation at Ser134 of the GR is ligand-independent and leads to the modulation of GC-mediated signaling in a manner different to that of GR phosphorylated at Ser404 (Galliher-Beckley et al., 2011, Lange et al., 2000)(Præstholm et al., 2020).

Importantly, besides phosphorylation, other post-translation modifications also occur which include acetylation, sumoylation and methylation. As shown in Figure 1.1.2.4.1, most post-translation modification sites are present in both PR isoforms; however, some phosphorylation sites are unique to PR-B (Fig. 1.1.2.4.1).

The ligand-dependent and -independent mechanisms of phosphorylation of SRs and the presence of multiple phosphorylation residues within SRs highlight the important role of SR phosphorylation in determining the resultant SR response.

1.1.2.5 Interaction with DNA

A ligand-bound SR needs to recognise a specific sequence within the promoters of genes to enhance or repress transcription (Fig. 1.1.1.1). This sequence is called the SR hormone response element (HRE). The HRE of an SR for transactivation by direct DNA-binding of an SR dimer consists of two 6-bp sequences (each referred to as a half site) with a 3-bp spacer region separating each palindrome (not shown in Fig. 1.1.1.1). One receptor in each SR dimer interacts with each half site (Whirledge & Cidlowski, 2019). The AR, GR, PR and MR share the same 6-bp consensus HRE separated by a 3-bp spacer region, i.e. 5'-GGTACAnnnTGTTCT-3' where 'n' represents any nucleotide (spacer region) (Beato & Klug, 2000, Horie-Inoue et al., 2006). Because of the high degree of similarity between the SREs for these SRs, the ligand-specific responses of gene regulation cannot be exclusively explained by this mechanism.

However, one mechanism which explains ligand-specific effects for each SR as indicated by *in vitro* studies, is the sequence variation in the spacer regions as well as

the nucleotides flanking the consensus sequence (Nelson et al., 1999). Additionally, the distance of the SRE from the promoter influences the resultant SR response (Nordeen et al., 1998). These variations in the interactions between SRs and DNA, contributes to the specificity of the SR-ligand interaction as well as to the complexity of ligand-responsiveness among genes.

1.1.2.6 Interaction with coregulatory proteins

Coregulatory proteins can either be coactivators or corepressors which, generally when a ligand-bound SR interacts with the former, transcription is enhanced while interaction with the latter results in the repression of transcription. Coactivators such as cyclic AMP response element binding protein (CREB) and p300 have acetyl transferase activity which modify nucleosomes to increase the accessibility of basal transcription machinery to promoters. The most well-characterised corepressors are nuclear receptor corepressor (NCoR) and silencing mediator of retinoid and thyroid receptor (SMRT). These corepressors were shown to interact with antagonist-bound PR to prevent transcription of genes that would normally be upregulated by agonist-bound PR (Gao & Nawaz, 2002, Li, H.; et al., 1997). These corepressors interact with SRs to repress transcription by increasing the recruitment of histone deacetylase 3 (HDAC) to decrease chromatin accessibility.

Besides the acetylase and deacetylase ability of coregulatory proteins, others have enzymatic functions such as methylation, demethylation, phosphorylation, dephosphorylation, ubiquitination and sumoylation (Perissi & Rosenfeld, 2005, Rosenfeld et al., 2006). Vicent *et al*. showed that in T47D cells which express both PR-A and -B, that the PR was able to bind PR response elements (PREs) and stabilise repressive complexes containing various coregulatory proteins such as heterochromatin protein 1γ (HP1γ), histone deacetylase 1/2 (HDAC 1/2) and lysine specific demethylase 1 (LSD1) (Vicent et al., 2013).

The resultant effect of cofactors on PR activity is cofactor-dependent and tissue-specific (Malbeteau et al., 2020, Rowan & O'Malley, 2000, Skowron et al., 2019, Wang, Z.; et al., 2021). For example, the coactivator p300 interacts with other coactivators such as steroid receptor coactivator 1 and 3 (SRC-1 and SRC-3), in

addition to the PR (Eckner et al., 1994) to bring about full agonist activity while another coactivator, ribosomal protein L7 (RPL7/ SPA), only interacts with RU486 (mifepristone, a PR antagonist) bound PR to bring about partial agonistic activity of the PR (Jackson, T. A.; et al., 1997). Additionally, the expression of cofactors is tissue-specific which suggests that there will be differential resultant PR activity depending on the tissue type (Wang, Z.; et al., 2021).

Changes in the expression of coregulatory proteins ultimately results in changes in SR activity and therefore contributes to SR-specific patterns of gene expression and the complexity of hormone action.

1.1.2.7 Interaction with other TFs

SRs can interact with other TFs to enhance or repress its activity in a process called 'tethering'. A well-studied example of this occurs between the GR and NFκB (Kuznetsova et al., 2015, Ling & Kumar, 2012, McKay & Cidlowski, 1999, Potamitis et al., 2019, Schesschowitsch et al., 2017). The ligand-bound GR primarily inhibits the expression of proinflammatory genes while NFκB enhances the proinflammatory response (McKay & Cidlowski, 1999, Potamitis et al., 2019). The GR is able to inhibit NFκB by direct and indirect interactions. Some evidence suggests that the GR-NFκB interaction prevents NFκB from binding to NFκB-response elements. Other evidence suggest that the GR does not block NFκB DNA binding but interacts with the transactivation domain of the p65 subunit of NFκB and therefore disrupts NFκB interactions with basal transcription machinery (McKay & Cidlowski, 1998). Another hypothesis is that the GR competes for the same coactivators required for NFκB activation (Caldenhoven et al., 1995, Hudson et al., 2018, Kuznetsova et al., 2015, Van de Stolpe et al., 1994).

Besides the GR, the PR also regulates gene expression by tethering mechanisms. In a study by Faivre *et al*., using T47D cells (a human breast cancer cell line), PR-B was phosphorylated by MAPK after which it associated with Sp-1. The PR-Sp-1 complex then regulated Sp-1-target genes (Faivre et al., 2008). Of note, the promoter sequences of the Sp-1-regulated genes did not contain PREs indicating that the PR

did not bind to the DNA (Faivre et al., 2008). When MAPK inhibitors were present, as expected, PR-B was not phosphorylated, the PR-B no longer associated with Sp-1 and tethering was blocked (Faivre et al., 2008). In agreement with the Faivre *et al*. study, an earlier study by Owen *et al*., showed in HeLa cells (a human cervical cell line) that in the presence of P4, PR affected the expression of the *p21* gene which is typically regulated by Sp-1 (Owen et al., 1998). Using co-immunoprecipitation assays they showed that Sp-1 and both PR isoforms existed in the same protein complex (Owen et al., 1998). In addition to Sp-1, the PR can tether to other transcription factors such as activator protein 1 (AP-1) (Cicatiello et al., 2004, Dinh et al., 2019, Flaqué et al., 2013) and STAT5 (Stoecklin et al., 1999).

The relative intracellular expression of TFs and SRs influences the resultant SR response. The *in vitro* data providing evidence of protein-protein interactions between SRs and TFs expands the already broad physiological role of SRs. However, the physiological role of these mechanisms *in vivo* requires additional work.

1.1.2.8 Signaling via second-messenger pathways

SRs can regulate transcriptional activity indirectly by rapid non genomic actions via the activation of second-messenger cascades. Studies have shown that MAPK pathways are activated after PR ligand treatment in cells expressing the PR (Treviño et al., 2013). Treviño *et al.* showed in T47D cells (breast cancer call line) which express both PR isoforms, that when the p42/p44 MAPK signaling pathway was inhibited, PR-mediated gene induction was impaired (Treviño et al., 2013). In other studies, it was shown that in the presence of a PR ligand, the PR can also activate the phosphoinositide 3-kinase (PI3K) and JAK/STAT pathway signal transducers and activators (Boonyaratanakornkit et al., 2008, Carnevale et al., 2007, Saitoh et al., 2005). Similar to the PR and the abovementioned signaling pathways, the second messenger, cAMP, has been shown to be activated in the presence of GR cognate ligands (Dong et al., 1989). In addition, in the presence of GCs, the ERK and kinase c-Jun N terminal MAPK signaling pathways have also been shown to be activated (Fürst et al., 2007, Kotitschke et al., 2009).

That SRs, in the presence of cognate ligands, can influence transcriptional responses indirectly by activating second-messenger pathways increases the complexity of SR action and provides another mechanism by which SRs can regulate transcription and influence physiological responses.

1.1.2.9 Interaction with microRNAs

There is increasing evidence for the role of microRNAs (miR) regulating the activity of SRs (Fletcher, 2014, Palagani, 2014, Tessel, 2010). It has been shown that miRNAs affect the activity of the PR, ER and the AR through feedback loops. For example, the PR inhibits miR-633, miR-29c, miR-29, miR-193b and miR-29 and upregulates a number of miRNAs such as miR-513a-5p which targets PR in a negative feedback loop (Fletcher, 2014). Evidence from another study by Tessel et al. shows the involvement of miRs in the regulation of the AR, PR and GR in hormone-responsive cancers. In addition, this paper shows that there is reciprocal modulation of miRs since several miRs are in fact regulated by SRs (Tessel, 2010). In a study by Palagani et al., 2014 it was shown that a specific miR-150-5p does not change the expression of the GR mRNA but rather indirectly regulates the expression of GR protein by interacting with the TFs required for successful GR protein expression (Palagani, 2014). Taken together, although the effect of miR on the activity of all SRs has not been investigated (Fletcher et al., 2014, Palagani et al., 2014), it cannot be excluded as another factor that influences the SR activity.

1.1.3 Strategies for investigating transcriptional effects by SRs

The dose-response approach is used to characterise the biological effects of a specific SR in the presence of different ligands (Fig. 1.1.3.1). This method allows for accurate determination of the maximum response (efficacy) and potency of a ligand. Potency or EC_{50}, is defined as the concentration of ligand required to generate the half maximum response (Hapgood, J. P.; et al., 2014b, Tocris, 2021). The efficacy can be used to determine the biocharacter of a ligand which can vary from full or partial agonism relative to a known full agonist response (Fig. 1.1.3.1a) (Tocris, 2021). Ligands can also act as neutral, partial or full antagonists relative to a known full agonist response (Fig. 1.1.3.1) (Hapgood, J. P.; et al., 2014b, Tocris, 2021). The definition of a “partial agonist” varies for different sources. Some define a partial

agonist as a ligand which induces SR maximal activity (efficacy) which is less than that of a full agonist, and that the ligand has also been shown experimentally to antagonize an agonist (Jackson, A., 2010, Tocris, 2021). On the other hand some define a ligand as a partial agonist whether or not antagonism has been demonstrated (Hapgood, J. P. et al., 2018), (Tocris, 2021). For the purposes of this study, the term "partial agonist" will be used to define a ligand that induces maximal activity that it less than a full agonist, whether or not antagonism has been investigated. Other important considerations for determining SR activity in the presence of different ligands are the relative binding affinity (RBA) reported as IC_{50} (determined from competitive binding analysis) and the K_d (the equilibrium dissociation constant). The K_d is determined using saturation binding using radiolabelled ligands or by competitive binding under certain conditions using a radiolabelled reference agonist (Ronacher et al., 2009). The RBA is experiment-specific because this value is dependent on the concentration of SR, as well as the final concentration of the radiolabelled ligand used (Ronacher et al., 2009). The K_d on the other hand, is constant regardless of experimental conditions.

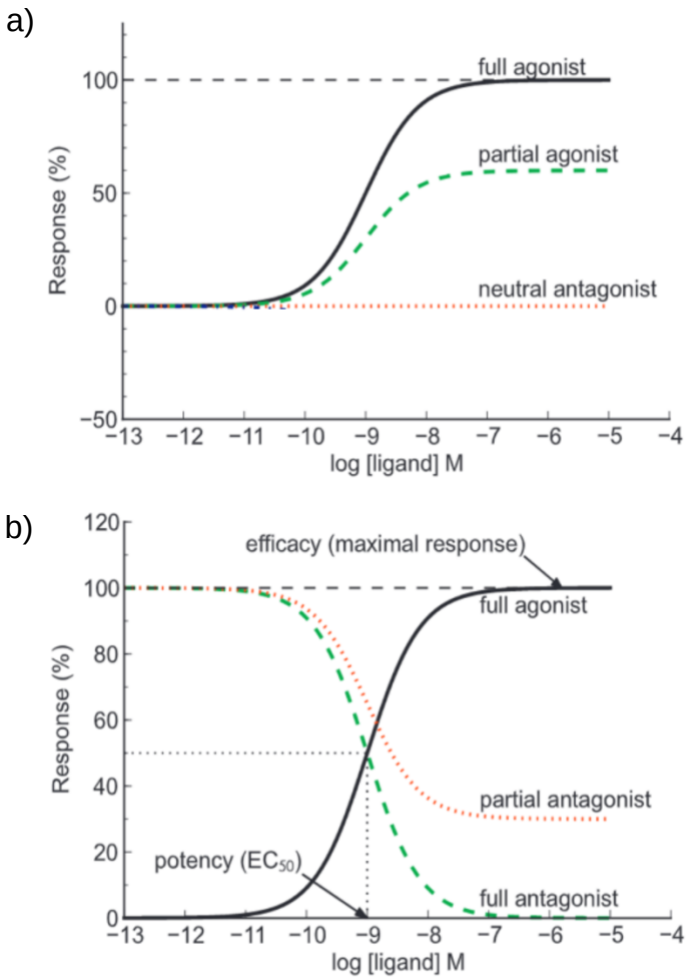

Figure 1.1.3.1: Schematic showing dose response curves for different ligands via a SR. a) A typical curve for a full agonist is shown in black, while the curve for a partial agonist is shown by the dashed green curve. A neutral antagonist response is shown by the dotted orange curve. In b) the EC_{50} (potency) is shown for the full agonist (black curve) as the concentration of ligand required to generate the half maximum response (indicated by the black arrow on the x-axis). A typical curve of a partial antagonist is shown by dotted orange curve while the curve for a full antagonist is shown by the dashed green curve. The image shown is adapted from Hapgood *et al.,* 2014.

It is important to note that although the RBA and K_d values are informative to a certain degree, this information does not always correlate to SR activity in the presence of a particular ligand (Ronacher et al., 2009). A common misconception in the field is that RBA or K_d of a particular ligand via an SR, is proportional to the ligand-induced transcriptional activity of that SR (Attardi et al., 2010, Kumar et al., 2017). One study showed that in the presence of GR agonists, there was a correlation between the RBA of ligands and the potencies via GR for transactivation (Ronacher et al., 2009). However, no correlation was observed for RBA and the potencies for transrepression

(Ronacher et al., 2009). Additionally, the efficacies for both transactivation and transrepression did not correlate to the RBAs (Ronacher et al., 2009). Therefore, in some cases, the RBA of ligand to a particular SR could be correlated to the transcriptional activity of that SR; however, as shown by the Ronacher *et al.* study; this is not always the case (i.e. the RBA is not the only factor that determines ligand responses via a particular SR).

The choice of model system used to investigate the activity of a particular SR is crucial. Although preclinical animal and clinical models are more physiologically relevant, they have several limitations including the presence of many SRs, multiple cofactors, species-specific effects and differences in ligand metabolism. Therefore, one cannot conclude whether the differences seen with different ligands are due to direct effects of the particular ligand on a particular SR or whether the differences are due to indirect effects of the confounding factors. Ideally, the system used needs to be easily manipulated to express only the SR of interest to reduce the number of confounding factors.

The technique by which the transcriptional activity of a ligand-activated SR is determined is another important consideration. These include promoter-reporter assays which can be conducted in cell lines, deficient in SRs, which are transiently transfected with the SR-expressing plasmid and the reporter plasmid. The reporter plasmid contains the cognate HRE upstream of a reporter gene (such as luciferase). By overexpressing the SR of interest, the use of promoter-reporter assays, allows one to determine the activity of the SR of interest specifically. While the physiological relevance of such promoter-reporter assays may be disputed by some, this assay yields direct evidence of receptor-specific transcriptional effects when experiments are performed in parallel which would otherwise be difficult to obtain.

Alternatively, cell lines can be used to investigate the expression of endogenous genes known to be regulated by a specific SR. Promoter-reporter assays may generate responses different to those obtained on endogenous genes. Regulatory *cis*-elements could be present in the proximal promoter region of endogenous genes or even far up- or down-stream thereof, which may not all be present in a promoter-reporter construct. Another important difference between promoter-reporter assays and

endogenous gene regulation is the chromatin structure. Plasmid DNA, used in promoter-reporter assays, is not packaged into endogenous chromatin, unlike endogenous genes, and thus not regulated by endogenous mechanisms such as epigenetic changes resulting in histone modification. For example, endogenous chromatin structure can either be in the form of methylated highly-condensed histones to form tightly-packed nucleosomes or loosely-compacted acetylated DNA (Mei et al., 2017, Xu et al., 2017), while this does not occur with plasmid DNA. An additional difference between plasmid DNA and endogenous genes is the ratio of DNA template to transcription machinery. In the case of plasmid DNA used in promoter-reporter assays, the copy number of target DNA is much higher than that of an endogenous gene, which could result in differential transcriptional responses (Whirledge & Cidlowski, 2019) between reporter gene and endogenous gene expression; however, this is not always the case and transcriptional responses between a reporter gene and an endogenous gene may be similar, as shown for synthetic GREs and GILZ (Ronacher et al., 2009). Measurement of endogenous gene expression may therefore provide more physiologically relevant data compared to promoter-reporter assays. However, given the complexity of transcriptional regulation by SRs (as discussed in section 1.1.2), differences in the nature, number and position of regulatory *cis*-elements in different endogenous gene promoters, result in gene-specific effects. The receptor-specific transcriptional effects when experiments are performed with multiple ligands in parallel could therefore be different on different endogenous genes, making the choice of which endogenous gene to investigate crucial.

Polymerase chain reaction (PCR) arrays can be used to investigate the expression of multiple endogenous genes in parallel. By using this technique global gene responses can be investigated. Thereafter, various groupings of genes can be made based on differential gene regulation. These groups can then be used to distinguish between different gene expression patterns for an SR using different ligands or under different experimental conditions.

Investigating the ligand-induced activity of SRs is particularly important due to the number of pharmaceutical drugs designed primarily to target a specific SR. For example, such drugs use GCs designed to target the GR for patients suffering from infections, allergies, inflammatory conditions or respiratory diseases to name a few

(Lu et al., 2006)(Nicolaides et al., 2018). Other drugs use progestogens designed to target the PR in female hormonal contraceptives (HCs) or hormone replacement therapy (HRT) (Stanczyk et al., 2013).

1.1.4 The progesterone receptor

In total there are seven transcripts transcribed from the PR gene (Weii et al., 1990) with evidence suggesting that only some are translated into functional protein (Jang & Yi, 2005, Yeates et al., 1998). Of these seven transcripts are those encoding the two well-known isoforms, PR-A and PR-B while a third less well-known isoform has also been identified in few studies, PR-C (Condon et al., 2006, Faivre & Lange, 2007, Taylor et al., 2009).

PR-A and PR-B are products of a single gene and are translated from the same messenger RNA transcript, transcribed from distinct promoters (Kastner et al., 1990). In terms of structure, PR-A contains a truncated N-terminal and PR-B houses an additional transcriptional activation (AF-3) (Fig. 1.1.2.4.1a) which is absent from PR-A (Fig. 1.1.2.4.1b) (Grimm et al., 2016, Sartorius et al., 1994). This is suggested to be part of the reason why PR-B is more transcriptionally active than PR-A (Sartorius et al., 1994) (Grimm et al., 2016). Additionally, the AF-3 unique to PR-B plays an essential role in specifying target genes that can only be activated by PR-B (Conneely & Lydon, 2000) and contributes to PR isoform tissue-specific expression patterns (Scarpin et al., 2009).

Less is known about the PR-C isoform. It is an N-terminally truncated PR form lacking the DBD and it is only cytoplasmic (Weii et al., 1990). The function of PR-C is relatively unknown. Weii *et al*., showed that P4 was able to bind PR-C so it is likely that other progestogens can also bind PR-C (Weii et al., 1990). There is evidence that suggests that PR-C has an inhibitory effect on PR-B activity by preventing ligand-bound PR-B from interacting with PREs (Weii et al., 1997). In a study by Condon *et al.*, the expression of PR-C and PR-B rapidly increased at the onset of labour in women suggesting that PR-C plays a role in regulating parturition in women (Condon et al., 2006).

1.1.4.1 Functions of the PR isoforms

Once bound by P4 or another progestogen, the PR forms either A:A or B:B homodimers, or A:B heterodimers in the nucleus (Conneely & Lydon, 2000). Progestogens are synthetic PR agonists that have been designed to have a better half-life and improved bioavailability compared to the endogenous hormone, P4. Half-life is defined as the time taken for the concentration of a progestogen to decrease to half the initial concentration (Tocris, 2021). Importantly, as shown in Figure 1.1.1.1 for the mechanisms of transcriptional regulation employed by SRs in general, dimerisation is not a requirement for PRs to initiate transcription and PR monomers can also regulate transcription (Jacobsen & Horwitz, 2012). In a study conducted by Mote *et al*., using human tissue samples, the PR-A and -B expression levels were similar in human breast, uteri and epithelial cells (Mote et al., 1999, Mote et al., 2002). However, there is evidence to suggest that equimolar expression of the PR isoforms is not always the case and drastic changes in the ratio of the PR isoforms are associated with malignancies in breast and endometrial tissues. These malignancies are not PR isoform-dependent and a ratio of either PR-A or -B dominance can be associated with malignant tissues (Mote et al., 2002).

The PR-A and -B isoforms regulate a suite of genes that are unique to each isoform, but they also share regulation of a subset of genes. In a microarray study in a breast cancer cell line (T47D), conducted by Richer *et al.,* of the 94 genes that met the criteria for further analysis, most genes (65) were identified to be regulated by PR-B but not PR-A, while only 4 were identified to be regulated by PR-A and not PR-B, and 25 genes were identified to be regulated by both PR isoforms (Richer et al., 2002). The Richer group used T47D cells which did not express PR and compared the gene expression patterns to T47D cells which expressed either PR-A or PR-B exclusively. The cells were treated with P4 for 3, 12 or 24 hours. Importantly, there were genes identified which were found to be regulated by either PR isoform at only one or two timepoints which was then lost at the other timepoint/s. In a similar study using the same cell lines, the Bray group found that the following genes, among others, were upregulated (and validated by real-time qPCR) in the T47D cells; *s100p, ppl, il-20ra, net1, atp1a1*, *hig2* and *cxcl12*. The gene products of these genes function as cytokines (*il-20ra*) or chemokines (*cxcl12*), are involved in the formation of epithelial cells (*s100p*

and *ppl*), play a role in DNA damage repair (*net1*) or form part of a signaling pathway activation complex (*hig2*) (Bray et al., 2005). The *atp1a1* gene product forms part of the subunit of the ATPase sodium/potassium transport enzyme (Bray et al., 2005, Lan et al., 2018). The studies by Richer *et al*. and the Bray group provide evidence that although some genes are regulated exclusively by PR-A or PR-B, there are a number of genes that are regulated by both PR isoforms. Both studies provide evidence of the dynamic role of the PR isoforms. The Bray *et al*. study shows that the physiological functions regulated by both PR isoforms are diverse and multifaceted while the Richer study shows that individually the PR isoforms exhibit distinct differences in the regulation of genes globally which highlights the unique functionality of each PR isoform.

The study by Vegeto *et al*. investigated the transcriptional effects of the PR isoforms individually. As discussed in section 1.1.2, Vegeto *et al*. showed that PR-A inhibited PR-B activity in two different cell lines using promoter-reporter assays (Vegeto et al., 1993). In the Vegeto study, PR-B activity increased in a PR-B concentration-dependent manner in CV-1 cells (monkey kidney fibroblast cell line) after a 24-hour incubation with 10 nM P4, while the activity of PR-A was no higher than background (-PR) for all amounts of transfected PR-A plasmid. This suggests that the activity of PR-B is dependent on PR-B levels and this is not the case for PR-A activity. Although the study by Vegeto *et al*. used a different strategy compared to both Richer *et al*. and Bray *et al*. to investigate PR transcriptional activity, this key study suggests that in cells where the expression of PR-A is dominant, the resultant transcriptional response will be blunted. This is primarily due to the fact that progestogen-induced responses via PR-A are significantly lower compared to PR-B which results in a ligand-bound PR-A-induced inhibition of the transcriptional activity of PR-B. The mechanism by which PR-A inhibits PR-B activity was not investigated in the Vegeto *et al.* study, however; the inhibition is most likely due to competition of ligand binding between PR-A and PR-B such that progestogen binding to PR-A decreases progestogen binding to PR-B.

The article by the Clarke lab investigated the effect of different ratios of the PR isoforms on breast cancer using tumour cytosols (Graham, 1995). Linear regression analysis revealed that high PR-A/-B ratios derived from a low concentration of PR-B rather than an upregulation of PR-A. Cells with higher PR-A expression were associated with a significant proportion of tumour cells (Graham, 1995). The group

suggests that, in agreement with the Vegeto *et al.* study, PR-A may indirectly inhibit the endocrine response by inhibiting PR-B.

While the studies discussed above used mammalian cell lines, few studies have investigated the function of the PR in whole organisms (Lydon et al., 1995, Park et al., 2020, Conneely & Lydon 2000). Lydon *et al*. showed that the PR isoforms have multifunctional roles in reproduction using female mice (Lydon et al., 1995). The expression of the PR was ablated by selectively crossbreeding mice. The Lydon group showed that female mice that did not express the PR, were completely infertile when crossed with wildtype males. Besides, the ovarian functions that were affected by the absence of the PR, the group also showed that uterine responses to P4, estrogen as well as decidual stimulation (morphological changes to the endometrial that would occur during a typical pregnancy) were reduced compared to wildtype mice. Additionally, the PR mutant mice were unresponsive to decidualisation (cell changes required for pregnancy) stimulation. This study also assessed mammary gland development by morphological analysis which revealed that in the PR mutant mice lacked the complex ductal arborisation in the periphery fat pad present in wildtype mice. This key study showed that when the PR expression was blated in mice; ovulatory-, uterine- and inflammatory functions, as well as mammary gland development were all negatively affected (Conneely & Lydon, 2000).

In agreement with the unique roles played by each PR isoform, in a more recent study by Singhal et al. the group showed by Chip-seq that the PR isoforms exhibit isoform-specific cistromes, interactomes and transcriptomes (Singhal, H.; Greene, M. E.; Zarnke, A. L.; Laine, M.; Al Abosy, R.; Chang, Y.; Dembo, A. G.; Schoenfelt, K.; Vadhi, R.; Qui, X.; Rao, P.; Santhamma, B.; Nair, H. B.; Nickisch, K. J.; Long, H. W.; Becker, L.; Brown, M.; Greene, G. L., 2018). In addition, using different PR agonists and antagonists, the group showed in the presence of both PR isoforms, that agonist-specific and gene-specific effects were observed. In terms of the unique functions of each PR isoform the group showed that PR-A inhibited gene expression and ER chromatin binding significantly more than PR-B (Singhal, H.; Greene, M. E.; Zarnke, A. L.; Laine, M.; Al Abosy, R.; Chang, Y.; Dembo, A. G.; Schoenfelt, K.; Vadhi, R.; Qui, X.; Rao, P.; Santhamma, B.; Nair, H. B.; Nickisch, K. J.; Long, H. W.; Becker, L.; Brown, M.; Greene, G. L., 2018). While this study provides important information

regarding PR isoform and ligand-specific functionality, no mechanistic insights explaining these differences were offered or investigated (Singhal, H.; Greene, M. E.; Zarnke, A. L.; Laine, M.; Al Abosy, R.; Chang, Y.; Dembo, A. G.; Schoenfelt, K.; Vadhi, R.; Qui, X.; Rao, P.; Santhamma, B.; Nair, H. B.; Nickisch, K. J.; Long, H. W.; Becker, L.; Brown, M.; Greene, G. L., 2018).

Once activated by P4, the PR isoforms play a crucial role in driving pregnancy-associated mammary ductal side-branching morphogenesis and alveologenesis without which would result in unsuccessful mammary gland development (Lain, 2013). However, in addition to P4 regulating functions related to reproduction, P4 also plays a pivotal role in other non-reproductive functions. These include cognition (Gibbs, 2000, Gonzalez et al., 2007), inflammation (Akison et al., 2018, Grimm et al., 2016, He et al., 2004, Park et al., 2020), mitochondrial function (Irwin et al., 2008) and neurogenesis (Giachino et al., 2003).

In a study by Park *et al.* it was discovered that the PR attenuated inflammation in the ovary and minimised tissue damage naturally caused by each ovulatory cycle (Park et al., 2020). Using this model, the group showed by RNA sequencing (RNA-Seq) that some genes were differentially expressed between the wildtype and a mutant mouse that could not successfully ovulate. Specifically, the expression of the *ptgs2* gene was significantly higher in the mice where PR expression was ablated (Park et al., 2020). The *ptgs2* gene encodes a rate-limiting enzyme involved in the synthesis of an inflammatory cytokine, prostaglandin E2 synthesis (PGE2) (Billich et al., 2005, Novak et al., 2009) that induces inflammation in the ovary. The group showed that higher levels of PTGS2 were associated with higher levels of NFκB which ultimately lead to an increase in PGE2 and a resultant increase in inflammation in the ovary. Park *et al.,* discovered that in mice, the PR functions to downregulate *ptgs2* expression by increasing the expression of the NFκB inhibitor-alpha (Park et al., 2020).

1.1.5 Functions of the GR

The GR is another ligand-activated SR that regulates the expression of genes via different mechanisms such as those shown in Figure 1.1.1.1 and discussed in section

1.1.2. The GR exists as two main isoforms, GRα and GRβ. GRα contains an additional 50 amino acids while GRβ contains an additional nonhomologous 15 amino acids (Nicolaides et al., 2010). For the purposes of this study, only information pertaining to the GRα will be discussed and will be referred to as GR.

The GR is ubiquitously expressed throughout the body and has a pleiotropic role throughout. The GR plays an essential role in regulating the immune response (Hammes & Levin, 2007), the central nervous system, digestive system, reproductive function and development, circadian clock as well as maintenance of metabolic homeostasis (Cohen & Steger, 2017, Garabedien et al., 2017, Præstholm et al., 2020, Rose et al., 2010).

1.1.6 Crosstalk between SRs

Primarily due to the high degree of structural homology between SRs (Fig. 1.1.1), the ability of SRs to form heterodimers and interact with each other has been investigated in several different studies which will be summarised in the present section.

In a study conducted by Mohammed *et al.,* the ability of the PR to influence ERα action was investigated. Using two human breast cancer cell lines (MCF-7 and T47D), after treatment with an ERα agonist followed by treatment with a PR agonist, the cells were cross-linked, and the PR was immunopurified. The group showed that there was a significant increase in the interaction between the PR and ERα after ligand treatment (Mohammed et al., 2015). Essentially, the group showed that the PR and the ERα could form direct protein-protein interactions and treatment with P4 inhibited the ERα proliferative effects in breast cancer cells, suggesting that the PR inhibits ERα-mediated cell proliferation (Mohammed et al., 2015).

Although the Mohammed group did not specify which PR isoform interacted with ERα, another study showed direct interaction between PR-B and ERα. In this study by Ballaré *et al*., the group showed that PR-B directly interacted with the ligand-binding domain of ERα (Ballaré et al., 2002). Because ERα is known to activate the Src/Erk pathway, the Src activity was also investigated. The group found that PR-B binding to

ERα resulted in activation of the Src/Erk pathway in presence of a PR agonist (Ballaré et al., 2002).

A similar effect was seen in another study by Singhal *et al.* which showed using human breast cancer tumours that the PR reprogrammed estrogen signaling in the presence of an estrogen, a progestin, and an estrogen in combination with a progestin (Singhal, H.; Greene, M. E.; Tarulli. G.; Zarnke, A. L.; Bourgo, R. J.; Laine, M.; Chang, Y.; Ma, S.; Dembo, A. G.; Raj, G. V.; Hickey, T. E.; Tilley, W. D.; Greene, G. L., 2016). The group went on to show by Chip-seq that the effect of the PR on ER function was as a result of PR altering ER chromatin binding (Singhal, H.; Greene, M. E.; Tarulli. G.; Zarnke, A. L.; Bourgo, R. J.; Laine, M.; Chang, Y.; Ma, S.; Dembo, A. G.; Raj, G. V.; Hickey, T. E.; Tilley, W. D.; Greene, G. L., 2016). Importantly, in this study no distinction was made between each PR isoform therefore, whether PR-A or PR-B or both PR isoforms reprograms ER signaling remains to be investigated.

The studies by Mohammed *et al*.,Ballaré *et al*. and Singhal *et al*., show that the PR modulates ERα activity by direct protein-protein interactions in a ligand-dependent manner. A similar relationship was observed between the MR and the GR; however, the interaction between these two SRs occurred ligand independently (Pooley et al., 2020). Of note, the study conducted by Pooley *et al*. proposed that the GR and MR interaction was not via a classical heterodimer but rather an allosteric and flexible interaction which occurred through oligomerisation like what has previously been described for other proteins (Stephens & Handel, 2013). With this mechanism of action in mind, the range of GR-MR interactions is expansive and allows for a variety of transcriptional outcomes in multiple tissue types that co-express both receptors (Pooley et al., 2020). Similar to the Pooley *et al.* study, another study also showed direct protein-protein interaction between SRs, in this case between the ER and the MR (Mueller et al., 2014).

In another study, it was discovered that GR-tethered to the MR leads to an increase in glucocorticoid-induced responses by competing for MR DNA-binding sites (Rivers et al., 2019). The Rivers group used chromatin immunoprecipitation (Zhang et al.) with nucleotide resolution to accurately characterise the binding profiles of the MR and the GR. In cells where the MR and GR were exclusively expressed, the MR and the GR

shared a number of overlapping binding sites in the presence of cortisol which is a ligand that binds both the MR and the GR (Rivers et al., 2019). In cells where the GR and MR were co-expressed, there was an amplified transcriptional response, and the MR was unable to bind DNA. Besides showing protein-protein interactions between SRs (Ballaré et al., 2002, Mohammed et al., 2015, Mueller et al., 2014, Pooley et al., 2020), the Rivers *et al*. study shows a different mechanism of SR crosstalk whereby liganded GR and MR compete for MR DNA binding sites (Rivers et al., 2019).

In a study by the Ogara group, researchers showed that PR-regulated responses were inhibited in the presence of a GC (Ogara et al., 2019). First, the group showed using T47D cells expressing both PR isoforms, by ChIP followed by sequencing (ChIP-seq), that the GR and PR share many genomic binding regions after treatment with their respective cognate ligands. Using select genes, real-time qPCR revealed that treatment with the synthetic GR agonist dexamethasone (dex), inhibited the expression of the following PR-regulated genes; *stat5* and *greb1.* However, this was not the case for all genes investigated. For *snai1* and *elf5*, dex in fact potentiated the PR-ligand response. Furthermore, the group showed that the GR and PR form part of the same protein complex using co-immunoprecipitation assays (Ogara et al., 2019). While the study by Ogara *et al*. provides compelling suggestive evidence that the GR has differential effects on PR-regulated genes by GR-PR crosstalk, the experiments were primarily conducted in the absence and presence of dex. Studies in which the GR is silenced are required to provide more direct evidence of SR crosstalk between the GR and the PR.

From the studies mentioned above it is evident that SR crosstalk occurs via different mechanisms which include direct protein-protein interactions as well as competition for DNA binding sites. The exact changes in the functionality of an SR after crosstalk with another SR need to be investigated further. The functionality of an SR could be altered, for example, by changes in the ability of the SR to bind or recognise SREs or changes in the phosphorylation site and/or degree of phosphorylation of the SR required to activate the SR.

1.2 Progestogens

HCs and HRT are hormonal therapies designed to target the PR to prevent unwanted pregnancy and to alleviate the symptoms of menopause, respectively, in women. HCs and HRT contain a progestin which is a synthetic PR agonist that has been designed to mimic the progestogenic actions of P4. Progestins are either structurally related to P4 or testosterone. 'Progestogens' is the collective term used to describe progestins and P4 that exert progestogenic effects.

When used in HCs, progestins differ in terms of their dose and mode of administration (Table 1.2.1). Some HCs contain a progestin only, while others contain a progestin in combination with an estrogen component (Table 1.2.1). According to 2019 statistics, 922 million women (or their partners) were contraceptive users worldwide (United Nations, 2019). It is evident that the type of contraceptive used varies widely by region. In sub-Saharan Africa, the most commonly used method of HC is the 3-monthly, intramuscular injectable contraceptive depot-medroxyprogesterone acetate (depo-MPA) (DMPA), followed by the levonorgestrel-containing implant, and then the oral pill (UNAIDS, 2019).

Table 1.2.1 summarises the most commonly used progestins in terms of structure, mode of administration, published potencies for the PR and serum concentrations detected in women. From the table, some progestogens are not administered as forms of HCs, such as P4 and R5020. These progestogens are often used as reference agonist for experimental comparison and determination of progestogen activity (Attardi et al., 2010, Bain et al., 2015, Enfield et al., 2020b, Sasagawa et al., 2008). On the other hand, some progestogens are administered in more than one form of HC method such as NET which is administered as a 2-monthly injectable (containing 200 mg NET-enanthate (NET-EN)) or as an oral pill (Table 1.2.1). NET-EN is administered in some forms of HC which is then converted to the metabolically active form, NET (Bayer, 2017, Bick et al., 2020). ETG and LNG are both administered as an implant as well as an oral pill (Table 1.2.1). Additionally, some progestogens share the same mode of administration in different HCs e.g. NET-EN used in the 2-monthly injectable and MPA used in the 3-monthly injectable. Of note, DMPA is the most commonly form of HC used in sub-Saharan Africa (UNAIDS, 2019).

Table 1.2.1: Progestogens widely used in contraception in sub-Saharan Africa and investigated in this study.

Structurally related to[a]	Progestogen (abbr.)	Structure	Published potencies (pM) for human PR[b]	Contraceptive examples[c]		
				Product	Mode of administration	Serum concentration (pM)[e]
-	Progesterone (P4)	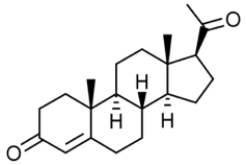	98[#], 400[#], 580* 800[#], 1000 – 5810*	-	-	650 – 600 000
-	Promegestone (R5020)	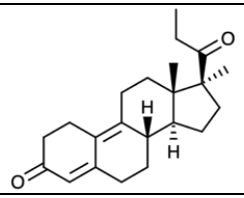	2.23[#], 60.5[§], 120[#], 5000*	-	-	-
P4	Medroxyprogesterone acetate (MPA)	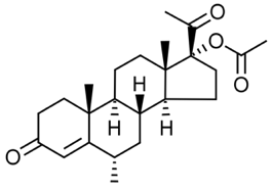	50*, 100*, 120[#], 150*	Depo-SubQ Provera®	104 mg single dose MPA, subcutaneous injection (every 3 months)	3300 – 21 000
	Nestorone (Tegley et al.)(Tegley et al.)(Tegley et al.) (NES)	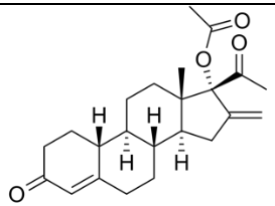	8.2[#], 29.7*	-	Ongoing trial: Vaginal ring 150 and 15, 150 and 20 and 200 and 15 µg/day of NES and ethinyl estradiol (EE)	-
Testosterone	Norethisterone (NET)	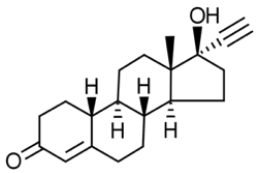	53[#], 380*, 400 –1550*	Nur-isterate®	200 mg single dose NET-EN, subcutaneous injection (2 months)	10 000 – 50 000
				Camila®	Daily mini-pill containing 0.35 mg NET	
				Norinyl-1/28®	Daily pill, 1 mg NET-EN and 50 µg Mestranol	

	Levonorgestrel (LNG)	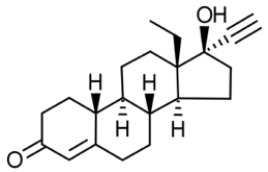	5.8[#], 169*,190*, 342[*]	Escapelle®/Levonelle® One Step[d]	Once-off emergency contraceptive pill, 1.5 mg LNG	300 – 28 000
				Nordette®	Daily pill, 0.15 mg LNG and 30 µg EE	
				Mirena®	Intrauterine device (Houshdaran et al.), 52 mg LNG (5 years)	
				Jadelle®	Slow-release subdermal implant containing 2 rods of 75 mg LNG (7 years)	
	Etonogestrel (ETG)	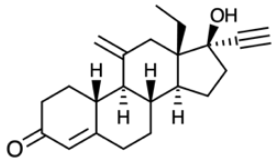	30*, 257*	Marvelon®	Daily pill containing 0.15 mg Desogestrel (DSG) (prodrug – ETG is the active metabolite) and 30 µg EE	2500 – 7500
				Implanon®	Slow-release subdermal implant containing 68 mg ETG (3 years)	
				NuvaRing®	Vaginal ring containing 11.7 mg ETG and 2.7 mg EE (3 weeks)	

[a](Stanczyk et al., 2013); [b](Attardi et al., 2010, Austin et al., 2002, Bain et al., 2015, Bray et al., 2005, Escande et al., 2009, Kumar et al., 2017, Lim et al., 1999, Madauss et al., 2004, Sasagawa et al., 2008, Tegley et al., 1998, Zhang et al., 2005); [c](Archer, D. F.; et al., 2019, Barr Laboratories, 2002, Bayer Healthcare Pharmaceuticals, 2011, Bayer Healthcare Pharmaceuticals, 2014a, Bayer Healthcare Pharmaceuticals, 2014b, Bayer Healthcare Pharmaceuticals, 2015, Merck, 2018a, Merck, 2018b, Pfizer, 2016, Teva, 2013); [d]The same product and formulation marketed under different names. [e](Hapgood et al., 2004, Speroff & Darney, 2010). *Authors did not specify which PR isoform was used. [#]EC_{50} values of progestins specifically via PR-B. [§]EC_{50} values of progestins specifically via PR-A.

1.2.1 Progestogen activity via the PR isoforms

Given the multifunctional roles of the PR isoforms and the widespread global use of HCs which target the PR, surprisingly there are no studies investigating the activity of a wide panel of progestogens via each PR isoform in a reliably comparable manner. The limited studies that have investigated the activity of progestogens via the PR isoforms, suggest that the progestogens exhibit distinct differences in potencies via the PR isoforms (Table 1.2.1). However, in each study, there are several limitations which may confound the reported PR data obtained.

In a study conducted by Attardi *et al*., promoter-reporter assays were used to determine the activity of P4, LNG, NET and nestorone (NES). Relative to the P4 transactivation response, LNG, NET and NES were all more potent than the P4 response (Table 1.2.1) (Attardi et al., 2010). Unfortunately, the group did not assess differences in maximal response (efficacy) of the progestogens via the PR isoforms. Additionally, because the study was conducted in a cell line expressing both PR isoforms, one cannot conclude PR-A or -B exclusive activity. Similarly, in a study by Bain *et al*., using U2OS cells stably transfected to express the PR and using P4 as the reference agonist, P4 was the least potent via the PR followed by NET and LNG. ETG generated the most potent response via the PR (Table 1.2.1). In terms of efficacy, surprisingly, even though it was least potent via the PR, P4 was determined to be the most efficacious, followed by ETG, LNG and then NET (Table 1.2.1) (Bain et al., 2015). However, yet again in this study by Bain *et al*. there is no clear indication about which PR isoform was investigated.

The Sasagawa group used COS-1 cells (African green monkey kidney fibroblast cells) to conduct promoter-reporter assays to investigate the activity of P4, NET and MPA via PR-B using P4 as the reference agonist. The group showed that NET and P4 had similar potencies while MPA was more potent (Table 1.2.1). However, it is unclear how reproducible the data is since there were no biological repeats and the experiment containing NET was not conducted in parallel with the experiment containing MPA. Additionally, like the study by the Attardi *et al.* group, the study by Sasagawa *et al.* did not report differences in efficacies of the progestogens via PR-B.

In a study where the PR-A and PR-B responses were compared, promoter-reporter assays were used in 1471.1 cells (mouse mammary tumour cell line) which were transfected to express either PR-A or PR-B (Lim, C. S.; et al., 1999). This study showed that the PR-A activity was much lower than that of PR-B; however, responses were more potent via PR-B than PR-A (Table 1.2.1) (Lim, C. S.; et al., 1999). A major shortfall of this study is the fact that the data obtained were not normalised to a single PR response which resulted in large error and data that is hard to interpret. Another shortcoming of the study by Lim *et al.* is that the differences in efficacies were not reported.

In a study by Kumar *et al*., the activity of P4, NET, LNG and NES were investigated using promoter-reporter assays in HEK293T cells (human embryonic kidney cell line) transfected to express PR-B (Kumar et al., 2017). Using only 3 (LNG and NES) or 4 (P4 and NET) different concentrations, LNG was determined to be the most potent progestogen followed by NES, NET and lastly P4 (Kumar et al., 2017). Although the efficacies are not reported in this study, LNG appeared to be the most efficacious progestogen followed by NES, NET (appeared to be equally as efficacious as NES) and then P4 (Kumar et al., 2017) (Table 1.2.1). Because so few concentration points were used to investigate the activity of the PR isoforms and the data were not analysed relative to a reference progestogen, it is difficult to interpret the reported potencies and efficacies via PR-B.

Only one study to date has reported results for mRNA levels of various endogenous genes by the PR in the presence of progestogens by dose response analysis. In the study by the Bray group, T47D cells expressing both PR-A and PR-B were used therefore, the effect of each individual PR isoform was not assessed. Nonetheless the PR activity was assessed in the presence of P4, NET, LNG and MPA using quantitative real-time qPCR (Table 1.2.1) (Bray et al., 2005). In general, the potencies and efficacies were gene-dependent (Bray et al., 2005). For most genes the potencies for the progestogens were very similar with only a few genes showing some distinct differences on the dose-response curves. For one gene, P4 was the least efficacious progestogen while for another gene, it generated the most efficacious response (Bray et al., 2005). Importantly, however, one cannot conclude PR-A or -B-exclusive activity. Furthermore, no potency and efficacies values were reported.

Taken together, current studies investigating the activity of progestogens via the PR isoforms have several limitations which include; limited use of physiologically relevant concentrations of progestogens which fall within the progestogen serum concentration range detected in women (Table 1.2.1) (Kumar et al., 2017). Some studies investigating the activity of progestogens via the PR isoforms use both PR isoforms which therefore means one cannot conclude PR isoform-specific activity (Attardi et al., 2010, Bain et al., 2015, Bray et al., 2005). Lastly in all studies to date, there is a limited panel of progestogens investigated. The activity of R5020, P4, NET, ETG, LNG, MPA and NES via each PR isoform therefore requires further investigation to determine whether these progestogens exhibit differential effects via each PR isoform. Characterising the activity of the progestogens via the PR isoforms will add to the body of knowledge leading to a better insight into choice of progestin for HC.

1.2.2 Progestogen activity via the GR

There are some studies investigating the effect of off-target progestogen-induced activity via SRs other than the PR.

Promoter-reporter assays in CV-1 cells transiently transfected to express the GR, showed that ETG is a weak partial agonist via the GR (Fuhrmann et al., 1995). In agreement with the study conducted by Fuhrmann *et al*., another study showed using cytosols prepared from rat tissues that ETG is a partial agonist for the GR while NET, LNG and NES showed no GR activity (Pollow et al., 1992). In addition to these results for ETG, others have shown that MPA, but not NET, activates GR-regulated genes (Hapgood, J. P.; et al., 2004, Hapgood, J. P.; et al., 2013, Maritz et al., 2018, Ronacher et al., 2009, Tomasicchio et al., 2013).

The off-target activation of the GR by progestogens may have important physiological implications on the immune response and other biological functions of individuals using treatments which contain progestogens. The transcriptional response of the GR in the presence of progestogens requires further investigation.

1.2.3 Metabolism of progestogens

Although some studies have investigated the differential transactivation effects of progestogens via PR-B (summarised above), the metabolism of progestogens is another important consideration in determining the final PR response. When PR transactivation studies are conducted, one assumes that the specific concentrations used remain constant for the duration of the experiment. However, hormone availability by differential synthesis and metabolism of ligands is a factor that influences the SR activity (Whirledge & Cidlowski, 2019). Most studies have researched progestogen metabolism in a clinical setting focussing on the serum and urine concentration of progestogens (Arici et al., 1999, Helmreich & Huseby, 1962, Huber, 1998, Hümpel et al., 1978, Prasad et al., 2010, Ravinder et al., 1997) (Table 1.2.1). From these studies, it is well-established that hormones are primarily metabolised in the liver (Charni-Natan et al., 2019, Shen & Shi, 2015). While these studies provide important information in characterising the pharmacodynamics of progestogens *in vivo*, they do not provide information regarding whether different cell types are affected differently or provide information about the potential mechanism allowing for the potential progestogen-specific responses.

As discussed in section 1.1.2.1, some studies have investigated the metabolism of ligands *in vitro*; however, these are surprisingly limited. The P4 metabolites formed are classified into those that retain the double bond of P4 in the carbon-4 position of ring A (4-pregnenes) and those that are 5α-reduced (5α-pregnanes). 3α-hydroxy-4-pregnen-20-one (3αHP) (a 4-pregnene) was reported as the major metabolite of P4, being produced via the aldo-keto reductase 1 (AKR1C1) enzyme (Hevir et al., 2011, Lewis et al., 2004), while 5α-pregnane-3,20,-dione (5αP) (a 5α-pregnane) was also reported as another P4 metabolite (Wiebe et al., 2000) produced by 5α reductase enzymes such as; SRD5A1 and SRD5A2 (Lewis et al., 2004) and CYP3A (Klein-Szanto & Conti, 2002, Wang, H.; et al., 2000).

Whether the P4 metabolites are active via SRs remains to be investigated. One study suggests that the P4 metabolites have differential physiological effects such that an elevated level of 5αP is associated with unfavourable outcomes using breast cancer cell lines *in vitro* while 3αHP is not (Wiebe et al., 2000). In agreement, another study

showed that the 5α reductase enzymes are expressed at elevated levels in breast cancer tissues compared to normal breast tissue while the converse was true for the AKR1C1 enzyme (Lewis et al., 2004). In contrast, one study, showed that increased expression of AKR1C1, AKR1C2 and AKR1C3 was associated with ovarian endometriosis (Hevir et al., 2011). It is likely that the expression of the enzymes involved in P4 metabolism therefore play an important role in determining the fate of breast and ovarian tissues (Lewis et al., 2004). Additionally, the metabolites and the enzymes involved in the metabolism of other progestogens besides P4, requires more investigation.

Metabolites of NET have been identified which include dihydro- (5α-NET and 5β-NET) and tetrahydro- (3α,5α-NET, 3β,5α-NET, 3α,5β-NET and 3β,5β-NET) metabolites (Bick et al., 2020). Evidence suggests that the dominant NET metabolite produced may be dependent on the dose of NET (2 or 25 mg) administered (Bick et al., 2020, Stanczyk & Roy, 1990). The enzymes involved in the metabolism of NET require further investigation. The cytochrome P450 3A polypeptide 4 (CYP3A4) enzyme has been implicated in the metabolism of ETG to produce hydroxylated metabolites (Bick et al., 2020, Korhonen et al., 2005). The exact metabolites produced by ETG metabolism remain to be investigated further. The metabolites of LNG are more well-studied than those of ETG. Like NET, LNG is reduced to form dihydro- (5α-LNG and 5β-LNG) and tetrahydro- (3α,5α-LNG, 3β,5α-LNG, 3α,5β-LNG and 3β,5β-LNG) metabolites (Stanczyk & Roy, 1990); however, the enzymes involved in LNG metabolism require further investigation (Bick et al., 2020). Even though MPA is the most commonly used progestogen in sub-Saharan Africa (UNAIDS, 2019), very little is known about its metabolism. Studies have shown that MPA can be hydroxylated to produce 6β, 21-dihydroxy-MPA as the major metabolite (Bick et al., 2020, Helmreich & Huseby, 1962). Although, CYP3A4 has been suggested to be responsible for hydroxylating MPA (Zhang et al., 2005), more research is required to confirm this. The metabolites of NES have not been identified in humans (Bick et al., 2020). Using rodent models, some metabolites have been identified which include 17α-deacetyl-NES and 4,5-dihydro-17α-deacetyl-NES (Prasad et al., 2010), 5α-dihydronestorone (5α-DHNES), 20α-dihydronestorone (20α-DHNES), 3α, 5α-tetrahydronestorone (3α, 5α-THNES) and 3β, 5α-tetrahydronestorone (3β, 5α-THNES) (Kumar et al., 2017).

Whether these NES metabolites are produced in humans remains to be investigated (Bick et al., 2020).

Differential metabolism of progestogens could affect the final concentration of ligand available to interact with SRs and therefore will influence the resultant SR activity. Whether there is differential metabolism of different progestins and how this compares to P4 metabolism remains to be determined. Additionally, although it is generally understood that the metabolism of progestogens occurs in the liver (Schiffer et al., 2019), whether progestogens are cell-specifically metabolised requires further investigation.

1.3 Antiretroviral drugs

Human immunodeficiency virus and acquired immunodeficiency syndrome (HIV/AIDS) continues to be one of the deadliest diseases in the world which continues to increase yearly (UNAIDS, 2019). In 2019, there were 38 million people living with HIV (an increase from 37.3 million in 2018) with about 7.1 million people unaware that they were infected (UNAIDS, 2019). Although there is no cure for HIV/AIDS, effective use of antiretroviral drugs (ARVs) as combined antiretroviral therapy (cART) has shown great success in allowing HIV-infected individuals to lead long lives (Frank et al., 2019). Moreover, due to the great success rate, ARVs are currently being used as a preexposure prophylactic (PrEP) measure for individuals at high risk of infection (Baeten et al., 2016, Keller, Marla J et al., 2019, Keller, M. J. et al., 2016, Nel et al., 2016). Furthermore, ARVs are currently being investigated for use as multipurpose prevention technologies (MPTs) which, in combination with a progestin, provides dual protection against both HIV and unwanted pregnancy (Dlamini et al., 2019). MPTs have been proposed as a result of millions of women taking ARVs (UNAIDS, 2019) and HCs (Fig. 1.2.1) concurrently. However, concerns over long-term use of ARVs need to be explored. Patients receiving cART have an increased mortality from a variety of complications such as cardiovascular disease, renal failure, bone disease and cancer (Deeks, 2011).

Tenofovir disoproxil fumarate (TDF) which is the prodrug of tenofovir (TFV) is a nucleotide reverse transcriptase inhibitor currently used in cART along with other ARVs. TDF is also the front-runner ARV for use as PrEP and in MPTs (Keller, Marla J et al., 2019, Keller, M. J. et al., 2016). Of note, TDF use has adverse effects such as negatively affecting renal function and bone density (Grigsby et al., 2010, Horberg et al., 2010). Dapivirine (DPV) is a non-nucleoside reverse transcriptase inhibitor and is the most clinically advanced ARVs in terms of PrEP, already having shown a reduced HIV infection risk of 30% in a phase III clinical trial. Modelling data from follow-up open-label extension shows a further increase in the reduction of HIV risk to approximately 50% (Baeten et al., 2016, Nel et al., 2016). Currently the DPV vaginal ring is under regulatory review for use for individuals at high risk of infection (Dlamini et al., 2019). Lastly, Maraviroc (MVC) is another ARV used in cART and is currently being investigated for PrEP (Gulick et al., 2017). It is a C-C chemokine receptor 5 (CCR5) antagonist that prevents the interaction between HIV gp120 and the human CCR5 (Dorr et al., 2005). There is limited research into the adverse effects long-term MVC use may have on individuals. Some studies suggest MVC may have proinflammatory effects (Madrid-Elena et al., 2018), while others suggest that it may have anti-inflammatory effects (Arberas et al., 2013, Díaz-Delfín et al., 2013).

1.3.1 ARVs and nuclear receptors

Whether any of the side-effects (cardiovascular disease, renal failure, bone disease and cancer) observed after long-term ARV use occur in part via the nuclear receptor family requires investigation. One study suggests that some side-effects may occur via off-target activation of nuclear receptors.

Svärd *et al*. conducted an investigation into the ARV-induced activity of the Liver X receptors (LXRα and β), ERs (ERα and β) and the GR in the presence of a number of ARVs including MVC (Svärd et al., 2014). Initially the group used an *in silico* approach to predict the ability of the ARVs to bind to the DBD of the above-mentioned receptors followed by *in vitro* promoter-reporter assays. The *in silico* and *in vitro* approaches showed that that MVC was able to bind the DBD of both LXR receptors. Using promoter-reporter assays in HepG2 cells, they showed that MVC activates the LXRβ. The LXRs belong to the nuclear receptor family but are not classified as SRs (Svärd

et al., 2014). In the study by Svard *et al.* no ARV-induced activity was detected via the SRs investigated (ER-α, -β and the GR).

Because SRs belong to the nuclear receptor family, the ability of ARVs to activate SRs may indeed occur. In a study in which the candidate is a co-author, the *in silico* binding of DPV and TDF to the PR was predicated (Dlamini et al., 2019). It was shown that DPV could bind PR-B however, TDF could not (Dlamini et al., 2019). The ARV-induced activity observed via nuclear receptors (Svärd et al., 2014) emphasizes the need for a thorough investigation of the potential off-target ARV-induced activity via SRs. This is especially important in light of the number of people using ARVs to combat HIV infection as well as increased research into other pharmaceuticals which would contain an ARV such as PrEP and MPTs.

1.4 Thesis rationale and hypotheses

There is a range of progestogen-containing HCs available which differ in terms of dose, type of progestogen used, mode and frequency of administration. Limited studies that have investigated progestogen-induced activity via the PR and its isoforms suggest that progestogens have differential effects on PR transcriptional activity. Given the number of HC use among women of reproductive age (15-49 years) (UNAIDS, 2019), the importance of accurately determining and comparing the activity of the different progestogens to each other and to the endogenous hormone P4 becomes apparent. However, such studies are limited and are likely to be confounded due to limitations which include the way the experiment was conducted (Kumar et al., 2017) or in the way the data were analysed (Lim, C. S.; et al., 1999, Sasagawa et al., 2008). Additionally, some studies do not specify which PR isoform was being assessed (Attardi et al., 2010, Bain et al., 2015). In the current study there are four central hypotheses, each one containing separate aims.

The first central hypothesis of the current study was that the progestogens exhibit progestogen-, model system-, promoter- and isoform-specific effects. The aims of this hypothesis are summarized below.

1. The first aim of the present study was to determine whether the progestogens exhibit **progestogen-specific transcriptional effects via the PR-B.** In order to address this aim, the activity of five clinically-relevant progestins used in HCs (as well as R5020 and P4) via PR-B in terms of potency, efficacy and biocharacter were determined. Dose-response analysis was performed using promoter-reporter constructs in PR-B transfected U2OS cells. The promoter-reporter assay, using synthetic PREs upstream of a reporter gene, has proven to be a viable method of investigating the mechanisms of progestogens via SRs (Enfield et al., 2020b, Kumar et al., 2017, Lim, C. S.; et al., 1999).

2. The second aim was to determine the effect of **model systems on progestogen-induced PR activity**. Under this aim, two aspects were investigated. First, it was investigated whether the transfection condition used in the promoter-reporter assays influenced the progestogen-induced PR activity. This was investigated using two different transient transfection conditions in U2OS cells (TC 1 or TC 2) to compare how different transient transfection conditions in the same cells (U2OS) influenced progestogen responses on promoter-reporters via the PR. Secondly, the effect of model system of progestogen-induced transcriptional effects via PR-B was investigated. To do this, the promoter-reporter progestogen-induced PR efficacies, potencies and biocharacters using TC 1 in transiently transfected U2OS cells were compared to those obtained in MDA-MB-231 PR-B-stably-transfected (MDA-PR-B+) cells.

3. The third aim was to investigate **the promoter-specific effects of progestogen-induced PR-B transcriptional responses**. To do this, the expression of three endogenous PR-regulated genes was assessed by real-time qPCR in MDA-PR-B+ cells. The relative efficacies, potencies and biocharacters for each gene were compared.

4. The fourth aim under the first central hypothesis was to determine whether the progestogens displayed **PR isoform-specific transcriptional responses**. This was done using comparing the PR progestogen-induced promoter-

reporter responses in the two cell lines stably expressing either PR-A or PR-B. The PR-A and -B responses could be reliably compared due to the fact that the promoter-reporter assays were conducted in the same cell line containing the same cofactors and other regulatory proteins where the only known difference was the PR isoform that was expressed.

The second hypothesis of the current study is that progestogens are differentially metabolised in extra-hepatic cells. Published studies investigating the transcriptional effects of progestogens via the PR have not considered progestogen metabolism to be a factor that could influence the final PR response to progestogens. The aims of this hypothesis are summarised below.

1. The first aim under the second hypothesis was to **establish whether progestogen metabolism occurred in one of the cell lines** used in the current study (U2OS cells). The degree of metabolism of the seven progestogens mentioned above was investigated using ultra performance liquid chromatography with tandem mass spectrometry (UHPSFC-MS/MS).

2. The second aim was to determine if **the relative extent of metabolism correlates with relative PR activity of different progestogens**. The progestogen-specific promoter-reporter PR-B potencies and efficacies in U2OS cells were assessed for correlation with progestogen metabolism data by Pearson correlation analyses.

The PR regulates multiple target genes which contribute to normal physiological functions. The fact that millions of women are using ARVs while simultaneously using HCs raises the question of whether these two combined treatments can affect the resultant PR activity. Given that some ARVs exhibit side-effects and that some have been shown to activate nuclear receptors (Svärd et al., 2014), this raises the question of whether ARVs can affect the activity of the PR and its isoforms. **The third central hypothesis is that the ARVs, TDF, DPV and MVC modulate PR-B activity.**

1. Therefore, the next aim of the current study was to **investigate the potential transcriptional effects of MVC, in addition to TDF and DPV, on the activity of the more transcriptionally active PR isoform, PR-B**. To investigate this aim promoter-reporter assays were used in U2OS cells transfected to exogenously express PR-B and in MDAPR-B+. The induced PR-B transcriptional responses were determined relative to P4 or LNG. LNG was selected for the investigation of ARV-induced activity via PR-B because it is currently the front-runner progestogen for use in MPTs (Polis et al., 2016b) and P4 was selected because it is the endogenous ligand for the PR. PR-B activity in the presence of ARVs alone and in combination with a progestogen was further investigated on endogenously PR regulated genes by real-time qPCR. Typical PR activation mechanisms were then investigated in the presence of the ARVs. These include effects on PR agonist binding using competitive binding assays as well as the investigation of PR-phosphorylation of the Ser294 hormone-inducible phosphorylation residue within the N-terminal domain of PR-B, Ser294.

There are published studies which have investigated the modulatory effect of one SR on the transcriptional activity of another SR (Ballaré et al., 2002, Mohammed et al., 2015, Mueller et al., 2014, Ogara et al., 2019, Pooley et al., 2020, Rivers et al., 2019). These have been summarised earlier in section 1.1.6. The ability of an SR to affect the transcriptional activity of another SR is particularly important in light of the number of pharmaceutical products designed to target a single SR. These include progestogens used in HCs or HRT designed to target the PR and GCs which target the GR when used to treat inflammatory conditions. The findings that ETG and MPA exhibit off-target activation of the GR (Fuhrmann et al., 1995, Hapgood, J. P.; et al., 2004, Hapgood, J. P.; et al., 2013, Maritz et al., 2018, Pollow et al., 1992, Ronacher et al., 2009, Tomasicchio et al., 2013) raise the important question of whether the GR influences PR-mediated responses in the presence of progestogens. **The final hypothesis of the current study is that the GR modulates progestogen-induced effects via the PR.**

1. The final aim of the current study was to **investigate the effect of the GR on PR transcriptional activity**. This aim was initially investigated by promoter-reporter assays in both PR-B transfected U2OS cells and the MDA-PR-B+ cells using siRNA specific for the GR. Both of these cell lines contain some endogenous GR as characterised in the present study. The PR-B response in the presence of progestogens was then investigated and compared under higher and lower GR levels using GR- or PR-specific ligands (i.e. not ETG or MPA). To gain insight into the global effects of the GR on endogenously regulated genes, a PCR array was performed. Furthermore, the potential mechanisms behind the GR inhibitory effect on PR-B responses were investigated using co-immunoprecipitation studies and investigating the degree of PR-phosphorylation at Ser294.

Chapter 2

Materials and Methods

2.1 Ethics and biosafety

This research formed part of a sub-study of HREC 210/2011, which was approved by the Human Research Ethics Committee at the University of Cape Town for use of human cervical explant tissue from Groote Schuur and Tygerberg Hospitals. Donors provided written informed consent.

This study, for a doctoral degree, was approved by the Human Research Ethics Committee at the University of Cape Town with reference number 072/2021.

All work was carried out according to the biosafety procedures established by the Health and Safety Committee of the Department of Molecular and Cell Biology at the University of Cape Town.

2.2 Compounds and antibodies

The following compounds were purchased from Sigma Aldrich, RSA: (11β,16α)-9-fluoro-11,17,21-trihydroxy-16-methylpregna-1,4-diene-3,20-dione (dex, catalogue no. D4902); 6α-methyl-17α- hydroxy-progesterone acetate (MPA, catalogue no. M0250000); 4-pregnene-3,20-dione (P4, catalogue no. P8783); 17α-ethynyl-19-nortestosterone (NET, catalogue no. BP266); 1-methylene-17α-ethynyl-18-methyl-19-nortestosterone (ETG, catalogue no. SML0356); 13β-Ethyl-17α-hydroxy-18,19-dinorpregn-4-en-20-yn-3-one (LNG, catalogue no. 1362602); 17-acetyl-13-methyl-16-methylidene-3-oxo-2,6,7,8,9,10,11,12,14,15-decahydro-1H-cyclopenta[a]phenanthren-17-yl] acetate (NES, catalogue no. SML0550). 17,21-dimethyl-19-norpregna-4,9-dien-3,20-dione (R5020) was purchased form PerkinElmer Life and Analytical Sciences, USA (catalogue no. NLP004005MG). All steroids were prepared in absolute ethanol (EtOH) and added to cells such that final [EtOH] was 0.1% (v/v). 3-(4,5- dimethylthiazol-2-yl)-2,5-diphenyltetrazolium bromide

(MTT) was also obtained from Sigma Aldrich, RSA (catalogue no. M5655). 4-carboxy-2',4'-dinitrodiphenylamine (dinitrodiphenylamine, DNPN, catalogue no. S746657-50MG) was purchased from Sigma Aldrich, RSA. 4,4-difluoro-N-[(1S)-3-[(1R,5S)-3-(3-methyl-5-propan-2-yl-1,2,4-triazol-4-yl)-8-azabicyclo[3.2.1]octan-8-yl]-1-phenylpropyl]cyclohexane-1-carboxamide (MVC) was purchased from Sigma Aldrich, RSA (catalogue no. PZ0002). [[(2*R*)-1-(6-aminopurin-9-yl)propan-2-yl]oxymethyl-(propan-2-yloxycarbonyloxymethoxy)phosphoryl]oxymethyl propan-2-yl carbonate but-2-enedioic acid (TDF) was purchased from the AIDS Research and Reference Reagent Program, Division of AIDS, NIAID, NIH (USA) (catalogue no. 10198). 4-[[4-(2,4,6-trimethylanilino)pyrimidin-2-yl]amino]benzonitrile (DPV) was purchased from and Selleck Chemicals (USA) (catalogue no. TMC120). The ARVs and DNPN were made up to a stock concentration of 10 mM and 500 mM, respectively, and diluted 1:1000 in dimethyl sulfoxide (DMSO, catalogue no. D2438, Sigma Aldrich, RSA) respectively. [^{3}H]-Progesterone (50 Ci/mmol) was obtained from AEC-Amersham, RSA (catalogue no. NET381001MC) and was used as a final concentration of 40 nM diluted in serum-free, phenol-red free media.

For western blotting, antibodies against human glyceraldehyde 3-phosphate dehydrogenase (GAPDH) (catalogue no. 0411; sc-47724), GR (G5, catalogue no. sc-393232), AR (catalogue no. H-280 sc-13062) and ER (catalogue no. HC-20 sc-543) were obtained from Santa Cruz Biotechnology, USA. Anti-PR (catalogue no. NCL-LPGR-312) was obtained from Leica Biosystems (Novacastra, UK). The antibody against Phospho-human PR (Ser294) (catalogue no. MA1414) was obtained from ThermoFisher Scientific, RSA. Horseradish peroxidise-conjugated secondary antibodies, anti-mouse (catalogue no. sc-2005) and anti-rabbit (catalogue no. sc-2313), were purchased from Santa Cruz Biotechnology, USA.

2.3 Plasmids

The luciferase reporter gene plasmid, pTAT-GRE-E1b-LUC (TAT-GRE-LUC), containing two glucocorticoid response elements (GREs) from the rat tyrosine amino transferase (TAT) gene under the control of the E1b promoter, was a gift from G. Jenster (Erasmus University of Rotterdam, Rotterdam, Netherlands) (Jenster et al., 1997). The empty vector, pcDNA3.1, containing a CMV promoter and no downstream

DNA sequence, was obtained from Invitrogen, UK (catalogue no. V79020). The steroid receptor plasmid for the GR, pcDNA3-hGR, containing full-length human GRα cloned into the pcDNA3 vector, was a gift from D. W. Ray (University of Manchester, UK) (Ray et al., 1999). The human PR-B (pSG5-hPR-B) and the human PR-A (pSG5-hPR-A) expression vectors were received from Eric Kalkhoven (University Medical Centre Utrecht, The Netherlands) (Kastner et al., 1990). The human AR plasmid, pSVARo (Brinkmann et al., 1999) and the human ERα plasmid, pSG5h-ERα (Chen et al., 2001) were obtained from F. Claessens (University of Leuven, Leuven, Belgium).

2.3.1 Plasmid transformation and purification

Plasmids were transformed into *Escherichia coli* DH5α cells using heat shock as previously described (Sambrook & Russel, 2006). Competent DH5α cells (100 µL) were incubated with 10 ng plasmid DNA on ice for 30 minutes, then at 42°C for 2 minutes and on ice for 2 minutes. Cells were subsequently mixed into 900 µL Luria broth (LB, 1% (w/v) tryptone, 0.5% (w/v) yeast extract, 0.5% (w/v) NaCl) and incubated at 37°C for 1 hour with shaking. Transformed cells were then plated onto LB-agar plates (1% (w/v) tryptone, 0.5% yeast extract, 1% NaCl, 1.5% agar) containing 100 µg/mL final concentration of the antibiotic ampicillin (catalogue no. 10835242001, Sigma Aldrich, RSA) and incubated overnight at 37°C. Day cultures of 5 mL LB containing 100 µg/mL ampicillin were inoculated with single colonies and incubated at 37°C for 8 hours with shaking. Plasmid glycerol stocks were prepared by mixing 500 µL 70% (v/v) glycerol with 500 µL transformed cell suspension and storage at -80°C. Overnight cultures of 200 mL LB containing 100 µg/mL ampicillin were inoculated with 200 µL day culture cell suspension and incubated at 37°C for 16 hours with shaking. Plasmid DNA was subsequently purified using the Nucleobond Xtra Midi kit for transfection-grade plasmid DNA (catalogue no. NC0389369, Thermo Scientific, USA), according to the manufacturer's instruction. The purity and yield of the plasmid preparation were assessed using a Nanodrop ND-1000 spectrophotometer (NanoDrop Technologies).

2.3.2 Restriction enzyme digestion

The supercoiled conformation of plasmid DNA was assessed by agarose gel electrophoresis by comparison with the linearized plasmid after restriction enzyme digestion. According to the manufacturer's instructions, reactions containing 300 ng DNA, 1 unit (U)/µL restriction enzyme (or equivalent volume of water for the undigested control) and 1 X FastDigest universal buffer containing sample application dye (Fermentas, Thermo Scientific, USA) were incubated for 10 minutes at 37°C. Digested and undigested samples were separated by electrophoresis on a 0.8% (w/v) 1 X Tris-Acetate-EDTA (TAE) agarose gel containing 10 µg/mL ethidium bromide (EtBr) (catalogue no. E1510, Sigma Aldrich, RSA). Samples were subsequently visualized under ultraviolet light on a Syngene, G:Box (Vacutec, England) and images acquired using GeneSnap version 7.08 (SynGene, England). The identity of the plasmids was assessed by restriction enzyme digestion pattern.

2.4 Cell lines

The African green monkey kidney fibroblast (COS-1, catalogue no. CRL-1650) and human osteosarcoma (U2OS, catalogue no. HTB-96) cell lines were purchased from the America Type Culture Collection (ATCC, USA). The MDA-MB-231 breast carcinoma PR-A or -B-stably-expressing cell lines (Lin et al., 2000) were obtained from V. Lin (Nanyang Technological University, Singapore).

Cells were cultured in humidified 37°C incubators containing 5% CO_2 in the BSL2 Mammalian Tissue Culture Facility in the Department of Molecular & Cell Biology at the University of Cape Town. COS-1 and U2OS cells were maintained in 75 cm^2 flasks (Greiner Bio-one International, Austria) in Dulbecco's modified Eagle's medium (catalogue no. D0819, DMEM, Sigma Aldrich, RSA) supplemented with 1 mM sodium pyruvate (catalogue no. P5280, Sigma Aldrich, RSA), 44 mM sodium bicarbonate (catalogue no. 144-55-8, Sigma Aldrich, RSA), 10% (v/v) foetal calf serum (FCS, catalogue no 26140, Thermo Scientific, RSA) and 100 IU/mL penicillin and 100 mg/mL streptomycin (catalogue no. 15140122, Gibco, Invitrogen, UK). The MDA-MB PR-stables were maintained as above; however, medium was supplemented with 7.5% (v/v) FCS and 500 µg/mL geneticin (G418, catalogue no. 11811023, Thermo Scientific, USA).

Transfections and stimulations were carried out in serum-free (SF) media for COS-1 and U2OS cells; however, phenol red-free DMEM (catalogue no. D4947, Sigma Aldrich, RSA) supplemented with 5% (v/v) charcoal-stripped FCS (cs-FCS, catalogue no. 12676029, Thermo Scientific, RSA) was used for the MDA-MB-231 PR stably-transfected MDA-MB-231 cell lines. For sub-culturing, cells were washed with warm 1 X phosphate-buffered saline (PBS, catalogue no. P4417, Sigma Aldrich, RSA) and incubated at 37°C with 2 mL 0.25% trypsin/0.1% EDTA in PBS (catalogue no. 252000056, Highveld Biological, RSA) for 5 minutes. Trypsin was neutralized by the addition of full DMEM containing 10% FCS (for COS-1 and U2OS) or 7.5% FCS (MDA-MB-231 PR-stables).

Cells were routinely checked for mycoplasma contamination by Hoescht staining (Freshney, 1987) and fluorescence microscopy (Department of Molecular and Cell Biology, University of Cape Town), and only mycoplasma-negative cells were used for experiments.

2.5 Transfections

Transient transfection of steroid receptor expression constructs and luciferase reporter vectors was carried out using XtremeGENE-9 transfection reagent (catalogue no. 06365787001, Roche Applied Science, RSA), according to the manufacturer's protocol at a ratio of 2:1 (XtremeGENE-9: DNA). Transfection mixes containing DNA and XtremeGENE-9 were incubated in serum-free (SF) -DMEM (COS-1 and U2OS) or phenol red-free DMEM supplemented with 5% (v/v) cs-FCS (PR stably-transfected MDA-MB-231 cell lines) at room temperature for 30 minutes before dropwise addition to the cells. For over-expression of PR-B, U2OS (1 X 10^5 cells/well) cells were seeded in 10 cm dishes (Greiner Bio-One International, Austria) for 24 hours, and transfected with pSG5-hPRB or equivalent pcDNA3.1 (as indicated in figure legends) for 24 hours before being reseeded (as indicated in figure legends) and treated in SF-DMEM (U2OS) or phenol red-free DMEM supplemented with 5% (v/v) cs-FCS (PR stably-transfected MDA-MB-231 cell lines) with the indicated ligands for a further 24 hours prior to harvesting for protein or supernatant media.

Positive controls for western blots were prepared by transfecting 1 X 10^5 cells per well COS-1 cells with 1 µg pSVARo, pSG5-hERα, pcDNA3-hGR, pSG5-hPRB or pSG5-hPRA for 24 hours prior to harvesting in 2 X sodium dodecyl sulphate (SDS) sample buffer (5 X SDS sample buffer: 100 mM TRIS-HCl pH 6.8, 5% (w/v) SDS, 20% (v/v) glycerol, 2% β-mercaptoethanol, 0.1% (w/v) bromophenol blue).

2.5.1 Promoter-reporter assays

Promoter-reporter assays using the luciferase reporter gene were carried out as described previously (Louw-du Toit et al., 2017) with a few modifications. Cells were seeded at 1.5 X 10^6 cells (U2OS) and 2.0 X 10^6 cells (MDA-MB-231 cells) in 10 cm dishes and allowed to adhere overnight. Transfection mixtures containing 9000 ng pTAT-GRE-LUC (for both U2OS and MDA-MB-231 cell) and 900 ng PR expression vector or empty vector (pcDNA3.1) (transfection condition 1) or 1410 ng pTAT-GRE-LUC and 3500 ng PR expression vector (transfection condition 2) for U2OS were prepared using XtremeGENE-9 transfection reagent and added dropwise onto cells. After 24 hours, 5 X 10^4 cells (U2OS cells) or 1 X 10^4 cells (MDA-MB-231 cells) were re-seeded into 96-well plates and allowed to adhere overnight. Twenty-four hours later, the cells were treated with the indicated ligands in SF-media (U2OS cells) or phenol red-free DMEM supplemented with 5% (v/v) cs-FCS (MDA-MB-231 PR-stables) for a further 24 hours, after which cells were washed in cold 1 X PBS and harvested in 25 µL 1 X reporter lysis buffer (catalogue no. PRE1501, Promega, USA) with a freeze-thaw step. Luciferase activity was assessed using the Luciferase Assay System (catalogue no. PRE1501, Promega, USA) by measuring relative light units (RLU) in 10 µL cell lysate after addition of 50 µL luciferin substrate in a Modulus microplate luminometer (Turner Biosystems, USA). Luciferase activity was calculated as RLU relative to total protein content per well as measured spectrophotometrically using the Bradford assay (Bradford, 1976). Thereafter, for dose responses, all data were expressed relative to the R5020 maximal response set as 100%. Data were analysed using the nonlinear regression model with three-parameters [log (agonist) vs response] with the hill slope set to 1 using Prism version 9. In the case where only one concentration was investigated, a full agonist was chosen as the reference ligand for maximum activity and all data were calculated relative to the reference ligand set as 100%.

2.5.2 Small interfering RNA (siRNA) transfections

Transfection with siRNA was carried out as previously described (Govender et al., 2014) with a few modifications. Cells were seeded at 1.5 X 10^6 cells (U2OS) and 2.0 X 10^6 cells (MDA-MB-231 cells) in 10 cm dishes and allowed to adhere overnight. Cells were transfected with 100 nM final concentration either validated GR HS_NR3C1_5 (GR5, referred to in this study as GR-KD) (catalogue no. SI02654757, Qiagen, RSA) siRNA targeting the human GR, PR HS_PGR_1 (referred to in this study as PR-KD) (catalogue no. SI00018683, Qiagen, RSA) or validated non-silencing control (NSC) scrambled sequence siRNA (catalogue no. 1027310, Qiagen, RSA) using 35 µL HiPerfect transfection reagent (catalogue no. 301704, Qiagen, RSA) in OptiMEM medium with GlutaMAX™ (catalogue no. 51985034, ThermoFisher Scientific, RSA) in a final volume of 400 µL transfection mixture. The transfection mixture was added in a dropwise manner after incubation at room temperature for 15 minutes. Cells were incubated with the siRNA transfection mixtures for 24 hours before being re-seeded at 5 X 10^4 cells (U2OS cells) or 1 X 10^4 cells (MDA-MB-231 cells) into 96-well plates. After 24 hours, the cells were transiently transfected with 9000 ng pTAT-GRE-LUC as described above (2.5.1). For RNA and protein extraction, cells were re-seeded at a density of 2.5 X 10^5 cells per well in 6-well plates and 1 X 10^5 cells per well in 12-well plates, respectively. After 24 hours, the cells were treated in SF-DMEM (U2OS) or phenol red-free DMEM supplemented with 5% (v/v) cs-FCS (PR stably-transfected MDA-MB-231 cell lines) with the indicated ligands for a further 24 hours prior to harvesting for protein, RNA or Luciferase activity. GR and PR protein knockdown was confirmed by western blotting.

2.6 Competition binding

Competitive whole cell binding assays were performed in U2OS cells as previously described (Bamberger et al., 1995), with a few modifications. Briefly, U2OS cells were seeded into 24-well plates at a density of 5 x 10^4 cells per well. Twenty-four hours later, the cells were transiently transfected with 250 ng pSG5hPR-B or pcDNA 3.1 vector using XtremeGene9. The following day, the cells were washed with PBS and incubated for 3 hours at 37°C with 40 nM [^{3}H]-Progesterone (50 Ci/mmol) in the

presence of 0.1% EtOH or 10 µM unlabelled competitor compound in antibiotic-free, phenol red-free and serum-free media. Working on ice at 4°C, cells were washed three times with ice-cold PBS containing 0.2% (w/v) bovine serum albumin (catalogue no. A9418, Sigma Aldrich, RSA) for 15 minutes. Cells were lysed in 1 X lysis buffer. The cell lysate was transferred to scintillation vials each containing 1 mL scintillation fluid (Flo-Scint^{TM} II, Perkin Elmer catalogue no. 6013529). Total binding ([^{3}H]-Progesterone only) was determined by scintillation counting using the Beckman Tri-Carb 2810 Beta-scintillation counter (Perkin Elmer machine purchased from Separations Scientific) which uses Quantasmart software (Perkin Elmer product purchased from Separations Scientific) and expressed as 100%. Specific bound [^{3}H]-Progesterone was calculated as the difference between total and non-specific binding ([^{3}H]-Progesterone + 10 µM P4) and expressed as a relative % of total binding. All values were normalised against total protein concentration as determined by the Bradford assay (Bradford, 1976).

2.7 Progestogen metabolism

2.7.1 Cell line incubations with progestogens

U2OS and MDA-MB-231 PR-B+ cells were seeded at 1 × 10^5 cells in 10% FCS or 7.5% FCS phenol red-containing media, respectively, in 24-well plates and cells were allowed to adhere for 24 hours. Thereafter, MDA-MB-231 cell media was replaced with phenol red-free media. For analysis of extent of metabolism, the cells and “no-cells” control (absence of cells) were washed with pre-warmed media then treated with 100 nM steroid or vehicle (0.1% v/v EtOH). U2OS cells were treated in phenol red-containing serum-free DMEM, while MDA-MB-231 cells were treated in phenol red-free 5% cs-FCS DMEM. For the P4 metabolism inhibition experiments, after seeding duplicate plates, MDA-MB-231 were pre-treated with 500 µM DNPN followed by a 24-hour incubation with 500 µM DNPN in combination with 100 nM P4. Upon treatment with ligand, 500 µL of the steroid- and vehicle-containing media were aliquoted into separate glass tubes and stored at −20°C; this served as the T0 control. After 24 hours, 500 µL aliquots of media were removed from the cells (and no-cell control) and transferred into clean glass tubes and stored at −20°C prior to extraction. Cells in the P4 metabolism duplicate plate were also assessed for cell viability. Cells were treated with MTT solution (5 mg/mL MTT in PBS, filter sterilised) to a final concentration of 0.5

mg/mL and incubated for another 2 hours at 37°C. Thereafter, the media was aspirated and 100 µL solubilisation solution (0.1 NHCl in isopropanol) was added to lyse the cells and resuspend the cells. The samples from each well were transferred in a new 96-well plate and the plate was read on a spectrophotometer (Thermo Scientific, USA) at 595 nm. The percentage cell viability was determined relative to the ctrl (vehicle) set to 100%.

2.7.2 Preparation of standards and samples

Individual stock solutions of the seven steroids (R5020, P4, NET, ETG, LNG, MPA and NES), as well as internal standard testosterone (T) were prepared in absolute ethanol (1 mg/mL) and stored at −20°C until use. These individual stock solutions were later used to prepare two standard master mixes (1 000 ng/mL and 1 ng/mL) containing all of the above-mentioned steroids in EtOH. These standard master mixes were subsequently used to prepare standards (1 mL, 0.01–100 ng/mL) by the addition of the appropriate volume of the standard master mix to the appropriate matrix (phenol-red containing DMEM without penicillin-streptomycin or FCS).

2.7.3 Progestogen extractions

Samples and standards were extracted using a 1:3 ratio of sample to methyl-tert-butyl-ether (MTBE) (v/v) (catalogue no. 20256-1L-F, Sigma Aldrich, RSA). The samples were shaken at 1 000 rpm for 15 minutes before being placed at −80°C for an hour to allow the aqueous phase to freeze. The MTBE layer containing steroids was transferred to glass tube and the MTBE was evaporated at room temperature in a fume hood overnight, or under a stream of nitrogen gas. Samples were subsequently reconstituted in 150 µL 50% methanol (v/v methanol and deionised water) and stored at −20°C prior to analysis.

2.7.4 Ultra-high performance supercritical fluid chromatography–tandem mass spectrometry (UHPSFC-MS/MS)

2.7.4.1 Instruments and chromatographic conditions for UHPSFC-MS/MS

The method was carried out and has been validated by someone else (Appendix A, Table A1). Briefly, the limit of detection (LOD) for each steroid was defined as the

lowest concentration at which the signal-to-noise (S/N) ratio was greater than 3 for the quantifier ion. The lower limit of quantification (LLOQ) was defined as the lowest concentration at which the S/N ratio was greater than 10 for the quantifier ion and greater than 3 for the qualifier ion. The upper limit of quantification (ULOQ) was defined as the highest concentration at which the % relative standard deviation (RSD) was no higher than 20. Precision was defined as the %RSD from the average calculated concentrations following the repeated injection of a single sample. Accuracy was defined as the %RSD from the analysis of independent replicate samples. The LOD, LLOQ, ULOQ, precision, accuracy, multiple reaction monitoring (MRM) mass transitions and retention time are summarised in Appendix A, Table A1.

2.7.4.2 UHPSFC-MS/MS method validation

Steroids were separated using an Acquity Ultra High Performance Convergence Chromatography (UPC^2) system (Waters Corporation, Milford, USA) with an Acquity UPC^2 Ethylene Bridged Hybrid (van de Stolpe et al.) column (3 mm x 100 mm, 1.7 µm particle size) as previously described (Skosana et al., 2019). The mobile phase consisted of liquid CO_2 (Mobile phase A) and methanol (Mobile phase B, MPB). A 2.5-minute gradient inlet method was used to separate the steroids using a constant flow rate of 1.9 mL/min according to the following protocol: 4% MPB from 0–1 min; 10% MPB from 1–1.5 min; 25% MPB from 1.5–2.5 min and back to 4% MPB at 2.5 min for re-equilibration. The column temperature and automated back pressure regulator were set to 60°C and 1700 pounds-force per square inch (psi), respectively. The injection volume was 2.0 µL. Quantitative mass spectrometric detection was carried out using a Xevo TQ-S triple quadrupole mass spectrometer (Waters, Milford, USA). A make-up pump fed 1% formic acid in methanol into the mixer preceding the MS line at a constant flow rate of 0.2 mL/min. All steroids were analysed in MRM mode using an electrospray probe in the positive ionisation mode (ESI+). The following settings were used: capillary voltage of 3.8 kV, desolvation temperature 350°C, desolvation gas 900 L/h and cone gas 150 L/h. MRM transitions are included in Appendix A, Table A1. Data collection and analysis were performed using MassLynx 4.1 (Waters Corporation). Using MassLynx, the area detected under the peak of each ligand was quantified and normalised to the respective internal standard peak area. Thereafter, the standard curve equation for each ligand (determined by MassLynx) was used to

calculate the concentration of the respective ligand in each sample (ng/mL). The concentration of ligand detected in the no-cells control was set to 100% and the concentration of ligand detected in the cells was calculated as a percentage thereof. Thereafter the % metabolism of all samples was expressed relative to the concentration of the respective no-cells control set to 0% metabolism.

2.8 Protein assays

2.8.1 Protein isolation

2.8.1.1 Cell lines

At the end of the experiment (transfection, knockdown, stimulation, etc.), cells seeded at 1 X 10^5 cells per well in 12-well plates were washed in ice cold 1 X PBS. Total protein was harvested by scraping in 50 µL 2 X SDS sample buffer (5 X SDS sample buffer: 100 mM TRIS-HCl pH 6.8, 5% (w/v) SDS, 20% (v/v) glycerol, 2% β-mercaptoethanol, 0.1% (w/v) bromophenol blue). After transfer to microfuge tubes, samples were boiled for 10 min at 100°C then stored at -20°C.

2.8.1.2 Cervical explants

Cervical explant protein samples were obtained from a post-doctorate research fellow and a research assistant. For completeness, the method they used to generate these samples, is given in Appendix A, section A2.8.1.2.

2.8.2 Western blotting

Western blotting was carried out as previously described (Avenant et al., 2010). Equal amounts of cell lysate were loaded onto 8% SDS-polyacrylamide gels and separated by electrophoresis at 75 V for 20 minutes then 110 V for 1 hour in 1 X running buffer (25 mM TRIS-HCl, 250 mM glycine and 0.1% (v/v) SDS pH 8.4) using a Bio-Rad Mini Protean II electrophoresis system (Bio-Rad, RSA). Proteins were blotted onto Hybond-ECL nitrocellulose membrane (AEC-Amersham, RSA) for 1 hour at 180 mA in cold 1 X transfer buffer (25 mM TRIS, 200 mM glycine, 20% (v/v) methanol). Membranes

were subsequently blocked for 1 hour at room temperature by shaking in 4% (w/v) ECL advance blocking powder (catalogue no. GERPN2232, AEC- Amersham, RSA) in 1 X TRIS-buffered saline (50 mM TRIS, 150 mM NaCl; TBS) containing 0.1% (v/v) Tween (catalogue no. P1379, Sigma Aldrich, RSA) (TBS-Tween; TBST). Primary antibodies were diluted in 4% ECL-TBST (Table 2.8.2.1) and incubated on membranes overnight with shaking at 4°C. Membranes were washed three times in 1 X TBST for 5 minutes and incubated with secondary antibodies diluted in 5% (w/v) skim milk powder in 1 X TBST (Table 2.8.2.1) for 1 hour at room temperature with shaking. After three 5-minute washes in 1 X TBST, membranes were placed in 1 X TBS prior to 1 minute incubation with Pierce ECL-chemiluminescent western blotting substrate (catalogue no. 32106, Thermo Scientific, USA). Proteins were visualised by autoradiography using Amersham Hyperfilm^{TM} MP higher performance autoradiography film (catalogue no. 28906842, AEC-Amersham, RSA). Densitometric quantification of film was carried out using ImageJ Software, version 1.8.0 (NIH, USA).

Table 2.8.2.1 Antibodies used in Western blot

Primary Antibody	Size (kDa)	Dilution	Secondary Antibody
AR	110	1:1000	Rabbit (1:3000)
ER	66	1:1000	Rabbit (1:3000)
GRα	95	1:3000	Mouse (1:5000)
PR-A/-B	94/114	1:1000	Mouse (1:5000)
PR-A/-B Ser294	94/114	1:100	Mouse (1:5000)
GAPDH	37	1:2000	Mouse (1:5000)

2.8.3 Co-immunoprecipitation (Co-IP) assay

The Co-IP assay was carried out as previously described (Avenant et al., 2010) with a few modifications. MDA-MB-231 PR-B+ cells were seeded at a density of 2 X 10^6 in 10 cm dishes and were allowed to adhere for 24 hours. Cells were treated with ligand or vehicle in phenol red-free DMEM supplemented with 5% (v/v) cs-FCS for 1 hour, washed once with cold 1 X PBS and lysed by scraping in 500 µL CytoBuster^{TM} protein extraction reagent (catalogue no. 71009-M, Novagen®) containing protease inhibitors (1 X Complete Mini protease inhibitor tablet [catalogue no. 11836153001, Roche,

RSA] per 10 mL). Cellular debris was pelleted by centrifugation at 16 000 x g for 5 min at 4ºC and 18 µL of supernatant were collected for inputs. From the supernatants of ligand-treated and vehicle control samples, equal volumes (200 µL each) were combined and incubated with 1.6 µg donkey anti-rabbit IgG antibody (catalogue no. sc-2313, Santa Cruz Biotechnology) at 4°C overnight with rotation. 200 µL of the remaining supernatants were incubated with 1.6 µg anti-GR (G-5) at 4°C overnight with rotation. Antibody-bound protein complexes were precipitated the following day by the addition of 20 µL PureProteome^{TM} Protein A/G magnetic beads (catalogue no. LSKMAGG02, Millipore, Merck, RSA) for 2 hours with rotation at 4°C. The complexes were washed twice with 1 X PBS by centrifugation at 2000 x g for 1 minute at 4°C. GR-bound proteins were then released from the beads by boiling in 25 µL 2 X SDS sample buffer for 5 minutes, then were separated using 8% SDS-PAGE and western blotting as described in 2.8.2. Samples were run on duplicate gels and duplicate blots were obtained which were probed with anti-GR (G-5) or anti-PR antibodies. The input signal quantified using ImageJ Software, version 1.8.0 (NIH, USA), was set to 100% and each IP signal was calculated as a percentage of the respective input signal.

2.9 Quantification of mRNA levels

2.9.1 RNA isolation

RNA was isolated from cell lines using Tri-Reagent® (catalogue no. T9429, Sigma-Aldrich, RSA). Cells seeded in 12-well plates were incubated in 400 µL Tri-Reagent® for 5 minutes at room temperature. Lysed cells were transferred from the 12 well plates into microfuge tubes. After the addition of 80 µL chloroform (catalogue no. 288306, Sigma Aldrich, RSA), tubes were vortexed vigorously for 15 seconds then centrifuged at 20 000 x g at 4°C for 15 minutes. The aqueous phase was removed carefully by pipetting and transferred into a new microfuge tube, into which 200 µL isopropanol (catalogue no. I9516, Sigma Aldrich, RSA) was then added. Samples were mixed by gentle inversion and incubated for 10 minutes at room temperature. RNA was pelleted by centrifugation at 4°C for 10 minutes at 20 000 x g. The supernatants were discarded, and the RNA pellet was washed twice in 75 % (v/v) EtOH in diethyl pyrocarbonate [(DEPC) catalogue no. D4758, Sigma Aldrich, RSA]-treated water (1:1000). Samples were air dried and RNA pellets were resuspended in 12 µL DEPC-

treated water. RNA was precipitated by the addition of 24 µL 100% (v/v) EtOH and 1.2 µL 3 M sodium acetate pH 5.5 followed by storage at -80°C for 30 min. RNA was then pelleted by centrifugation at 20 000 x g for 15 min at 4°C, washed in 75 % (v/v) EtOH (in DEPC-treated water), air dried and resuspended in 12 µL DEPC-treated water. Following the clean-up procedure, RNA was quantified by spectrophotometry (NanoDrop Technologies) and integrity was measured by denaturing formaldehyde agarose gel electrophoresis (Sambrook and Russell 2006). Briefly, 500 ng RNA was mixed with sample loading buffer [12% (v/v) DEPC-treated water, 5% (v/v) bromophenol blue, 7% (v/v) glycerol, 10% (v/v) 10X MOPS buffer (0.2 M MOPS in DEPC-treated water, 0.05 M sodium acetate, 0.01 M EDTA), 17% (v/v) 12.3 M formaldehyde and 49% (v/v) formamide] and 20 µg/mL EtBr. Samples were then electrophoresed on a 1% formaldehyde agarose gel [70% (v/v) DEPC-treated water, 10% (v/v) 10 X MOPS buffer, 20% (v/v) formaldehyde] in 1 X MOPS buffer (40 mM MOPS; 10 mM sodium acetate; 1 mM EDTA, pH 8.00) at 65V for 40 minutes. Samples were visualized under ultraviolet light on a Syngene, G:Box (Vacutec, England) and images acquired using GeneSnap version 7.08 (SynGene, England). RNA was stored at -80°C in 2 X volume ethanol + 1 X volume sodium acetate (catalogue no. S2889-250g, ThermoFisher Scientific, RSA) as a precipitate until cDNA synthesis.

2.9.2 cDNA synthesis

cDNA was synthesized from 250 ng RNA using the Transcriptor First Strand Synthesis cDNA kit (catalogue no. 04379012001, Roche Applied Science, RSA) according to the manufacturer's instructions. This reverse transcription method is based on anchored oligo d(T) priming. Samples were stored at -20°C.

2.9.3 Quantitative real-time RT-PCR (real-time qPCR)

Relative gene expression was determined by qPCR using 1 X SensiMix™ SYBR® no ROX master mix (catalogue no. QT650-05, Bioline, USA), forward and reverse primers (sequences and concentrations used are shown in Table 2.9.1) and 1 µL cDNA template in a 20 µL reaction. Samples were analysed on a RotorGene 3000 qPCR machine (Qiagen, Netherlands). Cycling conditions included an initial denaturation step at 95°C for 5 minutes, followed by 40 cycles of denaturation at 95°C for 8

seconds, annealing (primer-specific annealing temperatures are indicated in Table 2.9.1) for 10 seconds and elongation for 8 seconds at 72°C. Melting curve analysis and cycle threshold (Ct) determination were carried out by the RotorGene software (version 1.7). Real-time qPCR product samples were analysed by 2% agarose gel electrophoresis in 1 X TAE at 70 V for 1 hour. The primer efficiency was determined by standard curves. mRNA transcript levels normalized to the housekeeping gene GAPDH were calculated using the Pfaffl method (Pfaffl 2001). Fold change was calculated relative to the vehicle control (EtOH) set to 1. For dose responses, all data were calculated relative to the R5020 maximal response as 100%. Data were analysed using the nonlinear regression model with three-parameters [log (agonist) vs response] with the hill slope set to 1, = 100% using Prism version 9.

Table 2.9.1: Primers used for real-time qPCR reactions, primer sequences, concentrations, annealing temperatures and product sizes

Primer	Sequence	Final conc	Ta (ºC)	Product size (bp)	Reference
GAPDH	F: 5'-TGAACGGGAAGCTCACTGG-3' R: 5'-TGTCAGTTGATAAAACCGCTGCC-3'	200 nM	60	307	(Ishibashi et al., 2003)
GILZ	Quantitect Primer catalogue no. QT00091035	1 X	60	69	Qiagen, Netherlands
IL-6	F: 5'-TCTCCACAAGCGCCTTCG-3' R: 5'-CTCAGGGCTGAGATGCCG-3'	250 nM	60	193	(Wolf et al., 2002)
PTGS2	F: 5'-CATATTTACGGTGAAACTCTGGCT-3' R: 5'-CATTCAGGATGCTCCTGTTTAAG-3'	500 nM	63	275	(Billich et al., 2005)
TLR4	F: 5'-TTGAGCAGGTCTAGGGTGATTGAAC-3' R: 5'-ATGCGGACACACACACTTTCAAATA-3'	1 µM	60	143	(Shan et al., 2011)
CXCL1	F: 5'-AACCGAAGTCATAGCCACAC-3' R: 5'-GTTGGATTTGTCACTGTTCAGC-3'	250 nM	60	109	(Wang, D.; et al., 2006)
ATP1A1	F: 5'-CACACAGCCTTCTTCGTCAGTATC-3' R: 5'-CGAATTCCTCCTGGTCTTACAGA-3'	1 µM	57	110	(Bray et al., 2005)

2.10 PCR Array

2.10.1 RNA isolation

MDA-MB-231 PR-B+ cells were seeded at 1 x 10^6 cells in 10 cm dishes and allowed to adhere overnight. Twenty-four hours later, the cells were transfected as stated in section 2.5.2. Cells were reseeded in 6-well plates at a density of 2.5 x10^5 cells per well 24 hours later. Parallel western blot samples were reseeded at a density of 1 x 10^5 cells per well in a 12-well plate. The following day, the cells were treated with the indicated ligands in phenol red-free DMEM supplemented with 5% (v/v) cs-FCS for 24 hours. RNA was isolated from cells using the RNeasy Plus Mini Kit (catalogue no. QIA/74134, Qiagen, RSA) according to the manufacturer's instructions. All samples were sent to the Centre for Proteomic and Genomic Research (GPGR, RSA) for quality assessment. According to the CPGR, for RNA samples to be considered free of contaminants and salts the A260/280 ratio should be between 1.7 and 2.0 and the A260/230 ratio between 1.5 and 3. In addition to A260/280 and A260/A230 ratios, the RNA integrity number (RIN) applicability (Good RIN between 7 and 10), rRNA ratio (18s/ 28s) (Good ratio between 1.0 and 2.6) and quantitative range (25 - 500 ng/µl) were also assessed by the CPGR. Only RNA samples which met these criteria were converted to cDNA.

2.10.2 cDNA synthesis using the RT^2 first strand kit

cDNA was synthesized from 25 ng RNA using the RT^2 First Strand Kit, (catalogue no. QIA/330404, Qiagen, RSA) according to the manufacturer's instructions. Samples were then loaded on the RT^2 Profiler PCR Array, (catalogue no. 330231E-4 PAHS-181Z, Human Cancer Inflammation & Immunity Crosstalk, Qiagen, RSA) according to the manufacturer's instructions.

2.10.3 Analysis

Gapdh was used as the reference gene and the fold change for each gene was determined using the delta-delta Ct method. The average fold change for each gene was calculated and assessed for statistical significance using paired t-tests. Based on significant gene expression changes, a total of nine gene groups (A-I) was identified.

For genes that were upregulated:

Group A: Genes upregulated by NET when GR and PR-B are present (significant increase between non silencing control (NSC ctrl) compared to NSC NET). Group B: Genes upregulated only when GR is low (significant increase between GR knockdown control (GR-KD ctrl) compared to GR-KD NET with the condition that there is no significant increase between NSC ctrl and NSC NET). Therefore, groups A and B are mutually exclusive. Group C: Genes upregulated by NET with potentiated activation when GR is low (significant increase between NSC NET compared to GR-KD NET with the condition that there is also a significant increase between NSC ctrl and NSC NET). Group D: Genes upregulated by NET when GR and PR-B are present which is lost when GR is low (significant increase between NSC ctrl compared to NSC NET with the condition that there is no significant difference between GR-KD ctrl and GR-KD NET). Therefore, groups C and D are mutually exclusive. Additionally, groups B and D are mutually exclusive.

For genes that were downregulated:
Group E: Genes downregulated by NET when GR and PR-B are present (significant decrease between NSC ctrl compared to NSC NET). Group F: Genes downregulated only when GR is low (significant decrease between GR-KD ctrl compared to GR-KD NET with the condition that there is no significant decrease between NSC ctrl and NSC NET). Therefore, groups E and D are mutually exclusive. Group G: Genes downregulated by NET with potentiated repression when GR is low (significant decrease between NSC NET compared to GR-KD NET with the condition that there is also a significant decrease between NSC ctrl and NSC NET). Group H: Genes downregulated by NET when GR and PR-B are present which is lost when GR is low (significant decrease between NSC ctrl compared to NSC NET with the condition that there is no significant difference between GR-KD ctrl and GR-KD NET). Therefore, groups G and H are mutually exclusive. Additionally, groups F and H are mutually exclusive.

Group I contained genes where the expression did not change regardless of NET or high or low levels of the GR.

2.11 Statistical analysis

All statistical tests were performed using GraphPad Prism software (version 9) and are indicated, as well as n values indicating number of independent experiments, in the figure legends. All data were first analysed for normal distribution using a Shapiro Wilk normality test. Normally distributed data were analysed using either one-way or two-way ANOVA with a Tukey post-test for multiple comparisons or two-tailed paired t-tests for comparison between two samples. Non-normally distributed data were analysed using a non-parametric Kruskal-Wallis test (non-parametric one-way ANOVA) with Dunn's post-test (compared to control sample) for multiple comparisons or a Wilcoxon signed-rank test for comparisons between two samples. Graphs are plotted as mean ± SEM and the variation between independent experiments is represented by the spread of the black dots, indicating individual experiments.

Chapter 3

Progestogens exhibit progestogen-, model system-, promoter- and isoform-specific effects

3.1 Background and aims

Different progestogens are widely used in hormonal therapy and mediate their therapeutic actions via the PR. The literature is limited with characterising the activity of progestogens via the PR isoforms in a single model system. Most studies lack the use of comparable concentrations of various progestins. Additionally, it is difficult to exclusively conclude PR activity because of the type of system used which contains multiple SRs and other factors that could influence progestin activity. Accurately characterising the activity of progestins via the PR isoforms provides important information predictive of clinical relevance and side-effects.

Therefore, the initial aim of this chapter was to determine whether the progestogens exhibit **progestogen-specific** transcriptional effects via the PR-B. Initially, dose-response analysis was performed using promoter-reporter constructs in PR-B-transfected U2OS cells. Table 3.1.1 summarises the different cell lines and conditions used in this chapter. Thereafter, to address the second aim of determining the effect of **model system** on PR-B activity, two different transient transfection conditions were compared in U2OS cells to directly determine how different transfection conditions (TC 1 and TC 2) (Table 3.1.1) influenced progestogen responses via the PR. Following this, the PR-B responses obtained in U2OS cells using TC 1 were compared to those obtained in a second cell line which were stably-transfected to express PR-B (MDA-PR-B+ cells) to determine if PR-B responses were affected by the differences in these model systems (Table 3.1.1). To address the third aim, the **promoter-specific effects** of the progestogen-induced transcriptional effects on PR-B were compared and the expression of three endogenous PR-regulated genes was assessed by real-time qPCR in the MDA-PR-B+ cells. Lastly, the fourth aim was addressed by assessing the activity observed via PR-B in this stably-expressing system and comparing it to the

PR-A transcriptional responses observed in the PR-A stably-expressing MDA-MB-231 cells (MDA-PR-A+) (Table 3.1.1). This was to determine if the progestogens induced **PR-isoform specific** transcriptional responses. The only known difference between the MDA cell lines is the PR isoform expressed. The U2OS cell line was selected due to the negligible expression levels of other SRs (Africander et al., 2011 and Appendix B, Fig. B1). These cell lines were also selected since P4-activated PR plays a role in bone formation and/or bone turnover (Rickard, 2008, Prior, 2018) and the progression of certain breast cancers (Cui, 2016, Daniel, A. R.; et al., 2015). Although the MDA-MB-231 cells and U2OS cells express the GR, the PR expression level in these cells and in U2OS cells using TC 1, is similar to PR expression levels within an endocervical human explant sample (Appendix B, Fig. B2). While the physiological relevance in terms of the PR response in these models could be disputed, they do yield direct evidence of relative receptor-specific effects of different progestins when performed in parallel experiments. Part of the data shown in this chapter has been used in a publication by the present author (Enfield et al., 2020b).

Table 3.1.1: Summary of the different cell lines and conditions used in the present thesis

Cell line	Condition
U2OS. Human osteosarcoma cell line.	Transiently co-transfected to express PR-B and the reporter plasmid, 2XPRE-E1b-luc. Transfection condition 1 (TC 1): 1:10 ratio of PR-B expression vector to reporter plasmid. Transfection condition 2 (TC 2): 2.5:1 ratio of PR-B expression vector to reporter plasmid.
MDA-MB-231 PR-A+ (MDA-PR-A+). Human breast cancer cell line.	Transiently transfected to express the reporter plasmid 2XPRE-E1b-luc.
MDA-MB-231 PR-B+ (MDA-PR-B+). Human breast cancer cell line.	Transiently transfected to express the reporter plasmid 2XPRE-E1b-luc.

3.2 PR-B activity

3.2.1 Some progestogens have different efficacies but are equally as potent via PR-B in U2OS cells

To investigate the progestogen-specific effects, the activity of five clinically-relevant progestins used in HCs (as well as R5020 and P4) via PR-B in terms of potency, efficacy and biocharacter on a synthetic promoter-reporter construct were determined. Initially, transfection condition 1 (TC 1) containing a 1:10 ratio of PR-B expression vector to reporter plasmid was used. Following this, to investigate the effect of model system on PR-B transcriptional effects, a second transfection condition (TC 2) containing a 2.5:1 ratio of PR-B expression vector to reporter plasmid was investigated in U2OS cells. These conditions were selected because they had been previously used in the present author's laboratory and in the laboratory of their collaborator's. Part of the data shown in this chapter has been used in a publication by the present author (Enfield et al., 2020b). Thereafter, the effect of cell line on progestogen-induced PR-B transcriptional responses was investigated. This was done by comparing the PR-B responses obtained in U2OS using TC 1 to those obtained in MDA-PR-B+ cells.

In the U2OS cell line, using TC 1, the responses in the absence of PR-B generated some negligible background responses (Fig. 3.2.1.1a). In the presence of PR-B;

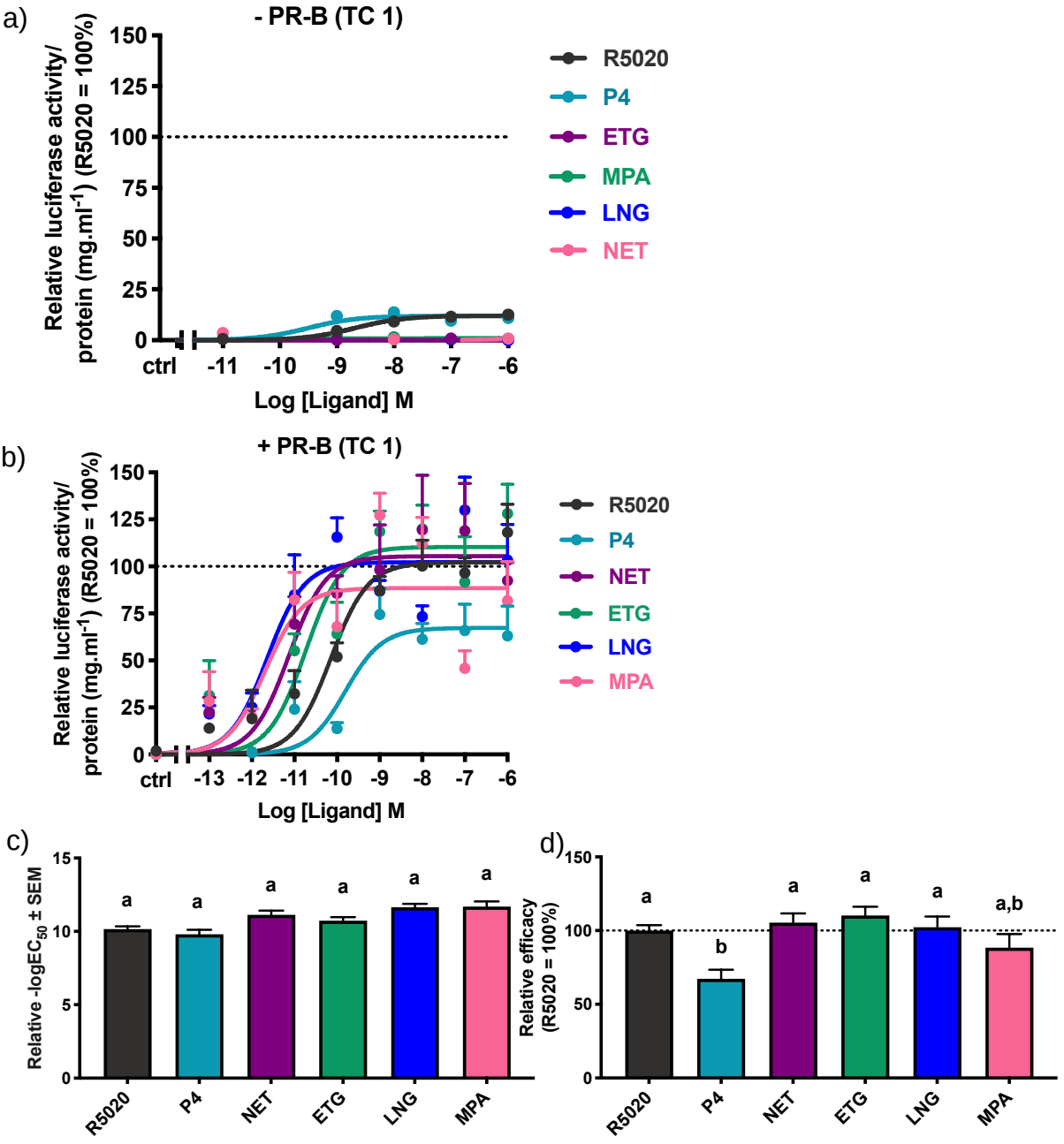

	R5020	P4	NET	ETG	LNG	MPA
Potency/ -logEC$_{50}$	10.15 ± 0.20	9.80 ± 0.31	11.13 ± 0.28	10.73 ± 0.24	11.64 ± 0.25	11.69 ± 0.36
Efficacy	100 ± 6.20	67.32 ± 6.55	105.4 ± 8.27	110.3 ± 7.50	102.3 ± 6.39	88.48 ± 8.11

Figure 3.2.1.1: The progestins and are full agonists and no significant differences were detected in potency in PR-B transiently transfected U2OS cells using transfection condition 1. U2OS cells were seeded and after 24 hours, the cells were transiently transfected with 900 ng pSG5hPR-B and 9 µg 2XPRE-E1b-luc reporter

plasmid (transfection condition 1, TC 1). Twenty-four hours later, the cells were re-seeded into 96-well plates and allowed to adhere overnight. The next day, the cells were treated with increasing concentrations ($1X10^{-13}$ M – $1X10^{-6}$ M) of each ligand or vehicle/ctrl (0.1% EtOH) for 24 hours. Thereafter, the cells were harvested and the Luciferase and Bradford assays were performed. a) & b) Show the % PR-B activity at increasing concentrations of each progestogen relative to the +PR-B R5020 efficacy = 100%. c) The bar graph shows the mean -logEC_{50} values relative to PR-B R5020 ± standard error of the mean (SEM) of each ligand via PR-B while d) shows the mean efficacies ± SEM of each progestogen via PR-B relative to R5020. Relative -logEC_{50} values and efficacies were analysed using one-way ANOVA with a Tukey post-test where different letters denote statistically significant differences while the same letters denote no significant difference. The table summarises the -logEC_{50} values and efficacies ± SEM. The SEM of the above data is calculated based on the following number of biological repeats: R5020 = 8; P4, ETG, MPA = 6; NET = 5; LNG = 4 each containing three technical repeats of each condition.

however, the progestins were all full agonists for transactivation compared to R5020, while P4 appeared to act as a partial agonist (Fig. 3.2.1.1b). The progestins were all equally as potent relative to R5020 = 100 % (Fig. 3.2.1.1c).

Although no significant differences were detected, the absolute -logEC_{50} values of the progestins from most potent to least potent were MPA (11.69), LNG (11.64), NET (11.13), ETG (10.73), R5020 (10.15) and P4 (9.84) (Fig. 3.2.1.1). The EC50 concentrations ranged from 2.02 ± 19.58 – 157.00 ± 10.89 pM (Table 7.1.1).

In terms of maximal response, P4 was significantly less efficacious than all the other progestogens investigated (Fig. 3.2.1.1d). This is unusual and suggests that the progestogens acted like “super-agonists” which has only been reported to occur via G-protein coupled receptors (Schrage et al., 2016) and not SRs.

3.2.2 Relative and absolute potencies and efficacies are mostly not significantly affected by transfection conditions

To determine whether the model system affects the efficacies and potencies of the progestogens via PR-B, the effect of transfection conditions was investigated next. This was done by repeating the promoter-reporter dose response analysis in U2OS cells; however, this time using transfection condition 2 (TC 2) to assess PR-B activity. Consistent with the amount of PR-B transfected using the second transfection

condition, about 4-fold more PR-B protein was expressed under TC 2 compared to TC 1 in U2OS cells, which was significantly higher than the PR-B expression levels found in the human endocervical tissue (Appendix B, Fig. B2).

In terms of PR-B activity, once again, in the absence of PR-B, there was negligible induction of the reporter plasmid in the presence of the progestogens (Appendix B, Fig. B3a). In the presence of PR-B, using TC 2 relative to the R5020 efficacy = 100%, all progestogens, except MPA were full agonists via PR-B (Appendix B, Fig. B3b). MPA was significantly less efficacious than R5020 and equally as efficacious as P4, NET and ETG (Appendix B, Fig. B3d), suggesting it is a partial agonist relative to R5020 and LNG. There were no significant differences detected in potency for all progestogens using TC 2 (Appendix B, Fig. B3c).

When comparing the first (Fig. 3.2.1.1) to the second (Appendix B, Fig. B3) transfection condition, few significant differences were detected (Appendix B, Fig. B4). Of note, only R5020 displayed a significantly lower potency while MPA was more potent using TC 2 (Appendix B, Fig. B4a). Although there were no significant differences detected in efficacy between TC 1 and TC 2, relative to R5020, MPA was much less efficacious using TC 2 compared to TC 1 (Appendix B, Fig. B4b).

3.2.3 Progestogens exhibit model system-specific transcriptional effects via PR-B

Following this, a second cell line which stably expresses PR-B was then used to investigate whether model system-specific differences could affect PR activity. Because the PR-B protein expression levels in U2OS cells using TC 2 were significantly higher (p-value < 0.0001) than the PR-B protein expression in endocervical tissue (Appendix B, Fig. B2), the PR-B data obtained using TC 1 (Fig. 3.2.1.1) were compared to the second cell line (MDA-PR-B+). Additionally, similar levels of PR-B protein were expressed when comparing U2OS using TC 1 and MDA-PR-B+ cells (Appendix B, Fig. B2).

The promoter-reporter dose response was carried out using MDA-PR-B+ cells which were transiently transfected with 9000 ng reporter plasmid. In the MDA-PR-B+ cells,

compared to P4, all progestogens were full agonists for transactivation via PR-B (Fig.

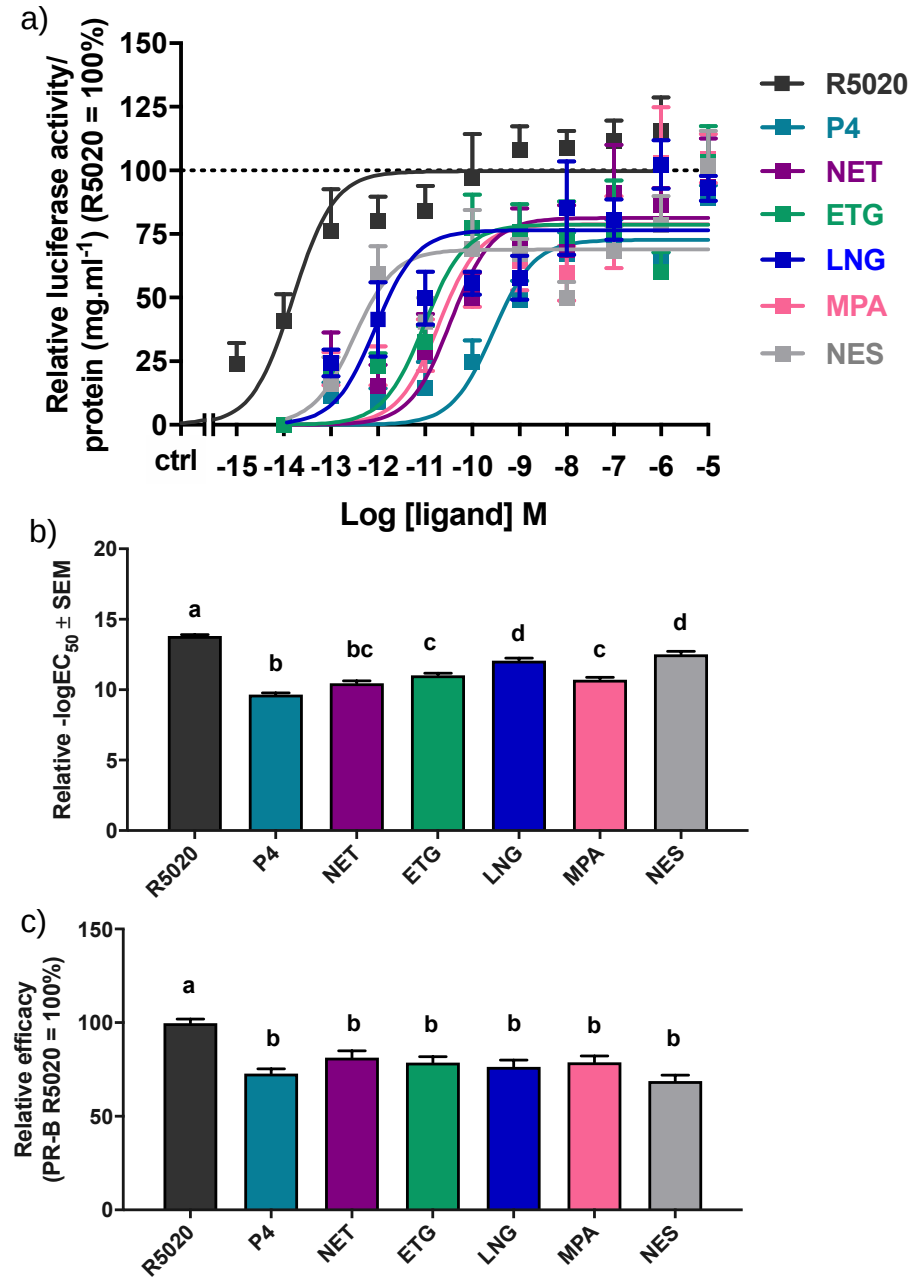

	R5020	P4	NET	ETG	LNG	MPA	NES
Potency/ -logEC$_{50}$	13.80 ±0.11	9.65 ±0.12	10.46 ±0.17	11.02 ±0.15	12.05 ±0.19	10.71 ±0.16	12.51 ±0.21
Efficacy	100 ±2.25	72.7 ±2.55	81.31 ±3.61	78.72 ±3.12	76.47 ±3.60	78.82 ±3.37	68.86 ±3.08

Figure 3.2.3.1: In MDA-MB-231 PR-B stably-expressing cells the progestins are full agonists for transactivation and show some significant differences in potency via PR-B. MDA-PR-B+ cells were seeded and after 24 hours, the cells were transiently transfected with 9 µg 2XPRE-E1b-luc reporter plasmid. Twenty-four hours later, the cells were re-seeded into 96-well plates and allowed to adhere overnight. After 24 hours, the cells were treated with increasing concentrations ($1.0X10^{-13}$ M – $1.0X10^{-5}$ M) of each ligand or vehicle/ctrl (0.1% EtOH) for 24 hours. Thereafter, the cells were harvested and the

Luciferase and Bradford assays were performed. a) Shows the % PR-B activity at increasing concentrations of each progestogen relative to R5020 efficacy = 100%. b) Shows the mean -logEC_{50} values relative to R5020 ± SEM of each ligand while c) shows the mean efficacies ± SEM of each progestogen relative to PR-B R5020 obtained in MDA-PR-B+ cells, respectively. One-way ANOVA with a Tukey post-test was performed to determine statistical differences between progestogens where different letters denote statistically significant differences while the same letters denote no significant difference. The table summarises the -logEC_{50} values and efficacies ± SEM. The SEM of the above MDA-PR-B+ data is calculated based on the following number of biological repeats: R5020, MPA = 6; P4, NET, LNG, NES = 4, ETG = 5, each containing three technical repeats of each condition.

3.2.3.1). Unexpectedly, in MDA-PR-B+ cells, the R5020 response was significantly higher compared to the other progestogens (Fig. 3.2.3.1a). Unlike in U2OS cells, significant differences in potency were found via PR-B in the MDA-PR-B+ cells (Fig. 3.2.3.1b). R5020 was significantly more potent than the other progestogens (Fig. 3.2.3.1b). Additionally, NET, ETG and MPA were similar in potency while LNG and NES had similar potencies (Fig. 3.2.3.1b). The absolute -logEC_{50} values showed that R5020 was the most potent (13.80) followed by NES (12.51) ≥ LNG (12.05) > ETG (11.02) ≥ MPA (10.71) ≥ NET (10.46) > P4 (9.56) (Fig 3.2.3.1b and Table in Fig. 3.2.3.1). The EC_{50} concentrations ranged from 0.016 ± 0.007 – 273.80 ± 114.00 pM (Table 7.1.1). In terms of efficacy, R5020 was significantly higher than the other progestogens and no significant difference was detected between the other progestogens (Fig. 3.2.3.1c).

When comparing the PR-B responses obtained in U2OS and MDA-PR-B+ cells, for potency R5020 was significantly less potent in U2OS cells while MPA was significantly more potent in U2OS cells (Fig. 3.2.3.2a). Additionally, there were significant differences in efficacy. NET, ETG and LNG were all significantly more efficacious in U2OS cells than in MDA-PR-B+ cells (Fig. 3.2.3.2b).

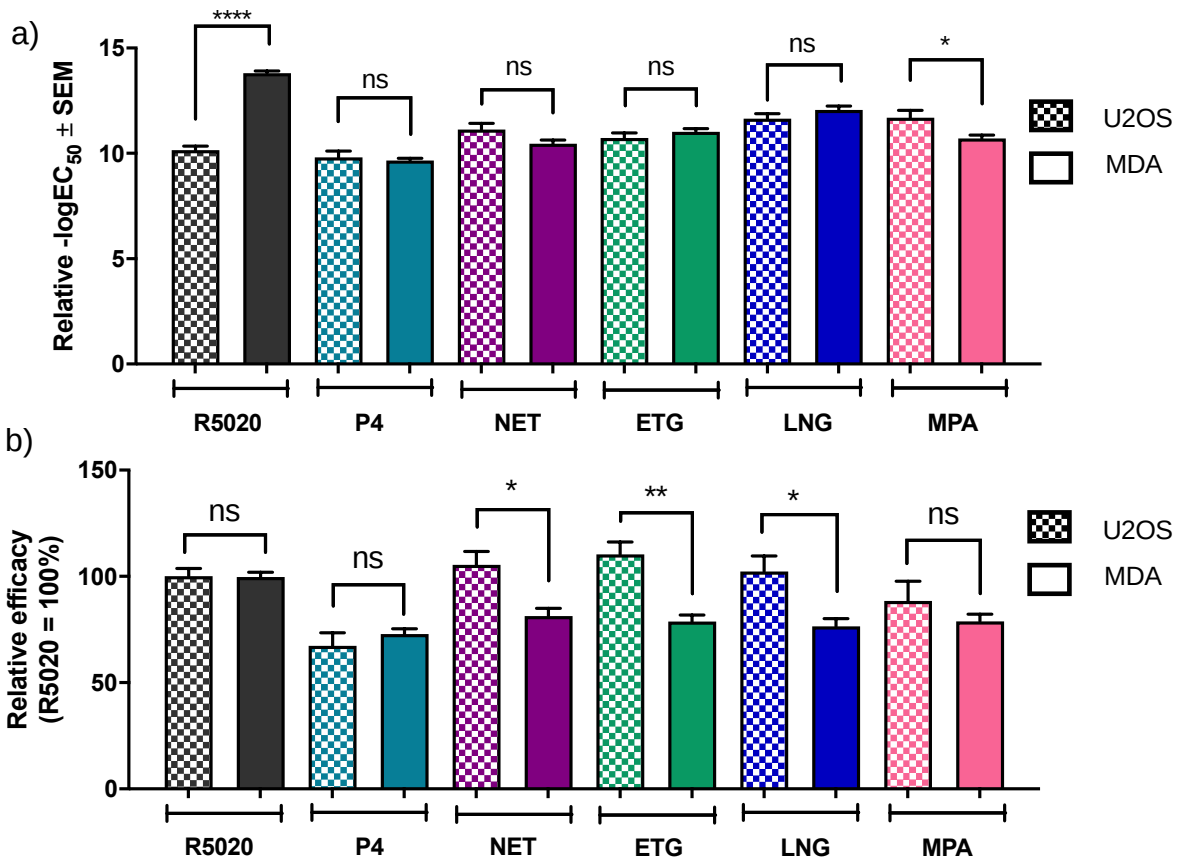

Figure 3.2.3.2: There are significant differences in PR-B responses using promoter-reporter assays in two different model systems. a) Shows the mean -logEC$_{50}$ values of each progestogen relative to R5020 ± SEM while b) shows the mean efficacies ± SEM of each progestogen relative to PR-B R5020 obtained in U2OS and MDA-PR-B+ cells, respectively. Relative -logEC$_{50}$ values and efficacies were analysed using unpaired t-tests where *, ** and **** denote p-value <0.05, <0.01 and <0.0001, respectively. The data shown in Figures 3.2.1.1 and 3.2.3.1 are shown again for comparative purposes.

3.2.4 There is significantly more PR-B protein expressed in MDA-PR-B+ cells than in U2OS cells using TC 1

To determine whether total PR-B protein levels could be a confounding factor contributing to the differences seen in the -logEC_{50} values or efficacies between the two cell lines investigated, PR-B protein expression level in these cell lines was next investigated. Having shown that the PR-B expression in both U2OS cells using TC 1 and in MDA-PR-B+ is similar to the PR-B expression within an endocervical human explant sample (Appendix B, Fig. B2), the difference in PR-B expression between these two cell lines was investigated.

Relative to vehicle (ctrl) = 100%, in U2OS cells using TC 1, there was significantly less PR-B protein levels after treatment with LNG and MPA. This was signifcantly less than PR-B levels after R5020 and ETG treatment (Fig. 3.2.4.1a and b). For MDA-PR-B+ cells, there was significant PR-B protein turnover for all progestogens compared to vehicle (ctrl) (Fig. 3.2.4.1a and c).

When comparing the PR-B levels between the two model systems, there was significantly more PR-B protein present in MDA-PR-B+ cells than U2OS cells before and after treatment with the progestogens (Fig. 3.2.4.1a and d).

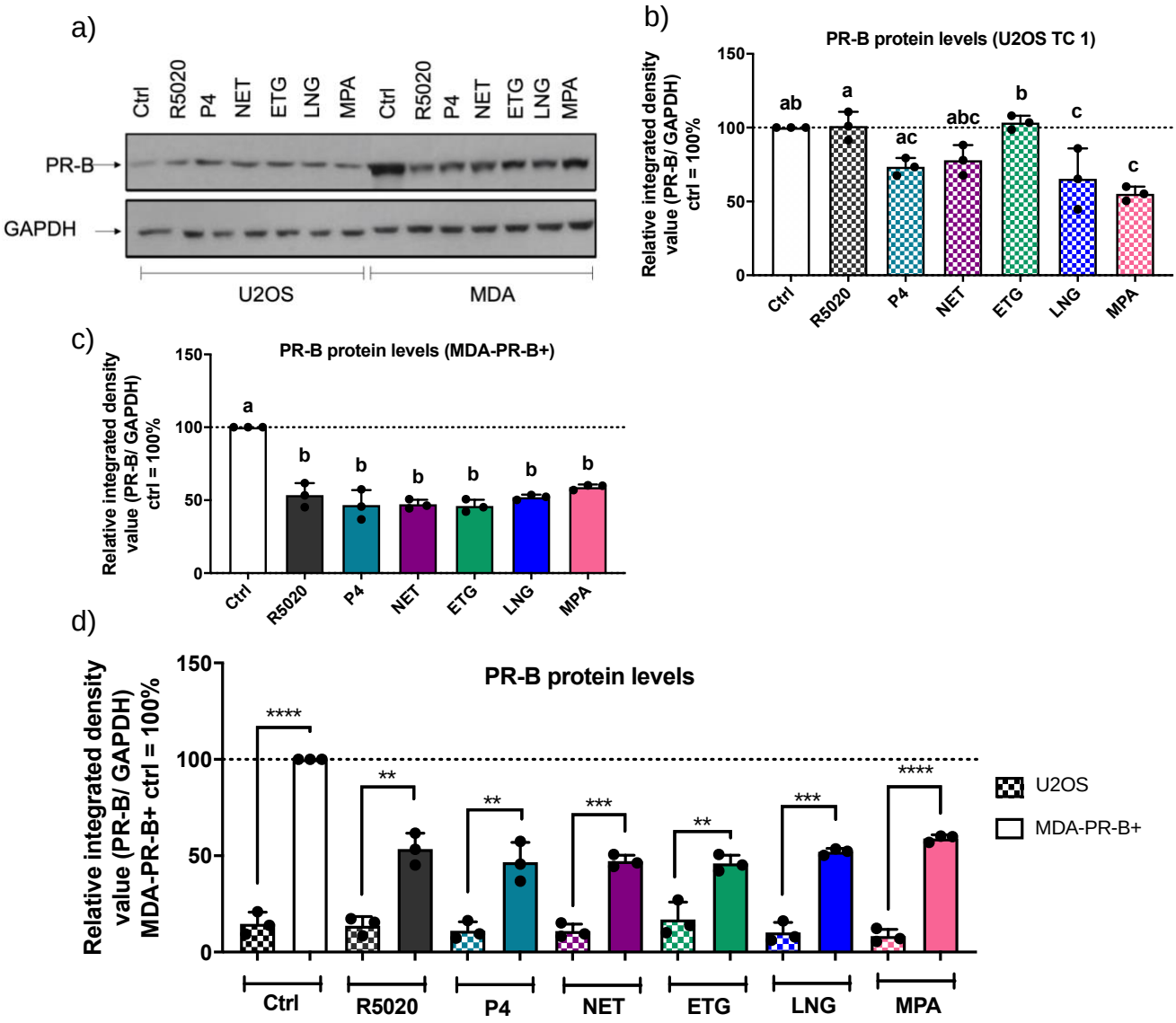

Figure 3.2.4.1: There is significantly more PR-B in MDA-PR-B+ cells compared to U2OS cells before and after a 24-hour incubation period with progestogens. Total protein lysates from U2OS and MDA-PR-B+ cells were analysed for PR-B protein levels by western blotting using GAPDH as a loading control. Blots were scanned and quantified for relative PR levels by calculating integrated density values. PR protein levels normalised to GAPDH are plotted relative to each respective vehicle control (ctrl) set to 100% in a) Shows a representative western blot of the PR-B and GAPDH protein levels. b) U2OS cells using TC 1 and c) MDA-PR-B+ cells which were assessed for statistical significance using one-way ANOVA with a Tukey post-test where different letters denote statistically significant differences while the same letters do not. d) Shows the statistical differences between U2OS and MDA-PR-B+ cells relative to MDA-PR-B+ ctrl = 100% which were determined using unpaired t-tests where **, *** and **** denote p-values <0.05, <0.001 and < 0.0001, respectively. d) The data are pooled from 3 independent experiments.

3.2.5 Progestogens exhibit gene-specific transcriptional effects

Next, the effect of the progestogen-induced transcriptional effects on endogenous PR-regulated genes was investigated. The progestogen responses via PR-B were investigated on three endogenous PR-regulated genes namely, *ptgs2, gilz* and *atp1a1,* to determine whether the progestogens exhibit promoter-specific transcriptional effects. These genes were selected because the promoter sequences either contain PREs or the expression has been shown previously to be regulated by the PR. Therefore, the expression of these genes will indicate the PR transactivation response via classical mechanisms. MDA-PR-B+ cells were treated with increasing concentrations of R5020, P4, NET or MPA for 24 hours and the mRNA levels were then measured and quantified. MPA was selected since it is used in the three-monthly injectable HC which is the most commonly used form of HC among women in Sub-Saharan Africa (UNAIDS, 2019). NET is used in the two-monthly injectable HC and has been proposed to act differently to MPA (Maritz et al., 2018). R5020 was selected to serve as the reference progestogen for determining PR activity and P4 would provide information about how the progestogen induced PR activity compares to the endogenous hormone response.

Different progestogen responses were generated for all three genes (Fig. 3.2.5.1 and 3.2.5.2). For the *ptgs2* gene, R5020, P4 and NET acted as full agonists via PR-B; however, MPA appeared to act as a partial agonist (Fig. 3.2.5.1a). All the progestogens acted as full agonists for *gilz* expression via PR-B (Fig. 3.2.5.1b). For the *atp1a1* gene, MPA generated the most efficacious response while unexpectedly, P4 appeared to act as a partial agonist (Fig. 3.2.5.1c).

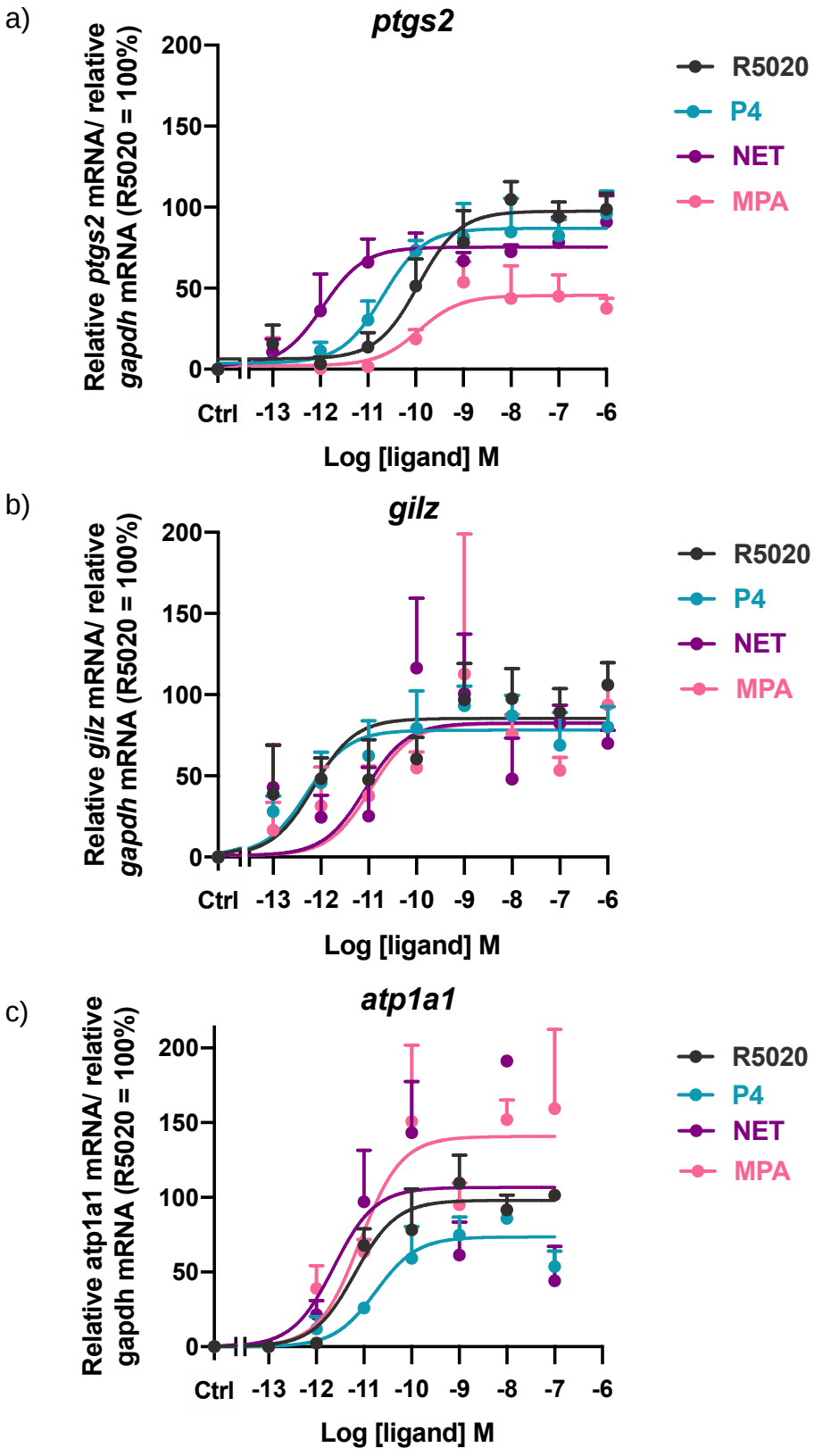

Figure 3.2.5.1: Different progestogen PR-B ligands trigger differential transcriptional regulation of *ptgs2*, *gilz* and *atp1a1* mRNA. MDA-MB-231-PRB+ cells were seeded and allowed to

adhere overnight. After 24 hours, the cells were treated with increasing concentrations ($1.0X10^{-13}$ M – $1.0X10^{-5}$ M) of each ligand or vehicle/ctrl (0.1% EtOH) for 24 hours. Thereafter the cells were harvested in Trizol. RNA was extracted and cDNA was synthesized from 250 ng RNA then used in real-time qPCR. Relative mRNA levels of a) *ptgs2*, b) *gilz* and c) *atp1a1* were normalized to *gapdh* mRNA levels. Relative expression was determined by normalising to ctrl set to 1. Thereafter, data were set relative to R5020 efficacy = 100%. The SEM of above data is calculated based on three biological repeats.

There were some significant differences in potencies and efficacies for the progestogens via PR-B on the expression of all three genes (Fig. 3.2.5.2). For the *ptgs2* gene, NET generated the most potent response which was significantly more potent than R5020 and MPA (Fig. 3.2.5.2a). For efficacy, MPA generated a significantly less efficacious response compared to the other progestogens for *ptgs2* expression. For *gilz* expression, there were no significant differences in $-\log EC_{50}$ values (Fig. 3.2.5.2c) nor efficacies (Fig. 3.2.5.2d) between progestogens. Similar to the *gilz* gene expression, there were no significant differences in potency for *atp1a1* gene expression (Fig. 3.2.5.2e). In terms of efficacy; however, the *atp1a1* gene was expressed significantly more in the presence of MPA compared to P4 (Fig. 3.2.5.2f).

When comparing the potencies and efficacies between the progestogens across all three genes, there were no significant differences in potencies (Fig. 3.2.5.3a); however, MPA generated a significantly higher efficacy for the *atp1a1* gene compared to the *ptgs2* gene while it approached a significant difference between *ptgs2* and *gilz* expression (p-value = 0.08) (Fig. 3.2.5.3b). These results suggest that R5020, P4 and NET act similarly on the three genes investigated while MPA may elicit more differential efficacies via different promoters in the same cell.

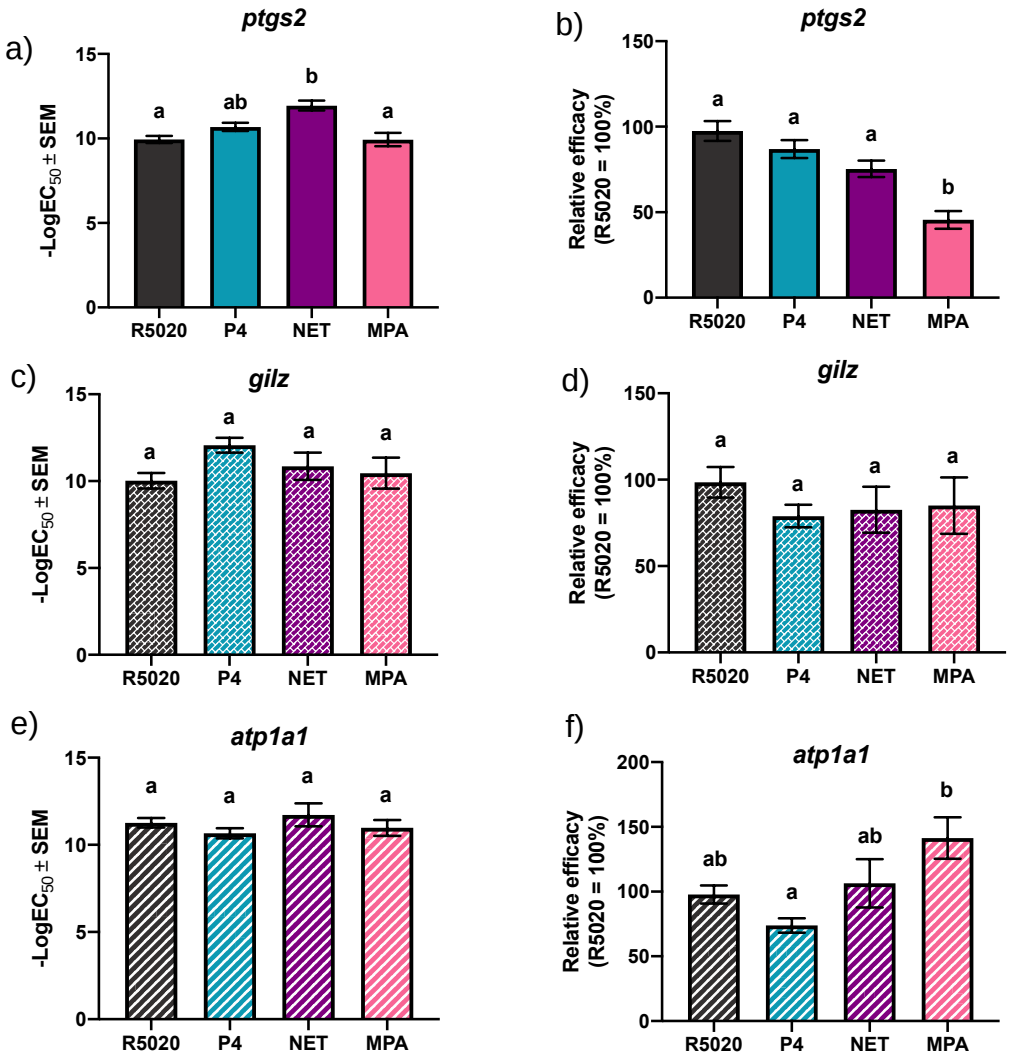

		R5020	P4	NET	MPA
ptgs2	Potency/ -logEC$_{50}$	9.94 ± 0.21	10.69 ± 0.24	11.95 ± 0.29	9.93 ± 0.39
	Efficacy	100 ± 5.80	86.93 ± 5.24	75.36 ± 4.86	45.52 ± 5.22
gilz	Potency/ -logEC$_{50}$	10.03 ± 0.44	12.07 ± 0.42	10.86 ± 0.79	10.46 ± 0.89
	Efficacy	100 ± 8.83	78.99 ± 6.54	82.57 ± 13.32	85.02 ± 16.35
atp1a1	Potency/ -logEC$_{50}$	11.27 ± 0.28	10.66 ± 0.29	11.72 ± 0.66	10.98 ± 0.46
	Efficacy	100 ± 6.99	73.85 ± 5.53	106.41 ± 18.71	141.42 ± 16.05

Figure 3.2.5.2: MPA generates the most variable efficacy via three different endogenous PR regulated genes. Mean relative a), c) and e) -logEC$_{50}$ values and b), d) and f) efficacies ± SEM from Fig. 3.2.5.1 were analysed using one-way ANOVA with a Tukey post-test, where different letters denote statistically significant differences while the same letters denote no significant difference.

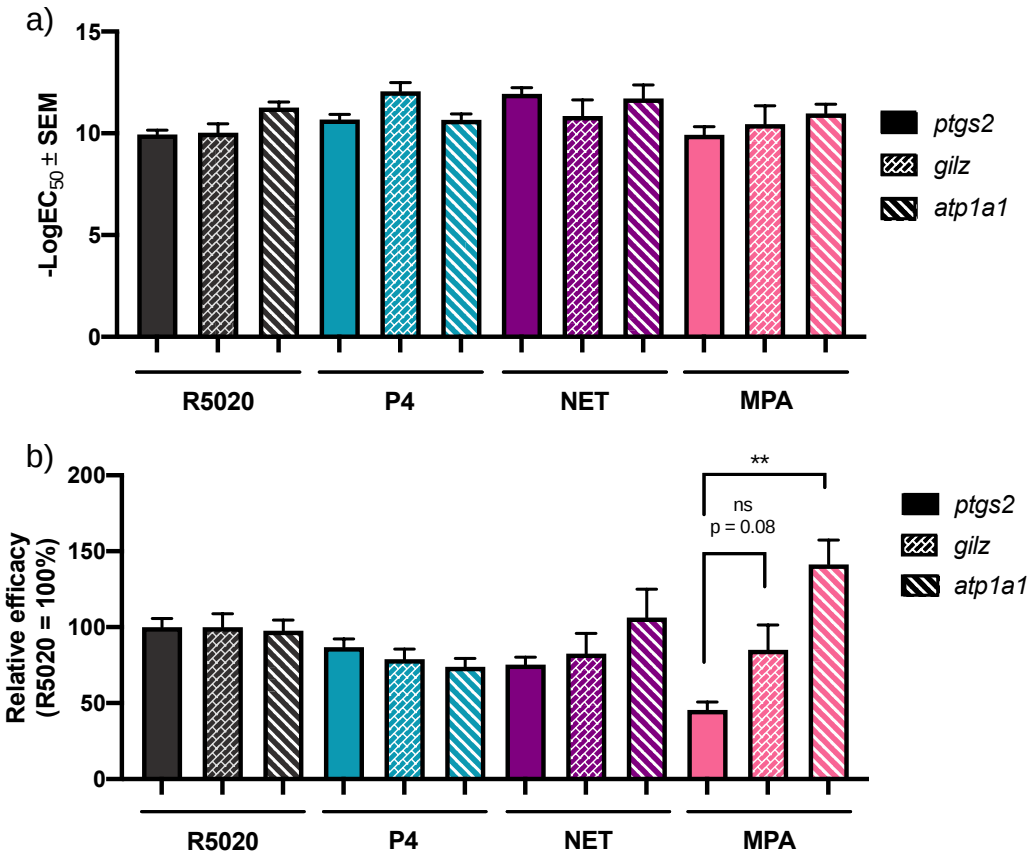

Figure 3.2.5.3: Few significant differences in potencies and efficacies for progestogen responses were detected via PR-B for different endogenous genes. Mean relative a) potency/ -logEC_{50} values and b) efficacies from Fig. 3.2.5.1 were analysed using paired t-tests where ** denotes p-value < 0.01 while ns indicates no significant difference.

3.3 PR-B and PR-A activity

3.3.1 Most progestogen responses via PR-A are significantly more potent and less efficacious than PR-B

The relative progestogen-induced PR isoform responses were investigated next. The MDA-PR-A+ cell line served as the best-suited model for directly comparing the PR-B activity observed in the MDA-PR-B+ cells.

For the PR-A responses, two ways were used to represent the activity of progestogens via this isoform namely; presenting the PR-A activity 1) relative to the efficacy of R5020 via PR-B = 100% or 2) relative to the efficacy of R5020 via PR-A = 100%. For option 1, promoter-reporter assays revealed that relative to the PR-B R5020 response, the

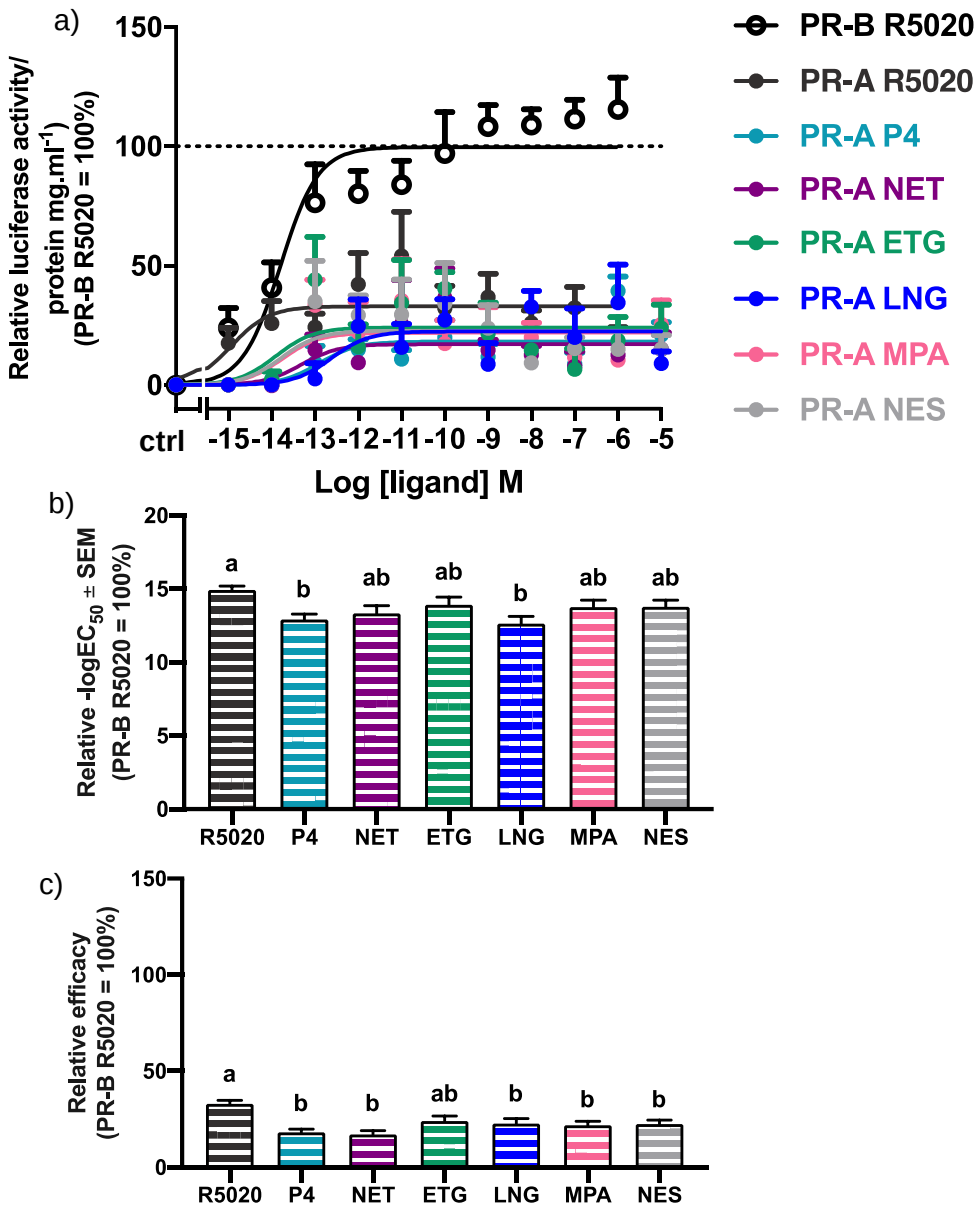

	R5020	P4	NET	ETG	LNG	MPA	NES
Potency/ -logEC$_{50}$	14.93 ±0.26	12.90 ±0.38	13.32 ±0.53	13.91 ±0.54	12.62 ±0.51	13.76 ±0.46	13.78 ±0.44
Efficacy	32.96 ±1.81	18.22 ±1.56	17.10 ±1.94	24.08 ±2.67	22.17 ±2.56	21.87 ±2.08	22.45 ±2.10

Figure 3.3.1.1: The progestogens are significantly less efficacious but more potent (except LNG) via PR-A than PR-B relative to PR-B R5020 efficacy = 100%. MDA-PR-A+ cells were seeded and after 24 hours, the cells were transiently transfected with 9 µg 2XPRE-E1b-luc reporter plasmid. Twenty-four hours later, the cells were re-seeded into 96-well tissue culture plates and allowed to adhere overnight. After 24 hours, the cells were treated with increasing concentrations ($1X10^{-13}$ M–$1X10^{-5}$ M) of each ligand or vehicle/ctrl (0.1% EtOH) or 24 hours. Thereafter, the cells were harvested

and the Luciferase and Bradford assays were performed. a) Shows % PR-A activity at increasing concentrations of each progestogen relative to PR-B R5020 efficacy = 100%. b) Shows the mean -logEC_{50} values relative to PR-B R5020 ± SEM of each ligand while c) shows the mean efficacies ± SEM of each progestogen relative to PR-B R5020 efficacy = 100%, in MDA-PR-A+ cells. Relative -logEC_{50} values and efficacies were analysed using one-way ANOVA with a Tukey post-test between progestogens, where different letters denote statistically significant differences while the same letters denote no significant difference. The SEM of the above data is calculated based on the following number of biological repeats: R5020, P4, NES = 5; NET, ETG, MPA = 4 and LNG = 3, each containing three technical repeats of each condition.

efficacies of the progestogens via PR-A were much lower than the PR-B R5020 response (Fig. 3.3.1.1a). From the dose response curves, all the progestogen responses appeared to be more potent via PR-A than the PR-B R5020 potency (Fig. 3.3.1.1a). When assessing the progestogen responses via PR-A relative to the PR-B R5020 response, both P4 and LNG were significantly less potent than R5020 via PR-A (Fig. 3.3.1.1b). Additionally, all progestogen responses except ETG were significantly less efficacious than R5020 via PR-A (Fig. 3.3.1.1c).

Relative to the PR-B R5020 efficacy = 100%, when comparing the progestogen-induced PR-A and PR-B responses, statistically, all progestogens, except LNG, were significantly more potent via PR-A (Fig. 3.3.1.2a). All progestogen responses were significantly less efficacious via PR-A than PR-B (Fig. 3.3.1.2b).

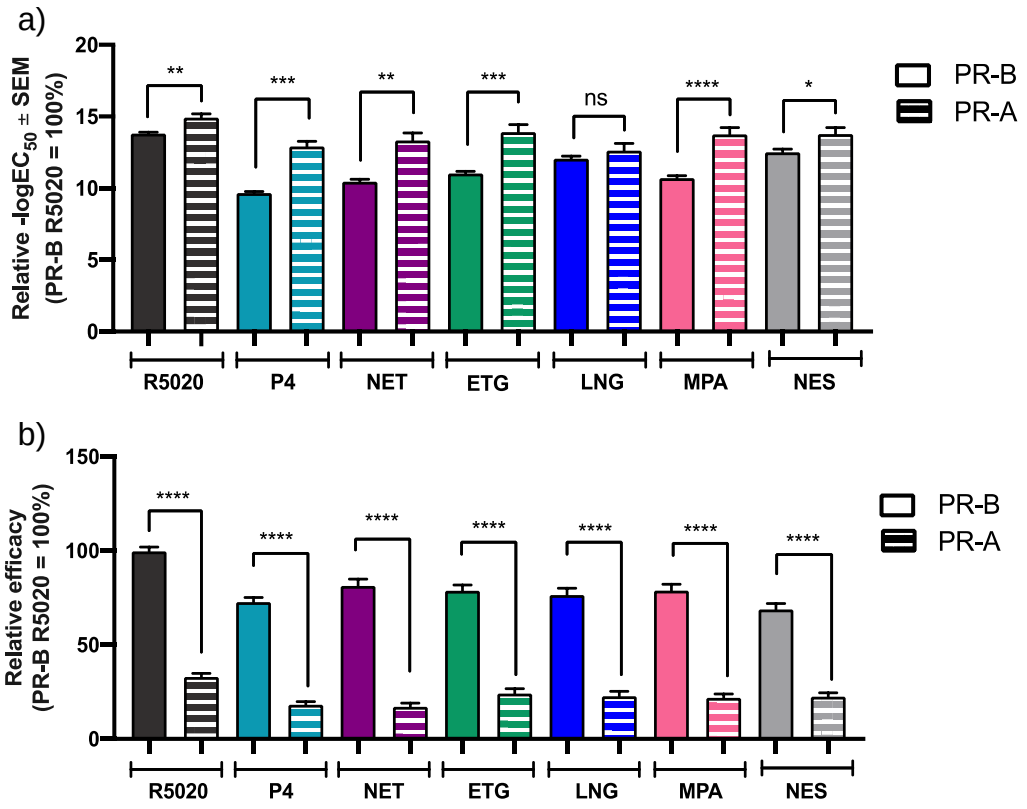

Figure 3.3.1.2: Most progestogens were significantly more potent and less efficacious via PR-A relative to PR-B. Mean relative ± SEM a) potency/ -logEC_{50} values and b) efficacies for PR-B and PR-A are shown from Fig. 3.2.3.1 and Fig. 3.3.1.1, respectively. PR-B efficacy was set to 100%. Paired t-tests were used to determine statistical differences between cell lines for each progestogen where *, **, *** and **** denote p-value < 0.5, 0.01, 0.001 and 0.0001, respectively.

When the same data were represented relative to the PR-A R5020 response (i.e. option 2) all progestogens were significantly less efficacious than the reference progestin R5020 (Appendix B, Fig. B5a and B5c). Additionally, consistent with the promoter-reporter PR-B responses in the other two cell lines (U2OS TC 1 and MDA-PR-B+) (Fig. 3.2.1.1 and Fig. 3.2.3.1), when assessing the absolute values, R5020 was the most potent progestogen; however, not significantly different to NET, ETG, MPA and NES (Appendix B, Fig. B5b). As shown in Figure B5, the potency of P4 was significantly less than R5020 while LNG was significantly less potent than all of the progestogens (Appendix B, Fig. B5b). In terms of efficacy, R5020 was significantly more efficacious than all the progestogens (Appendix B, Fig. B5c). Additionally, no significant differences were detected between ETG, MPA and NES which were all significantly more efficacious than NET and LNG (Appendix B, Fig. B5c).

3.3.2 There is significantly more PR-A protein compared to PR-B before and after treatment with progestogens

As with the U2OS and MDA-PR-B+ data comparison, the PR protein expression levels between the two PR stably-expressing MDA cell lines was investigated next to determine whether the protein levels of these receptors contributed to differences in potencies or efficacies between the cell lines.

For both MDA-PR-B+ cells and MDA-PR-A+ cells, no significant differences in PR protein levels were detected before and after progestogen treatments (Fig. 3.3.2.1a, b and c).

When the protein levels were set relative to PR-B vehicle (ctrl) = 100%, the PR-A protein levels were significantly higher than PR-B before and after all progestogen treatments (Fig. 3.3.2.1a and d).

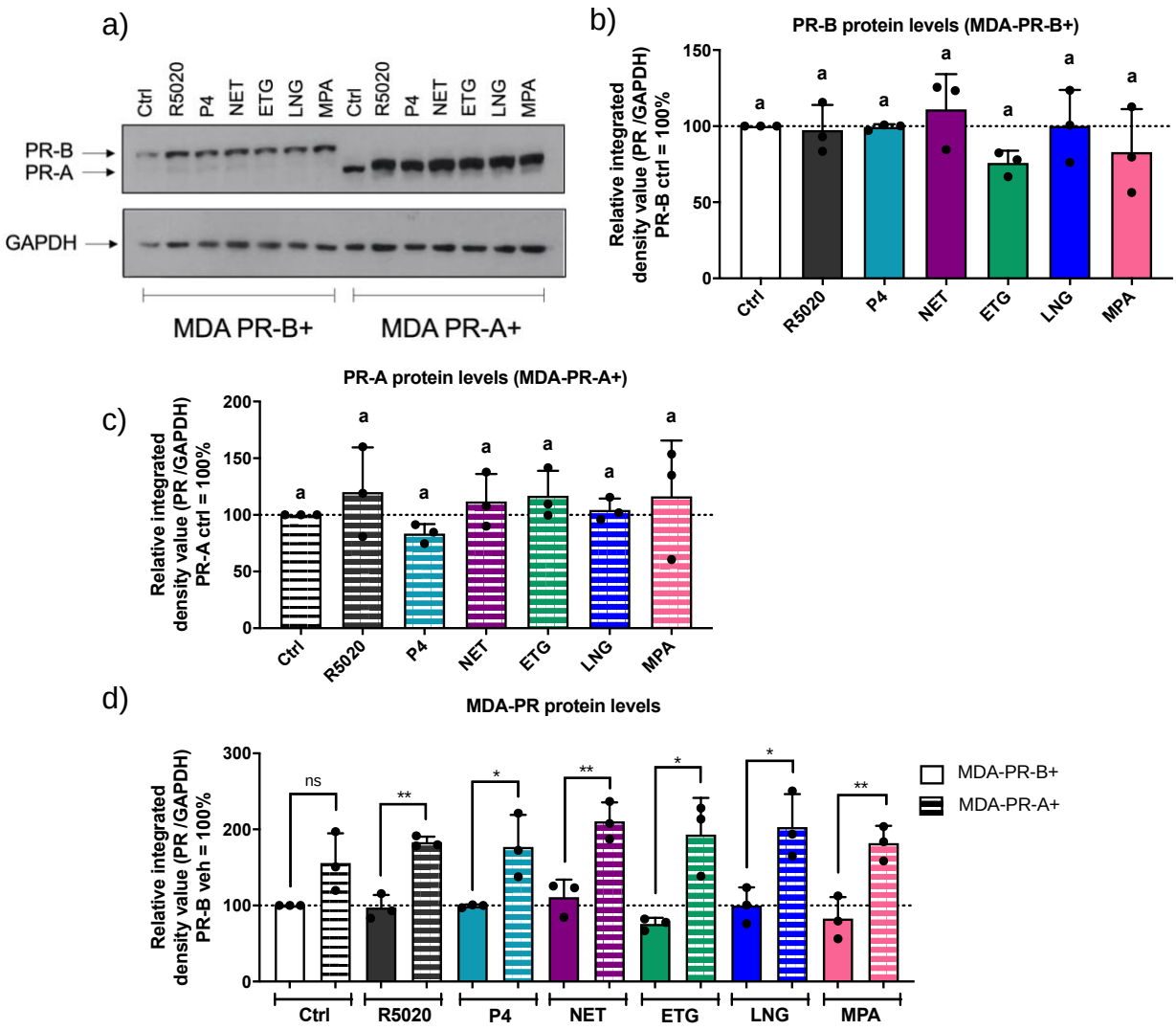

Figure 3.3.2.1: There is significantly more PR-A than PR-B protein in the MDA-MB-231 PR stable cell lines after a 24-hour incubation period with progestogens. Total protein lysates from MDA-PR-B+ and MDA-PR-A+ cells were analysed for PR protein levels by western blotting using GAPDH as a loading control. Blots were scanned and quantified for relative PR levels by calculating integrated density values. Total a) PR-B and b) PR-A protein levels normalised to GAPDH after progestogen treatment, relative to each respective vehicle control (ctrl) = 100%. c) PR protein levels normalised to GAPDH are plotted relative to the PR-B ctrl set to 100%. d) Shows a representative western blot of the PR-B, PR-A and GAPDH protein levels. For a) Shows a representative western blot of the PR-A, PR-B and GAPDH protein levels. b) MDA-PR-B+ cells using TC 1 and c) MDA-PR-A+ cells which were assessed for statistical significance using one-way ANOVA with a Tukey post-test where different letters denote statistically significant differences while the same letters do not. For d) statistical comparisons were carried out using parametric unpaired t-tests to determine significant differences between cell lines for each progestogen where * and ** denote p-values <0.05 and <0.01 respectively while ns indicates no significant difference. The data are pooled from three independent experiments.

3.3.3 Neither progestogen potency nor efficacy via PR-A or PR-B correlate with relative binding affinity

The correlation between published relative binding affinities (RBAs) of the progestogens and the progestogen-induced PR activity was next investigated.

Contrary to what is commonly suggested to be correlated in the field of SR activity (Ronacher et al., 2009), it was shown in Figure 3.3.3.1 that there was no significant correlation between RBAs and the progestogen-induced PR-B or PR-A activity obtained in PR-B exogenously-expressing U2OS cells (TC 1) (Fig. 3.3.3.1a and b), MDA-PR-B+ cells (Fig. 3.3.3.1c and d) or MDA-PR-A+ cells (Fig. 3.3.3.1e and f). For all three cell lines investigated in the present study, there was no correlation between PR -logEC_{50} and RBA or PR efficacy and RBA (Fig. 3.3.3.1).

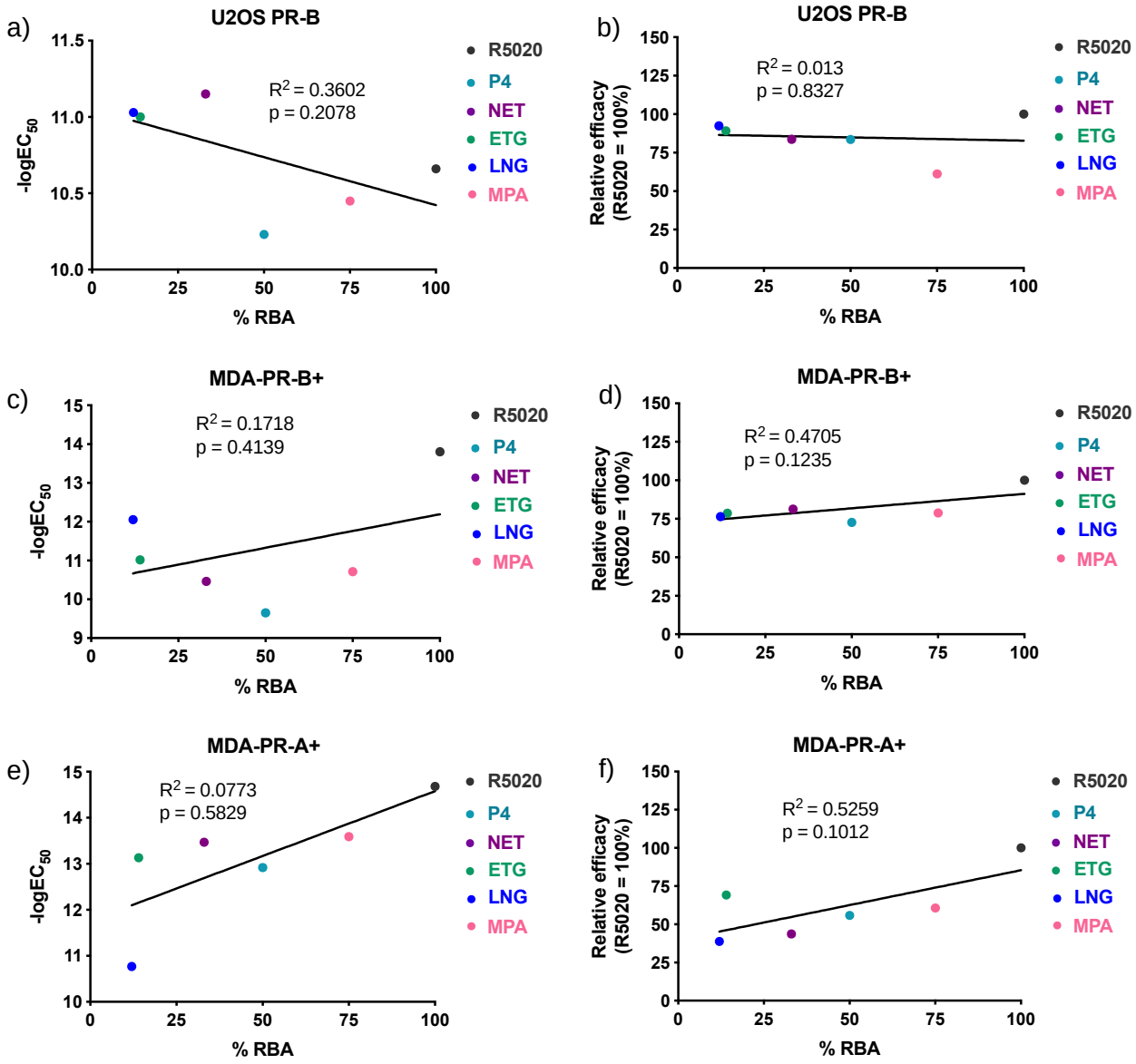

Figure 3.3.3.1: Pearson correlation analyses do not show a significant correlation between relative binding affinity and potency or efficacy for PR-B and PR-A. a), c) and e) Show the Pearson correlation analysis between the relative -logEC_{50} values and % relative binding affinity (RBA) while b), d) and f) show the Pearson correlation analysis between the relative efficacies and % RBA of each progestogen via PR-B in U2OS cells (using TC 1), MDA-PR-B+ cells and PR-A activity in MDA-PR-A+ cells, respectively. The PR data from Figures 3.2.1.1, Fig. 3.2.3.1 and Appendix B, Fig. B5 (relative PR-A R5020 = 100%) are shown for comparative purposes while the RBA values are shown in Table 7.1.1. In the case where a range was given for RBA, the lowest value was selected.

Chapter 4

Progestogen potency via PR-B is negatively correlated to progestogen metabolism

4.1 Background and aims

Having shown that there were differences in potency and efficacy via PR-B between the different progestogens, it was next investigated whether the progestogens are metabolised in these extra-hepatic (U2OS) cells and whether differential progestogen metabolism could contribute to these differences in PR-B potency and efficacy. Metabolism would result in a lower concentration of progestogens. The potential differential degrees of metabolism between progestogens may account, at least in part, for their differential activity via the PRs. The aims of this chapter were therefore to determine 1) if the progestogens were significantly and differentially metabolised in U2OS cells, and 2) if so, does the metabolism of the progestogens correlate to potency and/or efficacy?

UHPSFC-MS/MS was used to determine the concentration of progestogens remaining in the cell culture supernatant after a 24-hour incubation in the presence of U2OS cells. The UHPSFC-MS/MS method required for determining progestogen concentrations was optimised and validated in a previous study (Skosana et al., 2019), of which part of the data is presented in the present study. The lower limit of detection (LOD), lower limit of quantification (LLOQ), precision, accuracy, multiple reaction monitoring (MRM) mass transitions and retention time were all validated as previously described (Skosana et al., 2019) (Appendix A, Table A1).

The relative metabolism of the progestogens was investigated after a 24-hour incubation period in the absence and presence of U2OS cells. 100 nM of each progestogen was incubated in the absence of cells (no-cells) to determine the relative progestogen metabolism in the presence of cells. UHPSFC-MS/MS was then used to

determine the concentration of progestogen remaining in the presence of cells relative to a no-cells control. The concentration of progestogen remaining in the no-cells control was set to 100% and the concentration of the progestogens remaining in the presence of the U2OS cells was calculated relative to that. Thereafter, the % progestogen metabolised was calculated by subtracting the concentration of progestogen remaining (% relative to no-cell control set to 100%) from 100% (i.e. no metabolism).

4.2 Progestogens are differentially metabolised in U2OS cells (extra-hepatic cells)

The data shown in Figure 4.2.1 revealed that of all the progestogens investigated, only P4, NET and MPA were significantly metabolised relative to the no-cells control (Fig. 4.2.1). P4 showed the greatest % metabolism after 24 hours compared to the no-cells control (Fig. 4.2.1). Additionally, all progestogens were metabolised significantly less than P4 (Fig. 4.2.1). Furthermore, MPA was metabolised significantly more than both ETG and LNG (Fig. 4.2.1). Therefore, the progestogen metabolism trend from most to least metabolised was as follows: P4 (79%) > MPA (29.94%) ≥ NET (22.17%) ≥ NES (21.46%) ≥ R5020 (20.55%) ≥ ETG (6.03%) ≥ LNG (3.16%) (Fig. 4.2.1).

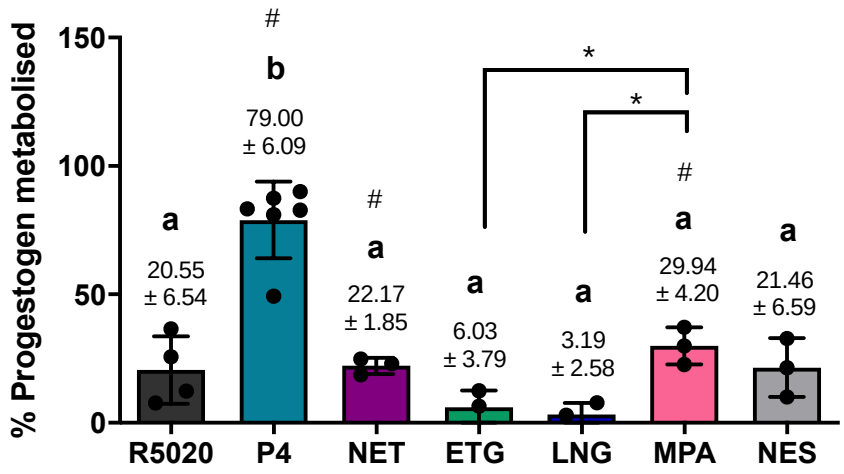

Figure 4.2.1: The endogenous hormone, P4 demonstrates the greatest percentage metabolism, while NET and MPA are also significantly metabolised in U2OS cells. U2OS cells were seeded and after 24 hours, the cells were treated with the ligand at 100 nM or vehicle (0.1% EtOH) for 24 hours. Thereafter the supernatant was harvested, and the MTBE steroid extraction method was followed. The bar graph shows the mean % progestogen metabolised ± SEM which was determined by UHPSFC-MS/MS. Initially, the concentration of progestogen remaining in the no-cells control was set to 100%. Thereafter, the % progestogen metabolised was calculated by subtracting the concentration of progestogen remaining (% relative to no-cell control set to 100%) from 100% (i.e. no metabolism). The data were analysed using one-way ANOVA with a Tukey post-test followed by paired t-tests where different letters indicate statistically significant differences while the same letters denote no significant difference. For the paired t-tests * denotes p-value <0.05 while # denotes significant metabolism relative to no-cells control (0%). The above data show the result of at least three biological repeats, except for P4, which is representative of six biological repeats, each with four technical repeats.

Although it is well established in the literature that the endogenous hormone, P4 is metabolised *in vivo* (Di Renzo et al., 2020, Kamergorodsky et al., 2020, Quinkler et al., 2004, Schumacher et al., 2017, Stanczyk, 2003), the extent to which this occurs is not well-studied. Therefore, a P4 metabolism time-course was performed. U2OS cells were incubated with P4 for increasing incubation times, the supernatants were harvested and the relative metabolism of P4 was investigated after different incubation periods in the absence and presence of U2OS cells.

Figure 4.2.2 shows the metabolism of P4 increased rapidly over time such that after 1.5 hours, already around 50% of the initial P4 (0h) was metabolised which then continued to increase until nearly 80% of the starting amount of P4 was metabolised (Fig. 4.2.2).

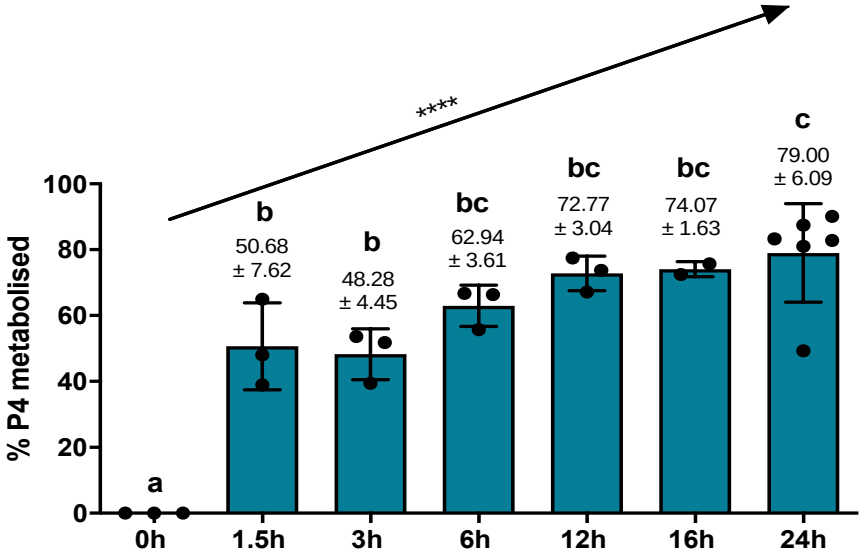

Figure 4.2.2: Time-dependent metabolism of P4 is observed in U2OS cells. U2OS cells were seeded and after 24 hours, the cells and no-cells control, were treated with 100 nM P4 in serum-free media. Thereafter the supernatant was harvested at the respective time-points, and the MTBE steroid extraction method was followed. The bar graph shows the mean % P4 metabolised ± SEM which was determined by UHPSFC-MS/MS. Initially, the concentration of P4 remaining in the no-cells control was set to 100%. Thereafter, the % metabolism was calculated by subtracting the concentration of P4 remaining (% relative to no-cell control set to 100%) at each P4 at time point from 100% (i.e. no metabolism). The data shown are representative of three biological repeats, except for 24h, which is representative of six biological repeats, each with four technical repeats of each condition. The data were analysed using one-way ANOVA with a Tukey post-test where different letters indicate statistically significant differences while the same letters denote no significant difference, followed by a linear trend post-test where **** denotes p-value <0.0001.

4.3 Progestogen-induced PR potency is negatively correlated to progestogen metabolism

Next, the Pearson correlation analysis was performed to determine whether progestogen metabolism correlated to either the progestogen -logEC_{50} values or efficacies via PR-B. The PR-B responses determined in U2OS cells (Fig. 3.2.1.1) were compared for correlation to the metabolism results obtained in Figure 5.1.2. As shown in Figure 4.3.1, a negative correlation was seen between the progestogen -logEC_{50} values and metabolism with an R^2 value of 0.6695 and a p-value of 0.0466 (Fig. 4.3.1a). However, no correlation was found between progestogen efficacy and metabolism with an R^2 value of 0.0756 and a p-value of 0.5978 (Fig. 4.3.1b).

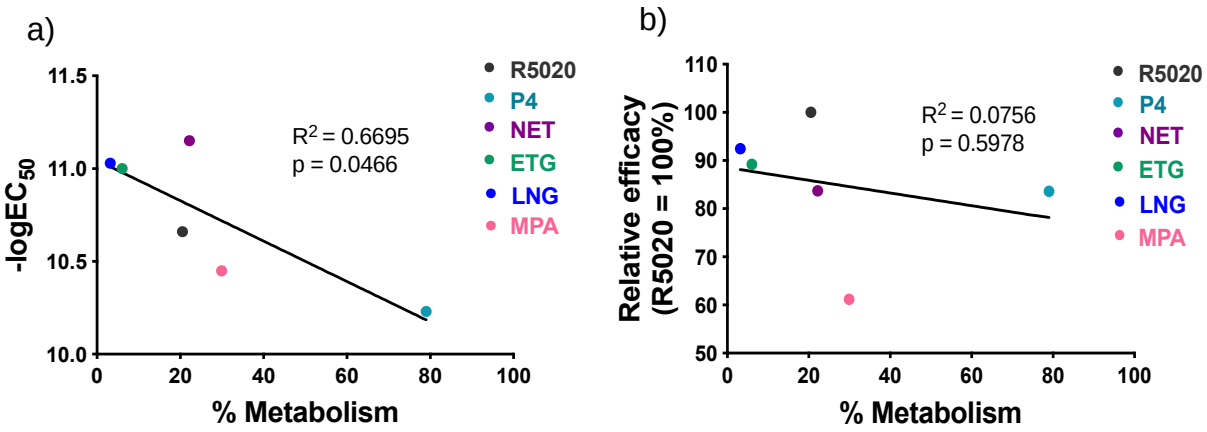

Figure 4.3.1: Pearson correlation analysis shows a significant negative correlation between metabolism and potency and no correlation between metabolism and efficacy in U2OS cells. Data obtained in Fig. 3.2.1.1 and Fig. 4.2.1 are shown for comparative purposes. a) Shows the Pearson correlation analysis between the relative -logEC_{50} values and % metabolism while b) shows the Pearson correlation analysis between the relative efficacies and % metabolism of each progestogen.

These data show that the greater the metabolism of a progestogen, the less potent the progestogen response will be via PR-B. However, the amount of metabolism does not correlate to the efficacy of a progestogen via PR-B.

Having shown that progestin metabolism negatively correlates with progestin potency, it was next investigated whether inhibiting P4 metabolism influenced the P4 response via PR-B and more specifically, whether P4 becomes more potent via PR-B when metabolism of P4 is inhibited. This was done by incubating the MDA-PR-B+ cells with 4-Carboxy-2' 4'-Dinitrophenylamine (DNPN) that has previously been shown to inhibit the primary enzyme responsible for P4 metabolism, AKR1C1 (Byrns & Penning,

2009). Using DNPN to inhibit P4 metabolism by targeting AKR1C1 had not been investigated prior to the present study. Before investigating the effect of DNPN on P4 transactivation via PR-B, it first needed to be verified that by inhibiting the primary enzyme responsible for P4 metabolism, P4 metabolism would be inhibited in MDA-PR-B+ cells.

Initially, increasing concentrations of DNPN were investigated to determine their effects on cell viability. 100 µM – 500 µM DNPN had no significant effect on cell viability after a 24-hour incubation period (Appendix B, Fig. B6). It was therefore decided to use 500 µM DNPN to investigate P4 metabolism inhibition. As shown in Figure 4.3.2, 97.97% metabolism of P4 was seen in MDA-PR-B+ cells after a 24-hour incubation period (Fig. 4.3.2). In the presence of the P4 metabolism enzyme inhibitor, DNPN, the total P4 metabolism dropped from 97.97% to 43.59% after 24 hours (Fig. 4.3.2). Therefore, the effect of P4 metabolism on the P4 transactivation response via PR-B was investigated in the MDA-PR-B+ cell line.

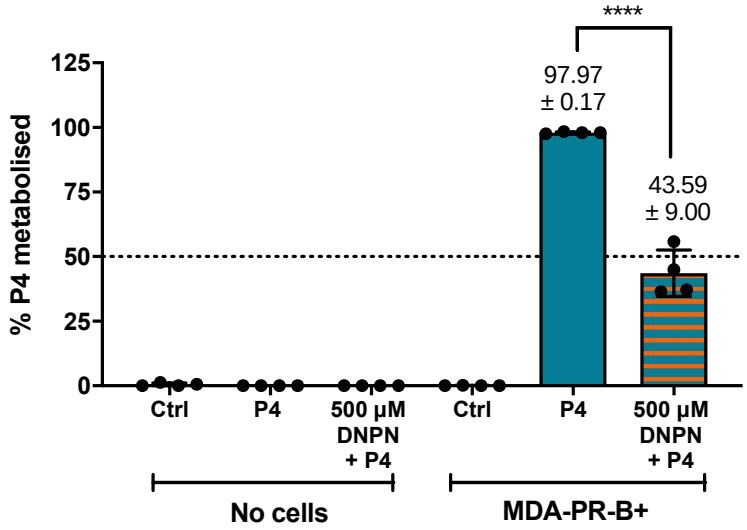

Figure 4.3.2: Using 4-Carboxy-2' 4'-Dinitrophenylamine (DNPN) to target the enzyme, AKR1C1, results in 54.58% reduction in P4 metabolism in MDA-PR-B+ cells. Cells were seeded and after twenty-four hours, the cells were treated with either 500 µM DNPN or vehicle/ctrl (0.1% DMSO) for 2 hours. Thereafter, the cells were treated with 100 nM P4 with either 500 µM DNPN or vehicle/ctrl (0.1% DMSO and 0.1% ethanol) for 24 hours. The supernatant from each well was then harvested and the MTBE steroid extraction method was performed. In parallel the MTT cell viability assay was performed. The bar graph shows the mean % P4 metabolised ± SEM which was determined by UHPSFC-MS/MS and calculated as the difference between no-cells control (set to 100%) and the % P4 remaining after 24 hours in the presence of MDA-PR-B+ cells. The data were analysed using paired t-tests with **** denoting p-value < 0.0001. The SEM of the above data is calculated based on four of biological repeats each containing three technical repeats of each condition.

Next, a P4 promoter-reporter dose response assay was performed in the absence or presence of DNPN and the resultant PR-B biocharacter was assessed. Consistent with the correlation analysis showing no correlation between metabolism and efficacy (Fig. 4.3.1), Figure 4.3.3a shows that relative to the P4 response in the absence of DNPN, the P4 maximum response in the presence of DNPN was not affected and resulted in a full agonist response of P4 via PR-B. Furthermore, as predicted by the negative correlation analysis between metabolism and potency, when preventing P4 metabolism with DNPN, the P4 + DNPN curve appeared to be left-shifted (i.e. more potent) compared to the P4 curve in the absence of DNPN (Fig. 4.3.3a). However, when the -logEC_{50} values were statistically assessed, no significant difference was detected between the two treatments although the difference approached significance (p-value = 0.073) (Fig. 4.3.3b). No significant difference was detected in cell viability for all conditions tested as indicated by the MTT cell viability assay (Fig. 4.3.3d). Therefore, any changes seen in the PR-B transactivation response in the absence and presence of DNPN were not attributed to changes in cell viability.

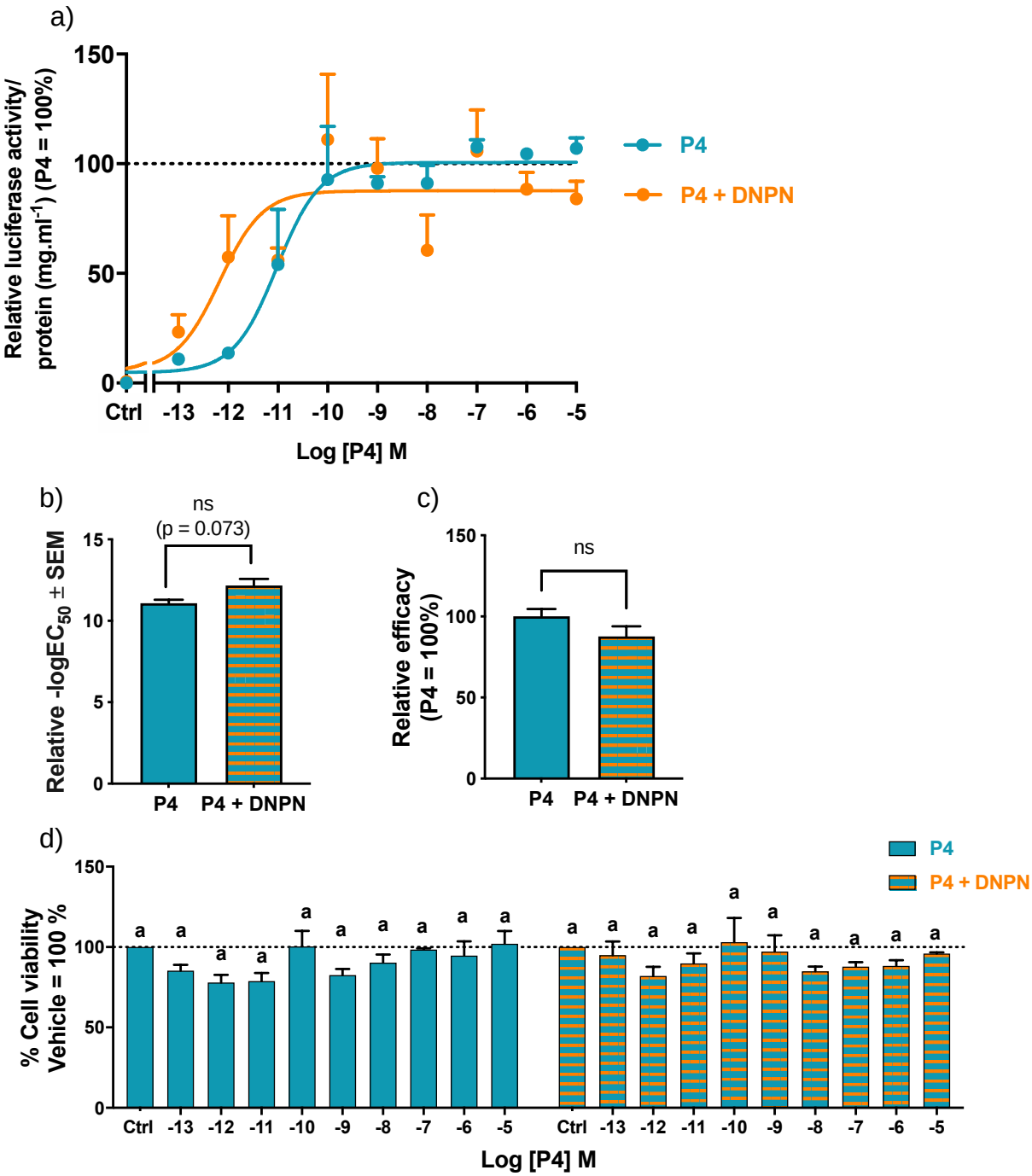

Figure 4.3.3: The P4 dose response curve appears to be left-shifted in the presence of 4-Carboxy-2' 4'-Dinitrophenylamine (DNPN) in MDA-PR-B+ cells. MDA-PR-B+ cells were seeded and after 24 hours, the cells were transiently transfected with 9 µg 2XPRE-E1b-luc reporter plasmid. Twenty-four hours later, the cells were re-seeded into 96-well tissue culture plates and allowed to adhere overnight. After 24 hours, the cells were treated with either 500 µM DNPN or vehicle/ctrl (0.1% DMSO) for 2 hours. Thereafter, the cells were treated with increasing concentrations ($1.0X10^{-13}$ M – $1.0X10^{-5}$ M) of P4 alone or in the presence of 500 µM DNPN for 24 hours. Twenty-four hours later, the cells were harvested and

the Luciferase and Bradford assays were performed. Additionally, a parallel MTT cell viability assay was performed. a) Shows the % PR-B activity at increasing concentrations of each ligand relative to P4 only efficacy = 100%. b) Shows the mean -logEC_{50} values relative to P4 only ± SEM for each condition and c) shows the mean efficacies of P4 under each condition relative to P4 only ± SEM. d) Shows the % cell viability after each treatment. Relative -logEC_{50} values and efficacies were analysed using paired t-tests where ns indicates no significant difference. The MTT data were analysed by Two-way ANOVA with a Tukey post-test where different letters indicate statistically significant differences while the same letters denote no significant difference. The SEM of the above data is calculated based on three of biological repeats each containing three technical repeats of each condition.

Taken together, the data shown in this section reveal that the metabolism of P4 increased rapidly over a 24-hour period in U2OS cells which provides evidence that the use of P4 as the reference ligand for PR activity may not be appropriate. Of the progestogens investigated, P4, NET and MPA demonstrated significant metabolism in U2OS cells after 24 hours. Additionally, progestogen metabolism negatively correlated to -logEC_{50} values, but not efficacies, of progestogens via PR-B. Moreover, P4 metabolism inhibition data were consistent with the correlation data in terms of efficacy such that even though metabolism is inhibited by nearly 54%, there is still no significant change in efficacy via PR-B. The difference in P4 potency via PR-B in the absence compared to the presence of DNPN approached significance, as predicted by the progestogen metabolism and potency correlation data.

Chapter 5

Maraviroc, Tenofovir disoproxil fumarate and Dapivirine, activate PR-B in the absence of progestogens

5.1 Background and aims

Antiretroviral therapy has slowed the HIV/AIDS pandemic and is currently being used as a prophylactic measure for individuals at high risk of infection (Frank et al. 2017). However, concerns over adverse effects of long-term use need to be explored (Deeks et al. 2011). These adverse effects may occur, at least in part, through off-target SR effects.

In this section the primary aim was to investigate the effects of MVC, TDF, and DPV on PR-B transcriptional activity in the absence and presence of progestogens (P4 and LNG). The chemical structure of the ARVs differ vastly from each other and compared to P4 (Appendix B, Fig. B8). An additional aim was to determine the mechanism by which the ARVs alter the PR-B response. Part of the data shown in this chapter has been used in a publication by the present author (Enfield et al., 2020a).

The role of the ARVs on PR transactivation was investigated by promoter-reporter assays in either U2OS cells transiently transfected to express either PR-A or PR-B or in MDA-PR-B+ cells. Furthermore, the endogenous PR-regulated gene responses in the presence of ARVs alone or in combination with a progestogen were investigated by real-time qPCR in MDA-PR-B+ cells. The mechanisms investigated were effects of ARVs on direct ligand binding to PR-B, changes in PR-B protein expression levels and changes in PR-B phosphorylation at Ser294.

5.2 MVC, TDF and DPV activate PR-B in the absence of progestogens

The transcriptional activity of TDF and DPV via PR-B was initially investigated using promoter-reporter assays in U2OS cells exogenously expressing PR-B. P4 and LNG were selected to investigate combination treatments since P4 is in the endogenous hormone while LNG is being considered for use in multipurpose prevention technologies.

As shown is Fig. 5.2.1a, TDF significantly increased the potency of the P4 response via PR-B (Fig. 5.2.1a and d), while the efficacy of P4 via PR-B was not significantly affected (Fig. 5.2.1e). Unexpectedly, in the absence of P4 (Ctrl), TDF increased reporter activity in a PR-B specific manner since the increase in reporter activity was not seen in the absence of PR-B (Fig. 5.2.1a and c). Figure 5.2.1c shows that TDF alone activated PR-B with a response ~ 50% as efficacious as 100 nM P4 while DPV alone did not activate PR-B. DPV on the other hand, had no effect on both the potency (Fig. 5.2.1b and f) and efficacy (Fig. 5.2.1g) of LNG via PR-B, nor did it activate the PR-B in the absence of progestogens (Fig. 5.2.1c).

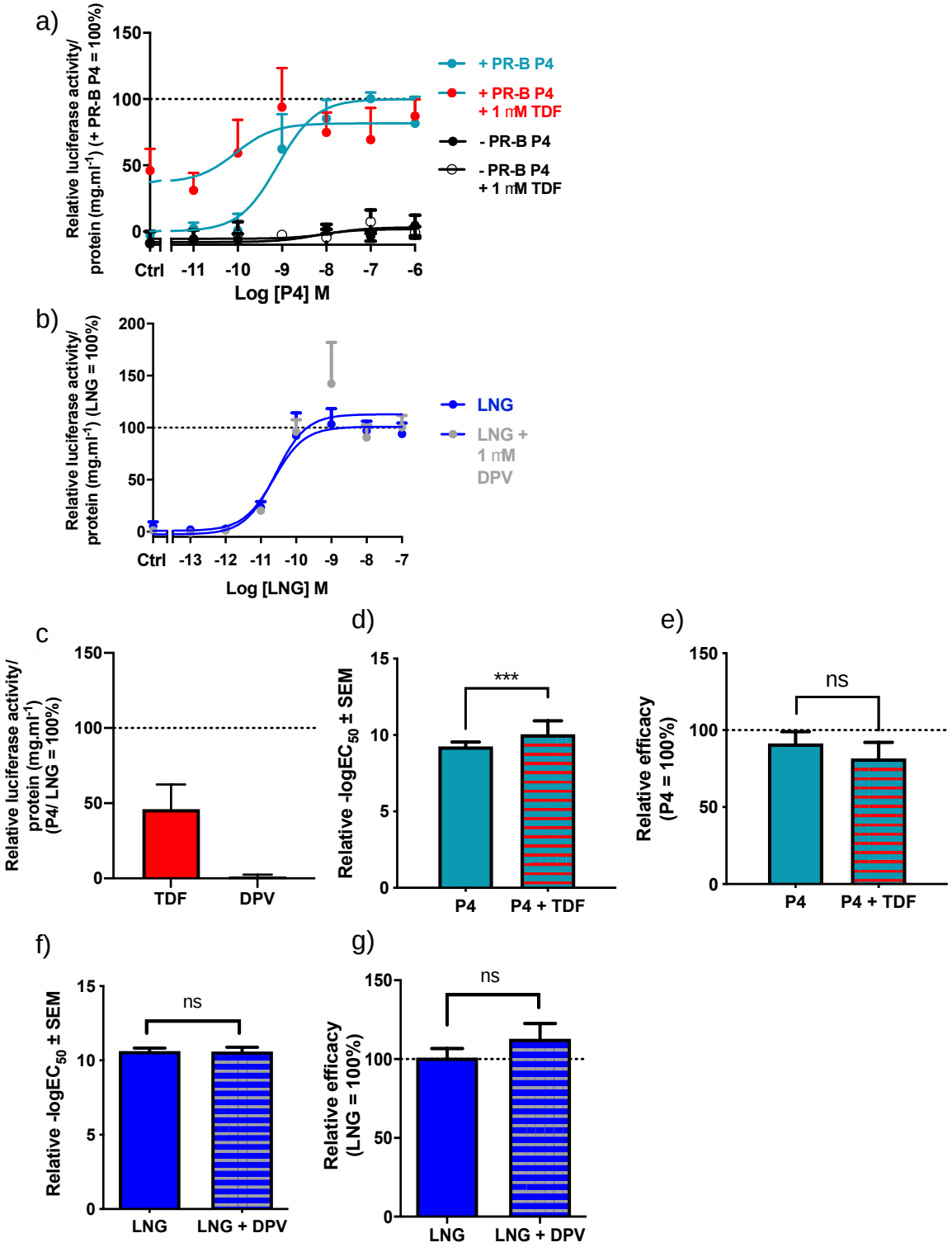

Figure 5.2.1: TDF and not DPV activates PR-B in the absence of progestogens in U2OS cells. U2OS cells were seeded and after 24 hours, the cells were transiently transfected with 900 ng pSG5hPR-B and 9 µg 2XPRE- E1b-luc reporter plasmid. Twenty-

four hours later, the cells were re-seeded into a 96-well tissue culture plates and allowed to adhere overnight. After 24 hours, the cells were treated with increasing concentrations ($1.0X10^{-11}$ M – $1.0X10^{-6}$ M) of P4 or LNG ($1.0X10^{-13}$ M – $1.0X10^{-7}$ M) and 0.1% DMSO (vehicle for the ARVs) or 1 µM TDF or DPV for 24 hours. Thereafter, the cells were harvested and the Luciferase and Bradford assays were performed. a) Shows % PR-B activity at increasing concentrations of P4 in combination with TDF relative to P4 efficacy = 100% while b) Shows % PR-B activity at increasing concentrations of LNG in combination with DPV relative to LNG efficacy = 100%. c) Shows the % PR-B activity in the presence of the ARVs alone relative to the respective progestogen. d) & f) Show the mean relative -logEC_{50} values for each condition while e) & g) show the mean efficacies ± SEM of each ligand relative to P4 or LNG efficacy = 100%. The data were analysed using paired t-tests with *** denoting p-value <0.001, while ns indicates no significant difference. The SEM of the above data is calculated based on four biological repeats, each containing three technical repeats of each condition.

A second cell line (MDA-PR-B+) was then used to investigate whether the results seen in U2OS cells were cell-specific. PR-B activity in the presence of TDF, DPV and additionally, MVC, in the absence and presence of LNG, was next investigated.

Similar to the results obtained in U2OS cells, Figure 5.2.2 shows that TDF and additionally MVC, but not DPV were able to activate PR-B in the absence of LNG (Ctrl) in MDA-PR-B+ cells (Fig. 5.2.2a and b). For the combination treatments, when assessed statistically, there was no significant difference in -logEC_{50} values for LNG alone and LNG in combination with DPV (Fig. 5.2.2c). As in the U2OS cells, there was however, a significant increase in the -logEC_{50} values for LNG alone compared to those observed with TDF in combination with LNG (p-value <0.01) and similarly with MVC in combination with LNG (p-value <0.05) (Fig. 5.2.2c).

In terms of efficacy, a similar trend was observed. As shown in Figure 5.2.2d, LNG in combination with either TDF or MVC resulted in a significantly higher efficacy compared to LNG alone via PR-B. There was no significant difference in efficacy between LNG alone and LNG in combination with DPV via PR-B (Fig. 5.2.2d).

Taken together, these data suggest that the LNG response via PR-B is significantly more potent and efficacious when in the presence of TDF or MVC but not DPV.

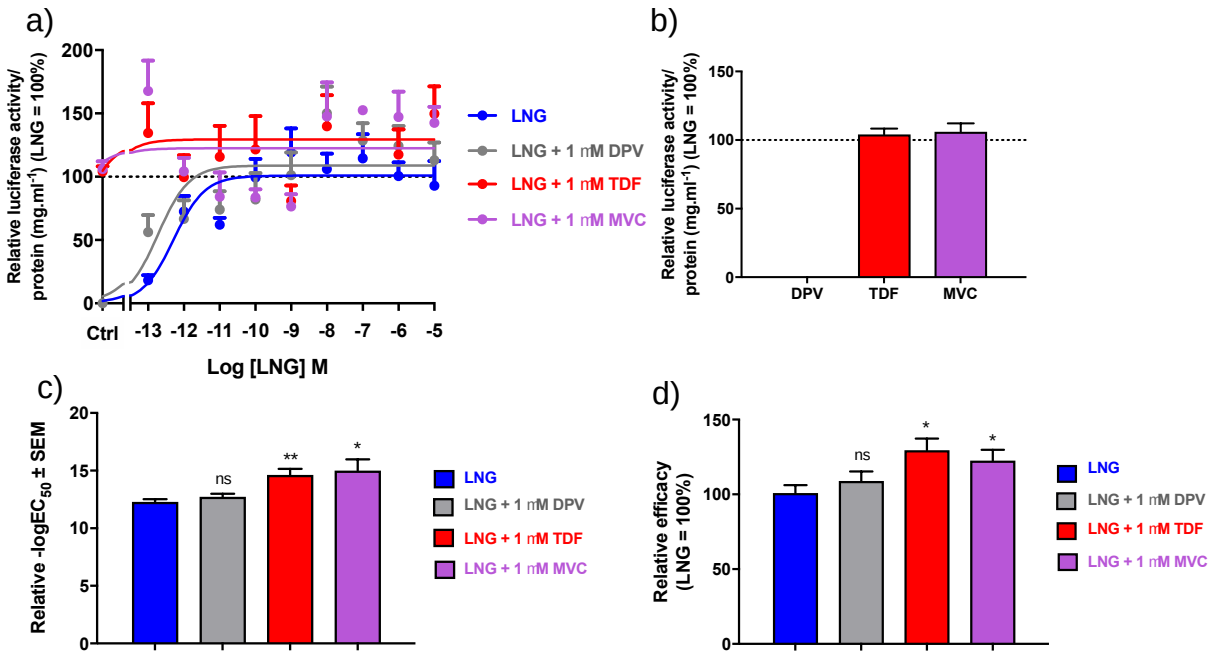

Figure 5.2.2: The ARVs, MVC and TDF, activate PR-B in the absence of LNG and potentiate the LNG-induced PR-B response. MDA-PR-B+ cells were seeded and after 24 hours, the cells were transiently transfected with 9 µg 2XPRE-E1b-luc reporter plasmid. Twenty-four hours later, the cells were re-seeded into a 96-well tissue culture plates and allowed to adhere overnight. After 24 hours, the cells were treated with increasing concentrations ($1.0X10^{-14}$ M – $1.0X10^{-5}$ M) of LNG and 0.1% DMSO (ARV vehicle) or 1 µM ARV for 24 hours. "Ctrl" indicates 0.1% DMSO + 0.1% EtOH or 0.1% EtOH + 1 µM ARV (combination treatment). Thereafter, the cells were harvested, and the Luciferase and Bradford assays were performed. a) Shows % PR-B activity at increasing concentrations of LNG in combination with 1 µM ARV relative to LNG efficacy = 100%. b) Shows the % PR-B activity of the ARVs alone relative to LNG efficacy = 100%. c) Shows the mean relative -logEC_{50} values for each condition while d) shows the mean efficacies ± SEM of each ligand relative to LNG efficacy = 100%. The data were analysed using paired t-tests with * and ** denoting p-value <0.05 and <0.01 respectively, while ns indicates no significant difference. The SEM of the above data is calculated based on four biological repeats each containing three technical repeats of each condition.

Next, the ARV responses via PR-B were investigated on endogenous genes. *Ptgs2* and *gilz* were chosen as examples as endogenous genes previously shown to be activated by the PR by others (Park et al., 2020) and in this thesis. *Il-6* was chosen as a transrepression model of PR activity. The *il-6* promoter contains binding elements for AP-1 and it has been shown previously that the PR can tether and interact with AP-1 (Cicatiello et al., 2004, Dinh et al., 2019, Flaqué et al., 2013).

As shown in Figure 5.2.3, real-time qPCR experiments revealed that, in agreement with the promoter-reporter assay in Figure 5.2.2, TDF treatment alone, was able to increase the mRNA levels of two PR-regulated genes (*ptgs2* and *gilz*) to similar extents as the PR agonists, LNG and NET (Fig. 5.2.3a and b). MVC alone was also able to upregulate both genes (1.23- and 1.78-fold, respectively) (Fig. 5.2.3a and b). Contrary to the results obtained in the promoter-reporter assays, DPV treatment alone was also able to upregulate mRNA levels of these two endogenous genes (Fig. 5.2.3a and b). When the ARVs were treated in combination with LNG, none of them potentiated the LNG response, contrary to what was observed for TDF and MVC in combination with LNG on the promoter-reporter assays (Fig. 5.2.3a and b).

In terms of transrepression, the progestins LNG and NET both resulted in a decrease in *il-6* mRNA levels (Fig. 5.2.3c). When treated with the ARVs alone, only TDF resulted in a decrease in *il-6* mRNA levels while DPV and MVC did not result in any significant changes compared to vehicle (Fig. 5.2.3c). When *il-6* expression was investigated in the presence of the ARVs in combination with LNG, all combination treatments resulted in a significant decrease in *il-6* mRNA levels compared to vehicle; however, this decrease was not significantly different to the response with LNG alone (Fig. 5.2.3c).

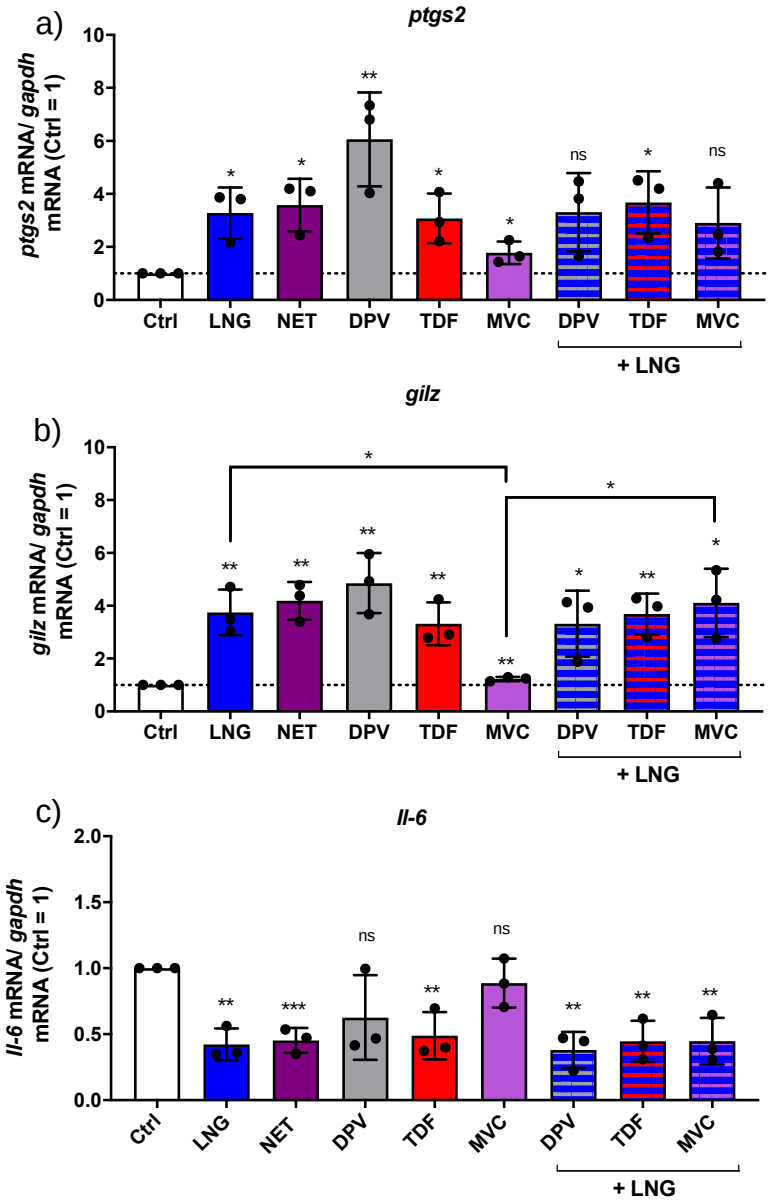

Figure 5.2.3: Three PR-regulated genes are transactivated or transrepressed by TDF alone while *ptgs2* and *gilz* are additionally transactivated by DPV and MVC. MDA-PRB+ cells were seeded and after 24 hours, the cells were treated with 100 nM progestin, 1 µM ARV alone or in combination with 100 nM LNG or vehicle/ctrl (0.1% DMSO and 0.1% ethanol) for 24 hours. Thereafter the cells were harvested in Trizol. RNA was extracted and cDNA was synthesized from 250 ng RNA then used in real time qPCR. Relative mRNA levels of a) *ptgs2*, b) *gilz* and c) *il-6* were normalized to *gapdh* mRNA levels ± SEM. Relative expression was determined by normalising to vehicle/ctrl set to 1. Relative fold-induction was analysed using paired t-tests with *, **, *** denoting p-value <0.05, <0.01, <0.001 respectively, while ns indicates no significant difference. The SEM of the above data is calculated based on three biological repeats.

Taken together, the data in this chapter suggest that the ARVs, TDF and MVC can activate PR-B in the absence of progestogens as shown on a promoter-reporter

response in two different cell lines, and consistent with endogenous gene responses. Additionally, the results suggest that while DPV can activate the PR-B in a manner that allows regulation of a PRE promoter-reporter gene, this does not affect levels of an endogenous PR-regulated gene. For the transrepression gene, only TDF was able to repress *il-6* mRNA levels in the absence of the progestogen. This suggests that in general, the LNG-independent ARV response for transrepression may not be as sensitive as transactivation and additionally, this may be ARV-specific. Furthermore, these data show that the activity of LNG via PR-B is not affected by the presence of the ARVs on endogenous gene responses, since there was no significant difference between the LNG alone and the combination treatment for all three genes that were investigated.

5.3 The ARVs appear to activate PR-B via different mechanisms

Having established that the ARVs can induce PR-B mediated transactivation on a reporter gene and/or an endogenous gene, the mechanism behind this action was next investigated. Competitive whole-cell binding was used to investigate the effect of ARVs on direct binding of P4 to the PR in U2OS cells transiently transfected to express either PR-A or PR-B. Binding of R5020 and LNG was also investigated as a positive control. U2OS cells were used because the conditions for investigating progestogen binding to the PR using this assay had previously been optimised in these cells by the candidate (data not shown).

Figure 5.3.1 shows that there was background ligand binding of both R5020 and LNG in the absence of expressed PR; however, binding of both these progestogens was significantly higher in the presence of PR-A and PR-B (Fig. 5.3.1). As expected, R5020 and LNG competed for binding of P4 to both PR-A and PR-B (Fig. 5.3.1). Interestingly, all the ARVs competed for binding of P4 to PR-A while only DPV competed for binding to PR-B.

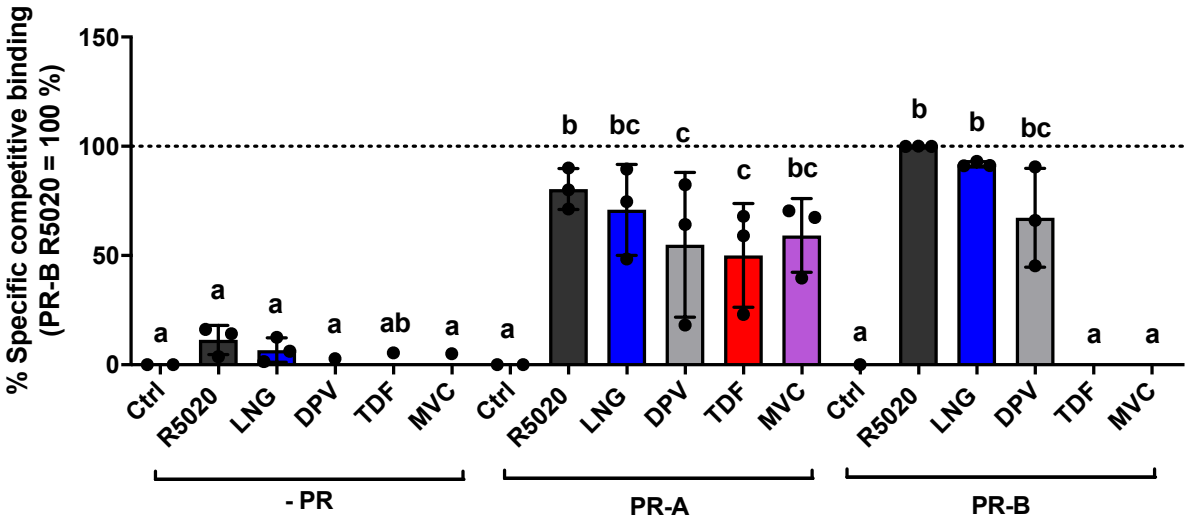

Figure 5.3.1: Whole cell binding of select progestogens and ARVs to PR-B in U2OS cells. The mean specific competitive binding (SB) was determined after a 3-hour incubation in the presence of 40nM [^{3}H]-P4 in the absence and presence of unlabelled competitor progestogens or ARVs. The U2OS cells were seeded into 24-well tissue culture plates and after 24 hours, each well was transiently transfected with 250 ng pcDNA vector (-PR), the pSG5hPR-A vector (PR-A) or the pSG5hPR-B vector (PR-B). The cells were incubated with 40nM ^{3}[H]-P4 in the absence or presence of the progestogens; R5020 and LNG at 1 µM, and the ARVs; DPV, TDF and MVC at 10 µM. "Ctrl" indicates 0.1% DMSO + 0.1% EtOH. The bar graph shows the mean ± SEM SB calculated as the difference between total binding (TB) and non-specific binding (NSB). The data were analysed using two-way ANOVA with a Tukey post-test followed by paired t-tests where different letters denote statistically significant differences while the same letters denote no significant difference. The SEM is calculated based on three independent experiments where each condition consisted of three technical repeats.

Next, since total SR protein levels affect the resultant SR activity, total PR protein levels were investigated after 3 hours of treatment with 100 nM R5020, LNG or 1 µM DPV, TDF or MVC. Additionally, because phosphorylation is another mechanism by which PR activity is regulated, the degree of PR phosphorylation at Ser294 was also investigated (Treviño & Weigel, 2013).

There were no significant changes in total PR-A and PR-B protein levels for all treatments investigated (Fig. 5.3.2a, b, and c). As expected, there was, however, a significant increase in both PR-A and PR-B phosphorylation upon stimulation with R5020 and LNG (Fig. 5.3.2a, b and d). Interestingly, the amount of PR-B phosphorylation for both progestins was significantly higher than that seen for PR-A (Fig. 5.3.2d). None of the ARVs resulted in significant changes in phosphorylation of

PR-A (Fig. 5.3.2a, b and d). However, TDF treatment resulted in a significant increase in PR-B phosphorylation compared to vehicle (Fig. 5.3.2b and d).

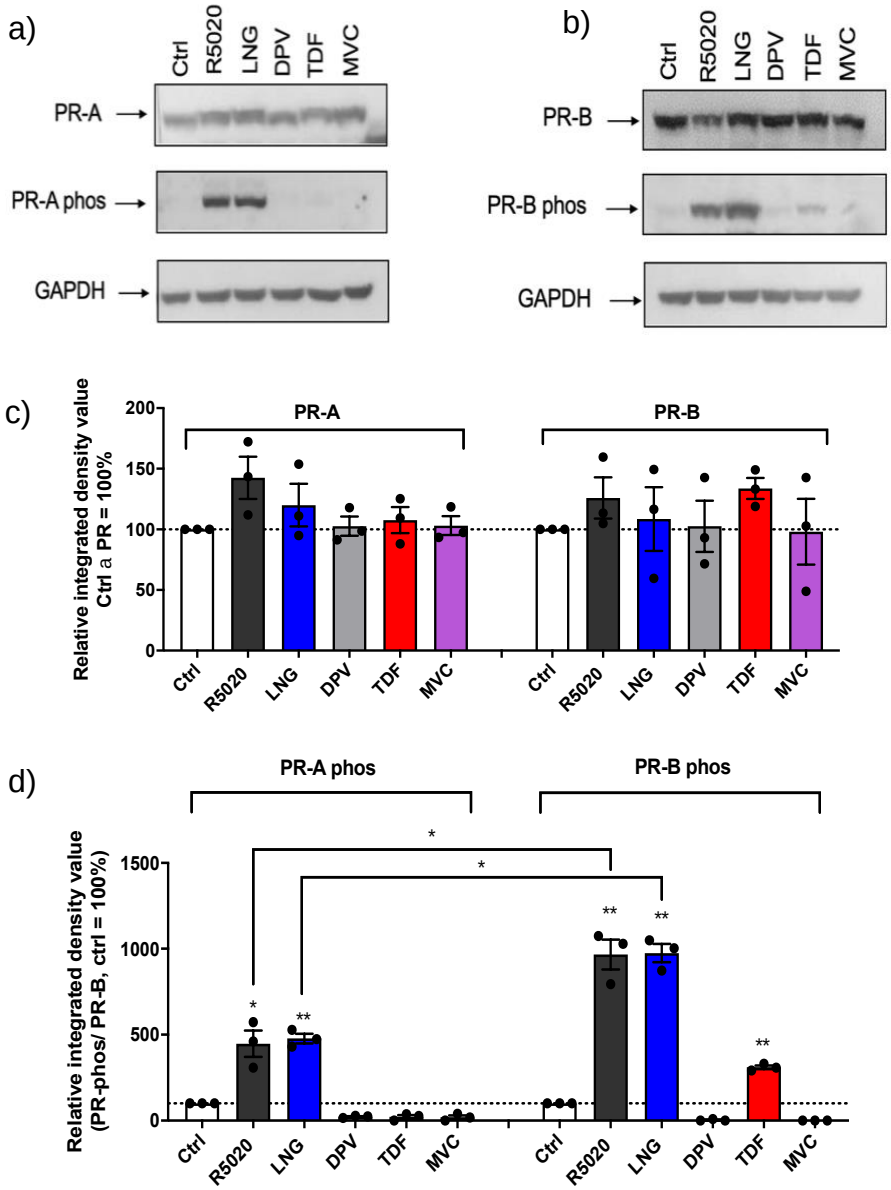

Figure 5.3.2: Three hours of treatment with R5020, LNG and TDF result in PR-B phosphorylation. MDA-PR-B+ and MDA-PR-A+ cells were seeded and after 24 hours, the cells were treated with 100 nM R5020, LNG or 1 µM ARV or ctrl (0.1% DMSO and 0.1% EtOH) for 3 hours. Thereafter, the cells were harvested, and a western blot was performed. a) & b) Representative western blots are shown for PR-A, PR-B, and PR phosphorylation, respectively. c) Shows the total PR-A and PR-B protein levels ± SEM relative to each ctrl = 100%. d) Shows the percentage phosphorylation for PR-A and PR-B normalised to total PR levels ± SEM relative to each ctrl = 100%. Relative protein levels were analysed using paired t-tests with * and ** denoting p-value <0.05 and <0.01, respectively. The SEM of the above data is calculated based on three biological repeats.

A summary of the data shown in this chapter is shown in Table 5.3.1 and suggests that even though TDF and MVC induced PR-B-mediated transcription on a reporter gene as well as endogenous genes, these ARVs appear to target PR-B using different mechanisms.

MVC and TDF both do not bind directly to the binding site of PR-B and TDF appears to activate PR-B by increasing PR-B phosphorylation, while MVC does not. DPV competes for binding with agonist to PR-B, but it did not increase PR phosphorylation at Ser294 and only induced PR-B mediated upregulation of endogenous genes but not of the reporter gene. It is possible that in the presence of ARVs, there may be multiple mechanisms at play resulting in PR activation.

Table 5.3.1: Summarised table of the ARV effects on PR activity determined in the present study. The data summarised below are presented in sections 5.2 and 5.3.

	TDF	DPV	MVC
Increases reporter gene expression	✓	-	✓
Increases mRNA endogenous gene (upregulated by progestogens)	✓	✓	✓
Decreases mRNA endogenous gene (downregulated by progestogens)	✓	-	-
Decreases binding of P4 to PR-A	✓	✓	✓
Decreases binding of P4 to PR-B	-	✓	-
Increases Ser294 phosphorylation of PR-A	-	-	-
Increases Ser294 phosphorylation of PR-B	✓	-	-

Chapter 6

GR inhibits PR-B activity

6.1 Background and aims

There is increasing evidence emerging from the literature which suggests that SRs can influence each other's activity. This has been shown for the ER which inhibits the MR (Mueller et al., 2014), the MR which enhances GR responses (Rivers et al. 2019) and the AR which inhibits the GR (Xie et al. 2015) to name a few. However, little is known about the interaction between the ubiquitously expressed GR, the target of glucocorticoids (GCs) which initiate a cascade of many biological responses and PR-B, the target of progestins used in female hormonal contraceptives (HCs) and hormone replacement therapies (Ogara et al., 2019). This is particularly important because many women simultaneously use HCs to prevent unwanted pregnancy as well as GCs to combat inflammatory conditions. Moreover, given that the GR is ubiquitously expressed, it is likely that PR-B and GR co-exist in cells.

The aim of the next chapter was to investigate whether the GR influences PR-B activity when treated with GR-specific or PR-specific ligands by promoter-reporter assays and real-time qPCR. Additionally, a PCR array was performed to determine if the effect of the GR on PR-B activity on endogenous genes was gene-specific. Lastly, the mechanism by which the modulation of the GR on PR-B was brought about was investigated by co-immunoprecipitation assays as well as PR-phosphorylation at Ser294. Two model systems were used, U2OS cells exogenously expressing PR-B as well as the MDA-PR-B+ cell line. Both cell lines were treated with SR-specific siRNA to knockdown either the GR (U2OS and MDA-PR-B+) or PR-B (MDA-PR-B+). The cells were treated with SR-specific ligands to generate responses via the respective SR only.

6.2 Changing GR or PR-B levels affects efficacy but not potency of SR-specific ligands

Promoter-reporter assays were initially used to investigate whether by changing GR levels relative to PR-B levels using GR-specific siRNA, the PR-B response to NET or P4 on a reporter gene is altered. Dose response analysis revealed that in agreement with Figure 3.2.1.1, in U2OS cells which express endogenous GR and were transiently transfected to exogenously express PR-B, NET and P4 were full agonists via PR-B (NSC) (Fig. 6.2.1a). When these cells were treated with GR-specific siRNA (GR-KD), the efficacy significantly increased for both NET and P4 (Fig. 6.2.1a and c). However, no significant change was detected in the -logEC_{50} values (Fig. 6.2.1b). A mock (using water instead of siRNA) condition was also investigated in parallel to ensure that the siRNA treatment was not affecting the cell responses (mock) (Fig. 6.2.1a) and there were no significant differences in -logEC_{50} values and efficacies between NSC and mock (Appendix B, Fig. B7). Figures 6.2.1d and e both show that GR knockdown was successful with a reduction in GR expression levels of ~ 50% while PR-B levels were unaffected by the GR siRNA treatment.

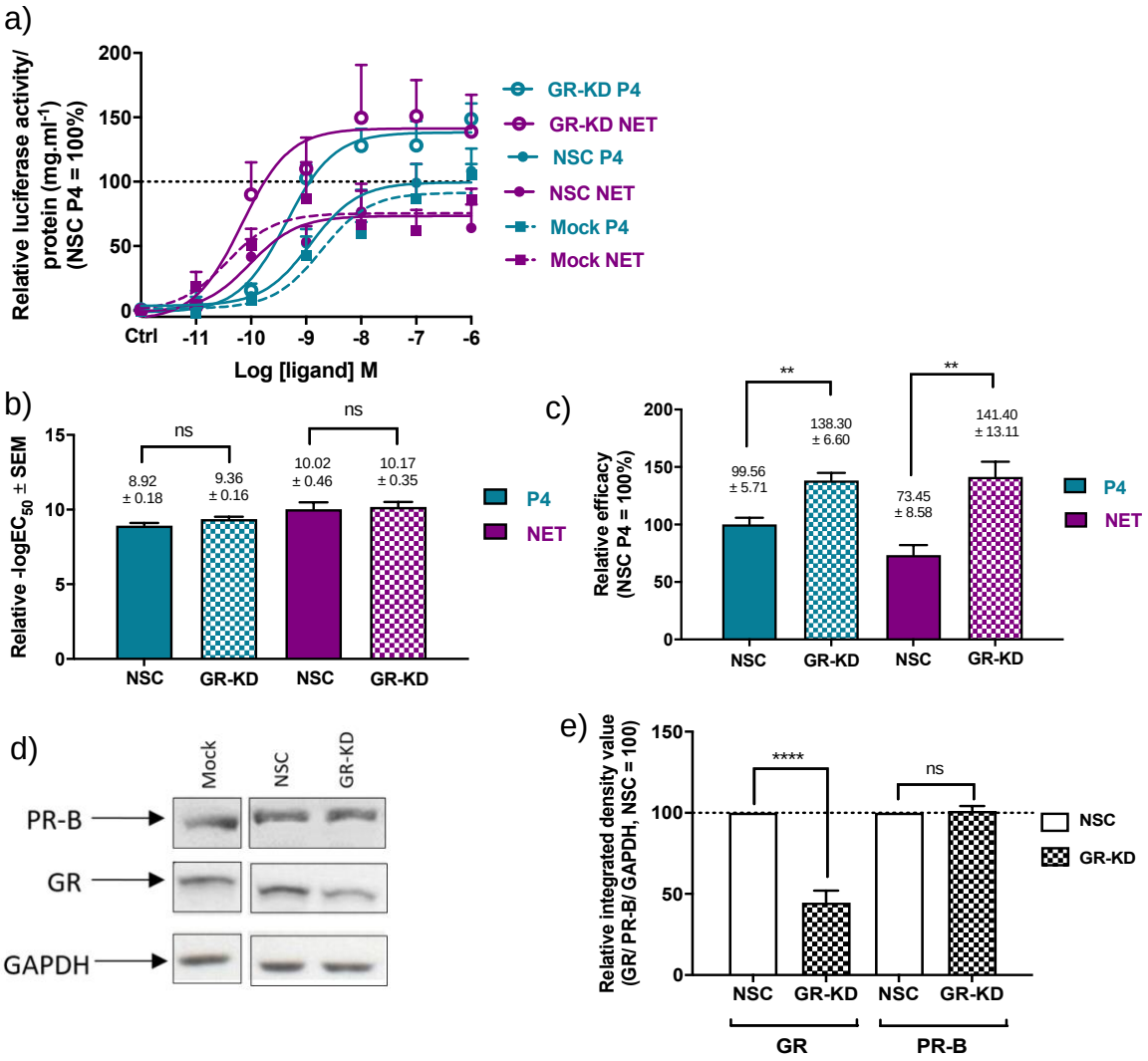

Figure 6.2.1: When GR levels decreased, the efficacy of both P4 and NET via PR-B significantly increased. U2OS cells were seeded and after 24 hours were treated with 100 nM GR-specific siRNA (GR-KD), non-silencing control siRNA (NSC) or mock (water instead of siRNA). After 24 hours, the cells were transiently transfected with 900 ng pSG5hPR-B and 9 µg 2XPRE-E1b-luc reporter plasmid. Twenty-four hours later the cells were re-seeded into 96-well tissue culture plates. After 24 hours, the cells were treated with increasing concentrations ($1X10^{-13}$ M – $1X10^{-6}$ M) of each ligand or vehicle (ctrl, 0.1% EtOH) for 24 hours. Thereafter, the cells were harvested, and the Luciferase and Bradford assays were performed. a) The % PR-B activity at increasing concentrations of each ligand relative to P4 NSC efficacy = 100%. b) The bar graph shows the mean -logEC_{50} values relative to P4 NSC ± SEM of each ligand via PR-B while c) shows the mean efficacies of each ligand via PR-B relative to P4 NSC ± SEM. d) Shows a representative western blot for the PR-B, GR and GAPDH protein levels and e) shows the quantified mean protein levels of each biological repeat after siRNA treatment. Mean relative -logEC_{50} values, efficacies and protein levels were analysed using paired t-tests where ** and **** denote p-value <0.01 and <0.0001 respectively, while ns indicates no significant difference. The SEM of the above data is calculated based six biological repeats each containing three technical repeats of each condition.

Next, promoter-reporter assays in a second cell line were performed to determine if the effect seen in U2OS cells was model system-dependent. Additionally, whether reciprocal modulation occurs was also investigated. Because it was shown in Figure 6.2.1 that only the efficacy was significantly affected when the GR is knocked down and not the -logEC_{50} values, only the concentration required to generate maximal response was investigated further. The MDA-PR-B+ cell line was used and treated with either NSC, PR- or GR-specific siRNA.

Like the data shown in Fig. 6.2.1c, the efficacies of the PR-B responses in the presence of PR-specific ligands (R5020, NET and MPA) were significantly higher when the GR levels were decreased (GR-KD) (Fig. 6.2.2a). Of note, reciprocal modulation appeared to occur when the PR levels were decreased. Using the GR-specific ligand, dex, the GR response was significantly higher when PR-B levels were lower (PR-KD) (Fig. 6.2.2a). MPA generated the most surprising response in that the efficacy via PR-B was significantly higher only when GR levels were lower but not when PR-B levels were lower (Fig. 6.2.2a). Importantly, the treatment with the PR-specific siRNA not only led to a significant decrease in PR-B protein expression but also a significant decrease of ~50% in GR protein expression in these cells (Fig. 6.2.2b and c). Therefore, GR levels were significantly lower under this condition (PR-KD) and the lack of MPA response via GR in the absence of the PR may be due to this decrease in GR levels compared to NSC. Treatment with the GR-specific siRNA significantly reduced GR protein expression and did not change PR-B expression levels (Fig. 6.2.2b and c).

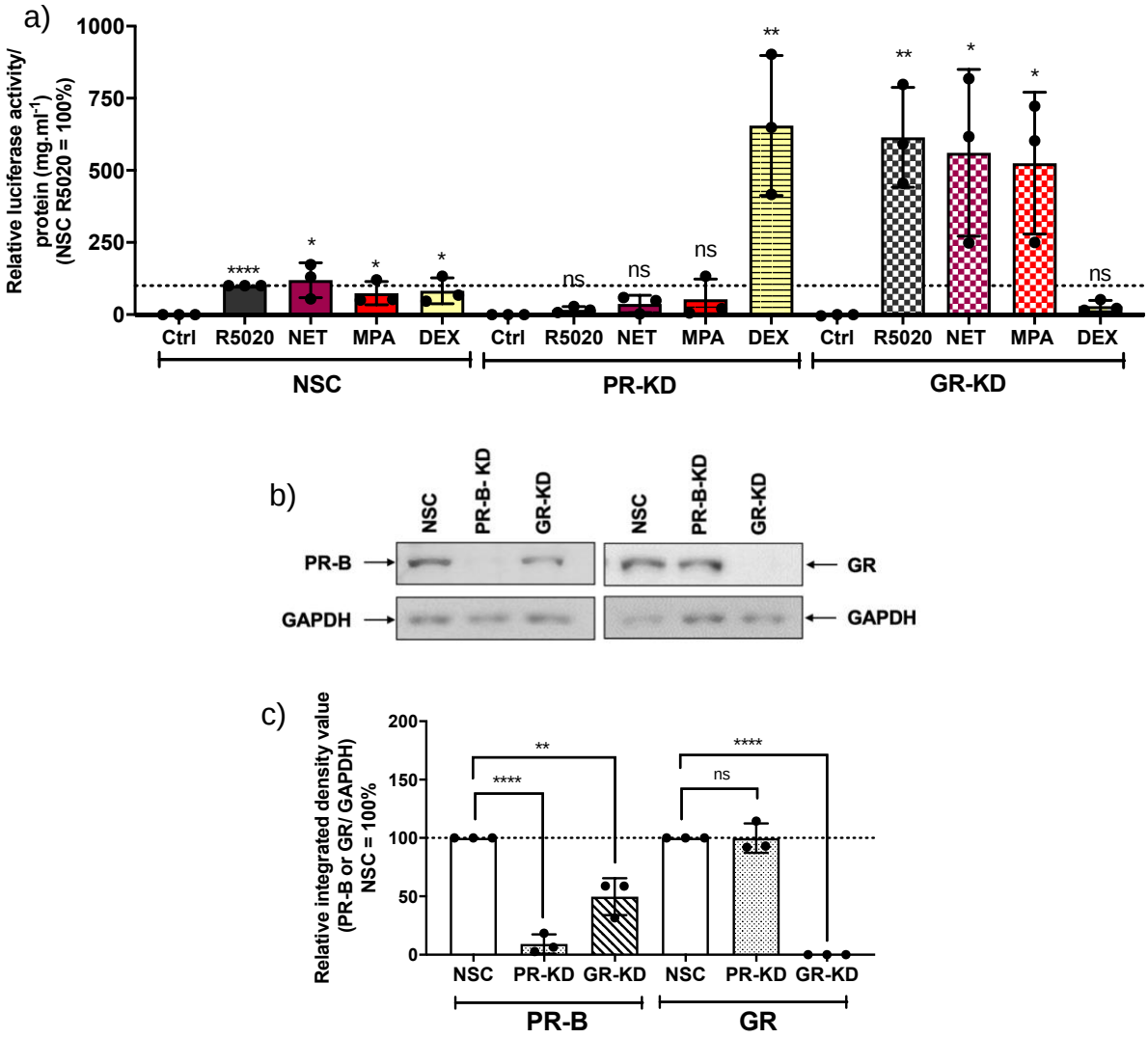

Figure 6.2.2: The efficacies of the GR and PR-B are reciprocally modulated by each other. MDA-PR-B+ cells were seeded and after 24 hours, the cells were treated with either 100 nM PR (PR-B-KD) or GR-specific siRNA (GR-KD) or non-silencing control siRNA (NSC). Twenty-four hours later, the cells were transiently transfected with 9 µg 2XPRE-E1b-luc reporter plasmid. The next day, the cells were re-seeded into 96-well tissue culture plates. After 24 hours, the cells were treated with 100 nM of each ligand or vehicle for 24 hours. Thereafter, the cells were harvested, and the Luciferase and Bradford assays were performed. a) Shows the % SR activity after treatment with each ligand or ctrl (vehicle, 0.1% ethanol) for 24 hours relative to NSC R5020 efficacy = 100%. b) Shows a representative western blot of the PR-B, GR and GAPDH protein levels while c) shows the quantified mean protein levels of the biological repeats. The above data were analysed using paired t-tests comparing data to the respective ctrl where *, ** and **** denote p-value <0.05, <0.01 and <0.0001 respectively, while ns indicates no significant difference. The SEM of the above data is calculated based three biological repeats each containing three technical repeats of each condition.

6.3 Global expression pattern of genes regulated by the PR agonist, NET reveals that the expression of some genes are dependent on relative GR levels

Given that the focus of this thesis is on the regulation of PR-mediated gene expression by progestogens, the effect of GR levels on PR-B mediated regulation of endogenous gene expression was further investigated. A PCR array was performed to investigate gene-specific effects of the GR on PR-B where a total of 89 genes relating to Human Cancer Inflammation & Immunity Crosstalk, were analysed for global GR-mediated inhibition of PR-B transcriptional regulation. The MDA-PR-B+ cell line which expresses endogenous GR (Appendix B, Fig. B1) was treated with NSC or GR-specific siRNA and then incubated with either 100 nM NET or vehicle for 24 hours. NET was chosen as is a PR agonist with no activity via the GR at 100 nM. Expression of the GR was significantly reduced while PR-B levels were unaffected after GR siRNA treatment (Appendix B, Fig. B9).

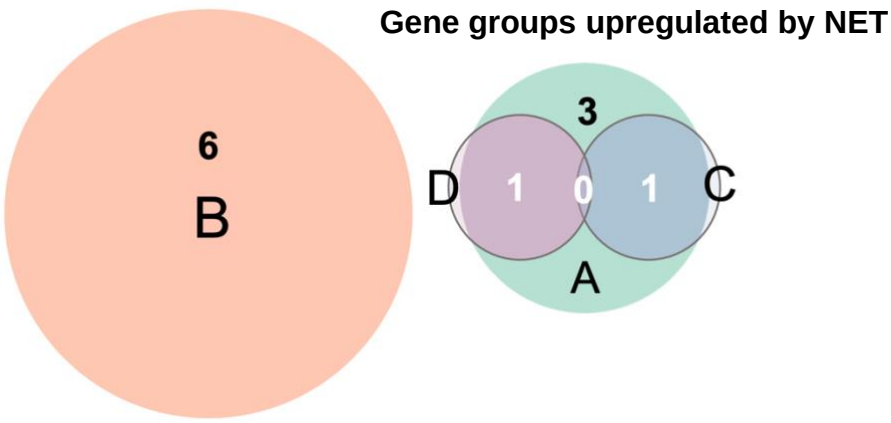

A: Genes upregulated by NET when GR + PR-B are present (significant increase between NSC ctrl and NSC NET) 3 genes

B: Genes upregulated by NET only when GR level is lower (significant increase between GR-KD ctrl and GR-KD NET and no change between NSC ctrl and NSC NET) 6 genes

C: Potentiated activation by NET when GR level is lower (significant increase between NSC ctrl and NSC NET, and GR-KD ctrl to GR-KD NET, and NSC NET to GR-KD NET) 1 gene

D: Genes upregulated by NET when GR + PR-B are present, but induction is lost when GR level is lower (significant increase between NSC ctrl and NSC NET and no change between GR-KD ctrl and GR-KD NET) 1 gene

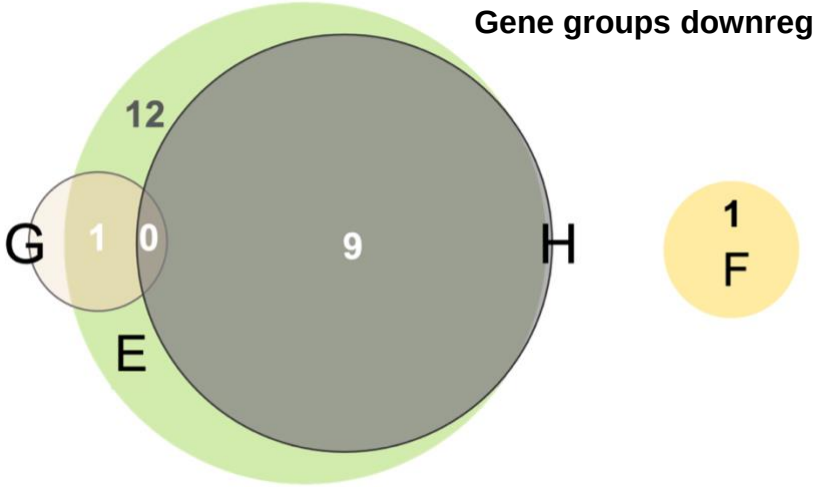

E: Genes downregulated by NET when GR + PR-B are present (significant decrease between NSC ctrl and NSC NET) 12 genes

F: Genes downregulated by NET only when GR level is lower (significant decrease between GR-KD ctrl and GR-KD NET and no change between NSC ctrl and NSC NET) 1 gene

G: Potentiated repression by NET when GR level is lower (significant decrease between NSC ctrl and NSC NET, and GR-KD ctrl to GR-KD NET, and NSC NET to GR-KD NET) 1 gene

H: Genes downregulated by NET when GR + PR-B are present, but repression is lost when GR level is lower (significant decrease between NSC ctrl and NSC NET and no change between GR-KD ctrl and GR-KD NET) 9 genes

Figure 6.3.1: Global gene expression pattern of genes regulated by NET grouped according to their dependence on relative GR levels. MDA-PR-B+ cells were seeded

and after 24 hours, the cells were treated with either 100 nM GR-specific siRNA or non-silencing control siRNA (NSC). Thereafter, the cells were re-seeded in 6-well tissue culture plates and allowed to adhere overnight. After 24 hours, the cells were treated with 100 nM NET or vehicle (ctrl, 0.1% ethanol) for 24 hours. Thereafter, RNA was extracted using the RNeasy extraction kit. cDNA was then synthesised, and the array plates were loaded according to the manufacturer's instructions. Relative expression was determined by normalising to ctrl = 1. The venn diagrams show the global gene expression patterns of 8 gene groups (group I not shown as these genes are not regulated by NET). The above data is calculated based on three biological repeats.

From the PCR array data, based on gene expression changes observed in the absence and presence of NET and the GR, nine gene groups were identified (A-I) as indicated in Figure 6.3.1 and Table 6.2.1. In general, there were fewer genes identified in the groups upregulated by NET (A-D) (Fig. 6.3.1, Table 6.3.1 and Appendix B, Fig. B9) than there were for gene groups downregulated by NET (E-H) (Fig. 6.3.1, Table 6.3.1 and Appendix B, Fig. B11). However, most genes did not change regardless of the presence of NET or higher or lower GR expression levels (group I) (Table 6.3.1 and Appendix B, Fig. B12). Although the expression of some genes appeared to change (increase or decrease) in the presence of NET, the mean fold difference compared to control was not significant and therefore did not meet the requirement to be classified into a gene group of which the expression was changed by NET (i.e. group I) (Table 6.3.1 and Appendix B, Fig. B12). From the PCR array, some genes did not generate a control (*gapdh)* signal. Therefore, the fold induction of that gene could not be determined so the gene was excluded from the grouping analysis. The PCR array data revealed that there were indeed genes that were upregulated in the presence of both GR and PR-B (NSC) (group A). Genes that were upregulated by NET in the presence of both SRs and fell into group A were *cxcl, ptgs2* and *cxcl11* (Table 6.3.1 and Appendix B, Fig. B9, group A). The genes that were downregulated when both SRs were present fell into group E (Table 6.3.1 and Appendix B, Fig. B11, group E).

When looking at the expression of genes that were upregulated by NET, GR knockdown either allowed for NET-induced upregulation (group B) (Table 6.3.1 and Appendix B, Fig. B9, group B) or seemed to enhance/ potentiate NET-induced upregulation (group C) (Table 6.3.1 and Appendix B, Fig. B9, group C). Additionally, one gene, *cxcl11*, was upregulated when both GR and PR-B were present (group A)

but when the GR was knocked down, the induction of this gene was lost (group D) (Table 6.3.1 and Appendix B, Fig. B9, groups A and D).

Table 6.3.1: Genes identified in the nine gene regulation groups identified in the PCR array. The genes highlighted in blue were selected for validation by real-time qPCR (*cxcl1, ptgs2* and *tlr4*). The data represents the data shown in Figure 6.3.2 and Appendix B, Figures B9, B10 and B11.

Group	Gene name
A	*cxcl1, cxcl11, ptgs2*
B	*actb, csf3, gzma, myc, stat1, vegfa*
C	*ptgs2*
D	*cxcl11*
E	*bcl2, csf2, cxcr3, egf, il-1a, cxcl8, irf1, mica, nfκb1, tlr4, tnfsf10, tp53*
F	*tgfb1*
G	*csf2*
H	*bcl2, egf, il-1a, cxcl8, irf1, mica, nfκb1, tnfsf10, tp53*
I	*ackr3, bcl21l1, ccl20,ccl28, ccl5, ccr10, cd274, csf1, cxcl2, cxcl5, cxcr2, cxcr4, egfr, foxp3, gbp1, gzmb, hif1a, hla-a, hla-b, il-1b, il-6, il-10, il-12a, il-13, il-15, kitlg, micb, mif, myd88, spp1, stat3, tlr2, tlr3*

Similarly, when looking at the expression of genes that were downregulated by NET, GR knockdown either allowed for NET-induced downregulation (group F) (e.g. *tgfb1*) (Table 6.3.1 and Appendix B, Fig. B11, group F) or potentiated NET-induced repression (group G) (e.g. *csf2)* (Table 6.3.1 and Appendix B, Fig. B11, group G). Like the *cxcl11* gene which was upregulated when both PR-B and GR were present but then lost its induction when the GR was knocked down, similarly the repression of the genes that fell into group H was also lost when GR levels were low (Appendix B, Fig. B11, group H). At first glance it appears as though the NET-induced repression of *cxcl8* and *irf1* was still maintained when GR was knocked down; however, statistically, it was revealed that the NET-induced repression was in fact lost (Appendix B, Fig. B11, group H). The repression of most of the genes that fell in group E was lost when the GR was knocked down and the expression of only two genes was unaffected by GR knockdown namely, *cxcr3* and *tlr4* (Table 6.3.1, Appendix B, Fig. B11, group E and Fig. 6.3.2e).

Due to the importance for this study, the results obtained in the PCR array for the *ptgs2* gene (groups A and C) was selected for validation using quantitative real-time qPCR. *Cxcl1* (group A) and *tlr4* (group E) were selected for validation because the

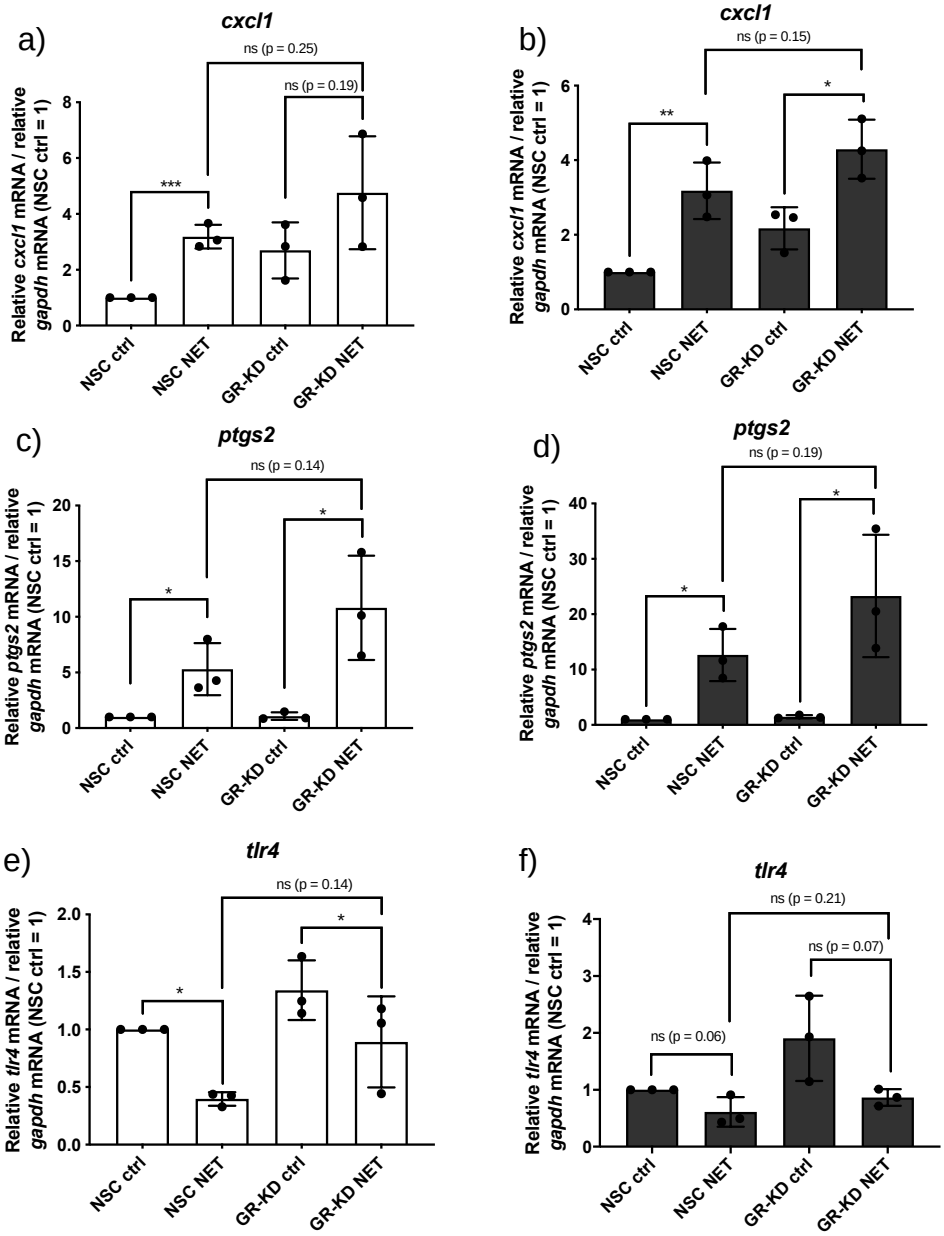

Figure 6.3.2: Quantitative real-time PCR validation (b, d and f) of selected target genes of array gene expression patterns (a, c and e). Using the same RNA that was used in the PCR array, cDNA was synthesized from 250 ng RNA then used in real-time qPCR. a-c) Relative mean mRNA levels of *cxcl1*, *ptgs2* and *tlr4* obtained from the PCR array. Relative mean mRNA levels of b) *cxcl1*, d) *ptgs2* and f) *tlr4* were normalized to *gapdh* mRNA levels. Relative expression was determined by normalising to NSC ctrl = 1. The above data were analysed using Two-way ANOVA with a Tukey post-test where *, ** and *** denote p-value < 0.05, < 0.01 and < 0.001 respectively. The mean ± SEM of the above data is calculated based on three biological repeats.

primers for these genes were available and had been optimised in the present author's lab (data not shown). The same RNA that was used for the PCR array was used again for the validation experiments. *Cxcl1, ptgs2* and *tlr4* were successfully validated by real-time qPCR because the expression of these genes showed the same fold induction pattern as those seen for the array data (Fig. 5.3.2). However, two of the genes chosen for validation from the PCR array (*cxcl2* and *il-6*) did not show the same result in the real-time qPCR experiment (Appendix B, Fig. B13) as obtained in the array.

Of particular interest to this study were genes that had an altered expression when GR levels were lower i.e. for NET-induced upregulation, groups B (only induced when GR levels were lower) and C (potentiated induction when GR levels were lower) and for NET-induced downregulation, groups F (only repressed when GR levels were lower) and G (potentiated repression when GR levels were lower). The change in expression of these genes when GR expression is lower emphasises and supports the inhibitory effect the GR has on PR-B activity suggested by the promoter-reporter assays (Fig. 5.2.1 and Fig. 5.2.2).

Taken together, the data shown in this chapter show that the GR inhibits PR-B activity as shown by the promoter-reporter data in both U2OS and MDA-PR-B+ cells, as well as on endogenous genes in MDA-PR-B+ cells. Additionally, GR mediated inhibition of PR-B regulation of endogenous genes seems to be highly promoter-specific as shown by the PCR array. Following this section, the mechanism behind the GR-mediated inhibition of PR-B activity was next investigated.

6.4 The GR and PR-B co-exist in a protein complex and PR-B phosphorylation is significantly lower in the presence of the GR

Having shown that GR and PR reciprocally modulate the activity of each other using promoter-reporter assays and that GR represses PR activity on select endogenous

genes, it was next investigated whether PR-B and GR could co-exist in a protein complex by co-immunoprecipitation assays. If this is the case, then these SRs have the potential to directly or indirectly interact and in doing so, this could be a mechanism for reciprocal modulation.

6.4.1 The GR and PR-B co-exist in the same protein complex

Co-immunoprecipitation assays were used to determine whether the GR and PR-B associate. MDA-PR-B+ cells expressing endogenous GR and stably-transfected to express PR-B, were treated with 1µM MPA or NET for 2 hours, before precipitation with an anti-GR antibody. As expected, there was no significant difference in GR or PR levels for the input samples for all treatments (lanes 1-4) (Fig. 6.4.1a and c). Additionally, as expected, after all treatments, the GR immunoprecipitated with anti-GR antibody (lanes 6-8) but not after immunoprecipitation with non-specific IgG (lane 5) (Fig. 6.4.1b and c). Interestingly, there was a significant amount of PR that co-immunoprecipitated with GR in the vehicle/ctrl after anti-GR immunoprecipitation (lane 5) (Fig. 6.4.1a and c). However, upon stimulation with both NET and MPA much less PR co-immunoprecipitated with the GR (lanes 6-8) (Fig. 6.4.1a and c). It is important to note that, although not significant, PR is detected in the IgG sample.

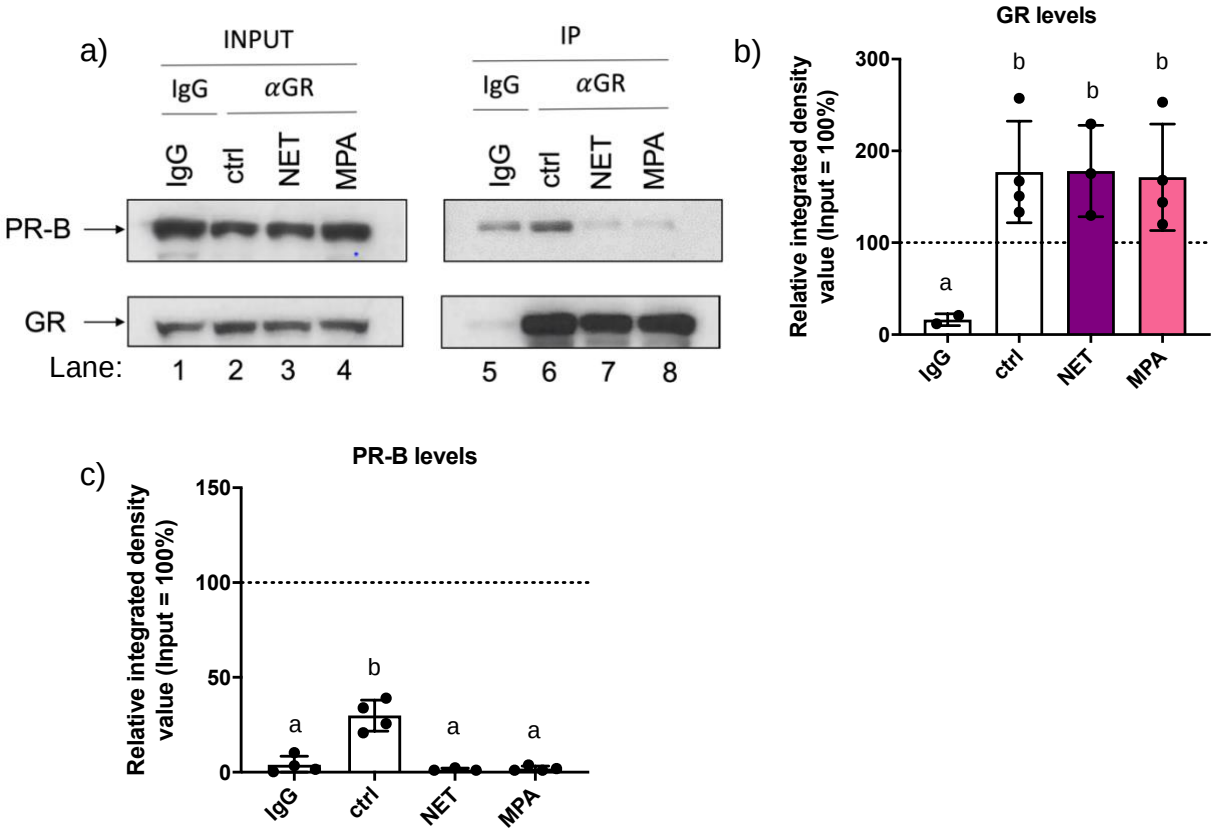

Figure 6.4.1: PR-B is co-immunoprecipitated with anti-GR antibody in MDA-PR-B+ cells. MDA-PR-B+ cells were seeded and after 24 hours, the cells were treated with 1 µM, MPA, NET or ctrl (vehicle, 0.1% ethanol) for 2 hours. Cells were lysed and an aliquot was analysed by western blotting for input levels (INPUT) of GR and PR-B. The remaining cell lysate was immunoprecipitated with anti-GR antibody and magnetic protein G beads (IP). From the supernatants of ligand-treated and vehicle control samples, equal volumes were combined and incubated with donkey anti-rabbit IgG antibody (IgG). The remaining supernatants were incubated with anti-GR antibody (αGR). Co-immunoprecipitated proteins were analysed by western blotting on separate blots for GR and PR-B. a) Shows a representative blot of PR-B and GR protein levels. Western blots were scanned and quantified for mean relative b) GR and c) PR-B levels by calculating integrated density values. Protein levels are plotted relative to the vehicle control for both IP and INPUT. The above data were analysed one-way ANOVA with a Tukey post-test where different letters indicate statistically significant differences while the same letters denote no significant difference. The SEM of the above data is based on four biological repeats.

These results show that the GR and PR can exist in the same complex in the absence of PR and GR ligand. Additionally, the data indicate that this GR-PR complex is most dominant when neither of the SRs are activated by ligand (i.e. unliganded GR associates with unliganded PR-B) and that stimulation/activation of the PR with progestogens, results in a dissociation of the complex. The reciprocal

immunoprecipitation using the anti-PR antibody was tried, but immunoprecipitation using the anti-PR antibody was not successful (Appendix B, Fig. B14).

6.4.2 PR-B is phosphorylated significantly more when GR levels are decreased

PR phosphorylation levels were investigated next, to gain more insight into the GR-PR interactions. The data in Figure 6.4.1 suggest that the GR and PR-B dissociate in the presence of ligands. Additionally, it is known that PR activation results in increased phosphorylation at Ser294 (Clemm et al., 2000, Grimm et al., 2016, Weigel & Moore, 2007). Therefore, PR phosphorylation was investigated to determine whether the PR was activated after it dissociates from the GR in the presence of MPA or NET.

Fig. 6.4.2 shows that there was a significant increase in PR-B phosphorylation levels after treatment with MPA and NET compared to vehicle (Fig. 6.4.2a and b) while total PR-B levels were unchanged for MPA and NET compared to vehicle (Fig. 6.4.2a and c).

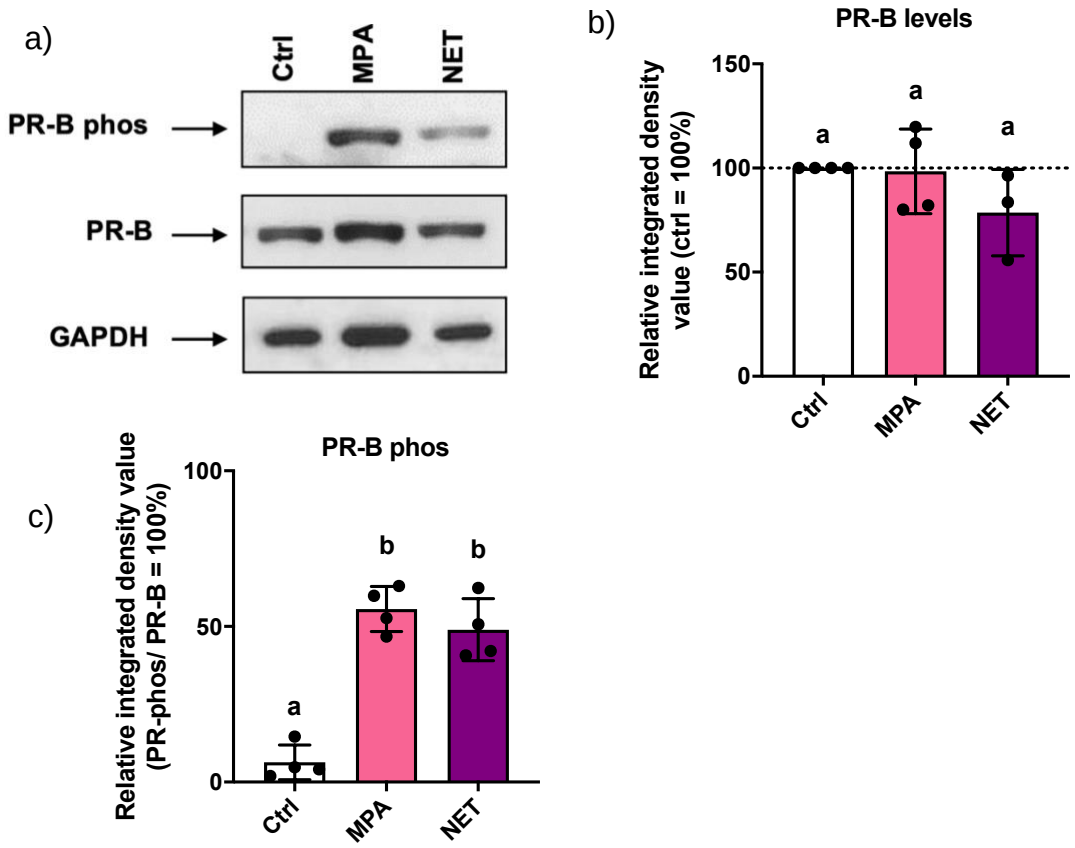

Figure 6.4.2: PR-B is phosphorylated in the presence of MPA and NET after a 2-hour incubation period. MDA-PR-B+ cells were seeded and after 24 hours, the cells were treated with 1 µM MPA, NET or ctrl (vehicle, 0.1% ethanol) for 2 hours. Thereafter, the cells were harvested in 2X sample buffer and a western blot was performed. a) Representative western blots are shown for phosphorylated PR-B (PR-B phos), total PR (PR-B) and GAPDH b) Shows the mean total PR-B protein levels relative to ctrl =100%. c)Shows the mean percentage phosphorylation for PR-B normalised to total PR-B levels relative to ctrl = 100%. . The above data were analysed using one-way ANOVA with a Tukey post-test where different letters indicate statistically significant differences while the same letters denote no significant difference. The SEM of the above data is based on four biological repeats.

Having shown in this section, that in the presence of progestogens, PR-B dissociated from the GR and is phosphorylated, it was next investigated whether the unliganded GR significantly modulates PR phosphorylation.

Figure 6.4.3 shows that, when both GR and PR-B+ were present (NSC), as expected PR-B was phosphorylated in the presence of the PR ligand NET (Fig. 6.4.3a and b). However, when the GR levels were decreased to undetectable levels (GR-KD) (Fig. 6.4.3a and d), there was a significant increase in PR-B phosphorylation compared to

when the GR was present (Fig. 6.4.3a and b). Importantly, total PR-B levels were not significantly different for all conditions investigated (Fig. 6.4.3a and c). These results indicate that in cells where the GR and PR-B are both present, the GR decreased PR-B phosphorylation and the resultant PR-B response was blunted. However, in cells where GR expression is undetectable and the PR-B is exclusively expressed, the PR-B response will be greater. Of note, the basal PR-B phosphorylation levels under low GR levels (GR-KD ctrl) appears to be lower than when GR is present (NSC ctrl) (Fig. 6.4.3a and d), although this was not statistically significant. These data support the idea that unliganded GR plays an important role in inhibiting PR-B activation responses.

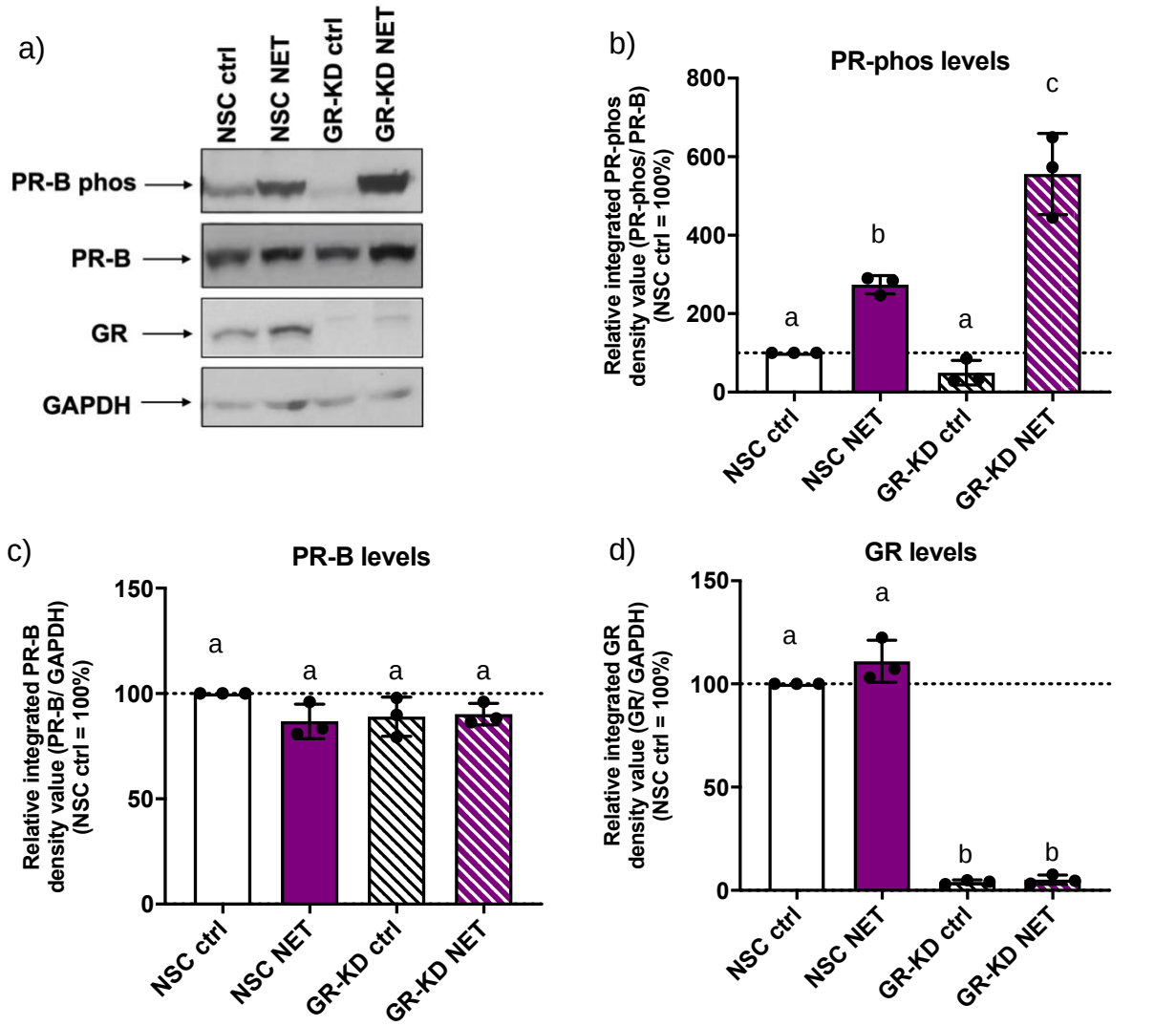

Figure 6.4.3: PR-B is phosphorylated significantly more in the presence of NET when GR levels are lower. MDA-PR-B+ cells were seeded and after 24 hours, the cells were treated with either 100 nM GR-specific siRNA (GR-KD) or non-silencing control siRNA (NSC). Thereafter, the cells were re-seeded into 12-well tissue culture plates. After 24 hours, the cells were treated with 100 nM NET or vehicle (ctrl, 0.1% ethanol) for 24 hours. Thereafter, the cells were harvested in 2X sample buffer and a western blot was performed. a) Representative western blots are shown for phosphorylated PR (PR-phos), total PR-B, GR and GAPDH. b) Shows the mean percentage phosphorylation for PR-B normalised to total PR-B levels. c) Shows the mean total PR-B levels while d) shows the mean GR levels quantified by relative integrated density values relative to NSC ctrl = 100%. Relative protein levels were analysed two-way using ANOVA with a Tukey post-test where different letters indicate statistically significant differences while the same letters denote no significant difference. The SEM is calculated based on three biological repeats.

In summary, the data in this chapter suggest that GR and PR-B can exist in the same protein complex. Moreover, the data in this chapter suggest that the unliganded GR

inhibits PR-B activity not only by association in the absence of ligand, but also by hindering PR-B phosphorylation in the presence of NET.

Chapter 7

Discussion

7.1 Characterising progestogen activity via the PR isoforms

HCs containing progestins are widely used globally (UNAIDS, 2019) and have been designed to target the PR to prevent unwanted pregnancy. Although the progestin-induced activity via the PR isoforms has been investigated before (Attardi et al., 2010, Bain et al., 2015, Bray et al., 2005, Kumar et al., 2017, Lim, C. S.; et al., 1999, Sasagawa et al., 2008), published data have shortcomings which make them hard to interpret. Therefore, although HC use among women of reproductive age (15 - 49 years) is widespread, the relative activities of most progestins have not been accurately determined via the target PR isoforms. Characterising the PR activity in the presence of different progestins is particularly important due to the high prevalence of HC use globally. In addition, many women using an HC to prevent unwanted pregnancy are also using ARVs to treat AIDs or prophylactically to prevent HIV-1 infection (PrEP). Whether combination treatment of a progestin and an ARV affects progestin-induced PR activity also needs investigation. The first central hypothesis of the present study was that the progestogens exhibit progestogen-, model system-, promoter- and isoform-specific effects.

7.1.1 Progestogens exhibit progestogen-, model system-, promoter- and isoform-specific effects

7.1.1.1 Progestogen-specific effects

The first aim under the first central hypothesis of the present study was to determine whether the progestogens exhibit progestogen-specific PR-B transcriptional effects.

7.1.1.1.1 Promoter-reporter gene expression

Data from the present study, part of which are presented in Enfield *et al.,* 2020b, show that in U2OS cells, all the progestins are full agonists via PR-B and no significant differences in potency were detected (Fig. 3.2.1.1). This suggests that the progestins do not exhibit progestogen-specific effects on potency in this cell line. Alternatively, the differences may occur, but they may be beyond the statistical power of the assay. Comparing the absolute pM values for potencies via PR-B obtained in U2OS cells using TC 1 and MDA-PR-B+ cells, P4 was consistently the least potent progestogen (Table 7.1.1) which is similar to what was observed in other studies (Bain et al., 2015, Bray et al., 2005). Similar to the present study, Kumar et al., showed that P4 and LNG have potencies of 98 pM and 5.8 pM, respectively, in HEK293 cells overexpressing human PR-B (Kumar et al., 2017). Other studies have; however, reported EC_{50} values for P4 of 3090 pM (Attardi et al., 2010) or a range of 400-800 pM (Sasagawa et al., 2008). For NET and MPA in U2OS cells using TC 1, the EC_{50} values determined for human PR-B in other studies were approximately ~2.5- and ~3.4-fold less potent, respectively (Kumar et al., 2017, Sasagawa et al., 2008), compared to the present study. For the PR-B responses obtained in MDA-PR-B+ cells (Fig. 3.2.3.1), the NET and MPA responses in the present study were ~1.5- and ~6-fold less potent respectively, compared to published potencies (Kumar et al., 2017). Considering that both these studies (Kumar et al., 2017, Sasagawa et al., 2008), in a manner similar to the present study, used promoter-reporter constructs containing two copies of the PRE, discrepancies between the results in the present study and these two studies could be attributed to other factors, such as the type and amount of PR-B expression vector used in transfection. For example, the study by Kumar et al., in HEK293 cells, used ~2 times less PR-B than in the present study and a different PR-B expression vector, namely pchPR-B (Kumar et al., 2017), while Sasawaga and co-workers used COS-1 cells and the pSG5-hPR-B, and did not specify the amount of PR transiently transfected (Sasagawa et al., 2008).

7.1.1.1.2 Endogenous gene expression

The endogenous gene response data (Fig. 3.2.5.1) provided more insight about progestogen-induced PR-B responses. The real-time qPCR data showed that the progestogen responses via PR-B were progestogen and promoter-specific.

When comparing the progestogen-induced PR-B responses on the promoter-reporter gene (Fig. 3.2.3.1) to the endogenous gene responses (Fig. 3.2.5.1), many differences were observed. For example, MPA was equally as efficacious as the other progestogens (except R5020) via PR-B for the promoter-reporter assay (Fig. 3.2.3.1); however, in terms of gene expression, MPA generated the least efficacious response for *ptgs2* expression but the most efficacious response for *atp1a1* expression (Fig. 3.2.5.1). For the *gilz* gene; however, more similarities between the promoter-reporter data and the endogenous gene responses were seen. Similar to the promoter-reporter data where NET and MPA generated overlapping dose-response curves, the same trend was seen for *gilz* expression. NET and MPA generated very similar responses for *gilz* expression with no significant differences detected between these ligands for both potency and efficacy (Fig. 3.2.5.1 and 3.2.5.2). Additionally, as seen for the promoter-reporter assays, R5020 was the most potent for *gilz* expression (Fig. 3.2.5.1). The similarities between the promoter-reporter assay data and *gilz* expression may be due to the fact that both promoters contain multiple copies of the PRE/GRE sequence (Bereshchenko et al., 2019, Ng et al., 2017). This suggests that the similarities in the expression of both the promoter-reporter gene and the *gilz* gene is highly dependent on GREs while the expression of the other genes may be dependent on other mechanisms.

Focussing specifically on the differences in the progestogen-induced expression of the endogenous genes (*ptgs2, gilz* and *atp1a1*), promoter- and progestogen-specific differences were observed (Fig. 3.2.5.1 and 3.2.5.2). All progestogens acted as full agonists when assessing the expression of all three PR-regulated genes, except MPA which acted as a partial agonist for *ptgs2* expression (Fig. 3.2.5.1 and 3.2.3.2). The progestogen-specific effects on the endogenous gene expression may be explained by the progestogen-specific PR conformational change induced upon ligand binding to the PR. Studies suggest that different PR ligands induce different ligand-bound PR conformations which ultimately results in the differential recruitment of cofactors in terms of number and type (Cabeza et al., 2014, Zheng et al., 2016). Alternatively, as

reviewed by Grimm *et al.,* some studies show that depending on the type of ligand (full or partial agonist or antagonist), the ligand-bound PR may act via different sequences in the genome (Grimm et al., 2016). This may be as a result of differential cofactor recruitment, chromatin remodelling and accessibility which ultimately results in ligand-induced differential gene expression patterns (Grimm et al., 2016). Importantly, the level of hsp does affect the binding affinity of ligands to SRs as has been shown for the AR (Eftekharzadeh, 2019) and the GR (Kirschke, 2014). Whether this occurs for the PR specifically remains to be investigated and was beyond the scope of the present study.

Taken together, the promoter-reporter gene and endogenous gene expression data support the first aim of the first central hypothesis that the progestogens exhibit progestogen-specific effects via PR-B.

7.1.1.2 Model system-specific effects

The second aim under the first central hypothesis of the present study was to determine whether the progestogens exhibit model system-specific PR-B transcriptional effects. This was assessed by investigating 1) the effect of transfection condition and 2) the effect of the model system on the resultant progestogen-induced PR-B transcriptional responses.

7.1.1.2.1 Transfection condition

In the present study, when the second transfection condition was investigated in U2OS cells (TC 2), no significant differences in potencies or efficacies were detected for the progestogen-induced activity via PR-B (Appendix B, Fig. B3). When comparing the transcriptional responses between TC 1 and TC 2, R5020 was significantly more potent using TC 1 and MPA was significantly less potent using TC 1 while no significant differences in efficacy were detected (Appendix B, Fig. B4). The lack of detectable significant differences for efficacies between these two transfection conditions is in agreement with the data using a different cell line, COS-1 cells, shown in the Enfield *et al.,* 2020b study. In the Enfield *et al.,* 2020b study, MPA was significantly less potent using TC 2 while NET was significantly less efficacious using

TC 2 in PR-B transiently transfected COS-1 cells (Enfield et al., 2020b), compared to TC 1. The results in the present study indicated that even though the PR-B expression level in U2OS cells was significantly higher using TC 2 (Appendix B, Fig. B2), total PR-B levels did not influence the progestogen-induced PR-B responses. While some studies suggest that expression levels of an SR can change the biocharacter, efficacy and/or potency (Abdel-Hafiz et al., 2009, Robertson et al., 2013, Zhao et al., 2003), this was not seen in the present study. Of note, however, in the present study, the amount of reporter plasmid also increased using TC 2. Therefore, not only did the amount of transiently transfected PR-expression vector change, but the total amount of transfected DNA between TC 1 and TC 2 also changed. From the present study, the progestogen-induced PR responses appear to be independent of PR expression levels and/or total amount of transiently transfected DNA. However, given that the amount of PR expression vector was not the only variable changed in this comparison, it is not possible to make a definitive conclusion on the effect of PR expression levels on PR activity in this study.

Table 7.1.1: Potency (EC_{50} values) determined in this study for different progestogens via PR-B (U2OS and MDA-PR-B+) or PR-A (MDA-PR-A+) using promoter-reporter assays compared to published relative binding affinities (RBAs) and serum progestogen concentrations. The Table below is adapted from Enfield et al., 2020b.

Progestogen	EC_{50} (pM ± SEM)			Relative EC_{50} (% ± SEM)			RBA (%)[a*]	Serum concentrations (pM)[a]
	U2OS	MDA-PR-B+	MDA-PR-A+	U2OS	MDA-PR-B+	MDA-PR-A+		
R5020	71.54 ± 33.09	0.016 ± 0.007	0.0021 ± 0.0008	100 ± 46.25	100 ± 43.75	100 ± 38.10	100	-
P4	157.00 ± 10.89	273.80 ± 114.00	0.12 ± 0.095	45.57 ± 6.94	0.01 ± 41.64	1.75 ± 79.17	50	650 - 600 000
NET	7.47 ± 54.00	35.07 ± 22.93	0.034 ± 0.031	957.70 ± 722.89	0.05 ± 65.38	6.18 ± 91.18	33-49	700 - 69 700
ETG	18.44 ± 10.99	9.55 ± 5.33	0.073 ± 0.064	387.96 ± 59.60	0.17 ± 55.81	2.88 ± 87.67	14-17	600 - 19 100
LNG	2.29 ± 15.07	0.89 ± 0.52	17.03 ± 18.83	3124.02 ± 658.08	1.80 ± 58.43	0.01 ± 110.57	12-48	300 - 84 800
MPA	2.02 ± 19.58	19.40 ± 11.64	0.025 ± 0.028	3541.58 ± 969.31	0.08 ± 60.00	8.40 ± 112.00	75	500- 99 600

[a][(Stanczyk et al., 2013), (Hapgood, J. P. et al., 2018)]; *Relative binding affinities for the human PR (isoforms not specified), are set relative to R5020 which is 100%.
R5020, promegestone; P4, progesterone; MPA, medroxyprogesterone acetate; NET, norethisterone; LNG, levonorgestrel; ETG, etonogestrel; SEM, standard error of the mean.

7.1.1.2.2 Model system effects

Given the apparent discrepancies in the literature, the effect of model system used on the resultant efficacies and potencies of the progestogens via PR-B were compared between U2OS cells and MDA-PR-B+ cells. The model system-dependent differential progestogen responses obtained in PR-B transiently transfected COS-1, U2OS and MDA-MB-231 cells, were also seen when comparing the PR-B responses using the same transient transfection condition (TC 1) (Enfield et al., 2020b). In the present study, the R5020 response obtained in the MDA-PR-B+ cells, was hard to understand as it appeared to act as a super-agonist via PR-B. A super-agonist response has only been reported for G-protein coupled receptors and none have been reported for SRs (Chapman, 2012, Schrage et al., 2016). Regardless, the significant differences in progestogen potencies and efficacies via PR-B between these cell lines suggests that there may be cell-specific, and possibly tissue-specific, PR-B transactivation responses. For example, the MPA response being less potent in MDA-PR-B+ cells compared to U2OS cells suggests that MPA may generate less potent responses in breast cancer cells compared to bone cancer cells while, the opposite is true for R5020. Additionally, the data suggest that a lower dose of NET, ETG and LNG is required to generate the same PR-B response in bone cancer cells compared to breast cancer cells.

The data shown in Figure 3.2.4.1 suggest that total PR-B protein is not associated with significant differences in PR-B -logEC_{50} values within U2OS or MDA-PR-B+, or between U2OS and MDA-PR-B+ cells. Furthermore, when comparing the PR-B responses between U2OS and MDA-PR-B+ cells, total PR-B protein did not influence PR-B efficacies. There were significantly higher PR-B protein expression levels after all progestogen treatments in MDA-PR-B+ cells compared to U2OS cells (Fig. 3.2.4.1); however, NET, ETG and LNG were significantly less efficacious in MDA-PR-B+ cells compared to U2OS cells (Fig. 3.2.3.1c). Therefore, the effect of PR-B expression on progestogen-induced PR activity is likely to be cell-specific and not dependent on total PR-B expression.

The significant and progestogen-specific responses between these cell lines could be explained by differential metabolism (Skosana et al., 2019), which either results in a decrease in the effective concentration of the progestogen, and/or an increase of a metabolite that is active via the PR. In addition, different cell lines could express different types and/or expression levels of co-regulators which may play a role in PR-B-mediated transcriptional regulation. Different ligands may cause differential recruitment of co-regulators (Scarpin et al., 2009). Indeed, in a study conducted by Liu *et al.,* it was shown that the ratio of co-activators and co-repressors could modulate the inhibitory or stimulatory effects of the PR/GR antagonist, RU486 (Liu, Z.; et al., 2002). The cell lines used in the present study contain the downstream factors necessary to support PR-mediated transcription as evident from the potent responses. It is possible that some co-factors that are present in PR-expressing cells *in vivo,* are not present in some or all of the cell lines used in the presence study and hence may result in different relative potencies and efficacies *in vivo*. It has, however, been shown that the MDA-MB-231 cells express multiple co-activators and co-repressors, including the SRC family of co-activators, the main co-activators involved in mediating PR transcription (Cai et al., 2019, Li, X.; et al., 2003, Nehdi et al., 2019).

In summary, the progestogen-induced transcriptional responses via PR-B using the two different transfection conditions in U2OS cells, and the comparison of the data of the progestogen-induced PR-B responses between U2OS (TC 1) and MDA-PR-B+ cells support the second aim of the first central hypothesis that the progestogens exhibit model system-specific transcriptional responses via PR-B.

7.1.1.3 Promoter-specific effects

The third aim under the first central hypothesis of the present study was to determine whether the progestogens exhibit promoter-specific PR-B transcriptional effects.

7.1.1.3.1 Endogenous gene expression

As mentioned in section 7.1.1.1.2, the progestogens generated different responses when comparing the transcriptional responses between the endogenous gene expression and the promoter-reporter responses. Additionally, each progestogen

induced different PR-B transcriptional responses on the expression of the endogenous genes that were investigated (Fig. 3.2.5.1). Although significant differences were not detected for all progestogen-induced transcriptional responses, it may be that the differences may occur beyond the statistical power of the assay used.

Of particular interest in the present study was the expression of the endogenous genes in the presence of MPA which suggested a highly promoter-specific response which may be as a result of PR as well as GR activation. The expression of the *ptgs2* gene in the presence of MPA was significantly less efficacious than the other progestogens and in contrast, it generated the most efficacious response on the *atp1a1* promoter (Fig. 3.2.5.3b). Additionally, since MPA acts via the GR as well as the PR isoforms, the variable response may be due to off-target GR activation (Hapgood, J. P.; et al., 2014a) resulting in promoter-specific activation of PR-regulated genes. The effect of activated GR is relevant for the expression of the *atp1a1* and *gilz* genes which both contain GREs (Kolla et al., 1999, Ng et al., 2017). Additionally, it was suggested by a previous study that the expression of the *ptgs2* gene may be inhibited by activated GR (Mitchell et al., 2011), which is consistent with the significantly lower efficacy seen in response to MPA for the *ptgs2* gene in the present study (Fig. 3.2.5.3b). Physiologically, the variable MPA response implies that the resultant *in vivo* MPA activity via PR-B may also be highly variable compared to the other progestogens. In the sub-Saharan context, this is concerning considering that the injectable containing MPA, is the most commonly used form of HC (UNAIDS, 2019).

A possible explanation for the promoter-specific differences in potencies and efficacies for endogenous gene expression could be due to differences in the sequence of DNA flanking the PREs and promoter architecture in terms of presence and frequency of different *cis*-elements and regulatory motifs within these genes (Nelson et al., 1999, Schöne et al., 2016, Whirledge & Cidlowski, 2019). The differences in the promoter sequences could allow for differential interaction of the progestogen-liganded PR-B with coregulatory proteins and/or other TFs. For example, the *gilz* gene contains five copies of the consensus GRE sequence (Ng et al., 2017) as well as a binding site for a leucine zipper-containing TF (Bereshchenko et al., 2019). Combined evidence from the literature suggests that the *gilz* gene is regulated by the GR and/or PR, by direct binding to GRE/PREs respectively, in the promoter (Cannarile et al., 2019, Flynn et

al., 2019, Kougioumtzi et al., 2014, Vétillard & Schlecht-Louf, 2018). In agreement with the Kougioumtzi *et al.* study, the present study showed that *gilz* expression increased in a dose-dependent manner in the presence of progestogens suggesting regulation by the PR supporting the fact that PREs are present within the *gilz* gene.

The *ptgs2* gene on the other hand, contains binding motifs for Runt-Related Transcription Factor 1 (RUNX1), myb, GATA-1, cAMP response element binding protein (CREB), NFκB and Sp-1 (Liu, J.; et al., 2009). To the present author's knowledge, a consensus GRE/PRE sequence has not been reported to be present in the promoter of the *ptgs2* gene. In agreement with the present study, P4 and MPA treatment resulted in a dose-dependent (1, 10, and 100 nM) increase in *ptgs2* mRNA levels using human primary umbilical vein cells (Hermenegildo et al., 2005). Although no PRE sequence has been identified within the *ptgs2* gene, experiments with the PR/GR antagonist, mifepristone (RU486) suggested the most likely mechanism resulting in *ptgs2* regulation is direct genomic action of activated PR (Hermenegildo et al., 2005). While determination of the mechanism whereby the PR regulates the *ptgs2* gene is beyond the scope of the present study, considering what is known about their promoters, it is likely to be different to that for the *gilz* gene, consistent with progestogen-specific and promoter-specific differences observed between responses on these promoters.

The *atp1a1* gene contains a potential TATA box (Shull et al., 1990), two GREs (Kolla et al., 1999) and potential binding sites for AP-1, AP-2 and AP-3 (Shull et al., 1990). The *atp1a1* gene also contains Sp-1 binding sites (Shull et al., 1990). Combined evidence from the literature suggests that the expression of the *atp1a1* gene is dependent on activated GR. To the present author's knowledge, the expression of *atp1a1* in the presence of progestogens has not been investigated previously; however, *atp1a1* expression in the presence of GCs has. In a study by Hatou *et al.* the expression of *atp1a1* protein increased after treatment with dex at 1 and 10 μM in primary mouse endothelial cells, suggesting that the expression of the *atp1a1* gene could be regulated by activated GR (Hatou et al., 2009). Consistent with this study, another study by Shimizu *et al.* showed that the recruitment of RNA polymerase II to the *atp1a1* promoter was dependent on dex-bound GR; however, this mechanism of

regulation of the *atp1a1* gene by the GR was dependent on cell type (Shimizu et al., 2008). The *atp1a1* gene contains two PRE/GREs in the promoter sequence (Kolla et al., 1999, Shull et al., 1990). Therefore, it is most likely that activated GR and/or PR as suggested by the present study, binds to these sites to initiate transcription of the *atp1a1* gene.

Some of the progestogen- and promoter-specific effects on mRNA levels observed in this study may be due to different epigenetic changes such as the degree of DNA methylation, histone modification and RNA silencing. Ligand-induced epigenetic changes to DNA as suggested by some studies (Houshdaran et al., 2020, Maekawa et al., 2019, McCarthy & Nugent, 2013, Xiong et al., 2017) contribute to differential gene expression patterns. Epigenetic changes to DNA occur largely by the addition of methyl groups via DNA-methylating enzymes (DNMTs), most commonly to cytosines that are next to guanines separated by a phosphate (CpG islands) in promoter sequences, which results in the repression of transcription (McCarthy & Nugent, 2013). While both MPA and P4 have been shown in separate studies to result in epigenetic changes to the genome (Maekawa et al., 2019, Houshdaran et al., 2020) compared to estrogen, whether the progestogens investigated in the present study induce differential epigenetic changes to the genome compared to each other on the same gene, or differences between genes for a particular progestogen, remains to be investigated. In addition, with increasing evidence for the role of miRs in regulating the activity of SRs (Fletcher, 2014, Palagani, 2014, Tessel, 2010), the effect of miRs on the expression of endogenous genes cannot be excluded.

Taken together, the differential progestogen-induced gene expression on PR-regulated genes supports the third aim of the first central hypothesis that the progestogens exhibit promoter-specific transcriptional effects via PR-B.

7.1.1.4 Isoform-specific effects

The final aim under the first central hypothesis of the present study was to determine whether the progestogens exhibit isoform-specific PR transcriptional effects.

To the best of the present author's knowledge, this is the first study to determine efficacies and potencies of a wide panel of progestogens in parallel via PR-A and PR-B in two cell lines that only differed in the PR isoform that was stably-expressed. Relative to the PR-B R5020 response, the progestogens; P4, NET, ETG, LNG, MPA and NES were significantly less efficacious via PR-A than PR-B (Fig. 3.3.1.2b). Progestogen activity being more efficacious via PR-B than PR-A is supported by previous PR isoform studies which investigated PR isoform activity in the presence of R5020 (Clemm et al., 2000), and P4 (Vegeto et al., 1993). Additionally, in the present study relative to the PR-B R5020 response, the progestogen responses via PR-A were significantly more potent via PR-A than PR-B (Fig. 3.3.1.2a) which is in agreement with another PR transactivation studies using P4, LNG and NES (Attardi et al., 2010). The study by Lim *et al.* showed that PR-B responses were more potent than PR-A, unlike another report (Lim et al., 1999). This could be explained by the fact that Lim *et al.* used a promoter which is known to be more specific for PR-B than PR-A (Lim et al., 1999). Additionally, in the Lim study, the PR responses were not normalised to a reference PR response therefore, the relative PR isoform-specific responses were not accurately determined. The data in the present study show for the first time that the differential activity of the PR-A and -B isoforms as shown for P4, LNG and NES in a previous study also occur for a wider panel of progestogens (R5020, P4, NET, ETG, LNG, MPA and NES). The present study also shows that not only are the progestogen responses via PR-A less efficacious than those observed via PR-B, and that they are also be more potent via PR-A.

A potential mechanism for the novel progestogenic responses via PR-A and PR-B may be due to isoform-specific phosphorylation signals. Of note, relative to the total PR levels, the present study shows that PR-B was phosphorylated significantly more than PR-A in the presence of LNG and R5020 (Fig. 5.3.2). Previous studies which have investigated effects on PR isoform activity suggest that the increased efficacy seen with PR-B is due to an additional activation function (AF-1) located in the N-terminal present in PR-B only (Sartorius et al., 1994). However, the data in the present study suggest that the increased efficacy seen with PR-B may be due to an increase in PR-B phosphorylation at Ser294 compared to PR-A. In agreement with this, a study by the Clemm group suggests that PR-B is preferentially phosphorylated at Ser294 compared to PR-A (Clemm et al., 2000).

The data in the present study therefore highlight the importance of PR ratios. These data suggest that in cells where the ratio of PR expression is in favour of PR-B (i.e. more PR-B than PR-A), the resultant progestogen response will be more efficacious and in cases where PR-A expression is favoured, the progestogen response may be more potent. A limitation, however, of the present study is that relative to PR-B protein, PR-A expression is significantly higher than PR-B (Fig. 3.3.1.3). However, if the antibody used to detect PR is more specific for PR-A than PR-B, relative PR signals might be misleading (Fabris et al., 2017). If there is similar sensitivity, the results in the present study suggest that total PR expression could be a contributing factor to the significantly more potent progestogen responses via PR-A. Moreover, even though PR-B expression appeared lower than PR-A for all progestogens (Fig. 3.3.1.3), the progestogen responses via PR-B were significantly more efficacious (Fig. 3.3.1.2b) and less potent relative to PR-B R5020 maximum response = 100% (Fig. 3.3.1.2a). Therefore, with regards to the PR isoforms, total PR-A/-B expression appeared to have a greater influence on potency values than efficacies such that more PR protein may allow for a more potent response; however, that does not necessarily result in a more efficacious response. The *in vitro* PR isoform data from the present study provide valuable proof of concept on the effects of differential progestogen action via these SR isoforms which, prior to this study, had not been thoroughly investigated.

Taken together, the data presented in the present study support the first central hypothesis that the progestogens exhibit progestogen-, model system-, promoter- and isoform-specific effects on PR transcriptional responses. These differential effects could be explained by the progestogen-specific conformational changes of the ligand-bound PR, the effect of the GR (in the presence of MPA), differential effects of other SRs/TFs, the presence and frequency of other *cis* regulatory elements as well as progestogen-specific epigenetic changes to the chromatin.

7.2 The progestogens are differentially metabolised in extra-hepatic cells

Most studies have investigated progestogen metabolism in a clinical setting while only one study to date, part of which is reported in this thesis, investigated progestogen metabolism *in vitro* (Skosana et al., 2019). *In vitro* approaches allow one to investigate the direct effects of a progestogen in a particular cell type which cannot be done using *in vivo* approaches. Therefore, determining the *in vitro* progestogen metabolism allows one to investigate the direct effects of progestogen metabolism on SR activity. Although one cannot be sure of whether this happens *in vivo*, *in vitro* data provide valuable proof of concept. The second central hypothesis of the present study was that the progestogens are differentially metabolised in extra-hepatic (U2OS) cells.

7.2.1 Differential progestogen metabolism

In the present study, the first aim under the second central hypothesis was to determine if the progestogens were differentially metabolised. Using U2OS cells, significant differences in progestogen metabolism were observed. In the study by Skosana *et al.,* P4 was significantly metabolised in all the cell lines investigated (Skosana et al., 2019). This may explain why the P4 efficacy via PR-B in U2OS cells using TC 1 was significantly lower for the other progestogens, except MPA (Fig. 3.2.1.1). The rapid P4 metabolism illustrates the justification for the use of R5020 as a reference progestogen for determining progestogen responses via the PR isoforms, since there is minimal metabolism of R5020 in most cell lines (Skosana et al., 2019). Moreover, cell-specific differences in progestogen metabolism were seen in the Skosana *et al.* 2019 study. This indicates that relative levels of enzymes that metabolise progestogens may be differentially expressed in these cell lines. The data in the present study provide compelling evidence that the progestogens are differentially metabolised in extra-hepatic cells.

7.2.2 Progestogen metabolism correlates with progestogen-induced PR activity

To address the second aim under this hypothesis, the progestogen-induced PR-B responses obtained in U2OS cells using TC 1 in the present study were assessed to determine whether a correlation occurred with progestogen metabolism observed in U2OS cells. For the first time, the present study shows that some progestogens (P4, NET and MPA) were significantly metabolised in U2OS cells while R5020, ETG, LNG

and NES were not. Furthermore, the present study shows that the PR-B EC_{50} values obtained in U2OS cells using TC 1, negatively correlate with metabolism, such that more metabolism of a progestogen is associated with a less potent progestogen response via PR-B (Fig. 4.3.1).

As shown in Fig. 4.3.3, when a P4 metabolising enzyme was inhibited by treatment with DNPN (Fig. 4.3.2), a significant difference in the resultant P4 response via PR-B was not detected in terms of potency and efficacy. However, the difference in P4 potencies via PR-B in the absence and presence of DNPN approached significance (Fig. 4.3.3b). The lack of a detectable significant difference could either be due to too few biological repeats and large error or because there was insufficient inhibition of P4 metabolism. From Figure 4.3.2, in the presence of DNPN, P4 metabolism was not fully inhibited. Using a higher concentration of DNPN may be required to fully inhibit the metabolism of P4 in order to detect significant differences in P4 potency and efficacy via PR-B. Unfortunately, at higher concentrations, DNPN was no longer soluble in the solvent.

The data in the present study provides compelling evidence to support the first aim of the second central hypothesis that progestogens are differentially metabolised. The data in the present study highlight the importance of progestogen metabolism in studies where SR biocharacter, potency and efficacy have been determined *in vitro*. The data shown in the present study provide evidence that the final progestogen concentration used *in vitro* may not be the same as the starting concentration and the progestogen metabolism is dependent on the cell line being used. The metabolism of ligands may confound the accurate determination of ligand-induced SR activity.

7.3 The ARVs activate PR-B in the absence of progestogens

7.3.1 MVC, TDF and DPV activate PR-B via different mechanisms

The data in the current study, which is presented in Enfield *et al.,* 2020a, show that not only were the PR-B transactivation responses with TDF observed using promoter-reporter assays in two different cell lines (Fig. 5.2.1 and 5.2.2), but these

transactivation responses were also seen using endogenously PR-regulated genes (Fig. 5.2.3). The fact that the TDF-induced PR-B transactivation was consistent in two different model systems (U2OS and MDA-PR-B+) suggests that this is not a cell-specific phenomenon. Additionally, in U2OS cells, the activation of the reporter gene with TDF was only seen in cells transiently transfected to express PR-B. This confirms that the response required the presence of PR-B and that the endogenous GR and other co-regulatory proteins did not activate the reporter gene in the presence of ARVs alone or in combination with progestogens (Fig. 5.2.1a and b). Of the three ARVs tested (TDF, DPV and MVC), TDF activated the *ptgs2* and *gilz* genes and was the only ARV that resulted in transrepression of the *il-6* gene (Table 5.3.1). The TDF data in the current study suggest that the mechanism by which TDF initiates transactivation by the PR is by phosphorylation at residue Ser294. This site is exclusively phosphorylated in the presence of progestogens by MAPKs (Treviño et al., 2013). Therefore, since TDF does not bind to PR-B, it may indirectly activate PR-B by activating MAPK pathways responsible for phosphorylating PR-B at the Ser294 residue such as the p42/p44 MAPK pathway (Treviño et al., 2013). The data in the present study suggest that phosphorylation at Ser294 of PR-B in the presence of TDF, is sufficient for PR-B transactivation and transrepression responses *in vitro*.

DPV, on the other hand, did not activate PR-B on the promoter-reporter assay in U2OS cells and MDA-PR-B+ cells (Fig. 5.2.1 and 5.2.2) but did on endogenous transactivation genes, *ptgs2* and *gilz* in MDA-PR-B+ cells (Fig. 5.2.3), suggesting that DPV-activated PR-B can only bring about activation of genes via endogenous PREs but not synthetic PREs. In addition, chromatin structure may play an important role for DPV-activated PR-B. The regulation of endogenous genes is modulated by endogenous chromatin structure which can either be in the form of methylated highly-condensed histones to form tightly-packed nucleosomes or loosely-compacted acetylated DNA (Mei et al., 2017, Xu et al., 2017), while this is not the case for plasmid DNA. Another distinct difference between plasmid DNA and endogenous genes is the ratio of DNA template to transcription machinery. For the promoter-reporter assay, the copy number of target DNA is much higher than that of an endogenous gene and this therefore may play a role in gene regulation in the presence of DPV. Unlike TDF, DPV did not result in transrepression of *il-6* (Fig. 5.2.3c). The mechanism employed by DPV to result in transactivation of PR-B may involve DPV competing for binding with P4 to

PR-B (Table 5.3.1). Although there is no PR-A transactivation data presented in this study, the binding data from the current study show that DPV also outcompetes P4 for binding to PR-A.

For MVC, transactivation by PR-B was seen on promoter-reporter assays and endogenous genes in MDA-PR-B+ cells (Table 5.3.1). These data suggest that the effect of MVC on PR-B activity is not dependent on PRE construct (synthetic or endogenous), on chromatin structure or the ratio of available DNA template to the transcription machinery. Similar to DPV, the transrepression of *il-6* was not seen in the presence of MVC. The transrepressive effects of the ARVs on PR-B endogenous gene responses may be ARV-specific. Only TDF was able to repress the expression of the *il-6* gene while DPV and MVC, although both able to increase the expression of *ptgs2* and *gilz*, had no effect on *il-6* expression. Because PR-B was phosphorylated in the presence of only TDF and not the other ARVs, this could mean that transrepression of *il-6* is only brought about by phosphorylated PR-B. In terms of the MVC mechanism of action for PR-B activation, the present study showed that MVC does not compete with P4 for binding to PR-B, nor does it increase PR-B phosphorylation (Table 5.3.1). Therefore, the mechanism by which MVC results in transactivation of PR-B responses remains to be investigated. PR-B could be phosphorylated at alternate sites, or the expression or activation status of PR-specific coregulators may be altered in the presence of MVC. Importantly the mechanisms identified in the present study may not be mutually exclusive and may be employed by TDF and DPV simultaneously.

Although this is not the first study to suggest ligand-independent activation of the PR, it is the first to investigate the potential mechanism. Previous studies have showed that the PR is activated in the presence of dopamine (Auger, 2001), growth factors (Daniel, A. R.; Lange, C. A., 2009, Mani, S.; Portillo, W., 2010) and cAMP (Mani, S.; Oyola, M. G., 2012) however, in each, the mechanism is not clearly defined. The data shown in the present study provide proof-of-concept that the ARVs TDF, DPV and MVC activate PR-B in an off-target manner via different mechanisms. The *in vitro* results indicate that these effects may have important physiological implications. Since the *ptgs2* gene plays a crucial role in modulating inflammation required for successful ovulation in women (Park et al., 2020), successful ovulation may be negatively affected because of the off-target PR-B activation. Similarly, the *gilz* and *il-6* genes are

involved in regulating the inflammatory response so in PR-expressing cells, in the presence of ARVs, the normal inflammatory response could be altered. The results in the present study show that TDF, DPV and MVC do not alter the LNG efficacy on endogenous genes transactivated by the PR, which is encouraging. This suggests that the biological effects of LNG will not be affected when in combination with ARVs. Additionally, it was shown by Dlamini *et al.* that LNG has no effect on the efficacy of TDF and DPV (Dlamini et al., 2019). Considering, the number of treatments which make use of ARVs alone (cART and PrEP) or in combination with a progestin (MPTs), emphasises the need for a thorough clinical investigation of the potential effects of off-target SR activation that these and other ARVs may have.

7.4 The GR inhibits PR-B activity

7.4.1 The GR modulates PR activity

The final aim of the present study was to determine the effect of the GR on PR transcriptional activity. In the present study the GR was determined to have an inhibitory effect on PR-B activity. It was shown by promoter-reporter assays that under high GR levels, the maximal PR response was inhibited in two cell lines (U2OS and MDA-PR-B+) (Fig. 6.2.1 and 6.2.2). Additionally, it was suggested by Fig. 6.2.2 that PR-B reciprocally modulated the GR response. Focussing on the effect the GR had on progestogen-mediated effects on endogenous mRNA levels via PR-B on a global scale, the PCR array showed that the GR had gene-specific effects on PR-B responses in the presence of NET (Fig. 6.3.1). The PCR array selected contained genes relating to human cancer, inflammation and immunity crosstalk. It is well known that one of the side-effects of unwanted PR activation is the development of breast cancer (Lim, E.; et al., 2016). Additionally, the PR plays an important role in regulating inflammation associated with ovulation in women (Park et al., 2020).

7.4.2 Gene-specific regulation of PR transcriptional responses by the GR

Results from the PCR array study revealed important insights both regarding gene-specific effects of NET as well as gene-specific modulation of PR actions by the GR. In the PCR array study, the ligand NET was chosen since it has no reported GR activity

at the chosen ligand concentration of 100 nM (Govender et al., 2014, Hapgood, J. P. et al., 2018). After treatment with NET in the presence of high or low levels of the GR, the PCR array results in the present study revealed 9 gene regulation groups (Fig. 6.3.1). The genes which fell into each group were categorised based on the gene expression changes from high to low levels of GR. These changes in expression were either present where it previously was not, potentiated or completely lost when GR expression was lower compared to when GR levels were higher. This section seeks to discuss the potential mechanisms allowing for and the physiological relevance of these significant changes in gene expression. Due to the number of genes in the array, for simplicity of this thesis only the genes that were validated will be discussed in more detail.

Surprisingly, 23/89 genes on the PCR array were regulated by NET. This suggests that the genes identified to be regulated by NET were PR-regulated genes. This implies that many of the pathways identified in this PCR array are influenced by the PR and these pathways may be modulated by the presence of the GR. Genes that fell into group A were upregulated by NET in the presence of PR-B and the GR. The pathways associated with these genes include chemokine signaling, regulation of the inflammatory response and TNF signaling. When the GR was removed, the expression of *ptgs2* was potentiated (group C) which suggests that the unliganded-GR had an inhibitory effect on the expression of this gene and therefore may affect the regulation of the ovulatory inflammatory response (Park et al., 2020). The genes that were upregulated only when the GR was absent (group B) were associated with pathways relating to metabolism, proliferation, cell survival, growth and angiogenesis such as the Jak-STAT signaling and PI3K-Akt signaling pathways. The fact that these genes were only expressed when the expression of the GR was reduced suggests that the unliganded-GR modulates the activity of these important cellular processes. Similar effects were observed for genes that were downregulated in the presence of PR-B and the GR (group E). The genes in group E were associated with regulating cellular apoptosis, prostate cancer, bladder cancer, cytokine-cytokine interaction, pancreatic cancer and chemokine signaling. Of note, when the expression of the GR was reduced, the repression of most of these genes was lost (group H) suggesting that the unliganded-GR and not PR-B, represses the expression of most of these important cellular functions.

The expression of *ptgs2* (groups A and C), *cxcl1* (group A) and *tlr4* (group E) from the PCR array were validated using real-time qPCR (Fig. 6.3.2). Previous research showed that the expression of *ptgs2* was upregulated after treatment with P4 (Hermenegildo et al., 2005, Siemieniuch et al., 2012), while the expression of *cxcl1* (Remus et al., 2015) and *tlr4* (Wang, Z.; et al., 2011, Zhu et al., 2013) was repressed after P4 treatment. To the present author's knowledge, the effect of progestins on the expression of these genes has not been investigated previously and this is the first study to show that these genes are regulated by NET-activated PR-B. Interestingly, these genes differ greatly in their promoter architecture which may explain the gene-specific expression differences observed for these genes in the presence of high and low GR levels. Motifs matching the consensus binding sites for NFκB, AP-1 and CREB have been identified in the *tlr4* gene sequence (Escoubet-Lozach et al., 2011, Nilsson et al., 2006). Although the *cxcl1* gene contains CREB and NFκB binding sites like the *tlr4* gene, it also contains CAAT displacement protein (CDP) binding sites (Amiri & Richmond, 2003, Saliba et al., 2019). The GR interacts differentially with the TFs binding to these sites. Therefore, the gene-specific differences in expression with and without GR knockdown in the presence or absence of NET may be explained by these differences in promoter architecture of these genes and others identified from the PCR array.

The expression of *cxcl1* (group A) and *tlr4* (group E) exhibited differential gene expression patterns in the presence of high GR compared to low GR (Fig. 6.3.2). Some studies suggest that these genes are regulated by activated GR. P4 has been shown to inhibit *cxcl1* expression through a mechanism involving inhibition of NFκB (Kavandi et al., 2012). A similar inhibitory effect on *cxcl1* gene expression in the presence of dex was observed in a different study (Shieh et al., 2014). Similarly, in two studies investigating *tlr4* gene expression, P4 treatment inhibited the expression of the *tlr4* gene through inhibition of the NFκB pathway (Wang, Z.; et al., 2011, Zhu et al., 2013). Importantly, it is accepted in the field that high concentrations of P4, such as those used in the studies mentioned above, can activate the GR (Africander et al., 2011, Lei et al., 2012, Polis et al., 2016a) and dex is a well-known GC. Therefore, it would not have been surprising if agonist-activated GR regulated the expression of

these genes. However, NET is not a GR agonist and would be predicted to have no influence on the differential expression of *cxcl1* and *tlr4* with and without GR knockdown. It is therefore likely that the responses by the 9 groups of genes showing differential sensitivity to low GR levels in the PCR array (Fig. 6.3.1) were due to gene-specific effects of the unliganded-GR. The potential mechanism by which the unliganded-GR carries out these effects are discussed in section 7.4 of this chapter.

Importantly, the expression of *il-6* and *cxcl2* from the PCR array were not validated using real-time qPCR. This is surprising since the other genes selected were validated even though the RNA from the same experiments was used and converted to cDNA for the validation experiments. Therefore, the lack of validation for *il-6* and *cxcl2* expression between the PCR array and the real-time qPCR data may be due to differences in the primer sequences and/or PCR conditions used in the PCR array compared to the real-time qPCR experiments.

The PCR array revealed that some genes were exclusively expressed when GR levels were lower (Fig. 6.3.1, group B, Table 6.3.1 and Appendix B, Fig. B9), while other genes were upregulated when both PR-B and GR were present (Fig. 6.3.1, group A, Table 6.3.1 and Appendix B, Fig. B10); however, the expression of other genes was potentiated when GR levels were lower (Fig. 6.3.1, group C, Table 6.3.1 and Appendix B, Fig. B10). Similar effects were seen for the expression of genes that were transrepressed (Fig. 6.3.1, groups E, F and G, Table 6.3.1 and Appendix B, Fig. B10). In summary, the PCR array revealed that majority of the genes (6/11, 55%) that were upregulated by NET were only expressed when GR levels were low (Fig. 6.3.1, group B) which is consistent with the GR inhibiting PR. However, the repression of the majority of the genes that were downregulated by NET (12/23, 52%) (Fig. 6.3.1, group E) was lost when GR levels were low (9/12, 75%) (Fig. 6.3.1, group H) which is inconsistent with the GR inhibiting the PR and rather suggests that the PR can only repress the expression of these genes if the GR is present.

The gene-specific regulation of PR transcriptional responses by the GR could be due to promoter-specific effects, such as the presence and frequency of PREs and/or other regulatory *cis*-elements. For example, *cxcl1* and *ptgs2* both fell into group A; however, only *ptgs2* fell into group C (Appendix B, Fig. B10). As discussed above, the *ptgs2*

gene contains binding sites for RUNX1, myb, GATA-1 (Liu et al., 2009), CREB and NFκB (Park et al., 2020) while the *cxcl1* gene contains binding sites for NFκB (Burke et al., 2014) and CDP (Saliba et al., 2019). These differences in the *cis* regulatory elements may have contributed to the difference in gene expression under high and low GR in the presence of NET. Of note, although no consensus PRE sequence has been identified in the *ptgs2* gene, the data from the present study suggests that PREs are present. This is because the expression vector used in the promoter-reporter assays contained PREs upstream of the reporter gene and the inhibitory effect of the GR on the PR-induced activity was observed (Fig 6.2.1 and 6.2.2). Furthermore, the same inhibitory effect of the GR on PR-induced efficacy was observed for the expression of the *ptgs2* gene (Appendix B, Fig. B10). A detailed analysis of all the known *cis*-elements (as well as putative *cis*-elements) for all the genes in each group is beyond the scope of this thesis. However, it would be important to do in future to better understand the mechanism of regulation of the genes within each group.

Importantly, because the expression of the GR was reduced but not completely ablated (Appendix B, Fig. B9), it is possible that the PR transcriptional response may be affected differently if the expression of the GR was completely lost. For example, the expression of genes that were potentiated when GR levels were low (group C), may be even more enhanced if GR expression was completely ablated. Nevertheless, the PR promoter-reporter gene expression data in the present study conducted in the presence and absence of the GR using PR-specific ligands provides compelling evidence which supports the hypothesis that the GR can modulate PR transcriptional responses. Furthermore, the PCR array data suggests there are gene-specific effects of NET and that the GR modulates PR transcriptional responses in a gene-specific manner. The extent to which the presence of the GR affected the determination of progestogen-, model system-, promoter- and isoform-specific responses of progestogens via the PR (first central hypothesis) in this study was not investigated for all models and genes. Importantly however, characterising PR activity in the absence of detectable GR expression is unlikely to be physiologically relevant because to the best of the present author's knowledge, all cells that express the PR also express the GR *in vivo*.

7.4.3 Mechanism behind the GR-mediated modulation of PR transcriptional responses

The co-immunoprecipitation data showed that PR-B and the GR can exist in the same protein complex in the absence of ligand (Fig. 6.3.1) and the assay to detect PR phosphorylation levels showed that PR-B was phosphorylated significantly more in the absence of the GR in the presence of NET, compared to in the presence of GR and NET (Fig. 6.4.3a). The fact that co-immunoprecipitation using the anti-PR antibody was unsuccessful (Appendix B, Fig. B14) may be due to the PR being inaccessible to the antibody when it is present in the GR-PR complex (Kotitschke et al., 2009).

Based on the data in the present study, the schematic shown in Figure 7.4.3.1 proposes one possible mechanism by which the GR could inhibit PR-B transcriptional responses via a PRE/GRE (Fig. 7.4.3.1). As shown in Figure 7.4.3.1a, in the absence of NET the PR is depicted as residing in the nucleus (Henríquez et al., 2017, Scarpin et al., 2009); however, some studies suggest that in the absence of ligand, the PR is mostly nuclear but some is cytoplasmic depending on cell type (not shown) (Asavasupreechar et al., 2020, Grimm et al., 2016). The unliganded-GR, on the other hand, is depicted as being mostly cytoplasmic with some being nuclear (Præstholm et al., 2020, Wikström et al., 1987). In the absence of NET, the PR exists as free monomers in the nucleus (Grimm et al., 2016) (Fig. 7.4.3.1a) and both the PR and GR are associated with HSPs and other co-regulatory proteins (not shown). In this model, in the presence of both GR and PR-B and in the absence of NET, the GR is associated with some PR-B in the same protein complex in the nucleus (Fig. 7.4.3.1a). Additionally, it is depicted in the model that an unliganded-GR dimer, as suggested by some studies directly occupies PRE/GREs (Hapgood, J. P.; et al., 2016, Ogara et al., 2019, Ritter & Mueller, 2012, Ritter & Mueller, 2014, Robertson et al., 2013) and modulates transcription of PR-regulated genes (Ogara et al., 2019, Ritter & Mueller, 2012, Ritter & Mueller, 2014) (Fig. 7.4.3.1a). In the study by Ogara *et al.,* it was revealed by ChIP-Seq that unliganded-GR can occupy the same binding sites as liganded-PR which prevented liganded-PR binding; however, transcription was still initiated from some genes (Ogara et al., 2019). In the study by Ritter and Mueller (2014), ChIP experiments showed that unliganded GR occupied and initiated

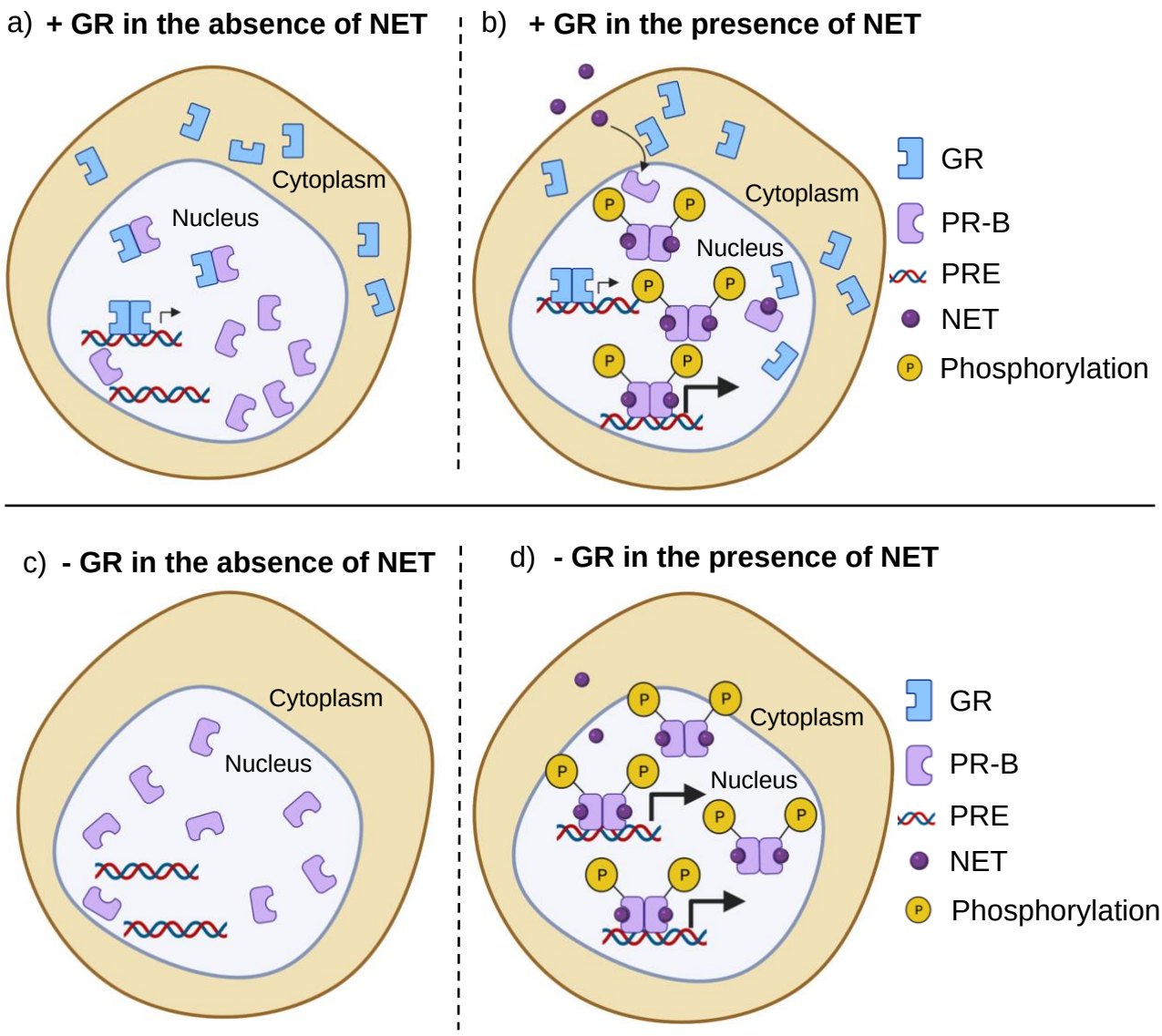

Figure 7.4.3.1: The proposed mechanism by which the GR inhibits PR-B activity.
The schematic is based on the data obtained in Chapter 6 of the present study.

transcription from promoter regions of some genes (Ritter & Mueller, 2014). Although previous studies provide compelling evidence to suggest that unliganded GR occupied PRE/GREs, this remains to be proven for the genes under investigation in the current study. The PR is basally phosphorylated in the absence of NET (not shown) (Clemm et al., 2000, Grimm et al., 2016, Pierson-Mullany & Lange, 2004).

According to the model, in the presence of NET and the GR, the PR undergoes a conformational change (not shown) upon NET binding and the GR dissociates from the PR. The PR is phosphorylated by MAPKs and the liganded PR monomers dimerise in the nucleus (Grimm et al., 2016, Kuiper & Brinkmann, 1994, Weigel & Moore, 2007)

(Fig. 7.4.3.1b). In the nucleus, the liganded PR dimers bind to PREs within the promoters of PR-regulated genes to initiate transcription (Fig. 7.4.3.1b). In the model, although two PRE sites are available for liganded PR dimers to bind, only one PRE site is occupied by a PR dimer to illustrate the concept that the unliganded-GR inhibits the binding of liganded PR dimers to some PREs and hence the progestogen-induced PR transcriptional response (Fig. 7.4.3.1b). This model would have to assume that the unliganded-GR dimer has a higher affinity for a PRE/GRE than the liganded-PR dimer, which remains to be investigated. The model suggests that in the presence of the GR and NET, the GR is no longer associated with PR as revealed by the co-immunoprecipitation data (Fig. 6.4.1). In the presence of NET (Fig. 7.4.3.1b), the unliganded-GR initiates the same transcriptional response from the PRE as in the absence of NET (Fig. 7.4.3.1a), but this is much less than the transcriptional response initiated from the liganded PR dimer bound to the PRE (Fig. 7.4.3.1b). The relative response of an unliganded GR dimer compared to a liganded PR dimer on a PRE/GRE remains to be determined.

In the absence of the GR and NET, there are more free PR monomers present in the nucleus compared to in the presence of the GR and the PREs are not occupied by the unliganded-GR dimer (Fig. 7.4.3.1c). In the absence of the GR and in the presence of NET, NET binds PR-B, which is phosphorylated, undergoes dimerization and binds to PREs (Fig. 7.4.3.1d). In the absence of the GR, all the PREs are free and available for liganded PR-B dimers to bind to initiate transcription (Fig. 7.4.3.1d). This is consistent with the data in Figure 6.2.1 and Figure 6.2.2 which revealed that there is a significant increase in progestogen-induced PR-B efficacy under low levels of GR compared to when GR levels are higher (Fig. 6.2.1 and 6.2.2). In addition, the model depicts that in the absence of the GR (Fig. 7.4.3.1d), phosphorylation of liganded-PR is increased compared to in the presence of the GR (Fig. 7.4.3.1b). Although it is thought that ligand-binding induces PR-B phosphorylation (Clemm et al., 2000, Grimm et al., 2016, Grimm et al., 2014), it is possible that when ligand binds to the PR when in a complex with GR, this phosphorylation process is inhibited or delayed. This could be due to the fact that the GR and PR first need to dissociate before phosphorylation can occur causing an inhibition of PR phosphorylation. This is supported by the data in the present study which showed a significant increase in phosphorylated PR-B when

GR levels were lower compared to when GR levels were higher in the presence of NET (Fig. 6.4.3).

In terms of the differential effects of the GR on PR-regulated genes (Fig. 6.3.1), this may be because some PR-regulated genes require Ser294-phosphorylated PR while others do not (Grimm et al., 2016, Grimm et al., 2014). This is because different PR phosphorylation sites allow for different coregulatory protein interactions (Grimm et al., 2016). According to the simplistic model proposed in this study, the presence of the GR prevents active PR dimers binding to PREs, thereby inhibiting transcription. This model therefore depicts PR-regulated genes that do not require Ser294-phosphorylation. However, at the same time this model shows that the presence of the GR reduces the number of active PR dimers phosphorylated at Ser294, which could play an important role on more complex promoters requiring Ser294-phosphorylated PR (not shown). In other words, this model suggests that the unliganded-GR can inhibit PR-regulated genes via two different mechanisms and is likely to affect PR-regulated genes that require Ser294-phosphorylated PR, as well as those that do not.

The physiological implications of these data and the proposed model are that in the absence and presence of PR ligands, the GR associates with PR-B and inhibits its function, more specifically the maximal response. Therefore, in cells where both the PR and GR are expressed, the final PR maximal response will be reduced for some genes. As a result, the following PR-regulated functions could be reduced; reproductive function (Lydon et al., 1995), regulation of inflammation (Grimm et al., 2016, He et al., 2004, Park et al., 2020), cognition (Gibbs, 2000, Gonzalez et al., 2007), mitochondrial function (Irwin et al., 2008) and neurogenesis (Giachino et al., 2003). Because of the number of treatments designed to target the PR specifically (HCs, HRT and MPTs), the effect of changing GR levels on PR activity needs to be critically assessed. Because the GR is ubiquitously expressed, this inhibitory effect is likely to occur in many cell- and possibly tissue types *in vivo*. The data in the present study emphasise the important role the GR plays in regulating progestogen-induced PR activity.

7.5 Study limitations

One limitation of the present study is that all the experiments were conducted *in vitro* and whether these effects would occur *in vivo* is unknown and, in some cases, not possible to determine. While *in vitro* methods allow for the determination of direct effects of a treatment in a particular cell type, these approaches are limited in that they do not capture the complexity of organ systems. *In vivo* approaches, on the other hand, allow for a holistic determination of the effect of various treatments on biological responses. In addition, it might have been useful to use ER/PR null cell lines for comparative purposes and the fact that these cell lines were not used does present a limitation to the present thesis. More specifically, the PR responses in the chosen MDA-231 cell line may not be the same as those observed in luminal breast cancer cells.

Another limitation of the present study is that the effect of PR levels on the resultant progestogen-induced PR responses using promoter-reporter assays in the two different cell lines tested (U2OS and MDA-PR-B+) could not be determined. This is because although the amount of the transiently transfected reporter plasmid was constant between the two cell lines, the total amount of transiently transfected DNA, changed between these two cell lines. Therefore, whether the cell line, amount of PR-B protein or amount of transiently transfected DNA affects the progestogen- induced PR responses, remains to be investigated. Additionally, the effect of total PR protein on progestogen-induced PR isoform activity could not be accurately determined since it has been suggested that the antibody used to detect PR protein may be more sensitive at detecting PR-A protein compared to PR-B (Fabris et al., 2017).

Importantly, because of the complexity of gene activation by SRs, other mechanisms by which the ARVs could result in transactivation of PR-B were not explored such as; phosphorylation at other residues, changes in post-translational modifications, or changes in expression of PR-specific co-activators such as p300 or SRC-1. Additionally, the present study only provides information at a single timepoint. ARV-induced PR activation by the mechanisms investigated in the present study, may have occurred at earlier or later timepoints.

One of the key findings of the present study is that in some cases it is difficult to establish statistically significant differences by dose-response analysis for efficacy and potency *in vitro*, when multiple ligands are investigated in parallel. It is common in the field for conclusions to be drawn as to whether one ligand is more potent than another on the basis of two or three independent dose-response experiments, without any statistical analysis of significance of difference (Bain et al., 2015, Kumar et al., 2017, Sasagawa et al., 2008). This can be misleading, as it is possible that where such differences are reported, they may in fact not be statistically significantly different. In addition, when no statistically significant differences are detected as in some of the data in the present study, differences may occur but be beyond the statistical power of the assays used. Thus, caution should be used when drawing conclusions about differences between ligands with or without any statistical analysis of significance of difference.

Lastly, this study is limited by the use of few biological repeats and a relatively large degree of biological variability and/or error in some experiments. For example, for the P4 metabolism inhibition investigation, although metabolism was inhibited, no significant differences in PR-B efficacy and potency were detected. To overcome this, a power analysis should be performed to determine the number of biological repeats required to appropriately detect statistically significant differences between treatments and conditions.

Chapter 8

Conclusions and future perspectives

8.1 Conclusions

Progestogen activity via the PR isoforms has been determined and accurately characterised *in vitro*. The progestogen responses via PR-B were determined to be largely influenced by model system, metabolism and by transfection condition in at least one cell line. The present study shows that relative potencies of the progestogens are more sensitive than efficacies to the model system used. Additionally, for the first time, the present study shows that for a wide panel of progestogens, the transcriptional responses were more potent and less efficacious via PR-A compared to PR-B which highlights the significance of varying ratios of PR-A and PR-B. Furthermore, as shown by endogenous gene responses, the MPA-induced PR responses were determined to be highly promoter-specific. One of the key findings of the progestogen-induced PR activation data is that it is difficult to establish statistically significant differences by dose-response analysis for efficacy and potency *in vitro*. In the present study several significant differences were detected between the efficacies and potencies of several progestogens. While some data are consistent across studies (Table 7.1.1), differences in absolute progestogen potencies between studies could be due to multiple factors, including differences in cell type, promoter-reporter constructs, method of dose-response analysis, or the PR isoform investigated. The present study shows that the potencies are well below the reported serum concentration range of these progestogens found in women (Table 7.1.1), which suggests that several other factors may contribute to the resultant PR response such as co-factors and cell-specific effects. The *in vitro* data shown in this study suggest that the absolute values of potencies and efficacies and even biocharacter via the PRs are likely to vary between cell types and possibly tissue types *in vivo*. Moreover, the present study shows that the rank order for progestogen efficacies and potencies does not correlate with rank order for RBAs for PR-B. The *in vitro* data from the present study therefore support the first central hypothesis which is that the progestogens have differential

and promoter-specific effects on PR activity which are cell-specific and correlated to progestogen metabolism.

Most surprisingly, PR-B was also shown to be activated by ARVs in the absence of progestogens. The mechanism by which the ARVs result in the PR-B activation appears to be ARV-specific and these mechanisms may all occur simultaneously. This off-target activation of PR-B provides a possible explanation for at least some of the side-effects that arise due to long-term ARV use. To confirm that the PR is directly involved, cells should be treated with PR-specific siRNA to knockdown the PR followed by treatment with the ARVs to determine if the same effect on the endogenously regulated genes is still observed. Lastly, the ubiquitously expressed GR was shown to inhibit PR efficacy in a gene-specific manner most likely by association with PR-B in the same protein complex. It is hypothesized that the unliganded-GR occupying PREs may prevent liganded-PR from binding. By associating with PR-B, the GR reduces phosphorylation of liganded-PR-B and therefore there is less progestogen-induced transcription. When the GR is absent, there is no GR-induced decrease in PR phosphorylation and no GR-induced inhibition of binding of liganded-PR to GRE/PREs. This therefore allows for an enhanced progestogen-induced PR transcriptional response compared to in the presence of the GR. Future studies should be done to investigate the reciprocal immunoprecipitation of the GR and the PR by overexpressing a flag-tagged PR followed by pulldown with an anti-flag antibody. The samples should then be probed by western blot using the GR antibody. In addition, the fact that there is PR pulldown in the IgG control sample shows that this assay may need to be optimised for future experiments.

Taken together, these data provide valuable insight into the complexity of determining PR activity and highlights the multiple factors which regulate PR responses. The present study has determined that a number of factors contribute to the final progestogen induced PR response. Table 8.1 shows that in addition to the progestogen type and concentration, the promoter sequence, progestogen metabolism, PR ratios, ARVs, the GR and phosphorylation at Ser294 of the PR, all affect the progestogen induced PR activity. The effect of cell type and PR protein expression on progestogen induced PR activity requires further investigation. In these

experiments, more than one variable was changed therefore, one cannot be sure of the exact effect of these two variables on progestogen-induced PR activity.

Table 8.1: Summary of factors investigated in the present study which influence PR activity.

Factor	Influences PR activity?
Progestogen type	✓
Progestogen concentration	✓
Transfection condition	✓
Cell type[1]	?
Promoter sequence	✓
Progestogen metabolism	✓
PR ratios	✓
PR protein expression[1]	?
TDF	✓
DPV	On endogenous promoters only
MVC	✓
GR	✓
Phosphorylation	✓

[1]More investigation is required for these factors to determine the effect on progestogen induced PR activity since more than one variable was altered in these experiments.

8.2 Future perspectives

Because of the PR isoform-specific progestogen responses, it would be interesting to investigate the final PR response in the presence of both PR isoforms. It was suggested by the Vegeto group that the PR-A inhibits PR-B responses (Vegeto et al., 1993). Future work should investigate PR activity in the presence of varying PR ratios to verify whether a PR-A dominant ratio would result in a less efficacious but more potent PR response as suggested by the present study.

To confirm the negative correlation between progestogen metabolism and potencies via PR-B, one should use a higher concentration of DNPN to prevent more P4 metabolism. Unfortunately, a higher concentration of DNPN could not be used in the present study due to solubility limitations of the solvent used. Future studies could investigate alternate solvents to allow for a higher final concentration of DNPN in solution. Additionally, alternative inhibitors of the other enzymes involved in P4 metabolism such as SRD5A1, SRD5A2 or CYP3A should be investigated. Since HCs have different modes of administration which may result in different sites of metabolism, future work could investigate the relative levels of progestogen-metabolising enzymes in different cells and tissues. This information could be used to further investigate whether progestogens are differentially metabolised in different cell and tissue types. Since P4, NET and MPA were all significantly metabolised, it would be interesting to determine which metabolites are produced and whether these metabolites can elicit activity via the PR.

For the MVC-induced PR-B activity, other mechanisms by which PR-B could be activated need to be explored. After a 3-hour incubation period, the present study has ruled out binding to PR-B and changes in PR-B phosphorylation at Ser294 as potential mechanisms for MVC-induced PR-B activity. Other mechanisms which could be investigated include changes in expression of PR-specific co-activators such as p300 or SRC-1 (Liu, Z. et al., 2001) or investigating the degree of phosphorylation at other PR phosphorylation sites. Other time-points should also be investigated as some changes may occur earlier or later than 3 hours. To further unravel the mechanism behind the TDF-induced activation of PR-B, Ser294 PR mutants could be used in promoter-reporter assays. This would confirm whether TDF-mediated phosphorylation of PR-B at this residue is required for generating a PR transcriptional response. Additionally, the ARVs, TDF, DPV and MVC were shown to bind to PR-A and did not alter the degree of PR-A phosphorylation at Ser294. Future studies should investigate whether the ARVs can transactivate PR-A activity in the absence and presence of progestogens.

The model of unliganded GR-induced inhibition of PR responses proposed in the present study presents some areas for future research. For example, the model

assumes that the unliganded-GR dimer has a higher affinity for a PRE/GRE than the liganded-PR dimer which is why the unliganded GR occupies the PRE/GRE even in the presence of NET. To confirm this, a DNA electrophoretic mobility shift assay (EMSA) should be performed. This assay will allow for a direct comparison of the binding of unliganded-GR dimers and liganded-PR dimers to the PRE/GRE oligonucleotide. Additionally, the model predicts that the relative response of the unliganded GR dimer is much lower compared to a liganded PR dimer on a PRE/GRE; however, this needs to be investigated. This could be investigated by ChIP to confirm which SR dimer is occupying the PRE/GRE followed by real-time qPCR investigating the expression of a PRE-dependent gene. Importantly, however, the unliganded-GR did not inhibit the PR transcriptional responses for all genes. Therefore, to better understand the mechanism behind the gene-specific regulation of PR genes by the GR, a detailed analysis of the pathways and *cis*-elements in the promoters of the genes in each group should be performed.

The current study provides compelling evidence that the PR-B/GR transcriptional responses may be reciprocally modulated. While the effect of the PR on GR activity was only investigated by promoter-reporter assays in the present study, more experiments are required to determine whether these receptors do in fact reciprocally modulate each other. As shown in the present study several differences between the promoter-reporter assay and the endogenous gene expression data using real-time qPCR were observed. Therefore, future studies should investigate the expression of GR-regulated genes in the presence and absence of the PR to obtain more physiologically relevant data.

Importantly, for all the *in vitro* data in the present study, whether these data are physiologically relevant remains to be investigated. To gain more insight into the different factors that affect PR activity (summarised in Table 8.1), future experiments could be conducted using female genital tract (FGT) cells (cells from the endometrium, uterus, cervix, vagina and/or ovaries) obtained from biopsies from women exclusively on ARVs, an HC or both an ARV and HC or neither. As suggested by the *in vitro* data shown in the present study, ARVs and the progestogens used in HCs affect PR transcriptional responses. The effect of these treatments on PR biological action such as uterine development (Lydon et al., 1995) and ovulatory inflammation (Park et al.,

2020) has not been investigated previously. This could be investigated by looking at the expression of specific genes by extracting RNA from the FGT cells and quantifying gene expression using real-time qPCR. These genes could include GATA binding protein 2 (*gata2*), SRY-Box Transcription Factor 17 (*sox17*) and enhancer of zeste homolog 2 (*ezh2*) for uterine function (Wu et al., 2018). Importantly obtaining these biopsies of women exclusively on ARVs, an HC or both an ARV and HC or neither would require a clinical trial and may be difficult to obtain. Nevertheless, this *in vivo* approach would provide more information about how some of the different factors (summarised in Table 8.1) influence the biological action of the PR.

The present study provides compelling evidence that progestogens induce promoter- and progestogen-specific responses on the expression of PR-regulated genes and that these effects may be carried out by different mechanisms. It is shown in the current study that ARVs can activate the PR by different mechanisms which may not be mutually exclusive. The present study also shows that the GR affects PR activity in a gene-specific manner. In terms of physiological implications, the data from the current study suggest that progestogens used in HCs and HRT have the potential to elicit differential PR action depending on the specific progestogen, the ratio of PR isoforms, the extent of progestogen metabolism, the promoter sequence, the levels of expression of the GR and whether or not the patient is using ARVs in addition to a progestogen treatment. The data from the present study highlight that progestogens act differently and that it cannot be assumed that the PR responses on cognition, regulation of inflammation, mitochondrial function, neurogenesis, female reproduction and disease will be the same for all progestogens.

References

Abdel-Hafiz, H., Dudevoir, M.L. & Horwitz, K.B. 2009. Mechanisms Underlying the Control of Progesterone Receptor Transcriptional Activity by SUMOylation. *J Biol Chem.* 284(14). DOI:10.1074/jbc.M805226200.

Africander, D., Verhoog, N. & Hapgood, J.P. 2011. Molecular mechanisms of steroid receptor-mediated actions by synthetic progestins used in HRT and contraception. *Steroids.* 76(7):636-652. DOI:10.1016/j.steroids.2011.03.001.

Agbo, L. & Lambert, J. 2019. Proteomics contribution to the elucidation of the steroid hormone receptors functions. *Journal of Steroid Biochemistry and Molecular Biology.* 192. DOI:10.1016/j.jsbmb.2019.105387.

Akison, L.K., Robertson, S., Gonzalez, M.B., Richards, J.S., Smith, C.W., Russel, D.L. & Robker, R.L. 2018. Regulation of the ovarian inflammatory response at ovulation by nuclear progesterone receptor. *AM J Reprod Immunol.* 76(6). DOI:10.1111/aji.12835.

Amiri, K.I. & Richmond, A. 2003. Fine Tuning the Transcriptional Regulation of the CXCL1 Chemokine. *Prog Nucleic Acid Res Mol Biol.* 74:1-36.

Arberas, H., Guardo, A., Bargallo, M., Maleno, M., Calvo, M., Blanco, J., Garcia, F., Gatell, J. et al. 2013. In vitro effects of the CCR5 inhibitor maraviroc on human T cell function. *Journal of Antimicrobial Chemotherapy.* 68(3):577-586.

Arici, A., Marshburn, P.B., MacDonald, P.C. & Dombrowski, R.A. 1999. Progesterone Metabolism in Human Endometrial Stromal and Gland Cells in Culture. *Steroids.* 64(8). DOI:10.1016/S0039-128X(99)00029-X.

Asavasupreechar, T., Saito, R., Miki, Y., Edwards, D.P., Boonyaratanakornkit, V. & Sasano, H. 2020. Systemic distribution of progesterone receptor subtypes in human tissues. *Journal of Steroid Biochemistry and Molecular Biology.* 199. DOI:10.1016/j.jsbmb.2020.105599.

Attardi, B.J., Koduri, S. & Hild, S.A. 2010. Relative progestational and androgenic activity of four progestins used for male hormonal contraception assessed in vitro in relation to their ability to suppress LH secretion in the castrate male rat. *Mol Cell Endocrinol.* 328. DOI:10.1016/j.mce.2010.06.010.

Auger, A.P. 2001. Ligand-independent activation of progestin receptors: relevance for female sexual behaviour. *Reproduction.* 122:847-855.

Avenant, C., Kotitschke, A. & Hapgood, J.P. 2010. Glucocorticoid receptor phosphorylation modulates transcription efficacy through GRIP-1 recruitment. *Biochemistry.* 49(5).

Baeten, J.M., Palanee-Phillips, T., Brown, E.R., Schwartz, K., Soto-Torres, L.E., Govender, V., Mgodi, N.M., Matovu Kiweewa, F. et al. 2016. Use of a Vaginal Ring Containing Dapivirine for HIV-1 Prevention in Women. *N Engl J Med.* 375(22):2121-2132. DOI:10.1056/NEJMoa1506110.

Bain, P.A., Kumar, A., Ogino, Y. & Iguchi, T. 2015. Nortestosterone-derived synthetic progestogens do not activate the progestogen receptor of Murray-Darling rainbowfish (Melanotaenia fluviatilis) but are potent agonists of androgen receptors alpha and beta. *Aquat Toxicol.* 163. DOI:10.1016/j.aquatox.2015.03.021.

Ballaré, C., Uhrig, M., Bechtold, T., Sancho, E., Domenico, M.D., Migliaccio, A., Auricchio, F. & Beato, M. 2002. Two Domains of the Progesterone Receptor Interact with the Estrogen Receptor and Are Required for Progesterone Activation of the c-Src/Erk Pathway in Mammalian Cells. *Molecular and Cellular Biology.* 23(6). DOI:10.1128/MCB.23.6.1994–2008.2003.

Bamberger, C.M., Bamberger, A.M., de Castro, M. & Chrousos, G.P. 1995. Glucocorticoid receptor beta, a potential endogenous inhibitor of glucocorticoid action in humans. *J Clin Invest.*

Bayer, P.L.C. 2017. *Product information for Noristat 200mg, solution for intramuscular injection*. Available: https://www.medicines.org.uk/emc/product/1134/smpc#gref [2021, 10 January].

Beato, M. & Klug, J. 2000. Steroid hormone receptors: an update. *Human Reproduction Update.* 6(3).

Bereshchenko, O., Migliorati, G., Bruscoli, S. & Riccardi, C. 2019. Glucocorticoid-Induced Leucine Zipper: A Novel Anti-inflammatory Molecule. *Front Pharmacol.* 10(308). DOI:10.3389/fphar.2019.00308.
Bick, A.J., Louw-du Toit, R., Skosana, S.B., Africander, D. & Hapgood, J.P. 2020. Pharmacokinetics, metabolism and serum concentrations of progestins used in contraception. *Pharmacol Ther.* 222. DOI:10.1016/j.pharmthera.2020.107789.
Billich, A., Bornancin, F., Mechtcheriakova, D. & Françios, N. 2005. Basal and induced sphingosine kinase 1 activity in A549 carcinoma cells: function in cell survival and IL-1β and TNF-α induced production of inflammatory mediators. *Cellular Signalling.* 17(10).
Bledsoe, R.K., Montana, V.G., Stanley, T.B., Delves, C.J., Apolito, C.J., McKee, D.D., Consler, T.G., Parks, D.J. et al. 2002. Crystal Structure of the Glucocorticoid Receptor Ligand Binding Domain Reveals a Novel Mode of Receptor Dimerization and Coactivator Recognition. *Cell.* 110(1). DOI:10.1016/S0092-8674(02)00817-6.
Boonyaratanakornkit, V., Bi, Y., Rudd, M. & Edwards, D.P. 2008. The role and mechanism of progesterone receptor activation of extra-nuclear signaling pathways in regulating gene transcription and cell cycle progression. *Steroids.* 73. DOI:10.1016/j.steroids.2008.01.010.
Bradford, M.M. 1976. A rapid sensitive method for the quantitation of microgram quantities of protein utilizing the principle of protein-dye binding. *Anal Biochem.* 72.
Bray, J.D., Jelinsky, S., Ghatge, R., Bray, J.A., Tunkey, C., Saraf, K., Jacobsen, B.M., Richer, J.K. et al. 2005. Quantitative analysis of gene regualtion by seven clinically relevant progestins suggests a highly similar mechanism of action through progesterone receptors in T47D breast cancer cells. *Journal of Steroid Biochemistry and Molecular Biology.* 97. DOI:10.1016/j.jsbmb.2005.06.032.
Brzozowski, A.M., Pike, A.C., Dauter, Z., Hubbard, R.E., Bonn, T., Engström, O., Ohman, L., Greene, G.L. et al. 1997. Molecular basis of agonism and antagonism in the oestrogen receptor. *Nature.* 389. DOI:10.1038/39645.
Bunma, T., Vonnahme, K.A., Vasquez-Hidalgo, M.A., Swanson, K.C., Dorsam, S.T., Ward, A.K., Navanukrav, C. & Grazul-Bilska, A.T. 2020. Nuclear and membrane progesterone receptors expression in placenta from early to late pregnancy in sheep: Effects of restricted nutrition and realimentation. *Theriogenology.* 148:95-102. DOI:10.1016/j.theriogenology.2020.02.041.
Burke, S.J., Lu, D., Sparer, T.E., Masi, T., Goff, M.R., Karlstad, M.D. & Collier, J.J. 2014. NF-κB and STAT1 control CXCL1 and CXCL2 gene transcription. *Endocrinology and Metabolism.* 306(2):131-149. DOI:10.1152/ajpendo.00347.2013.
Byrns, M.C. & Penning, T.M. 2009. Type 5 17β-Hydroxysteroid Dehydrogenase/Prostaglandin F Synthase (AKR1C3): Role In Breast Cancer and Inhibition by Nonsteroidal Antiinflammatory Drug Analogs. *Chem Biol Interact.* 178. DOI:10.1016/j.cbi.2008.10.024.
Cabeza, M., Heuze, Y., Sánchez, A., Garrido, M. & Bratoeff, E. 2014. Recent advances in structure of progestins and their binding to progesterone receptors. *Journal of Enzyme Inhibition and Medicinal Chemistry.* 30(1). DOI:10.3109/14756366.2014.895719.
Cai, M., Liang, X., Sun, X., Chen, H., Dong, Y., Wu, L., Gu, S. & Han, S. 2019. Nuclear Receptor Coactivator 2 Promotes Human Breast Cancer Cell Growth by Positively Regulating the MAPK/ERK Pathway. *Front Oncol.* 9(164). DOI:10.3389/fonc.2019.00164.
Caldenhoven, E., Liden, J., Wissink, S., Van de Stolpe, A., Raaijimakers, J., Koenderman, L., Okret, S., Gustafsson, J.A. et al. 1995. Negative cross-talk between Rel A and the glucocorticoid
receptor: a possible mechanism for the antiinflammatory action of glucocorticoids. *Mol Endocrinol.* 9:401-412.
Cannarile, L., Delfino, D.V., Adorisio, S., Riccardi, C. & Ayroldi, E. 2019. Implicating the Role of GILZ in Glucocorticoid Modulation of T-Cell Activation. *Front Immunol.* 10. DOI:10.3389/fimmu.2019.01823.
Carnevale, R.P., Proietti, C.J., Salatino, M., Urtreger, A., Peluffo, G., Edwards, D.P., Boonyaratanakornkit, V., Eduardo, H. et al. 2007. Progestin effects on breast cancer cell proliferation, proteases activation, and in vivo development of metastatic phenotype all

depend on progesterone receptor capacity to activate cytoplasmic signaling pathways. *Mol Endocrinol.* 21. DOI:10.1210/me.2006-0304.
Chapman, K.L. 2012. G Protein coupled receptors - exploiting flexible conformations. *European Pharmaceutical Review.* (4).
Chapman, K.L., Holmes, M. & Seckl, J. 2013. 11beta-hydroxysteroid dehydrogenases: intracellular gate-keepers of tissue glucocorticoid action. *Physiol Rev.* 93(3).
Charni-Natan, M., Aloni-Grinstein, R., Osher, E. & Rotter, V. 2019. Liver and Steroid Hormones- Can a Touch of p53 Make a Difference? *Front. Endocrinol.* 10(374). DOI:10.3389/fendo.2019.00374.
Chen, S., Zhou, D., Yang, C. & Sherman, M. 2001. Molecular Basis for the Constitutive Activity of Estrogen Related Receptor α-1 (ERRα-1). *The Journal of Biological Chemistry.* 276(30). DOI:10.1074/jbc.M102638200.
Cicatiello, L., Addeo, R., Sasso, A., Altucci, L., Petrizzi, V.B., Borgo, R., Cancemi, M., Caporali, S. et al. 2004. Estrogens and Progesterone Promote Persistent CCND1 Gene Activation during G1 by Inducing Transcriptional Derepression via c-Jun/c-Fos/Estrogen Receptor (Progesterone Receptor) Complex Assembly to a Distal Regulatory Element and Recruitment of Cyclin D1 to Its Own Gene Promoter. *Molecular and Cellular Biology.* 24(16). DOI:10.1128/MCB.24.16.7260-7274.2004.
Clemm, D.L., Sherman, L., Boonyaratanakornkit, V., Schrader, W.T., Weigel, N.L. & Edwards, D.P. 2000. Differential Hormone-Dependent Phosphorylation of Progesterone Receptor A and B Forms Revealed by a Phosphoserine Site-Specific Monoclonal Antibody. *Molecular Endocrinology.* 54.
Cohen, D.M. & Steger, D.J. 2017. Nuclear Receptor Function through Genomics: Lessons from the Glucocorticoid Receptor. *Trends in Endocrinology and Metabolism.* 28(7):531-540. DOI:10.1016/j.tem.2017.01.001.
Condon, J.C., Hardy, D.B., Kovaric, K. & Mendelson, C.R. 2006. Up-Regulation of the Progesterone Receptor (PR)-C Isoform in Laboring Myometrium by Activation of Nuclear Factor-k?B May Contribute to the Onset of Labor through Inhibition of PR Function. *Molecular Endocrinology.* 20(4). DOI:10.1210/me.2005-0242.
Conneely, O.M. & Lydon, J.P. 2000. Progesterone receptors in reproduction: functional impact of the A and B isoforms. *Steroids.* 65.
Cui, X.S., R.; Arpino, G.; Osborne, C. K.; Lee, A. V.; . 2016. Biology of Progesterone Receptor Loss in Breast Cancer and Its Implications for Endocrine Therapy. *Journal of Clinical Oncology.* 23(30). DOI:10.1200/JCO.2005.09.004.
Daniel, A.R., Hagan, C.R. & Lange, C.A. 2011. Progesterone receptor action: defining a role. *Expert Rev Endocrinol Metab.* 6(3). DOI:10.1586/eem.11.25.
Daniel, A.R., Gaviglio, A.L., Knutson, T.P., Ostrander, J.H., D'Assoro, A.B., Ravindranathan, P., Peng, Y., Raj, G.V. et al. 2015. Progesterone receptor-B enhances estrogen responsiveness of breast cancer cells via scaffolding PELP1- and estrogen receptor-containing transcription complexes. *Oncogene.* 34(4):506-515. DOI:10.1038/onc.2013.579.
Daniel, A.R.L., C. A. 2009. Protein kinases mediate ligand-independent depression of sumoylated progesterone receptors in breast cancer cells. *PNAS.* 106(34):14287-14292.
De Bosscher, K. & Haegeman, G. 2009. Minireview: latest perspectives on antiinflammatory actions of glucocorticoids *Mol Endocrinol.* 23.
Deeks, S.G. 2011. HIV infection, inflammation, immunosenescence, and aging. *Annu Rev Med.* 62. DOI:10.1146/annurev-med-042909-093756.
Di Renzo, G.C., Tosto, V. & Tsibizova, V. 2020. Progesterone: History, facts and artifacts. *Best Practice & Research Clinical Obstetrics and Gynaecology.* 69. DOI:10.1016/j.bpobgyn.2020.07.012.
Díaz-Delfín, J., Domingo, P., Giralt, M. & Villarroya, F. 2013. Maraviroc reduces cytokine expression and secretion in human adipose cells without altering adipogenic differentiation. *Cytokine.* 61(3):808-815.
Diep, C.H., Ahrendt, H. & Lange, C.A. 2016. Progesterone induces progesterone receptor (PGR) expression via rapid activation of protein kinase pathways required for cooperative

estrogen receptor alpha (ER) and progesterone receptor (PR) genomic action at ER/PR target genes. *Steroids.* 114. DOI:10.1010/j.steroids.2016.09.004.
Dinh, D.T., Breen, J., Akison, L.K., DeMayo, F.J., Brown, H.M., Robker, R.L. & Russel, D.L. 2019. Tissue-specific progesterone-chromatin binding and the regulation of progesterone-dependent gene regulation. *Nature Scientific Reports.* 9. DOI:10.1038/s41598-019-48333-8.
Dlamini, S., Kuipa, M., Enfield, K., Skosana, S., Woodland, J.G., Moliki, J.M., Bick, A.J., van der Spuy, Z. et al. 2019. Reciprocal Modulation of Antiretroviral Drug and Steroid Receptor Function In Vitro. *Antimicrobial Agents and Chemotherapy.* 64(1):e01890-01819. DOI:10.1128/aac.01890-19.
Dong, Y., Aronsson, M., Gustafsson, J.Å. & Okret, S. 1989. The Mechanism of cAMP-induced Glucocorticoid Receptor Expression. *The Journal of Biological Chemistry.* 264(23).
Dorr, P., Westby, M., Dobbs, S., Griffin, P., Irvine, B., Macartney, M., Mori, J., Rickett, G. et al. 2005. Maraviroc (UK-427,857), a potent, orally bioavailable, and selective small-molecule inhibitor of chemokine receptor CCR5 with broad-spectrum anti-human immunodeficiency virus type 1 activity. *Antimicrobial agents and chemotherapy.* 49(11):4721-4732. DOI:Doi 10.1128/Aac.49.11.4721-4732.2005.
Eckner, R., Ewen, M.E., Newsome, D., Gerdes, M., DeCaprio, J.A., Lawrence, J.B. & Livingston, D.M. 1994. Molecular cloning and functioning analysis of the adenovirus E1A-associated 300-kD protein (p300) reveals a protein with properties of a transcriptional adaptor. *Genes and Development.* 8. DOI:10.1101/gad.8.8.869.
Eftekharzadeh, B., ; Banduseela, V. C.; Chiesa, G.; Martínez-Cristóbal, P.; Rauch, J. N.; Nath, S. R.; Schwarz, D. M. C.; Shao, H.; Marin-Argany, M.; Di Sanza, C.; Giorgetti, E.; Yu, Z.; Pierattelli, R.; Felli, I. C.; Brun-Heath, I.; García, J.; Nebreda, A. R.; Gestwicki, J. E.; Lieberman A. P.; Salvatella, X. 2019. Hsp70 and Hsp40 inhibit an inter-domain interaction necessary for transcriptional activity in the androgen receptor. *Nature.* 10.
Enfield, K., Dlamini, S., Avenant, C., Kuipa, M. & Hapgood, J.P. 2020a. Maraviroc, tenofovir disoproxil fumarate and dapivirine, activate progesterone receptor B in the absence of progestogens. *Biochemical and Biophysical Research Communications.* 533(4). DOI:10.1016/j.bbrc.2020.09.107.
Enfield, K., Cartwright, M., Louw-du Toit, R., Avenant, C., Africander, D. & Hapgood, J.P. 2020b. Characterisation of progestins used in hormonal contraception and progesterone via the progesterone receptor. *Biochemical and Biophysical Research Communications.* 533(4). DOI:doi.org/10.1016/j.bbrc.2020.09.058.
Escoubet-Lozach, L., Benner, C., Kaikkonen, M.U., Lozach, J., Heinz, S., Spann, N.J., Crotti, A., Stender, J. et al. 2011. Mechanisms Establishing TLR4-Responsive Activation States of Inflammatory Response Genes. *PLoS Genet.* 12. DOI:10.1371/journal.pgen.1002401.
Estrada, M., Espinoso, A., Müller, M. & Jaimovich, E. 2003. Testosterone stimulates intracellular calcium release and mitogen-activated protein kinases via a G protein-coupled receptor in skeletal muscle cells. *Endocrinology.* 144.
Fabris, V., Abascal, M.F., Giulianelli, S., May, M., Sequeira, G.R., Jacobsen, B.M., Lombès, M., Han, J. et al. 2017. Isoform specificity of progesterone receptor antibodies. *J Pathol Clin Res.* 4. DOI:10.1002/cjp2.83.
Faivre, E.J. & Lange, C.A. 2007. Progesterone Receptors Upregulate Wnt-1 To Induce Epidermal Growth Factor Receptor Transactivation and c-Src-Dependent Sustained Activation of Erk1/2 Mitogen-Activated Protein Kinase in Breast Cancer Cells. *Molecular and Cellular Biology.* 27. DOI:10.1128/MCB.01539-06.
Flaqué, M.C.D., Galigniana, N.M., Béguelin, W., Vicario, R., Proietti, C.J., Russo, R.C., Rivas, M.A., Tkach, M. et al. 2013. Progesterone receptor assembly of a transcriptional complex along with activator protein 1, signal transducer and activator of transcription 3 and ErbB-2 governs breast cancer growth and predicts response to endocrine therapy. *Breast Cancer Res* 15. DOI:10.1186/bcr3587.
Fletcher, C.E.D., D. A.; Bevan, C. L. 2014. Interplay between steroid signalling and microRNAs: implications for hormone-dependent cancers. *Endocrinology.* 21. DOI:10.1530/ERC-14-0208.

Flynn, J.K., Dankers, W. & Morand, E.F. 2019. Could GILZ Be the Answer to Glucocorticoid Toxicity in Lupus? *Front Immunol.* 10. DOI:10.3389/fimmu.2019.01684.
Frank, T.D., Carter, A., Jahagirdar, D., Biehl, M.H., Douwes-Schultz, D., Larson, S.L. & Arora, M. 2019. Global, regional, and national incidence, prevalence, and mortality of HIV, 1980–2017, and forecasts to 2030, for 195 countries and territories: a systematic analysis for the Global Burden of Diseases, Injuries, and Risk Factors Study 2017. *Lancet.* 6. DOI:10.1016/S2352-3018(19)30196-1.
Freshney, I.R. 1987. Basic Principles of Cell Culture. In *Culture of Cells for Tissue Engineering.* G. Vunjak-Novakovic and I.R. Freshney, Eds.: John Wiley & Sons. 3-21. DOI:10.1002/0471741817.ch1.
Fuhrmann, U., Slater, E.P. & Fritzemeier, K.H. 1995. Characterization of the novel progestin gestodene by receptor binding studies and transactivation assays. *Contraception.* 51. DOI:10.1016/0010-7824(94)00003-f.
Fürst, R., Schroeder, T., Eilken, H.M., Bubik, M.F., Kiemer, A.K., Zahler, S. & Vollmar, A.M. 2007. MAPK phosphatase-1 represents a novel anti-inflammatory target of glucocorticoids in the human endothelium. *FASEB J.* 21. DOI:10.1096/fj.06-6752com.
Gadsby, J.E., Frandsen, S., Chang, J., Celestino, B., Tucker, E. & Poole, D.H. 2020. Progesterone inhibits cytokine/TNF-α production by porcine CL macrophages via the genomic progesterone receptor. *Domestic Animal Endocrinology.* 72. DOI:10.1016/j.domaniend.2019.106426Get.
Galliher-Beckley, A.J., Williams, J.G., Collins, J.B. & Cidlowski, J.A. 2008. Glycogen synthase kinase 3beta-mediated serine phosphorylation of the human glucocorticoid receptor redirects gene expression profiles. *Mol Cell Biol.* 24. DOI:10.1128/MCB.00808-08.
Gao, X. & Nawaz, Z. 2002. Role of steroid receptor coactivators and corepressors in progesterone receptors in breast cancer. *Breast Cancer Research.* 4(5).
Garabedien, M.J., Harris, C.A. & Jeanneteau, F. 2017. Glucocorticoid receptor action in metabolic and neuronal function. *F1000Research.* 6(1208). DOI:10.12688/f1000research.11375.1.
Giachino, C., Galbiati, M., Fasolo, A., Peretto, P. & Melcangi, R. 2003. Neurogenesis in the subependymal layer of the adult rat: a role for neuroactive derivatives of progesterone. *Ann NY Acad Sci.* 1007.
Gibbs, R.B. 2000. Long-term treatment with estrogen and progesterone enhances acquisition of spatial memory task by ovariectomized aged rats. *Neurobiology of Aging.* 21.
Gonzalez, D.M.C., Garay, L., Gonzalez, S., Saravia, F., Labombarda, F., Guennoun, R., Schumacher, M. & De Nicola, A.F. 2007. Progesterone modulates brain-derived neurotrophic factor and choline acetyltransferase in degenerating Wobbler motoneurons. *Exp Neurol.* 203.
Govender, Y., Avenant, C., Verhoog, N.J.D., Ray, R.M., Grantham, N.J., Africander, D. & Hapgood, J.P. 2014. The Injectable-Only Contraceptive Medroxyprogesterone Acetate, Unlike Norethisterone Acetate and Progesterone, Regulates Inflammatory Genes in Endocervical Cells via the Glucocorticoid Receptor. *Plos One.* 9(5). DOI:10.1371/journal.pone.0096497.
Graham, J.D.Y., C.; Balleine, R. L.; Harvey, S. S.; Milliken, J. S.; Bilous, A. M.; Clarke, C. L. 1995. Characterization of Progesterone Receptor A and B Expression in Human Breast Cancer. *Cancer Research.* 55:5063-5068.
Griekspoor, A., Zwart, W., Neefkes, J. & Michalides, R. 2007. Visualizing the action of steroid hormone receptors in living cells. *Nuclear Receptor Signaling.* 5. DOI:DOI: 10.1621/nrs.05003.
Grigsby, I.F., Pham, L., Mansky, L.M., Gopalakrishnan, R. & Mansky, K.C. 2010. Tenofovir-associated bone density loss. *Therapeutics and Clinical Risk Management.* 6:41.
Grimm, S.L., Hartig, S.M. & Edwards, D.P. 2016. Progesterone Receptor Signaling Mechanisms. *J Mol Biol.* 428(19):3831-3849. DOI:10.1016/j.jmb.2016.06.020.
Grimm, S.L., Ward, R.D., Obr, A.E., Franco, H.L., Fernandez-Valdivia, R., Kim, J., Roberts, J.M., Jeong, J. et al. 2014. A role for site-specific phosphorylation of mouse progesterone receptor at serine 191 in vivo. *Mol Endocrinol.* 12:2025-2037. DOI:10.1210/me.2014-1206.

Gulick, R.M., Wilkin, T.J., Chen, Y.Q., Landovitz, R.J., Amico, K.R., Young, A.M., Richardson, P., Marzinke, M.A. et al. 2017. Safety and tolerability of maraviroc-containing regimens to prevent HIV infection in women: a phase 2 randomized trial. *Annals of internal medicine.* 167(6):384-393.
Hammes, S.R. & Levin, E.R. 2007. Extranuclear steroid recptors: nature and actions. *Endocr Rev.* 28(7).
Hapgood, J.P., Avenant, C. & Moliki, J.M. 2016. Glucocorticoid-independent modulation of GR activity: implications for immunotherapy. *Pharmacol Ther.* 165. DOI:10.1016/j.pharmthera.2016.06.002.
Hapgood, J.P., Kaushic, C. & Hel, Z. 2018. Hormonal Contraception and HIV-1 Acquisition: Biological Mechanisms. *Endocr Rev.* 39:36-78.
Hapgood, J.P., Koubovec, D., Louw, A. & Africander, D. 2004. Not all progestins are the same: implications for usage. *Trends Pharmacol Sci.* 25. DOI:10.1016/j.tips.2004.09.005.
Hapgood, J.P., Ray, R.M., Govender, Y., Avenant, C. & Tomasicchio, M. 2013. Differential Glucocorticoid Receptor-Mediated Effects on Immunomodulatory Gene Expression by Progestin Contraceptives: Implications for HIV-1 Pathogenesis. *American Journal of Reproductive Immunology.* 71. DOI:10.1111/aji.12214.
Hapgood, J.P., Ray, R.M., Govender, Y., Avenant, C. & Tomasicchio, M. 2014a. Differential Glucocorticoid Receptor-Mediated Effects on Immunomodulatory Gene Expression by Progestin Contracpetives: Implications for HIV-1 Pathogenesis. *American Journal of Reproductive Immunology.* 71(6). DOI:10.1111/aji.12214.
Hapgood, J.P., Africander, D., Louw-du Toit, R., Ray, R.M. & Rohwer, J.M. 2014b. Potency of progestogens used in hormonal therapy: toward understanding differential actions. *J steroid Biochem Mol Biol.* 142:39-47. DOI:10.1016/j.jsbmb.2013.08.001.
Hatou, S., Yamada, M., Mochizuki, H., Shiraishi, A., Joko, T. & Nishida, T. 2009. The effects of dexamethasone on the Na,K-ATPase activity and pump function of corneal endothelial cells. *Curr Eye Res.* 34(5):347-354. DOI:10.1080/02713680902829624.
He, J., Evans, C.O., Hoffman, S.W., Oyesiku, N.M. & Stein, D.G. 2004. Progesterone and allopregnanolone reduce inflammatory cytokines after traumatic brain injury. *Exp Neurol.*
Helmreich, M.L. & Huseby, R.A. 1962. Identification of a 6,21-dihydroxylated metabolite of medroxyprogesterone acetate in human urine. *J Clin Endocrinol Metab.* 22.
Helzer, K.T., Hooper, C., Miyamoto, S. & Alarid, E.T. 2015. Ubiquitylation of nuclear receptors: new linkages and therapeutic implications. *J Mol Endocrinol.* 54(3). DOI:10.1530/JME-14-0308.
Henríquez, S., Kohen, P., Muñoz, A., Godoy, A., Orge, F., Strauss, J.F. & Devoto, L. 2017. In-vitro study of gonadotrophin signaling pathways in human granulosa cells in relation to progesterone receptor expression. *Reproductive Biomedicine Online.* 35. DOI:10.1016/j.rbmo.2017.06.011.
Hermenegildo, C., Oviedo, P.J., García-Martínez, M.C., García-Pérez, M.A., Tarín, J.J. & Cano, A. 2005. Progestogens stimulate prostacyclin production by human endothelial cells. *Hum Reprod.* 20(6). DOI:10.1093/humrep/deh803.
Hevir, N., Vouk, K., Sinkovec, J., Ribic-Pucelj, M. & Rizner, T.L. 2011. Aldo-keto reductases AKR1C1, AKR1C2 and AKR1C3 may enhance progesterone metabolism in ovarian endometriosis. *Chem Biol Interact.* 191. DOI:10.1016/j.cbi.2011.01.003.
Horberg, M., Tang, B., Towner, W., Silverberg, M., Bersoff-Matcha, S., Hurley, L., Chang, J., Blank, J. et al. 2010. Impact of Tenofovir on Renal Function in HIV-Infected, Antiretroviral-Naive Patients. *J Acquir Immune Defic Syndr.* 53(1).
Horie-Inoue, K., Takayama, K., Bono, U.H., Ouchi, Y., Okazaki, Y. & Inoue, S. 2006. Identification of novel steroid target genes through combination of bioinformatics and functional analysis of hormone response elements. *Biochemical and Biophysical Research Communications.* 339:99-106. DOI:10.1016/j.bbrc.2005.10.188.
Houshdaran, S., Oke, A.B., Fung, J.C., Vo, K.C., Nezhat, C. & Giudice, L.C. 2020. Steroid hormones regulate genome-wide epigenetic programming and gene transcription in human endometrial cells with marked aberrancies in endometriosis. *PLoS Genet.* 16(6). DOI:10.1371/journal.pgen.1008601.

Huang, P., Chandra, V. & Rastinejad, F. 2010. Structural overview of the nuclear recep- tor superfamily: insights into physiology and therapeutics. *Annu Rev Physiol.* 72.
Huber, J. 1998. Pharmacokinetics of Implanon. *Contraception.* 58.
Hudson, W.H., de Vera, I.M.S., Nwachukwu, J.C., Weikum, E.R., Herbst, A.G., Yang, Q., Bain, D.L., Nettles, K.W. et al. 2018. Cryptic glucocorticoid receptor-binding sites pervade genomic NF-κB response elements. *Nature communications.* 9(1337). DOI:10.1038/s41467-018-03780-1.
Hümpel, M., Wendt, H., Pommerenke, G., Weiβ, C. & Speck, U. 1978. Investigations od pharmacokinetics of levonorgestrel to specific consideration of a possible first-pass effect in women. *Contraception.* 17.
Ing, N.H. 2005. Steroid Hormones Regulate Gene Expression Posttranscriptionally by Altering the Stabilities of Messenger RNAs. *Biology of Reproduction.* 72:1290-1296. DOI:10.1095/biolreprod.105.040014.
Irwin, R.W., Yao, J., Hamilton, R., Cadena, E., Brinton, R.D. & Nilsen, J. 2008. Progesterone and estrogen regulate oxidative metabolism in brain mitochondria. *Endocrinology.* 149(6).
Ishibashi, H., Suzuki, T., Suzuki, S., Moriya, T., Kaneko, C., Takizawa, T., Sunamori, M., Handa, M. et al. 2003. Sex steroid hormone receptors in human thymoma. *J Clin Endocrinol Metab.* 88(5). DOI:10.1210/jc.2002-021353.
Jackson, A. 2010. "Partial Agonist". *Encyclopedia of Psychopharmacology.* 2010. Springer, Berlin Heidelberg. Available: https://link.springer.com/referenceworkentry/10.1007%2F978-3-540-68706-1_548.
Jackson, T.A., Richer, J.K., Bain, D.L., Takimoto, G., Tung, L. & Horwitz, K.B. 1997. The partial agonist activity of antagonist-occupied steroid recep- tors is controlled by a novel hinge domain-binding coactivator L7/ SPA and the corepressors N-CoR or SMRT. *Mol Endocrinol.* 11.
Jacobsen, B.M. & Horwitz, K.B. 2012. Progesterone Receptors, their isoforms and the Progesterone Regulated Transcription. *Mol Cell Endocrinol.* 357. DOI:10.1016/j.mce.2011.09.016.
Jang, S. & Yi, L.S. 2005. Identification of a 71 kDa protein as a putative non-genomic membrane progesterone receptor in boar spermatozoa. *Journal of Endocrinology.* 184(2).
Jenster, G., Spencer, T., Burcin, M., Tsai, M.J. & O'Malley, B.W. 1997. Steroid receptor induction of gene transcription: A two-stepmodel. *PNAS.* 94(15). DOI:10.1073/pnas.94.15.7879.
Kamat, A., Hinshelwood, M.M. & Murray, B.A. 2002. Mechanisms in tissue-specific regulation of estrogen biosynthesis in humans. *Trends Endocrinol Metab.* 13(3).
Kamergorodsky, G., Invitti, A.L., D'Amora, P., Parreira, R.M., Kopelman, A., Bonetti, T.C.S., Girão, M.J.B.C. & Schor, E. 2020. Progesterone's role in deep infiltrating endometriosis: Progesterone receptor and estrogen metabolism enzymes expression and physiological changes in primary endometrial stromal cell culture. *Molecular and Cellular Endocrinology.* 505. DOI:10.1016/j.mce.2020.110743.
Kang, H.Y., Cho, C.L., Huang, K.L., Wang, J.C., Hu, Y.C., Lin, H.K., Chawnshang, C. & Huang, K. 2004. Nongenomic androgen activation of phosphatidylinositol 3-kinase/Akt signaling pathway in MC3T3-E1 osteoblasts. *J Bone Miner Res.* 19(7). DOI:10.1359/JBMR.040306.
Kassel, O. & Herrlich, P. 2007. Crosstalk between the glucocorticoid receptor and other transcription factors: molecular aspects. *Mol Cell Endocrinol.* 275.
Kastner, P., Bocquel, M., Turcotte, B., Garnier, J.M., Horwitz, K.B., Chambon, P. & Gronemeyer, H. 1990. Transient expression of human and chicken progesterone receptors does not support alternative translational initiation from a single mRNA as the mechanism generating two receptor isoforms. *J Biol Chem.* 265(21).
Kavandi, L., Collier, M.A., Nguyen, H. & Syed, V. 2012. Progesterone and calcitriol attenuate inflammatory cytokines CXCL1 and CXCL2 in ovarian and endometrial cancer cells. *J Cell Biochem.* 113(10):3143-3152. DOI:10.1002/jcb.24191.
Keller, M.J., Wood, L., Billingsley, J.M., Ray, L.L., Goymer, J., Sinclair, S., McGinn, A.P., Marzinke, M.A. et al. 2019. Tenofovir disoproxil fumarate intravaginal ring for HIV pre-

exposure prophylaxis in sexually active women: a phase 1, single-blind, randomised, controlled trial. *The Lancet HIV.* 6(8):e498-e508.
Keller, M.J., Mesquita, P.M., Marzinke, M.A., Teller, R., Espinoza, L., Atrio, J.M., Lo, Y., Frank, B. et al. 2016. A phase 1 randomized placebo-controlled safety and pharmacokinetic trial of a tenofovir disoproxil fumarate vaginal ring. *Aids.* 30(5):743-751. DOI:10.1097/QAD.0000000000000979.
Kirschke, E.G., D.; Southworth, D.; Griffin, P.R.; Agard, D. 2014. Glucocorticoid Receptor Function Regulated by Coordinated Action of the Hsp90 and Hsp70 Chaperone Cycles. *Cell.* 157(7).
Klein-Szanto, A.J.P. & Conti, C.J. 2002. Skin and Oral Mucosa. In *Organ-Specific Toxicologic Pathology.* "Second Edition" ed. W.M. Haschek, M.A. Wallig and C.G. Rousseaux, Eds.: Elsevier. 85 - 119. DOI:https://doi.org/10.1016/B978-012330215-1/50030-2.
Kolla, V., Robertson, N.M. & Litwack, G. 1999. Identification of a mineralocorticoid/ glucocorticoid response element in the human Na/K ATPase alpha1 gene promoter. *Biochem. Biophys. Res. Commun.* 266. DOI:10.1006/bbrc.1999.1765.
Korhonen, T., Tolonen, A., Uusitalo, J., Lundgren, S., Jalonen, J. & Laine, K. 2005. The role of CYP2C and CYP3A in the disposition of 3-keto-desogestrel after administration of desogestrel. *J Clin Pharmacol.* 60:60-75.
Kotitschke, A., Gijsen, H., Avenant, C., Fernandes, S. & Hapgood, J.P. 2009. Genomic and Nongenomic Cross Talk between the Gonadotropin-Releasing Hormone Receptor and Glucocorticoid Receptor Signaling Pathways. *Molecular Endocrinology.* 23(11).
Kougioumtzi, A., Tsapara, P. & Magklara, A. 2014. Deep Sequencing Reveals New Aspects of Progesterone Receptor Signaling in Breast Cancer Cells. *Plos One.* 9(6). DOI:10.1371/journal.pone.0098404.
Kuiper, G.G. & Brinkmann, A.O. 1994. Steroid hormone receptor phosphorylation: is there a physiological role? *Mol Cell Endocrinol.* 100. DOI:10.1016/0303-7207(94)90287-9.
Kumar, N., Fagart, J., Liere, P., Mitchell, S.J., Knibb, A.R., Petit-Topin, I., Rame, M., El-Etr, M. et al. 2017. Nestorone® as a Novel Progestin for Nonoral Contraception: Structure-Activity Relationships and Brain Metabolism Studies. *Endocrinology.* 158(1).
Kuznetsova, T., Wang, S., Rao, N.A., Mandoli, A., Martens, J.H.A., Rother, N., Aartse, A., Groh, L. et al. 2015. Glucocorticoid receptor and nuclear factor kappa-b affect three-dimensional chromatin organization. *Genome Biology.* 16(264). DOI:10.1186/s13059-015-0832-9.
Lain, A.R.C., C. J.; Conneely, O. M. 2013. Research Resource: Progesterone Receptor Targetome Underlying Mammary Gland Branching Morphogenesis. *Mol Endocrinol.* 27(10):1743-1761. DOI:10.1210/me.2013-114.
Lan, Y., Wang, X., Lou, J., Xing, J., Yu, Z., Wang, H., Shuang, Z., Ma, X. et al. 2018. Bufalin inhibits glioblastoma growth by promoting proteasomal degradation of the Na+/ K+ -ATPase α1 subunit. *Biomedicine & Pharmacotherapy.* 103.
Lange, C.A., Shen, T. & Horwitz, K.B. 2000. Phosphorylation of human progesterone receptors at serine-294 by mitogen-activated protein kinase signals their degradation by the 26S proteasome. *PNAS.* 97(3).
Lauber, A.H., Romano, G.J. & Pfaff, D.W. 1991. Sex difference in estradiol regulation of progestin receptor mRNA in rat mediobasal hypothalamus as demonstrated by in situ hybridization. *Neuroendocrinology.* 53.
Lei, K., Chen, L., Georgious, E.X., Sooranna, S.R., Khanjani, S., Brosens, J.J., Bennett, P.R. & Johnson, M.R. 2012. Progesterone Acts via the Nuclear Glucocorticoid Receptor to Suppress IL-1β-Induced COX-2 Expression in Human Term Myometrial Cells. *Plos One.* 7(11). DOI:10.1371/journal.pone.0050167.
Lewis, M.J., Wiebe, J.P. & Heathcote, J.G. 2004. Expression of progesterone metabolizing enzyme genes (AKR1C1, AKR1C2, AKR1C3, SRD5A1, SRD5A2) is altered in human breast carcinoma. *BMC Cancer.* 4:27. DOI:10.1186/1471-2407-4-27.
Li, H., Leo, C., Schroen, D.J. & Chen, J.D. 1997. Characterization of receptor interaction and transcriptional repression by the corepressor SMRT. *Mol Endocrinol.* 11.

Li, X., Wong, J., Tsai, S.Y., Tsai, M.J. & O'Malley, B.W. 2003. Progesterone and Glucocorticoid Receptors Recruit Distinct Coactivator Complexes and Promote Distinct Patterns of Local Chromatin Modification. *Molecular and Cellular Biology.* 11. DOI:10.1128/MCB.23.11.3763-3773.2003.
Lim, C.S., Baumann, C.T., Htun, H., Xian, W., Irie, M., Smith, C.L. & Hager, G.L. 1999. Differential Localization and Activity of the A- and B-Forms of the Human Progesterone Receptor Using Green Fluorescent Protein Chimeras. *Mol Endocrinol.* 13. DOI:10.1210/mend.13.3.0247.
Lim, E., Palmieri, C. & Tilley, W.D. 2016. Renewed interest in the progesterone receptor in breast cancer. *Br J Cancer.* 115(8):909-911. DOI:10.1038/bjc.2016.303.
Lin, V.C., Ng, E.H., Aw, S.E., Tan, M.G. & Bay, B.H. 2000. Progesterone induces focal adhesion in breast cancer cells MDA-MB-231 transfected with progesterone receptor complementary DNA. *Mol Endocrinol.* 3. DOI:10.1210/mend.14.3.0426.
Ling, J. & Kumar, R. 2012. Crosstalk between NFkB and glucocorticoid signaling: A potential target of breast cancer therapy. *Cancer Letters.* 322. DOI:10.1016/j.canlet.2012.02.033.
Liu, J., Park, E. & Jo, M. 2009. Runt-Related Transcription Factor 1 Regulates Luteinized Hormone-Induced Prostaglandin-Endoperoxide Synthase 2 Expression in Rat Periovulatory Granulosa Cells. *Endocrinology.* 150(7):3291-3300. DOI:10.1210/en.2008-1527.
Liu, Z., Wong, J., Tsai, S.Y., Tsai, M.J. & O'Malley, B.W. 2001. Sequential recruitment of steroid receptor coactivator-1 (SRC-1) and p300 enhances progesterone receptor-dependent initiation and reinitiation of transcription from chromatin. *Proc Natl Acad Sci U S A.* 98(22):12426-12431. DOI:10.1073/pnas.231474798.
Liu, Z., Auboeuf, D., Wong, J., Chen, J.D., Tsai, S.Y., Tsai, M.J. & O'Malley, B.W. 2002. Coactivator/corepressor ratios modulate PR-mediated transcription by the selective receptor modulator RU486. *PNAS.* 99(12). DOI:10.1073/pnas.122225699
Louw-du Toit, R., Perkins, M., Hapgood, J.P. & Africander, D. 2017. Comparing the androgenic and estrogen properties of progestins used in contraception and hormone therapy. *Biochemical and Biophysical Research Communications.* 491(1). DOI:10.1016/j.bbrc.2017.07.063.
Lu, N.Z., Wardell, S.E., Burnstein, K.L., Defranco, D., Fuller, P.J., Giguere, V., Hochberg, R.B., McKay, L. et al. 2006. International Union of Pharmacology. LXV. The Pharmacology and Classification of the Nuclear Receptor Superfamily: Glucocorticoid, Mineralocorticoid, Progesterone, and Androgen Receptors. *Pharmacological Reviews.* 58. DOI:10.1124/pr.58.4.9.
Lydon, J.P., DeMayo, F.J., Funk, C.R., Mani, S.K., Hughes, A.R., Montgomery, C.A., Shyamala, G., Conneely, O.M. et al. 1995. Mice lacking progesterone receptor exhibit pleiotropic reproductive abnormalities. *Genes and Development.* 9.
Madrid-Elena, N., García-Bermejo, M.L., Serrano-Villar, S., Díaz-de Santiago, A., Sastre, B., Gutiérrez, C., Dronda, F., Díaz, M.C. et al. 2018. Maraviroc is associated with latent HIV-1 reactivation through NF-κB activation in resting CD4+ T cells from HIV-Infected Individuals on Suppressive Antiretroviral Therapy. *Journal of virology.*JVI. 01931-01917.
Maekawa, R., Tamura, I., Shinagawa, M., Mihara, Y., Sato, S., Okada, M., Taketani, T., Tamura, H. et al. 2019. Genome-wide DNA methylation analysis revealed stable DNA methylation status during decidualization in human endometrial stromal cells. *BMC Genomics* 20(1). DOI:10.1186/s12864-019-5695-0.
Malbeteau, L., Poulard, C., Languilaire, C., Mikaelian, I., Flamant, F., Le Romancer, M. & Corbo, L. 2020. PRMT1 Is Critical for the Transcriptional Activity and the Stability of the Progesterone Receptor. *iScience.* 23(6).
Mangal, R.K., Wiehle, R.D., Poindexter, A.N. & Weigel, N.L. 1997. Differential Expression of Uterine Progesterone Receptor Forms A and B during the Menstrual Cycle. *J Steroid Biochem.* 63.
Mani, S.O., M. G. 2012. Progesterone signaling mechanisms in brain and behavior. *Frontiers in endocrinology.* 3(7).
Mani, S.P., W. 2010. Activation of Progestin Receptors in Female Reproductive Behavior: Interactions with Neurotransmitters. *Neuroendocrinol.* 31(2):157-171.

Maritz, M.F., Ray, R.M., Bick, A.J., Tomasicchio, M., Woodland, J.G., Govender, Y., Avenant, C. & Hapgood, J.P. 2018. Medroxyprogesterone acetate, unlike norethisterone, increases HIV-1 replication in human peripheral blood mononuclear cells and an indicator cell line, via mechanisms involving the glucocorticoid receptor, increased CD4/CD8 ratios and CCR5 levels. *Plos One.* 13(4). DOI:10.1371/journal.pone.0196043.
Matias, P.M., Carrondo, M.A., Coelho, R., Thomaz, M., Zhao, X., Wegg, A., Crusius, K., Egner, U. et al. 2002. Structural basis for the glucocorticoid response in a mutant human androgen receptor (AR(ccr)) derived from an androgen-independent prostate cancer. *J Med Chem.* 45(7). DOI:10.1021/jm011072j.
McCarthy, M.M. & Nugent, B.M. 2013. Epigenetic Contributions to Hormonally-Mediated Sexual Differentiation of the Brain. *J Neuroendocrinol.* 25(11):1133-1140. DOI:10.1111/jne.12072.
McEwan, I.J., Lavery, D., Fischer, K. & Watt, K. 2007. Natural disordered sequences in the amino terminal domain of nuclear receptors: lessons from the androgen and glucocorticoid receptors. *Nuclear Receptor Signaling.* 5. DOI:DOI: 10.1621/nrs.05001.
McKay, L.I. & Cidlowski, J.A. 1998. Cross-talk between nuclear factor k B and ther steroid hormone receptors: mechanisms of mutual antagonism. *Mol Endocrinol.* 12:45-56.
McKay, L.I. & Cidlowski, J.A. 1999. Molecular control of immune/inflammatory responses: interactions between nuclear factor-kappa B and steroid receptor-signaling pathways. *Endocr Rev.* 20.
Mei, Q., Huang, J., Chen, W., Tang, J., Xu, C., Yu, Q., Cheng, Y., Ma, L. et al. 2017. Regulation of DNA replication-coupled histone gene expression. *Oncotarget.* 55. DOI:10.18632/oncotarget.21887.
Mitchell, C., Johnson, R., Bisits, A., Hirst, J. & Zakar, T. 2011. PTGS2 (prostaglandin endoperoxide synthase-2) expression in term human amnion in vivo involves rapid mRNA turnover, polymerase-II 5'-pausing, and glucocorticoid transrepression. *Endocrinology.* 152(5):2113-2122. DOI:10.1210/en.2010-1327.
Mohammed, H., Russell, I.A., Stark, R., Rueda, O.M., Hickey, T.E., Tarulli, G.A., Serandour, A.A.A., Birell, S.N. et al. 2015. Progesterone receptor modulates estrogen receptor-α action in breast cancer. *Nature.* 523. DOI:10.1038/nature14583.
Mote, P.A., Balleine, R.L., McGowan, E.M. & Clarke, C.L. 1999. Colocalization of progesterone receptors A and B by dual immunofluorescence histochemistry in human endometrium during the menstrual cycle *J Clin Endocrinol Metab.* 84.
Mote, P.A., Bartow, S., Tran, N. & Clarke, C.L. 2002. oss of co-ordinate expression of progesterone receptors A and B is an early event in breast carcinogenesis *Breast Cancer Res Treat.* 72.
Mueller, K.B., Lu, Q., Mohammad, N.N., Luu, V., McCurley, A., Williams, G.H., Adler, G.K., Karas, R.H. et al. 2014. Estrogen receptor inhibits mineralocorticoid receptor transcriptional regulatory function. *Endocrinology.* 155(11):4461-4472. DOI:10.1210/en.2014-1270.
Nehdi, A., Ali, R., Alhallaj, A., Alzahrani, H., Samman, N., Mashhour, A., Baz, O., Barhoumi, T. et al. 2019. Nuclear Receptors Are Differentially Expressed and Activated in KAIMRC1 Compared to MCF7 and MDA-MB231 Breast Cancer Cells *Molecules.* 24(11). DOI:10.3390/molecules24112028.
Nel, A., van Niekerk, N., Kapiga, S., Bekker, L.-G., Gama, C., Gill, K., Kamali, A., Kotze, P. et al. 2016. Safety and efficacy of a dapivirine vaginal ring for HIV prevention in women. *New England Journal of Medicine.* 375(22):2133-2143.
Nelson, C.C., Hendy, S.C. & Schukin, R.J. 1999. Determinants of DNA sequence specificity of the androgen, progesterone, and glucocorticoid receptors: evidence for differential steroid receptor response elements. *Mol Endocrinol.* 13.
Ng, H.P., Jennings, S., Wang, J., Molina, P.E., Nelson, S. & Wang, G. 2017. Non-canonical Glucocorticoid Receptor Transactivation of gilz by Alcohol Suppresses Cell Inflammatory Response. *Front. Immunol.* 10.3389/fimmu.2017.00661. DOI:10.3389/fimmu.2017.00661.
Nicolaides, N.C., Pavlaki, A.N., Alexandra, M.A.M. & Chrousos, G.P. 2018. Glucocorticoid Therapy and Adrenal Suppression. In *Endotext.* K.R. Feingold, B. Anawalk and A. Boyce, Eds. South Dartmouth (MA). DOI:www.ncbi.nlm.nih.gov/books/NBK279156/.

Nicolaides, N.C., Galata, Z., Kino, T., Chrousos, G.P. & Charmandari, E. 2010. The Human Glucocorticoid Receptor: Molecular Basis of Biologic Function. *Steroids.* 75(1). DOI:10.1016/j.steroids.2009.09.002.
Nilsson, R., Bajic, V.B., Suzuki, H., di Bernado, D., Björkegren, J., Katayama, S., Reid, J.F., Sweet, M.J. et al. 2006. Transcriptional network dynamics in macrophage activation. *Genomics.* 88(2). DOI:10.1016/j.ygeno.2006.03.022.
Nordeen, S.K., Ogden, C.A., Taraseviciene, L. & Lieberman, B.A. 1998. Extreme Position Dependence of a Canonical Hormone Response Element *Molecular Endocrinology.* 12(6). DOI:10.1210/mend.12.6.0118.
Novak, M.L., Billich, W., Smith, S.M., Sukhija, K.B., McLoughlin, T.J., Hornberger, T.A. & Koh, T.J. 2009. COX-2 inhibitor reduces skeletal muscle hypertrophy in mice. *Am J Physiol Regul Integr Comp Physiol.* 296(4):R1132-1139. DOI:10.1152/ajpregu.90874.2008.
Oakley, O.R. & Cidlowski, J.A. 2013. The biology of the Glucocorticoid Receptor: New Signaling Mechanisms in Health and Disease. *J Allergy Clin Immunol.* 132(5). DOI:10.1016/j.jaci.2013.09.007.
Ogara, M.F., Rodrıguez-Seguı, S.A., Marini, M., Nacht, A.S., Stortz, M., Levi, V., Presman, D.M., Vicent, G.P. et al. 2019. The glucocorticoid receptor interferes with progesterone receptor-dependent genomic regulation in breast cancer cells. *Nucleic Acids Research.* 47. DOI:10.1093/nar/gkz857.
Orang, A.V., Safaralizadeh, R. & Kazemzadeh-Bavili, M. 2014. Mechanisms of miRNA-Mediated Gene Regulation from Common Downregulation to mRNA-Specific Upregulation. *Int J Genomics.* 10. DOI:10.1155/2014/970607.
Owen, G.I., Richer, J.K., Tung, L., Takimoto, G. & Horwitz, K.B. 1998. Progesterone regulates transcription of the p21(WAF1) cyclin-dependent kinase inhibitor gene through Sp1 and CBP/p300. *J Biol Chem.* 273(17). DOI:10.1074/jbc.273.17.10696.
Palagani, A.O.d.B., K.; Naulaerts, S.; Diddens, J.; Chirumamilla, C. S.; Van Camp, G.; Laukens, K.; Heynick, K.; Gerlo, S.; Mestdagh, P.; Vandesompele, J.; Vanden Berghe, W. 2014. Ectopic MicroRNA-150-5p Transcription Sensitizes Glucocorticoid Therapy Response in MM1S Multiple Myeloma Cells but Fails to Overcome Hormone Therapy Resistance in MM1R cells. *Plos One.* 9(12). DOI:10.1371/journal.pone.0113842.
Panettieri, R.A., Schaafsma, D., Amrani, Y., Koziol-White, C., Ostrom, R. & Tliba, O. 2018. Non-genomic Effects of Glucocorticoids: An Updated View. *Cell Press.* 40(1). DOI:10.1016/j.tips.2018.11.002.
Park, C.J., Lin, P.C., Zhou, S., Barakat, R., Bashir, S.T., Choi, J.M., Cacioppo, J.A., Oakley, O.R. et al. 2020. Progesterone Receptor Serves the Ovary as a Trigger of Ovulation and a Terminator of Inflammation. *Cell Rep.* 31(2):107496. DOI:10.1016/j.celrep.2020.03.060.
Perissi, V. & Rosenfeld, M.G. 2005. Controlling nuclear receptors: the circular logic of cofactor cycles. *Nat Rev Mol Cell Biol.* 6(7). DOI:10.1038/nrm1680.
Pfaff, D.W., Schwanzel-Fukunda, M., Parhar, I.S., Lauber, A.H., McCarthy, L.M. & Kow, L.M. 1994. GnRH neurons and other cellular and molecular mechanisms for simple mammalian reproductive behaviors. *Recent Prog Horm Res.* 49. DOI:10.1016/b978-0-12-571149-4.50005-2.
Pierson-Mullany, L.K. & Lange, C.A. 2004. Phosphorylation of Progesterone Receptor Serine 400 Mediates Ligand-Independent Transcriptional Activity in Response to Activation of Cyclin-Dependent Protein Kinase 2. *Molecular and Cellular Biology.* 24(24). DOI:10.1128/MCB.24.24.10542–10557.2004.
Polikarpova, A.V., Levina, I.S., Sigai, N.V., Zavarzin, I.V., Morozov, I.A., Rubtsov, P.M., Guseva, A.A., Smirnova, O.V. et al. 2019. Immunomodulatory effects of progesterone and selective ligands of membrane progesterone receptors. *Steroids.* 145:5-18. DOI:10.1016/j.steroids.2019.02.009.
Polis, C.B., Phillips, S.J., Hillier, S.L. & Achilles, S.L. 2016a. Levonorgestrel in contraceptives and multipurpose prevention technologies: does this progestin increase HIV risk or interact with antiretrovirals? *AIDS.* 30(17):2571-2576. DOI:10.1097/QAD.0000000000001229.

Polis, C.B., Phillips, S.J., Hillier, S.L. & Achilles, S.L. 2016b. Levonorgestrel in contraceptives and multipurpose prevention technologies: does this progestin increase HIV risk or interact with antiretrovirals? *AIDS.* 30. DOI:10.1097/QAD.0000000000001229.
Pollow, K., Juchem, M., Elger, W., Jacobi, N., Hoffmann, G. & Möbus, V. 1992. Dihydrospirorenone (ZK30595): A novel synthetic progestagen-characterization of binding to different receptor protein. *Contraception.* 46. DOI:10.1016/0010-7824(92)90121-9.
Pooley, J.R., Rivers, C.A., Kilcooley, M.T., Paul, S.N., Cavga, A.D., Kershaw, Y.M., Muratcioglu, S., Gursoy, A. et al. 2020. Beyond the heterodimer model for mineralocorticoid and glucocorticoid receptor interactions in nuclei and at DNA. *Plos One.* 15(1):e0227520. DOI:10.1371/journal.pone.0227520.
Potamitis, C., Siakouli, D., Papavasileiou, K.D., Boulaka, A., Ganou, V., Roussaki, M., Calogeropoulou, T., Zoumpoulakis, P. et al. 2019. Discovery of New non-steroidal selective glucocorticoid receptor agonist. *Journal of Steroid Biochemistry and Molecular Biology.* 186:142-153. DOI:10.1016/j.jsbmb.2018.10.007.
Præstholm, S.M., Correia, C.M. & Grøntved, L. 2020. Multifaceted Control of GR Signaling and Its Impact on Hepatic Transcriptional Networks and Metabolism. *Frontiers in endocrinology.* 11. DOI:10.3389/fendo.2020.572981.
Prasad, P.V., Bashir, M., Sitruk-Ware, R. & Kumar, N. 2010. Single-dose pharmacokinetics of nestorone, a potential female-contraceptive. *Steroids.* 75. DOI:10.1016/j.steroids.2009.12.011.
Quinkler, M., Diederich, S., Bähr, V. & Oelkers, W. 2004. The role of progesterone metabolism and androgen synthesis in renal blood pressure regulation. *Horm Metab Res.* 36(6). DOI:10.1055/s-2004-814572.
Ravinder, P., Shatrugna, V., Madhavan, K. & Sivakumar, B. 1997. Pharmacokinetics of orally administered norethisterone enanthate in rabbit, monkey and women. *Contraception.* 55. DOI:10.1016/S0010-7824(97)00047-4.
Ray, D.W., Suen, C.S., Brass, J., Soden, J. & White, A. 1999. Structure/function of the human glucocorticoid receptor: tyrosine 735 is important for transactivation. *Mol Endocrinol.* 13(11).
Remus, E.W., Sayeed, I., Won, S., Lyle, A.N. & Stein, D.G. 2015. Progesterone protects endothelial cells after cerebrovascular occlusion by decreasing MCP-1- and CXCL1-mediated macrophage infiltration. *Exp Neurol.* 271:401-408. DOI:10.1016/j.expneurol.2015.07.010.
Richer, J.K., Jacobsen, B.M., Manning, N.G., Abel, M.G., Wolf, D.M. & Horwitz, K.B. 2002. Differential gene regulation by the two progesterone receptor isoforms in human breast cancer cells. *J Biol Chem.* 277.
Rickard, D.J.I., U. T.; Evans, G.; Hefferan, T. E.; Hunter, J. C.; Waters, K. M.; Lydon, J. P.; O'Malley, B. W.; Khosla, S.; Spelsberg, T. C.; Turner, R. T. . 2008. Bone Growth and Turnover in Progesterone Receptor Knockout Mice. *Endocrinology.* 149(5):2383-2390. DOI:10.1210/en.2007-1247.
Ritter, H.D. & Mueller, C.R. 2012. The unliganded glucocorticoid receptor positively regulates the tumor suppressor gene BRCA1 through GABP beta. *Mol Cancer Res.* 10(4):558-569.
Ritter, H.D. & Mueller, C.R. 2014. Expression microarray identifies the unliganded glucocorticoid receptor as a regulator of gene expression in mammary epithelial cells. *BMC Cancer.* 14(275).
Rivers, C.A., Rogers, M.F., Stubbs, F.E., Conway-Campbell, B.L., Lightman, S.L. & Pooley, J.R. 2019. Glucocorticoid Receptor-Tethered Mineralocorticoid Receptors Increase Glucocorticoid-Induced Transcriptional Responses. *Endocrinology.* 160(5):1044-1056. DOI:10.1210/en.2018-00819.
Robertson, S., Rohwer, J.M., Hapgood, J.P. & Louw, A. 2013. Impact of Glucocorticoid Receptor Density on Ligand-Independent Dimerization, Cooperative Ligand-Binding and Basal Priming of Transactivation: A Cell Culture Model. *PLoS One.* 8(5). DOI:10.1371/journal.pone.0064831.

Ronacher, K., Hadley, K., Avenant, C., Stubsrud, E., Simons, S.S.J., Louw, A. & Hapgood, J.P. 2009. Ligand-selective transactivation and transrepression via the glucocorticoid receptor: role of cofactor interaction. *Mol Cell Endocrinol.* 299(2). DOI:10.1016/j.mce.2008.10.008.
Rose, A.J., Vegiopoulos, A. & Herzig, S. 2010. Role of glucocorticoids and the glucocorticoid receptor in metabolism: Insights from genetic manipulations. *The Journal of Steroid Biochemistry and Molecular Biology.* 122. DOI:10.1016/j.jsbmb.2010.02.010.
Rosenfeld, M.G., Lunyak, V.V. & Glass, C.K. 2006. Sensors and signals: a coactivator/corepressor/epigenetic code for integrating signal-dependent programs of transcriptional response. *Genes Dev.* 20.
Rowan, B.G. & O'Malley, B.W. 2000. Progesterone receptor coactivators. *Steroids.* 65.
Saitoh, M., Ohmichi, M., Takahashi, K., Kawagoe, J., Ohta, T., Doshida, M., Takahashi, T., Igarashi, H. et al. 2005. Medroxyprogesterone acetate induces cell proliferation through up-regulation of cyclin D1 expression via phosphatidylinositol 3-kinase/Akt/nuclear factor-kappaB cascade in human breast cancer cells. *Endocrinology.* 146. DOI:10.1210/en.2004-1535.
Saliba, J., Coutaud, B., Solovieva, V., Lu, F. & Blank, V. 2019. Regulation of CXCL1 chemokine and CSF3 cytokine levels in myometrial cells by the MAFF transcription factor. *J Cell Mol Med.* 23(4). DOI:10.1111/jcmm.14136.
Sambrook, J. & Russel, D.W. 2006. *The condensed protocols from molecular cloning: a laboratory manual* Cold Spring Harbor, N.Y.: Cold Spring Harbor Laboratory Press.
Sartorius, C.A., Melville, M.Y., Hovland, A.R., Tung, L., Takimoto, G. & Horwitz, K.B. 1994. A third transactivation function (AF3) of human progesterone receptors located in the unique N-terminal segment of the B isoform. *Mol Endocrinol.* 8(10).
Sasagawa, S., Shimizu, Y., Kami, H., Takeuchi, T., Mita, S., Imada, K., Kato, S. & Mizuguchi, K. 2008. Dienogest is a selective progesterone receptor agonist in transactivation analysis with potent oral endometrial activity due to its efficient pharmacokinetic profile. *Steroids.* 73. DOI:10.1016/j.steroids.2007.10.003.
Scarpin, K.M., Graham, J.D., Mote, P.A. & Clarke, C.L. 2009. Progesterone action in human tissues: regulation by progesterone receptor (PR) isoform expression, nuclear positioning and coregulator expression. *Nuclear Receptor Signaling.* 7. DOI:10.1621/nrs.07009.
Schesschowitsch, K., Leite, J.A. & Assreuy, J. 2017. New Insights in Glucocorticoid Receptor Signaling - More Than Just a Ligand-Binding Receptor. *Frontiers in endocrinology.* 8(16). DOI:10.3389/fendo.2017.00016.
Schiffer, L., Barnard, L., Baranowski, E.S., Gilligan, L.C., Taylor, A.E., Arlt, W., Shackleton, C.H.L. & Storbeck, K.H. 2019. Human steroid biosynthesis, metabolism and excretion are differentially reflected by serum and urine steroid metabolomes: A comprehensive review. *J steroid Biochem Mol Biol.* 194. DOI:10.1016/j.jsbmb.2019.105439.
Schöne, S., Jurk, M., Helabad, B.M., Dror, I., Lebars, I., Kieffer, B., Imhof, P., Rohs, R. et al. 2016. Sequences flanking the core-binding site modulate glucocorticoid receptor structure and activity. *Nature communications.* 7.
Schrage, R., De Min, A., Kostenis, E. & Mohr, K. 2016. Superagonism at G protein-coupled recptors and beyond. *British Journal of Pharmacology.* 173(20). DOI:10.1111/bph.13278.
Schumacher, M., Zhu, X. & Guennoun, R. 2017. Progesterone: Synthesis, Metabolism, Mechanism of Action, and Effects in the Nervous System. In *Hormones, Brain and Behavior.* Third ed. D.W. Pfaff and M. Joëls, Eds.: Academic Press. 215-244. DOI:10.1016/B978-0-12-803592-4.00054-7.
Sever, R. & Glass, C.K. 2013. Signaling by Nuclear Receptors. *Cold Spring Harb Perspect Biol.* 5(3). DOI:10.1101/cshperspect.a016709.
Shan, J.Y., Ji, W.z., Li, H.T., Tuxun, T., Lin, R.Y. & Wen, H. 2011. TLR2 and TLR4 expression in peripheral blood mononuclear cells of patients with chronic cystic echinococcosis and its relationship with IL-10. *Parasite Immunology.* 33(12).
Shen, M. & Shi, H. 2015. Sex Hormones and Their Receptors Regulate Liver Energy Homeostasis. *International Journal of Endocrinology.* 2015:294278. DOI:10.1155/2015/294278.

Shiau, A., Barstad, D., Loria, P.M., Kushner, P.J., Agard, D.A. & Greene, G.L. 1998. The Structural Basis of Estrogen Receptor/Coactivator Recognition and the Antagonism of This Interaction by Tamoxifen. *Cell.* 95(7). DOI:10.1016/S0092-8674(00)81717-1.
Shieh, J.M., Tsai, Y.J., Tsou, C.J. & Wu, W.B. 2014. CXCL1 Regulation in Human Pulmonary Epithelial Cells by Tumor Necrosis Factor. *Cell Physiol Biochem.* 34:1373-1384. DOI:10.1159/000366344.
Shimizu, N., Yoshikawa, N., Wada, T., Handa, H., Sano, M., Fukuda, K., Suematsu, M., Sawai, T. et al. 2008. Tissue- and Context-Dependent Modulation of Hormonal Sensitivity of Glucocorticoid-Responsive Genes by Hexamethylene Bisacetamide-Inducible Protein 1. *Molecular Endocrinology.* 22(12):2609-2623. DOI:10.1210/me.2008-0101.
Shull, M.M., Pugh, D.G. & Lingrel, J.B. 1990. The human NA,K-ATPase α 1 gene: characterization of the 5" flanking region and identification of a restriction fragement length polymorphism. *Genomics.* 6:451-460. DOI:10.1016/0888-7543(90)90475-A.
Siemieniuch, M.J., Jursza, E., Kowalewski, M.P., Majewska, M. & Skarzynski, D.J. 2012. Prostaglandin endoperoxide synthase 2 (PTGS2) and prostaglandins F2α and E2 synthases (PGFS and PGES) expression and prostaglandin F2α and E2 secretion following oestrogen and/or progesterone stimulation of the feline endometrium. *Reprod Domest Anim.* 48(1). DOI:10.1111/j.1439-0531.2012.02031.
Singhal, H.G., M. E.; Tarulli. G.; Zarnke, A. L.; Bourgo, R. J.; Laine, M.; Chang, Y.; Ma, S.; Dembo, A. G.; Raj, G. V.; Hickey, T. E.; Tilley, W. D.; Greene, G. L. 2016. Genomic agonism and phenotypic antagonism between estrogen and progesterone receptors in breast cancer. *Oncology.* 2.
Singhal, H.G., M. E.; Zarnke, A. L.; Laine, M.; Al Abosy, R.; Chang, Y.; Dembo, A. G.; Schoenfelt, K.; Vadhi, R.; Qui, X.; Rao, P.; Santhamma, B.; Nair, H. B.; Nickisch, K. J.; Long, H. W.; Becker, L.; Brown, M.; Greene, G. L. 2018. Progesterone receptor isoforms, agonists and antagonists differentially reprogram estrogen signaling. *Oncotarget.* 9(4):4282-4300.
Skosana, S.B., Woodland, J.G., Cartwright, M.C., Enfield, K., Komane, M., Louw-du Toit, R., van der Spuy, Z., Avenant, C. et al. 2019. Differential metabolism of clinically-relevant progestogens in cell lines and tissue: Implications for biological mechanisms. *J Steroid Biochem.* 189. DOI:10.1016/j.jsbmb.2019.02.010.
Skowron, K.J., Booker, K., C.;, C., Creed, S., David, B.P., Lazzara, P.R., Lian, A., Siddiqui, Z. et al. 2019. Steroid receptor/coactivator binding inhibitors: An update. *Molecular and Cellular Endocrinology.* 493. DOI:10.1016/j.mce.2019.110471.
Stanczyk, F.Z. 2003. All progestins are not created equal. *Steroids.* 68(10). DOI:10.1016/j.steroids.2003.08.003.
Stanczyk, F.Z. & Roy, S. 1990. Metabolism of levonorgestrel, norethindrone, and structurally related contraceptive steroids. *Contraception.* 42:67-96. DOI:10.1016/0010-7824(90)90093-B.
Stanczyk, F.Z., Hapgood, J.P., Winer, S. & Mishell, D.R.J. 2013. Progestogens Used in Postmenopausal Hormone Therapy: Differences in Their Pharmacological Properties, Intracellular Actions, and Clinical Effects. *Endocr Rev.* 34(2).
Stephens, B. & Handel, T.M. 2013. Chemokine Receptor Oligomerization and Allostery. In *Progress in Molecular Biology and Translational Science.* T. Kenakin, Ed.: Elsevier BV. 375-420. DOI:10.1016/b978-0-12-394587-7.00009-9.
Stoecklin, E., Wissler, M., Schaetzle, D., Pfitzner, E. & Groner, B. 1999. Interactions in the transcriptional regulation exerted by Stat5 and by members of the steroid hormone receptor family. *Journal of Steroid Biochemistry and Molecular Biology.* 69. DOI:10.1016/S0960-0760(99)00052-7.
Svärd, J., Blanco, F., Nevin, D., Fayne, D., Mulcahy, F., Hennessy, M. & Spiers, J.P. 2014. Differential interactions of antiretroviral agents with LXR, ER and GR nuclear receptors: potential contributing factors to adverse events. *British Journal of Pharmacology.* 171. DOI:10.1111/bph.12480.
Tanenbaum, D.M., Wang, Y., Williams, S.P. & Sigler, P.B. 1998. Crystallographic comparison of the estrogen and progesterone receptor's ligand binding domains. *Proc Natl Acad Sci U S A.* 95.

Taylor, A.H., McParland, P.C., Taylor, D.J. & Bell, S.C. 2009. The cytoplasmic 60 kDa progesterone receptor isoform predominates in the human amniochorion and placenta at term. *Reproductive Biology and Endocrinology.* 7(22). DOI:10.1186/1477-7827-7-22.
Tegley, C.M., Zhi, L., Marschke, K.B., Gottardis, M.M., Yang, Q. & Jones, T.K. 1998. 5-Benzylidene 1,2-Dihydrochromeno[3,4-F]Quinolines, a Novel Class of Nonsteroidal Human Progesterone Receptor Agonists. *J Med Chem.* 41. DOI:10.1021/jm980366a.
Tessel, M.A.K., N.; Rosen, S. 2010. Steroid receptor and microRNA regulation in cancer. *Curr Opin Oncol.* 22(6). DOI:10.1097/CCO.0b013e32833ea80c.
Thiebaud, D. & Secrest, R.J. 2001. Selective estrogen receptor modulators: mechanism of action and clinical experience. Focus on raloxifene. *Reprod Fertil Dev.* 13.
Tocris. 2021. *Pharmacological Glossary*. Available: https://www.tocris.com/resources/pharmacological-glossary [2021, 9 January].
Tomasicchio, M., Avenant, C., Du Toit, A., Ray, R.M. & Hapgood, J.P. 2013. The Progestin-Only Contraceptive Medroxyprogesterone Acetate, but Not Norethisterone Acetate, Enhances HIV-1 Vpr-Mediated Apoptosis in Human CD4+ T Cells through the Glucocorticoid Receptor. *Plos One.* 8(5). DOI:10.1371/journal.pone.0062895.
Treviño, L.S. & Weigel, N.L. 2013. Phosphorylation: a Fundamental Regulator of Steroid Receptor Action. *Trends Endocrinol Metab.* 24(10). DOI:10.1016/j.tem.2013.05.008.
Treviño, L.S., Bingman, W.E.r., Edwards, D.P. & Weigel, N.L. 2013. The requirement for p42/p44 MAPK Activity in Progesterone Receptor-Mediated Gene Regulation is Target Gene-Specific. *Steroids.* 78(6). DOI:10.1016/j.steroids.2012.12.014.
UNAIDS. 2019. *Global HIV & AIDS statistics — 2020 fact sheet*.
United Nations. 2019. United Nations, Department of Economic and Social Affairs, Population Division (2019). In *Contraceptive Use by Method 2019: Data Booklet.*
Van de Stolpe, A., Caldenhoven, E., Stade, B.G., Koenderman, L., Raajimakers, J.A.M., Johnson, J.P. & Van der Saag, P.T. 1994. 12-O-tetradecanoylphorbol-13-acetate and tumor necrosis factor a-mediated induction of intracellular adhesion molecule-1 is inhibited by dexamethasone. *J Biol Chem.* 269:6185-6192.
van de Stolpe, A., Slycke, A.J., Reinders, M.O., Zomer, A.W.M., Goodenough, A., Behl, C., Seasholtz, A.F. & van der Saag, P.T. 2004. Estrogen Receptor (ER)-Mediated Transcriptional Regulation of the Human Corticotropin-Releasing Hormone-Binding Protein Promoter: Differential Effects of ERα and ERβ. *Molecular Endocrinology.* 18(12). DOI:10.1210/me.2003-0446.
Vegeto, E., Shahbaz, M.M., Wen, D.X., Goldman, M.E., O'Malley, B.W. & McDonnell, D.P. 1993. Human Progesterone Receptor A Form is a Cell- and Promoter-Specific Repressor of Human Progesterone Receptor B Function. *Molecular Endocrinology.* 7(10).
Vétillard, M. & Schlecht-Louf, G. 2018. Glucocorticoid-Induced Leucine Zipper: Fine-Tuning of Dendritic Cells Function. *Front Immunol.* 9. DOI:10.3389/fimmu.2018.01232.
Vicent, G.P., Nacht, A.S., Zaurin, R., Font-Mateu, J., Soronellas, D., Le Dily, F., Reyes, D. & Beato, M. 2013. Unliganded progesterone receptor-mediated targeting of an RNA-containing repressive complex silences a subset of hormone-inducible genes. *Genes and Development.* 27. DOI:10.1101/gad.215293.113.
Wan, Y., Coxe, K.K., Thackray, V.G., Housley, P.R. & Nordeen, S.K. 2001. Separable features of the ligand-binding domain determine the differential subcellular localization and ligand-binding specificity of glucocorticoid receptor and progesterone receptor. *Mol Endocrinol.* 15(1).
Wang, D., Wang, H., Brown, J., Daikokou, T., Ning, W., Richmond, A., Strieter, R., Dey, A.K. et al. 2006. CXCL1 induced by prostaglandin E2 promotes angiogenesis in colorectal cancer. *Jourrnal of Experimental Medicine.* 203(4).
Wang, H., Napoli, K.L. & Strobel, H.W. 2000. Cytochrome P4503A9 catalyzes the metabolism of progesterone and other steroid hormones. *Mol Cell Biochem.* 213. DOI:10.1023/a:1007124417566.
Wang, Z., Zuo, G., Shi, X.Y., Zhang, J., Fang, Q. & Chen, G. 2011. Progesterone administration modulates cortical TLR4/NF-κB signaling pathway after subarachnoid hemorrhage in male rats. *Mediators Inflammation.* 2011. DOI:10.1155/2011/848309.

Wang, Z., Wang, P., Li, Y., Peng, H., Zhu, Y., Mohandas, N. & Liu, J. 2021. Interplay between cofactors and transcription factors in hematopoiesis and hematological malignancies. *Signal Transduction and Targeted Therapy.* 6(24). DOI:10.1038/s41392-020-00422-1.
Weigel, N.L. & Moore, N.L. 2007. Steroid Receptor Phosphorylation: A Key Modulator of Multiple Receptor Functions. *Molecular Endocrinology.* 21(10). DOI:10.1210/me.2007-0101.
Weii, L.L., Norris, B.M. & Baker, C. 1997. An N-terminally truncated third progesterone receptor protein, PR(C), forms heterodimers with PR(B) but interferes in PR(B)-DNA binding. *J steroid Biochem Mol Biol.* 62.
Weii, L.L., Gonzalez-Aller, C., Wood, W.M., Miller, L.A. & Horwitz, K.B. 1990. Heterogeneity in human progesterone receptor transcripts predicts a new amino-terminal truncated “C”-receptor and unique A-receptor messages. *Mol Endocrinol.* 4.
Whirledge, S. & Cidlowski, J.A. 2019. Steroid Hormone Action. In *Yen and Jaffe's Reproductive Endocrinology (Eighth Edition).* J.F. Strauss and R.L. Barbieri, Eds.: Elsevier. 115-131.e114. DOI:10.1016/B978-0-323-47912-7.00005-6.
Wiebe, J.P., Muzia, D., Hu, J., Szwajcer, D., Hill, S.A. & Seachrist, J.L. 2000. The 4-Pregnene and 5a-Pregnane Progesterone Metabolites Formed in Nontumorous and Tumorous Breast Tissue Have Opposite Effects on Breast Cell Proliferation and Adhesion. *Cancer Research.* 60.
Wikström, A.C., Bakke, O., Okret, S., Brönnegård, M. & Gustafsson, J.A. 1987. Intracellular localization of the glucocorticoid receptor: evidence for cytoplasmic and nuclear localization. *Endocrinology.* 120(4). DOI:10.1210/endo-120-4-1232.
Wolf, K., Schulz, C., Reigger, G.A.J. & Pfeifer, M. 2002. Tumour necrosis factor-alpha induced CD70 and interleukin-7R mRNA expression in BEAS-2B cells. *Eur Respir J.* 2. DOI:10.1183/09031936.02.00303602.
Wu, S., Li, R. & DeMayo, F.J. 2018. Progesterone Receptor Regulation of Uterine Adaptation for Pregnancy. *Trends Endocrinol Metab.* 29(7):481-491. DOI:10.1016/j.tem.2018.04.001.
Xiong, Y., Wang, J., Liu, L., Chen, X., Xu, H., Li, T.C., Wang, C.C. & Zhang, S. 2017. Effects of high progesterone level on the day of human chorionic gonadotrophin administration in in vitro fertilization cycles on epigenetic modification of endometrium in the peri-implantation period. *Fertil Steril.* 108(2):269-276. DOI:10.1016/j.fertnstert.2017.06.004.
Xu, Y., Zhang, S., Lin, S., Guo, Y., Deng, W., Zhang, Z. & Xue, Y. 2017. WERAM: a database of writers, erasers and readers of histone acetylation and methylation in eukaryotes. *Nucleic Acids Research.* 45(D1). DOI:10.1093/nar/gkw1011.
Yeates, C., Hunt, S.M., Balleine, R.L. & Clarke, C.L. 1998. Characterization of a truncated progesterone receptor protein in breast tumors. *J Clin Endocrinol Metab.* 82(2).
Zhang, Z., Olland, A.M., Zhu, Y., Cohen, J., Berrodin, T., Chippari, S., Appavu, C., Li, S. et al. 2005. Molecular and pharmacological properties of a potent and selective novel nonsteroidal progesterone receptor agonist tanaproget. *J Biol Chem.* 280. DOI:10.1074/jbc.M504144200.
Zhao, Q., Pang, J., Favata, M.F. & Trzaskos, J.M. 2003. Receptor density dictates the behavior of a subset of steroid ligands in glucocorticoid receptor-mediated transrepression. *Int Immunopharmacol.* 3. DOI:10.1016/j.intimp.2003.08.005.
Zheng, L., Lin, C.V. & Mu, Y. 2016. Exploring Flexibility of Progesterone Receptor Ligand Binding Domain Using Molecular Dynamics. *Plos One.* 11(11). DOI:10.1371/journal.pone.0165824.
Zhou, J. & Cidlowski, J.A. 2005. The human glucocorticoid receptor: One gene, multiple proteins and diverse responses. *Steroids.* 70. DOI:10.1016/j.steroids.2005.02.006.
Zhu, Y., Wu, M., Wu, C. & Xia, G. 2013. Role of progesterone in TLR4-MyD88-dependent signaling pathway in pre-eclampsia. *J Huazhong Unvi Sci Technolog Med Sci.* 33(5). DOI:10.1007/s11596-013-1188-6.

Appendix A

Supporting information for Chapter 2

Table A1: Summary of the Molecular ion species, lower limit of detection (LOD), lower limit of quantification (LLOQ), precision, accuracy, multiple reaction monitoring (MRM) mass transitions and retention time. The information displayed is adapted from Skosana et al., 2019.

Abbrev.	LOD ng/mL (nM)	LLOQ ng/mL (nM)	Precision			Accuracy			Mass transition: Quantifier ion	Mass transition: Qualifier ion	Retention time
			1 ng/mL	10 ng/mL	100 ng/mL	1 ng/mL	10 ng/ mL	100 ng/mL			
R5020	5 (15.32)	50 (153.15)	/	/	14.07	/	/	13.45	327.28 > 57.06	327.28 > 129.01	0.96 min
P4	0.01 (0.03)	0.01 (0.03)	18.2	12.6	8.3	18.2	12.6	8.3	315.2 > 97.1	315.2 > 109.1	0.89 min
NET	0.5 (1.7)	1 (3.4)	14.3	11.5	9.8	14.1	4.4	9.7	299 > 109	299 > 231	1.46 min
ETG	1 (3.18)	5 (12.7)	/	13.1	8.0	/	10.9	8.7	325.2 > 109.1	325.2 > 147.1	1.28 min
LNG	0.01 (0.03)	5 (16.0)	/	4.7	11.2	/	7.4	9.7	313.1 > 109.4	313.1 > 131.1	1.30 min
MPA	0.5 (1.3)	1 (2.6)	10.9	11.1	9.7	14.0	6.7	9.3	387.3 > 123.3	387.3 > 285	1.00 min
NES	0.5 (1.3)	1 (1.3)	16.5	12.6	8.3	19.0	16.1	18.8	371.3 > 253.2	371.3 > 269	1.20 min

A2.8.1.2 Cervical explants

On the day of surgery, individual pieces of cervical explant tissue (approximately 3mm^3) were placed in cryovials containing 200 µL All-Protect® (Qiagen, Netherlands) and were stored at -80°C until use. Explants were thawed at room temperature and excess All-Protect® was removed by wiping explants on tissue paper using sterile forceps. Explants were then transferred to 2 mL microfuge tubes containing two 7 mm stainless steel beads (Qiagen, Netherlands) and 100 µL radio-immunoprecipitation (RIPA) buffer (50 mM TRIS-HCl pH 8.0, 150 mM NaCl, 1% NP-40, 0.5% sodium deoxycholate and 0.1% SDS) containing 1 mM final concentration PMSF and 1 X Complete Mini protease inhibitor tablet (1 tablet/ 10 mL buffer; Roche Applied Science, RSA). Total protein was harvested mechanically using the TissueLyser LT (Qiagen, Netherlands) at 50 Hz in 4 x 1 min steps, cooling on ice in between steps. Samples were centrifuged for 20 minutes at 12000 x g at 4°C, then transferred to new microfuge tubes. Total protein was quantified using the BCA protein assay kit according to the manufacturer's instructions (Pierce, Rockford, IL, USA) and 5 X SDS sample buffer was added to a final volume of 1 X (v/v) to the remaining sample. Samples were boiled at 100°C for 7 minutes and stored at -20°C.

Appendix B

Supporting data for chapters 3 - 6

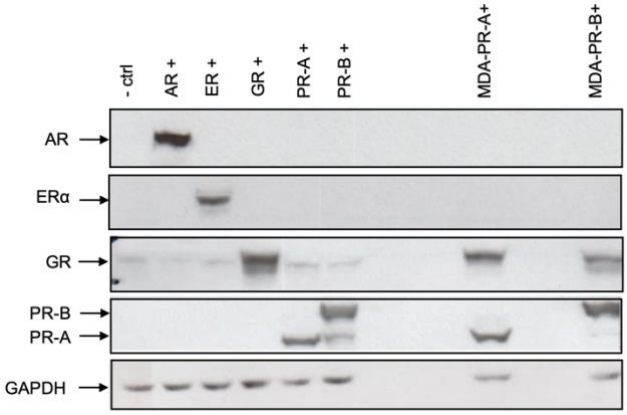

Figure B1: Endogenous expression of the PR-A and PR-B isoforms and the GR in the MDA-MB-231 PR-A/-B stably-transfected with PR-A or PR-B cell lines. MDA-MB-231-PR-A+ and -PR-B+ cells were seeded at $2.0x10^6$ cells per well in a 12-well plate. The positive controls were prepared in COS-1 cells which were seeded at 1 x 10^5 cells per well in a 12-well plate. Twenty-four hours later, the COS-1 cells were transfected with 1 µg pcDNA3.1 (empty), pSVARo, pSG5h-ERα, pcDNA3-hGR, pSG5-hPRA or pSG5-PRB. After 24 hours, the cells were harvested in 2X sample buffer and a western blot was performed. Blots were probed individually on separate blots for each primary antibody to avoid cross-reactivity between antibodies.

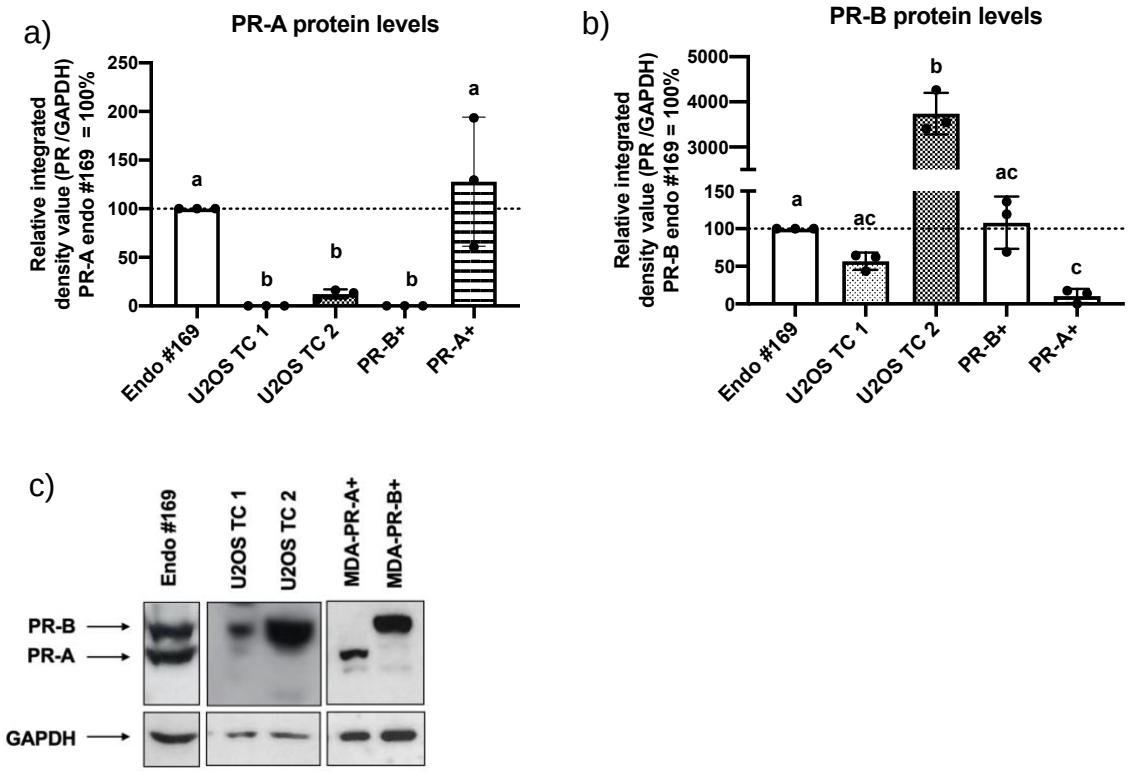

Figure B2: PR isoform expression levels in model systems are comparable to human endocervical explant. U2OS cells were seeded at $1.5x10^6$ cells per 10 cm dish. After 24 hours, the U2OS cells were transiently transfected with either 900 ng pSG5hPR-B and 9 µg 2XPRE-E1b-luc reporter (transfection condition 1, TC 1) or 3500 ng pSG5-hPR-B expression vector and 1410 ng pTAT-2xPRE-E1b-luciferase (transfection condition 2, TC 2). Twenty-four hours later, the cells were reseeded at $1.0x10^6$ cells per well in a 12-well plate. On this day MDA-MB-231-PR-A+ and MDA-MB-231-PR-B+ cells were seeded at $1.0x10^5$ cells per well in a 12-well plate. After 24 hours, U2OS TC 1, U2OS TC 2, MDA-PR-A+, MDA-PR-B+ cells were harvested in 2X sample buffer and a western blot was performed. a) Shows the mean total PR-A protein levels for each cell line, relative to endocervical tissue explant (Endo #169) = 100%. b) Shows mean total PR-B protein levels for each cell line, relative to endocervical tissue explant (Endo #169) = 100%. c) A representative western blot is shown for PR-A, PR-B and GAPDH protein levels. All samples were separated on the same gel and all samples were probed simultaneously. Three biological repeats were created for the cell line samples and compared to the endocervical sample. Relative protein levels were analysed using one-way ANOVA with a Tukey post-test, where different letters denote statistically significant differences while the same letters denote no significant difference. The SEM of the above data is calculated based on three biological repeats.

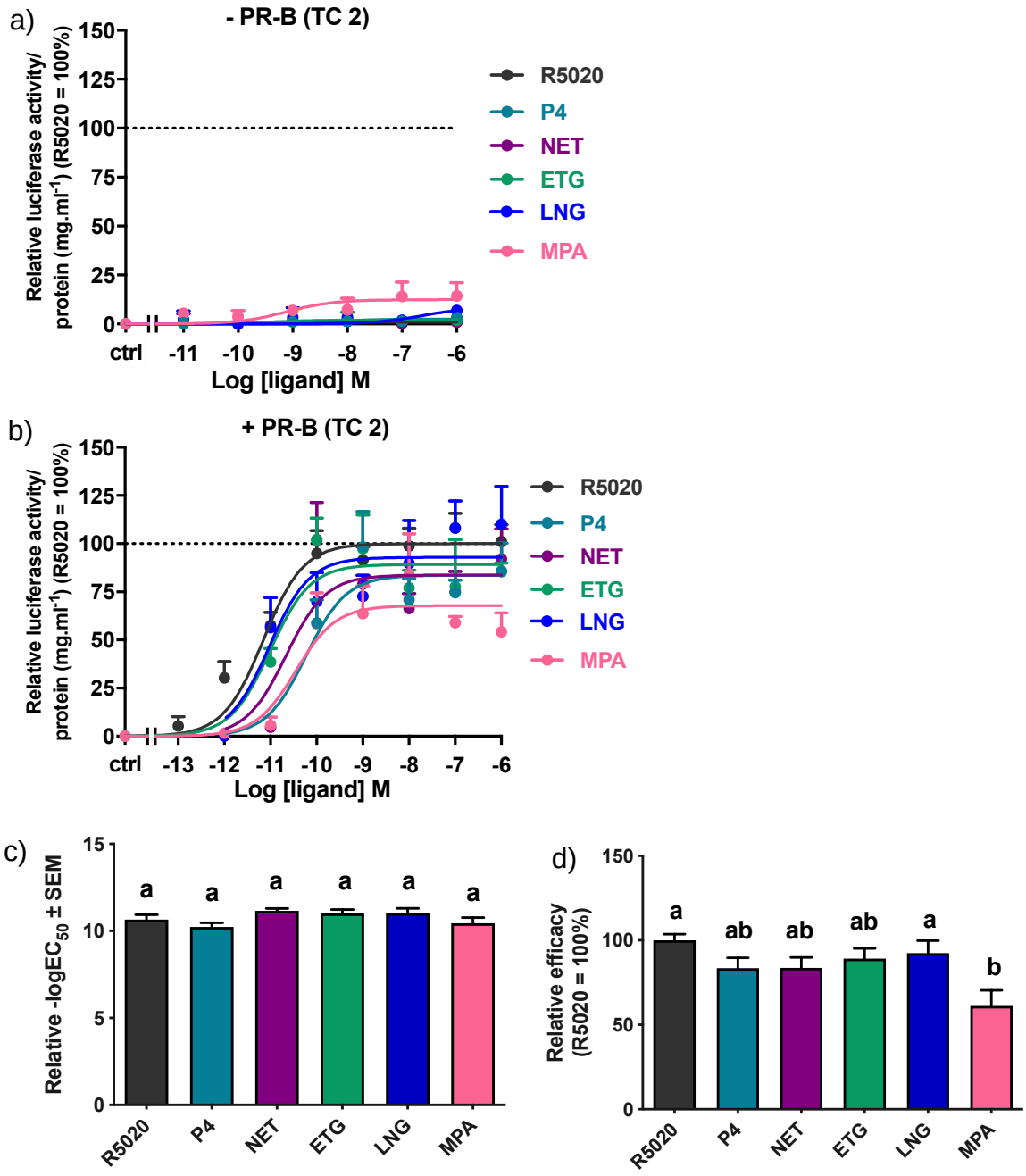

	R5020	P4	NET	ETG	LNG	MPA
-logEC$_{50}$	10.66 ± 0.27	10.23 ± 0.24	11.15 ± 0.14	11.00 ± 0.24	11.03 ± 0.28	10.45 ± 0.32
Efficacy	100 ± 3.70	83.61 ± 6.11	83.70 ± 6.26	89.22 ± 5.93	92.46 ± 7.30	61.19 ± 9.25

Figure B3: Progestogen efficacies and potencies via PR-B are minimally influenced by transfection conditions. U2OS cells were seeded and after 24 hours, the cells were transiently transfected with 3500 ng pSG5-hPR-B expression vector and 1410 ng 2xPRE-E1b-luciferase (transfection condition 2, TC 2). Twenty-four hours later, the cells were re-seeded and allowed to adhere overnight. The next day, the cells were treated with increasing concentrations (1X10^{-13} M – 1X10^{-6} M) of each ligand or vehicle (0.1% EtOH) for 24 hours.

Thereafter, the cells were harvested, and the Luciferase and Bradford assays were performed. a) & b) Show the % PR-B activity at increasing concentrations of each progestogen relative to the +PR-B R5020 efficacy = 100%. b) The bar graph shows the mean -logEC_{50} values relative to R5020 ± SEM of each ligand via PR-B while c) shows the mean efficacies of each ligand via PR-B relative to R5020 ± SEM. Relative -logEC_{50} values and efficacies were analysed using one-way ANOVA with a Tukey post-test was performed to determine statistical differences within each transfection condition different letters denote statistically significant differences while the same letters do not. The table summarises the -logEC_{50} values and efficacies ± SEM. The SEM of the above data is calculated based on the following number of biological repeats: R5020 = 7; P4 and ETG = 6; NET and MPA = 5; LNG = 4 each containing three technical repeats of each condition.

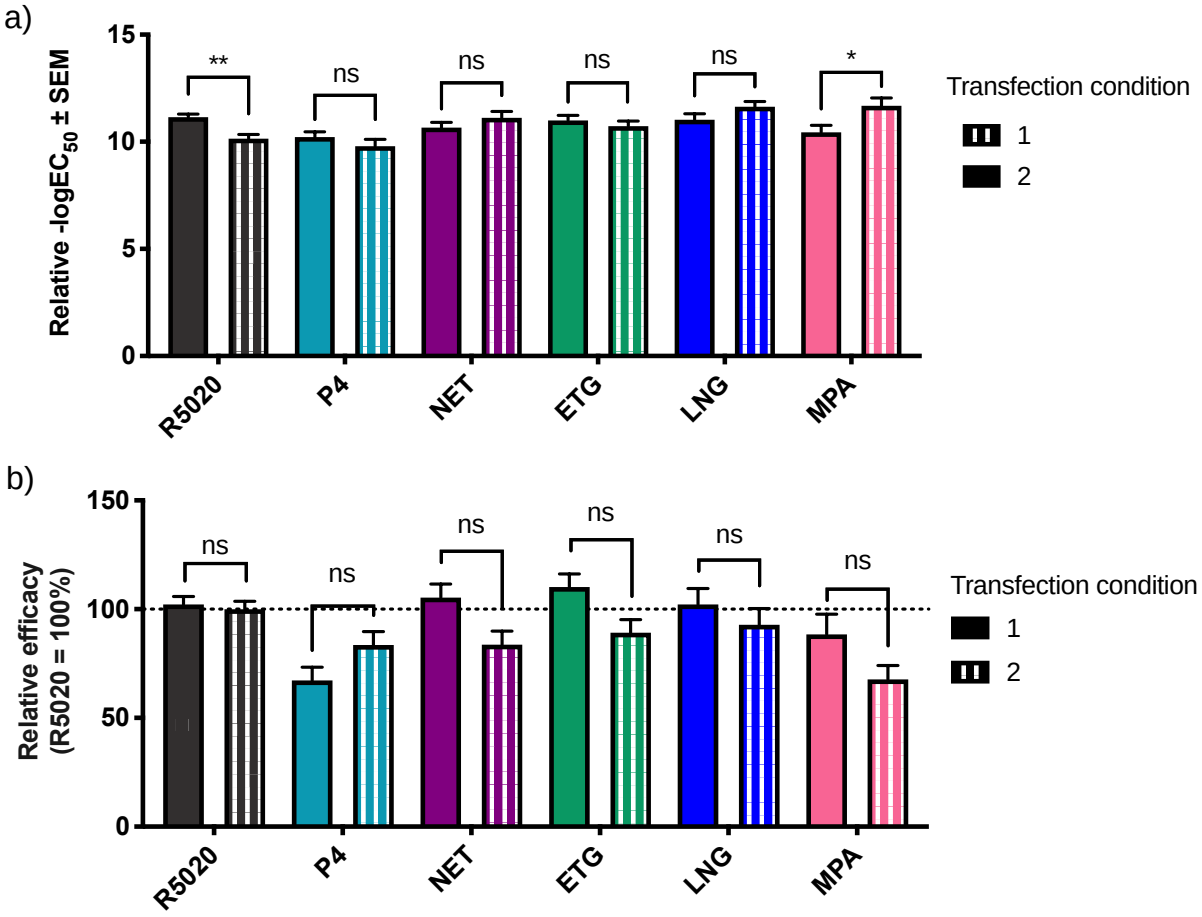

Figure B4: There are few significant differences between PR-B responses using two different transfection conditions in U2OS cells. a) The bar graph shows the mean -logEC_{50} values relative to R5020 ± SEM of each ligand via PR-B while b) shows the mean efficacies of each ligand via PR-B relative to R5020 ± SEM. The -logEC_{50} and efficacy data obtained in Fig. 3.2.1.1 (TC 1) and Fig C3 (TC 2) are shown to compare TC 1 with TC 2. A Two-way ANOVA with a Tukey post-test was performed to determine statistical differences between each cell transfection condition where * and ** denote p-value <0.05 and <0.01, respectively.

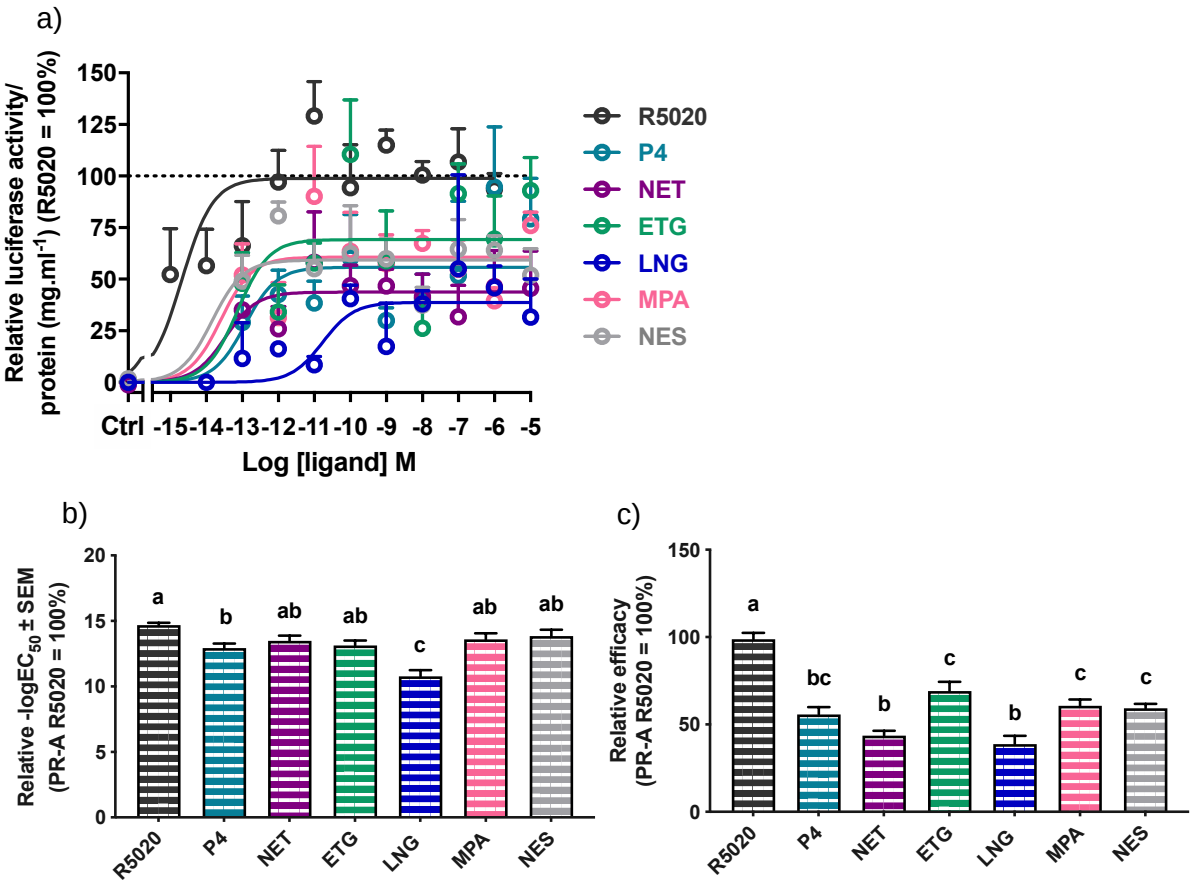

	R5020	P4	NET	ETG	LNG	MPA	NES
-logEC$_{50}$	14.68 ±0.17	12.92 ±0.34	13.47 ±0.39	13.13 ±0.37	10.77 ±0.48	13.59 ±0.47	13.84 ±0.49
Efficacy	100 ±3.55	55.79 ±4.20	43.73 ±2.69	69.20 ±5.29	38.78 ±4.79	60.68 ±3.68	59.27 ±2.51

Figure B5: R5020 is significantly more efficacious than the other progestogens via PR-A. MDA-PR-A+ cells were seeded and after 24 hours, the cells were transiently transfected with 9 µg 2XPRE-E1b-luc reporter plasmid. Twenty-four hours later, the cells were re-seeded into 96-well tissue culture plates. After 24 hours, the cells were treated with increasing concentrations ($1.0X10^{-13}$ M – $1.0X10^{-5}$ M) of each ligand or vehicle (0.1% EtOH) for 24 hours. Thereafter, the cells were harvested in 1X lysis buffer and the Luciferase and Bradford assays were performed. a) Shows the % PR-A activity at increasing concentrations of each progestogen relative to PR-A R5020 efficacy = 100%. b) Shows the mean -logEC$_{50}$ values relative to PR-B R5020 ± SEM of each ligand while c) shows the mean efficacies ± SEM of each progestogen relative to PR-A R5020 efficacy = 100%. The table summarises the mean -logEC$_{50}$ values and efficacies ± SEM. Relative -logEC$_{50}$ values and efficacies were analysed using one-way ANOVA with a Tukey post-test between progestogens where different letters denote statistically significant differences while the same letters denote no significant difference. The SEM of the above data is calculated based on the following number of biological repeats: R5020, P4, NES = 5; NET, ETG, MPA = 4 and LNG = 3, each containing three technical repeats of each condition.

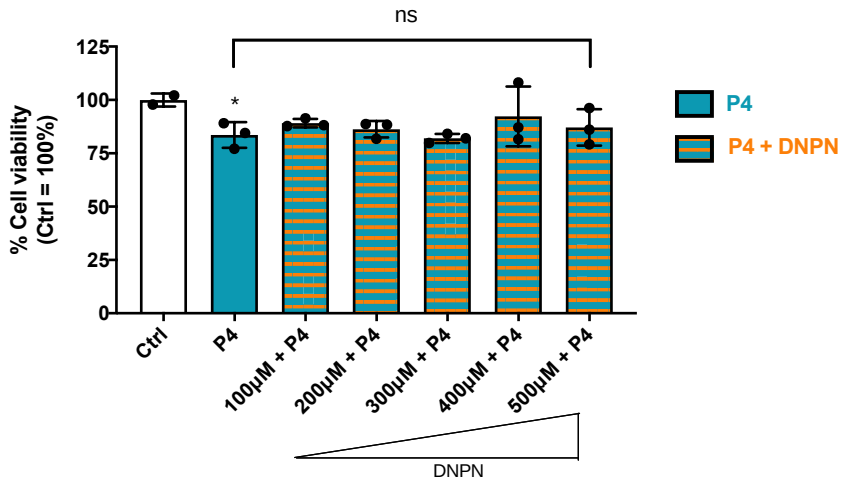

Figure B6: 4-Carboxy-2' 4'-Dinitrophenylamine (DNPN) does not significantly reduce cell viability in MDA-PR-B+ cells after a 24-hour incubation. Cells were seeded at $1x10^5$ cells per well in a 24-well tissue culture dish. 24 hours later the cells were treated with either 500 µM DNPN or vehicle (0.1% DMSO) for 2 hours. Thereafter the cells were treated with 100 nM P4 with either 500 µM DNPN or vehicle (0.1% DMSO and 0.1% ethanol) for 24 hours. The bar graph shows the mean MTT cell viability ± SEM. The data were analysed using unpaired t-test with * denoting p-value < 0.05. The SEM of the above data is calculated based on three biological repeats each containing three technical repeats of each condition.

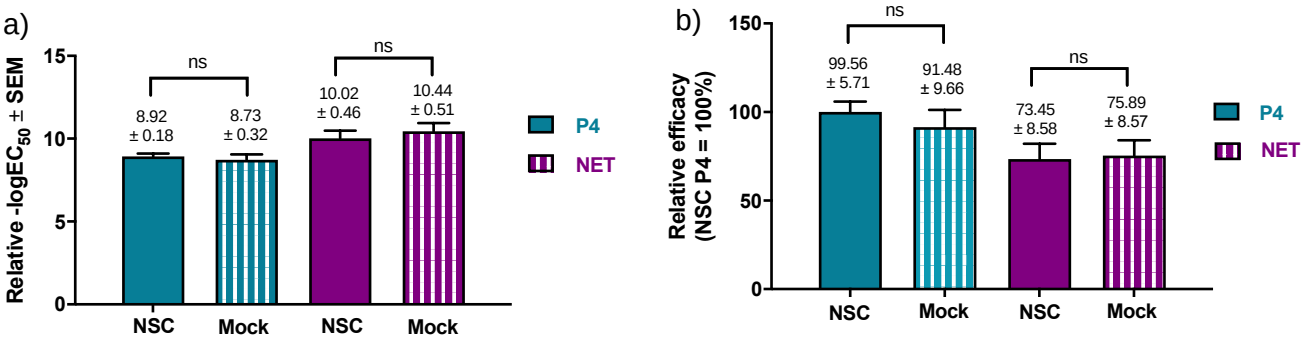

Figure B7: Potency and efficacy of P4 and NET via PR-B are not significantly different between NSC and Mock-treated U2OS cells. U2OS cells were seeded at $1.0x10^6$ cells per 10 cm dish. Twenty-four hours later, the cells were treated with 100 nM GR-specific siRNA (GR-KD) (shown in Fig. 6.2.1), non-silencing control siRNA (NSC) or mock (water instead of siRNA). After 24 hours, the cells were transiently transfected with 900 ng pSG5hPR-B and 9 µg 2XPRE-E1b-luc reporter plasmid. Twenty-four hours later the cells were re-seeded at $5x10^4$ cells per well in a 96-well tissue culture plate. After 24 hours, the cells were treated with increasing concentrations ($1X10^{-13}$ M – $1X10^{-6}$ M) of each ligand or vehicle (ctrl, 0.1% EtOH) for 24 hours. Thereafter, the cells were harvested in 1X lysis buffer and the Luciferase and Bradford assays were performed. a) The bar graph shows the -logEC_{50} values while c) shows the efficacies of each ligand via PR-B relative to P4 NSC efficacy = 100%. The above data were analysed using paired t-tests where ns indicates no significant difference. The SEM of the above data is calculated based six biological repeats each containing three technical repeats of each condition.

a)

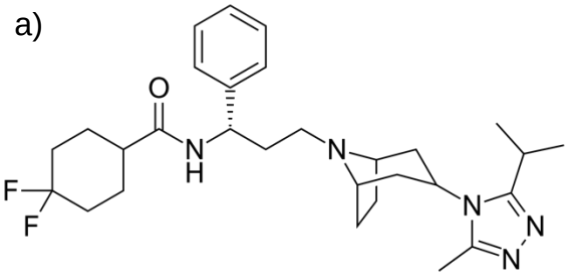

Maraviroc (MVC)

b)

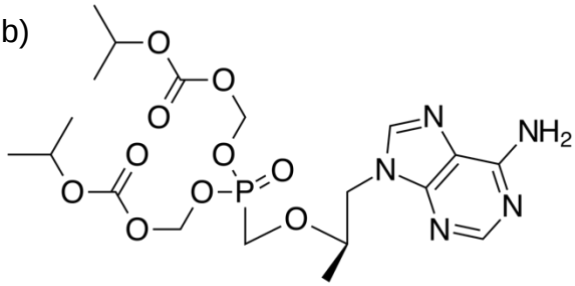

Tenofovir disoproxil fumarate (TDF)

c)

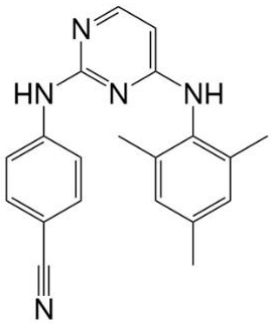

Dapivirine (DPV)

d)

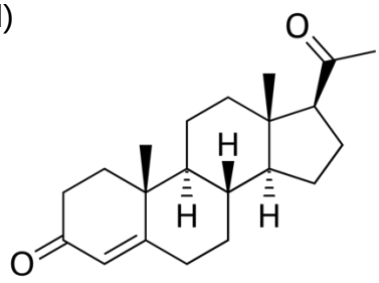

Progesterone (P4)

Figure B8: The chemical structures of MVC, TDF, DPV and P4 differ vastly.

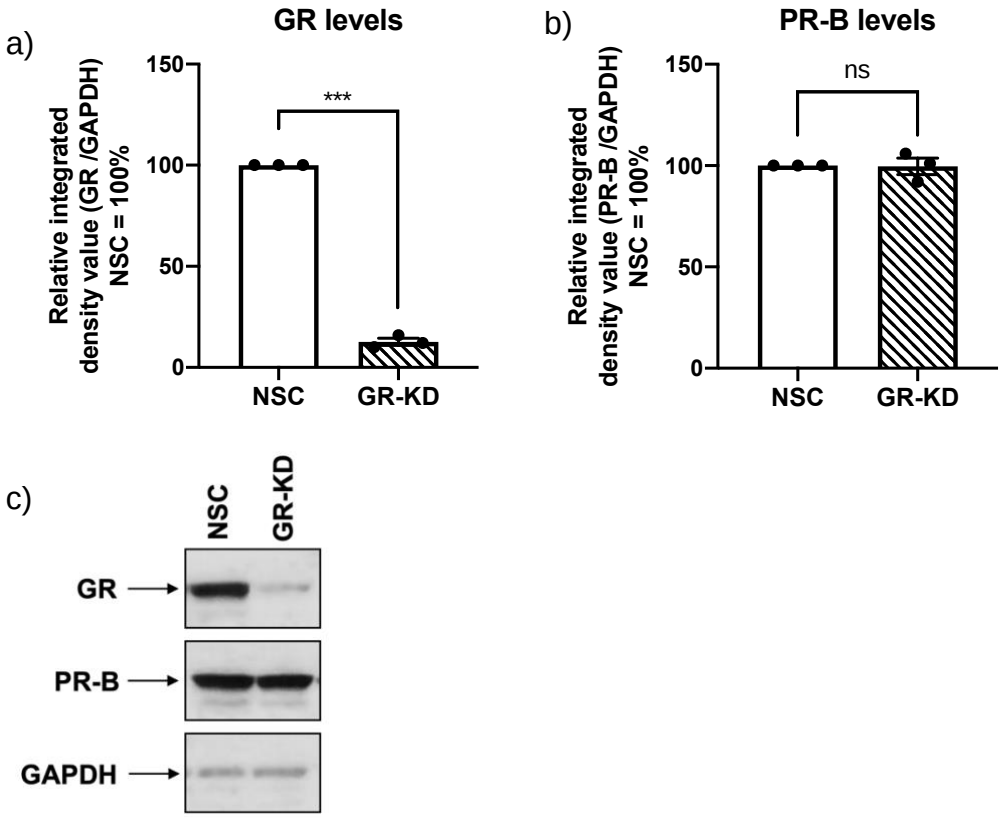

Figure B9: GR expression is reduced after GR siRNA treatment while PR-B levels are not significantly affected. MDA-PR-B+ cells were seeded and after 24 hours, the cells were treated with either 100 nM GR-specific siRNA (GR-KD) or non-silencing control siRNA (NSC). Thereafter, the cells were re-seeded in 12-well tissue culture plates and allowed to adhere overnight. After 24 hours, the cells were harvested in 2X sample buffer and a western blot was performed. a) Shows the mean GR levels while b) shows the mean total PR-B levels quantified by relative integrated density values relative to NSC ctrl = 100%. c) Representative western blots are shown for GR, PR-B and GAPDH. Relative protein levels were analysed using paired t-tests where *** denotes p-value < 0.001. The SEM is calculated based on three biological repeats.

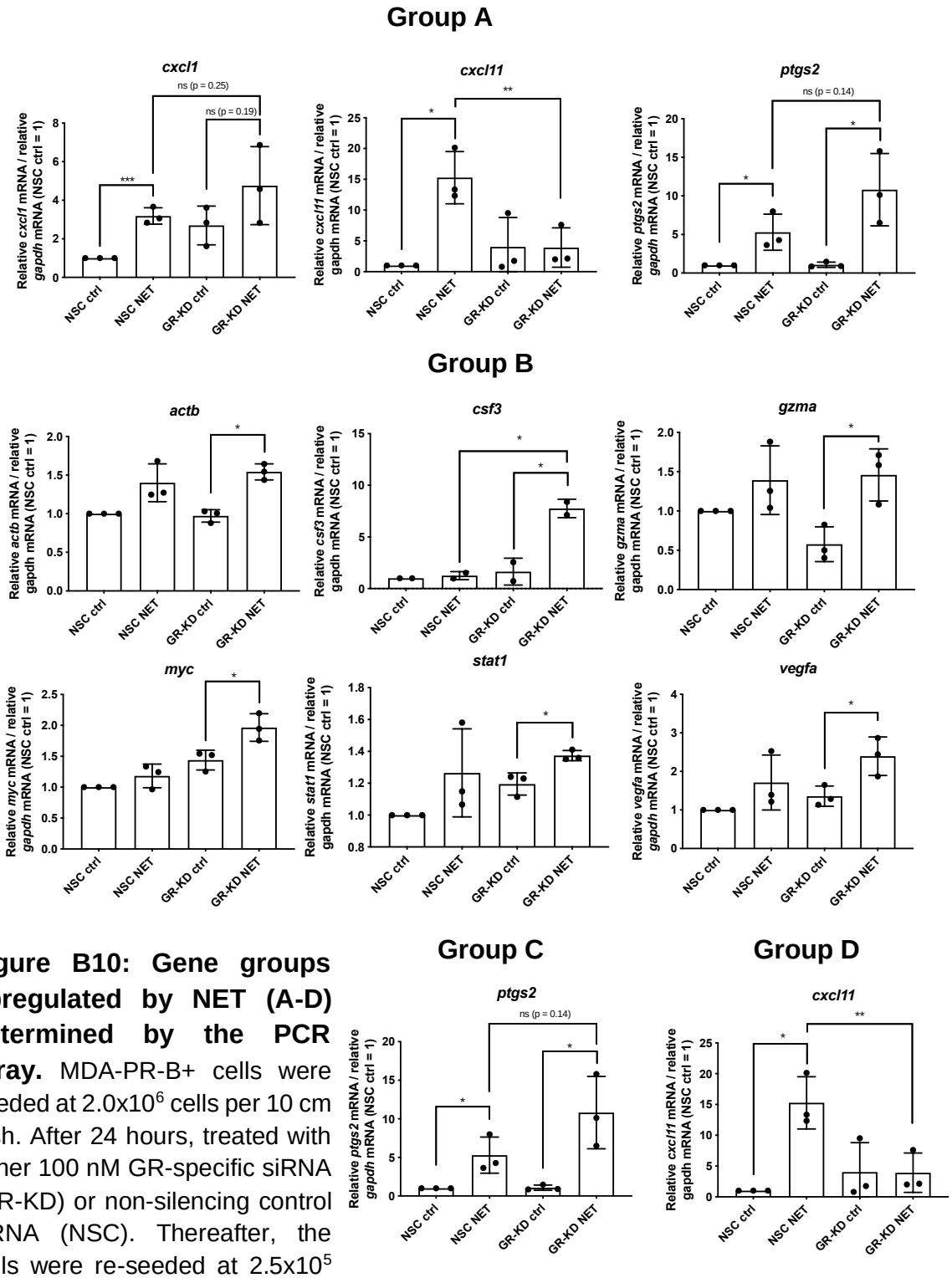

Figure B10: Gene groups upregulated by NET (A-D) determined by the PCR array. MDA-PR-B+ cells were seeded at 2.0x10^6 cells per 10 cm dish. After 24 hours, treated with either 100 nM GR-specific siRNA (GR-KD) or non-silencing control siRNA (NSC). Thereafter, the cells were re-seeded at 2.5x10^5 cells per 6-well tissue culture dish. After 24 hours, the cells were treated with 100 nM NET or vehicle (ctrl, 0.1% ethanol) for 24 hours. The cells were harvested, and the RNA was extracted using the RNeasy extraction protocol according to the manufacturer's instructions. Relative mRNA levels of the genes were normalized to *gapdh* mRNA levels. Relative expression was determined by the delta-delta Ct method normalising to NSC ctrl = 1. The above data were analysed using paired t-tests where * and ** denote p-value < 0.05 and 0.01 respectively. The SEM of the above data is calculated based on three biological repeats.

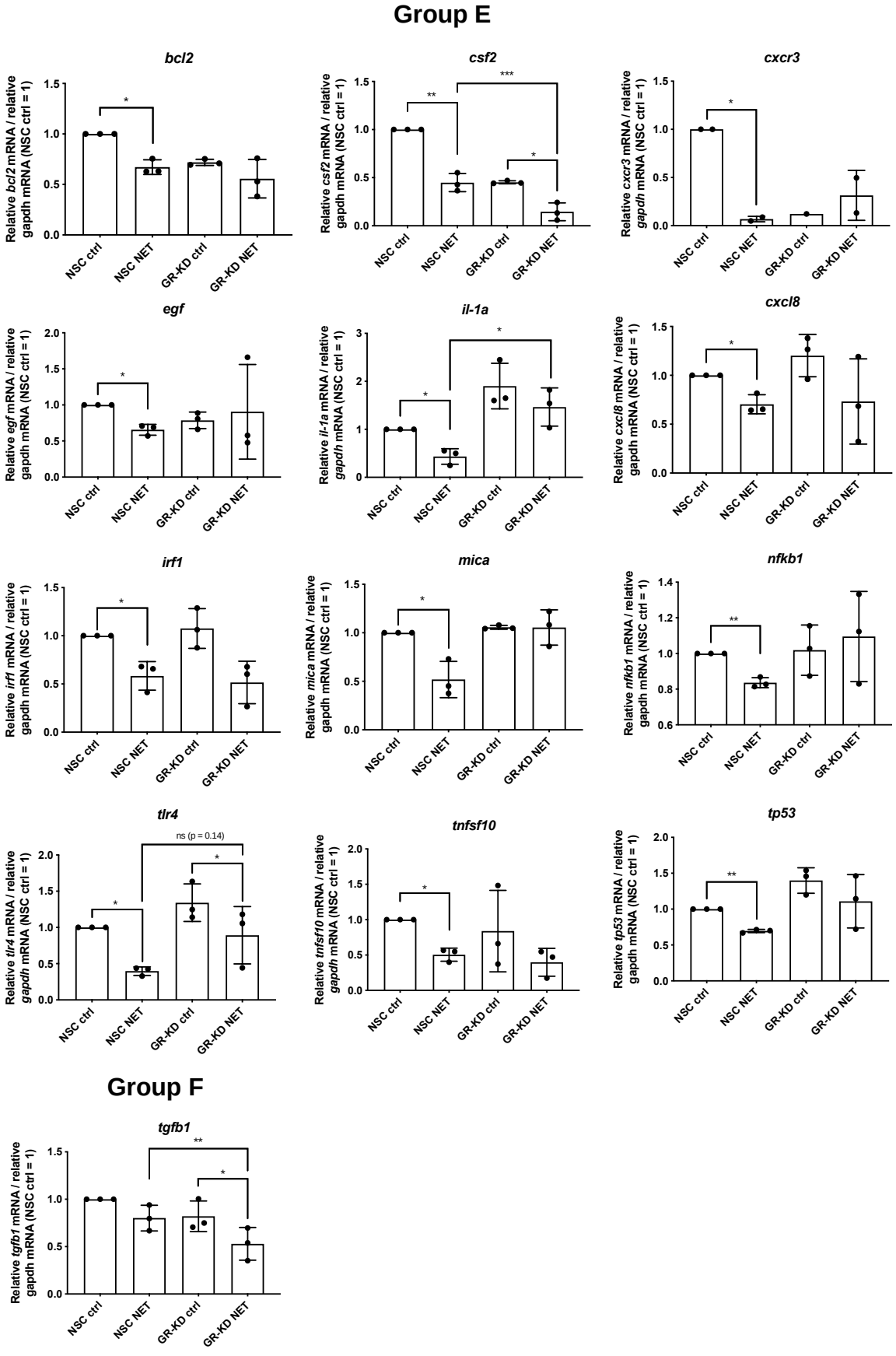

Figure B11: Gene groups downregulated by NET (E-H) determined by the PCR array. (continues on to next page).

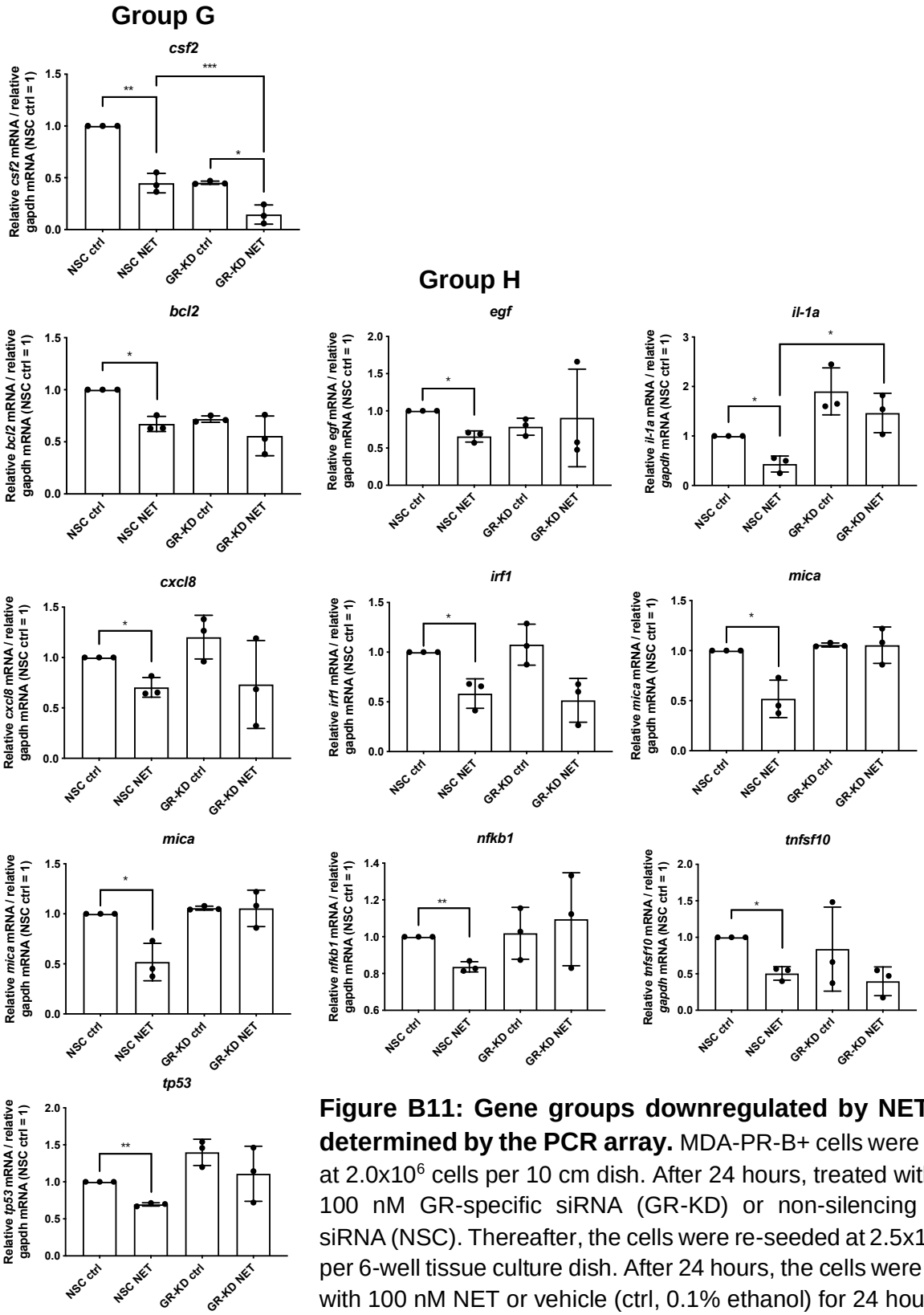

Figure B11: Gene groups downregulated by NET (E-H) determined by the PCR array. MDA-PR-B+ cells were seeded at 2.0x10^6 cells per 10 cm dish. After 24 hours, treated with either 100 nM GR-specific siRNA (GR-KD) or non-silencing control siRNA (NSC). Thereafter, the cells were re-seeded at 2.5x10^5 cells per 6-well tissue culture dish. After 24 hours, the cells were treated with 100 nM NET or vehicle (ctrl, 0.1% ethanol) for 24 hours. The cells were harvested, and the RNA was extracted using the RNeasy extraction protocol according to the manufacturer's instructions. Relative mRNA levels of the genes were normalized to *gapdh* mRNA levels. Relative expression was determined by the delta-delta Ct method normalising to NSC ctrl = 1. The above data were analysed using paired t-tests where * and ** denote p-value < 0.05 and 0.01 respectively. The SEM of the above data is calculated based on three biological repeats.

Group I

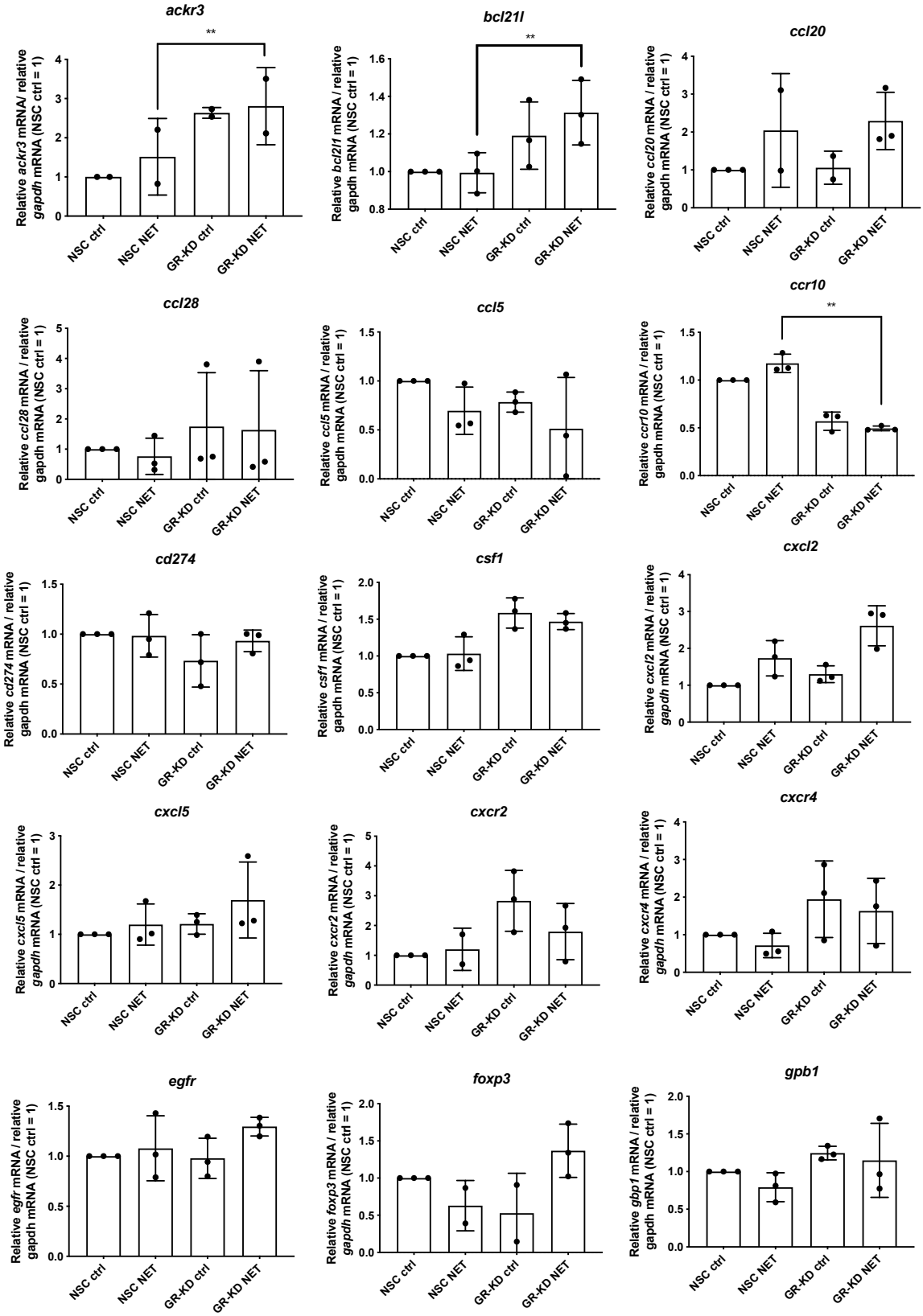

Figure B12: Gene group I shows gene expression patterns unaffected by the presence of NET determined by the PCR array. (continues on to next page).

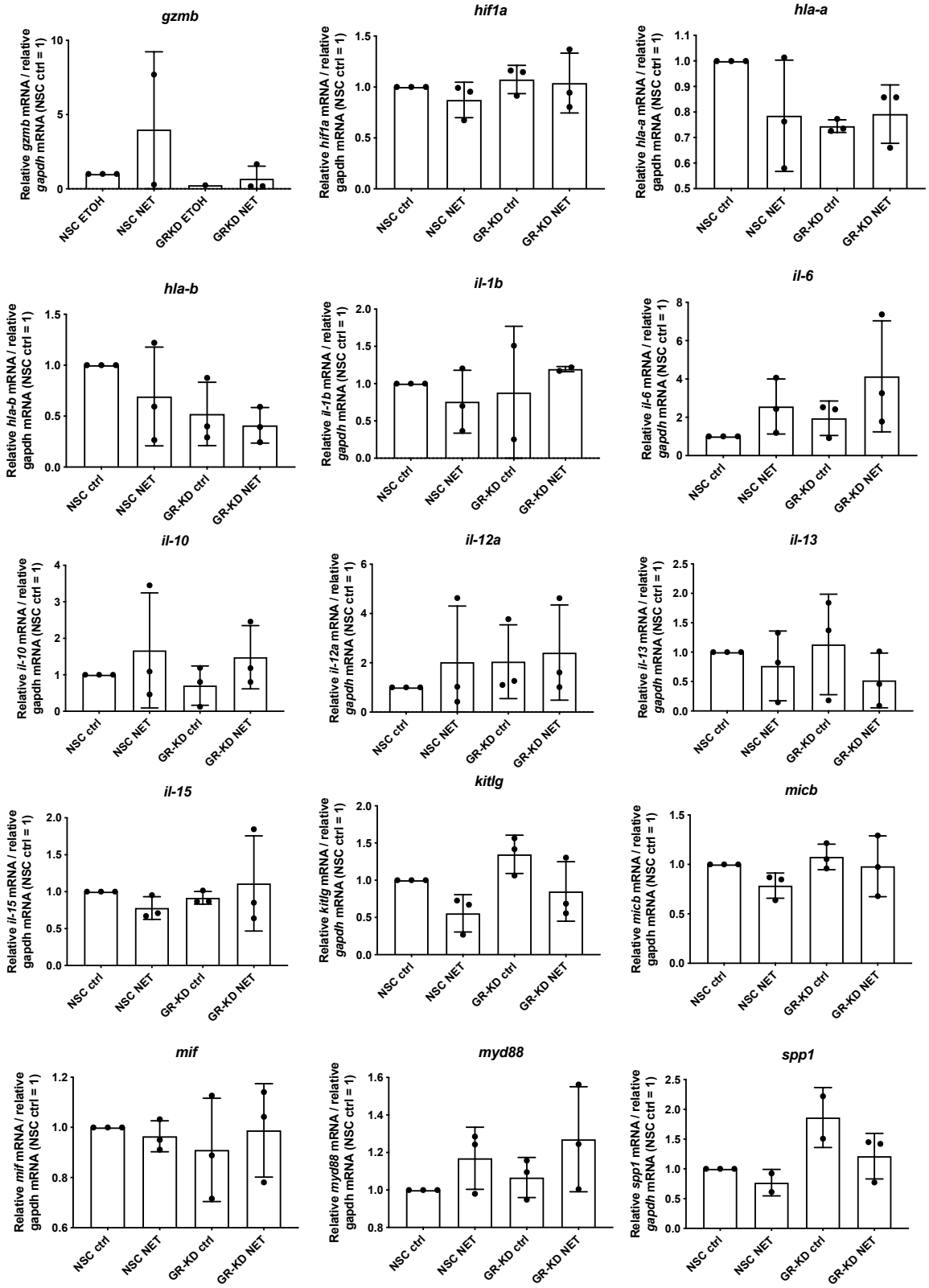

Figure B12: Gene group I shows gene expression patterns unaffected by the presence of NET determined by the PCR array. (continues on to next page).

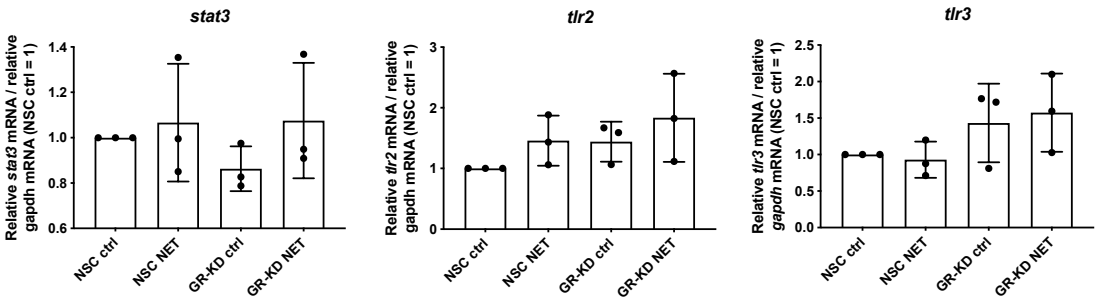

Figure B12: Gene group I shows gene expression patterns unaffected by the presence of NET determined by the PCR array. MDA-PR-B+ cells were seeded at $2.0x10^6$ cells per 10 cm dish. After 24 hours, treated with either 100 nM GR-specific siRNA (GR-KD) or non-silencing control siRNA (NSC). Thereafter, the cells were re-seeded at $2.5x10^5$ cells per 6-well tissue culture dish. After 24 hours, the cells were treated with 100 nM NET or vehicle (ctrl, 0.1% ethanol) for 24 hours. The cells were harvested, and the RNA was extracted using the RNeasy extraction protocol according to the manufacturer's instructions. Relative mRNA levels of the genes were normalized to *gapdh* mRNA levels. Relative expression was determined by the delta-delta Ct method normalising to NSC ctrl = 1. The above data were analysed using paired t-tests where * and ** denote p-value < 0.05 and 0.01 respectively. The SEM of the above data is calculated based on three biological repeats.

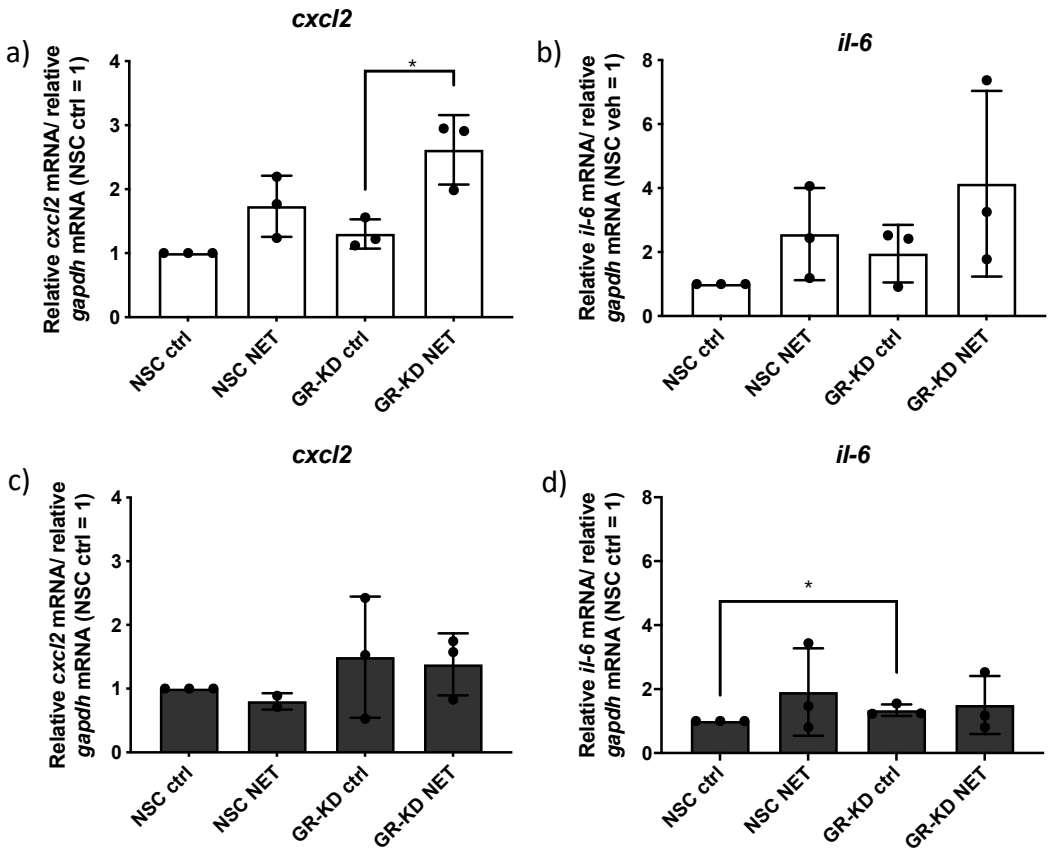

Figure B13: Two PCR array gene expression patterns (a & b) did not exhibit the same expression pattern compared to quantitative real time qPCR (c & d) experiments. Using the same RNA that was used in the PCR array, cDNA was synthesized from 250 ng RNA then used in real-time qPCR. a-b) Relative mean mRNA levels of *cxcl1*, *ptgs2* and *tlr4* obtained from the PCR array. Relative mean mRNA levels of c) *cxcl1*and d) *ptgs2* were normalized to *gapdh* mRNA levels. Relative expression was determined by normalising to NSC ctrl = 1. The above data were analysed using Two-way ANOVA with a Tukey post-test where *, ** and *** denote p-value < 0.05, < 0.01 and < 0.001 respectively. The mean ± SEM of the above data is calculated based on three biological repeats.

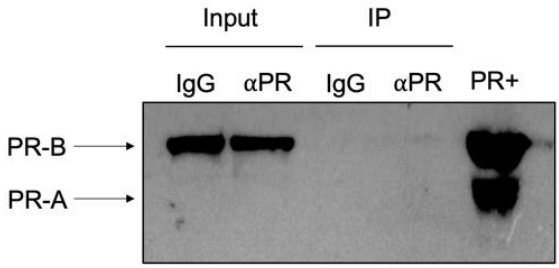

Figure B14: Representative blot showing that PR-B could not be immunoprecipitated using anti-PR antibody in MDA-PR-B+ cells. MDA-PR-B+ cells were seeded and after 24 hours, the cells were lysed, and an aliquot was analysed by western blotting for input levels (INPUT) of PR-B. The remaining cell lysate was immunoprecipitated with anti-PR antibody and magnetic protein G beads (IP). From the supernatants of ligand-treated and vehicle control samples, equal volumes were combined and incubated with donkey anti-rabbit IgG antibody (Wolf et al.). The remaining supernatants were incubated with anti-PR antibody (αPR). PR+ represents the PR positive control. Western blots were scanned for PR and the representative blot of PR protein levels is shown.

Appendix C

Publications, conference presentations and statement of work done by the candidate:

Part of the data shown chapters 3 (Fig. 3.2.1.1 and Appendix B, Fig. B3), 4 (Fig. 4.2.1) and 5 (Fig. 5.2.1, 5.2.2, 5.2.3, 5.3.1 and 5.3.2) are contained in the following publications:

Kim Enfield*, Meghan C. Cartwright*, Renate Louw-du Toit, Chanel Avenant, Donita Africander & Janet P. Hapgood (2020b). **Characterisation of progestins used in hormonal contraception and progesterone via the progesterone receptor.** *Biochemical and Biophysical Research Communications.* 553. DOI: 10.1016/j.bbrc.2020.09.058.

*co-first authors

Statement by the candidate: All data presented in which U2OS cells were used were conducted by the candidate which includes, all cell culture maintenance and experimental procedures such as promoter-reporter assays and western blotting. All statistical analyses and presentation of all the figures for both U2OS cells and other model systems were done by the candidate. The candidate also wrote the first draft of the 'Results' section contributed intellectually to the discussion and interpretation of all the results and proof-reading drafts and providing valuable feedback.

Salndave B. Skosana, John G. Woodland, Meghan C. Cartwright, **Kim Enfield**, Maleshigo Komane, Renate Louw-du Toit, Zephany van der Spuy, Chanel Avenant, Donita Africander, Karl. H. Storbeck, Janet P. Hapgood (2019). **Differential metabolism of clinically-relevant progestogens in cell lines and tissue: Implications for biological mechanisms.** *J Steroid Biochem.* 189. DOI:10.1016/j.jsbmb.2019.02.010.

Statement by the candidate: All data presented in which U2OS and END-1 cells were used were conducted by the candidate which includes all cell culture maintenance, the MTBE steroid extraction procedure as well as the UHPSFC-MS/MS experimental procedure. All statistical analyses on the U2OS and END-1 cells data

and preparation of associated figures were performed by the candidate. The candidate also contributed intellectually to the discussion and interpretation of all the results and by proof-reading drafts and providing valuable feedback.

Kim Enfield, Sigcinile Dlamini, Chanel Avenant, Michael Kuipa & Janet P. Hapgood (2020a). **Maraviroc, tenofovir disoproxil fumarate and dapivirine, activate progesterone receptor B in the absence of progestogens.** *Biochemical and Biophysical Research Communications.* 533. DOI:10.1016/j.bbrc.2020.09.107.
Statement by the candidate: All the work and figures presented in this publication were performed by the present author which includes all cell culture maintenance and experimental procedures such as promoter-reporter assays, western blotting, endogenous gene expression by real-time qPCR, competition binding, statistical analyses and presentation of results. The candidate also contributed intellectually by writing the first draft of the 'Results' and 'Methods and Materials' sections as well to the discussion and interpretation of all the results and in proof-reading drafts and providing valuable feedback.

Sigcinile Dlamini, Michael Kuipa, **Kim Enfield**, Salndave B. Skosana, John G. Woodland, Johnson M. Moliki, Alexis J. Bick, Zephany van der Spuy, Michelle F. Maritz, Chanel Avenant, Janet P. Hapgood (2019). **Reciprocal Modulation of Antiretroviral Drug and Steroid Receptor Function In Vitro**. *J. Antimicrobial Agents and Chemotherapy.* 64(1). DOI:10.1128/aac.01890-19.
Statement by the candidate: All data presented in which U2OS cells were used were conducted by the candidate which includes, all cell culture maintenance and the promoter-reporter experimental procedure. The candidate also contributed to the discussion and interpretation of all the results and in proof-reading drafts and providing valuable feedback.

Part of the data shown in chapters 3 (Fig. 3.2.3.1, 3.3.1.1, 3.3.1.2, Appendix B, Fig. B1) and 6 (Fig. 6.2.1 and 6.2.2) were presented by the candidate at the following conference presentations:

HIV Research for Prevention (HIVR4P), Madrid, Spain – Oct 2018

Alexis Bick, **Kim Enfield,** Roslyn Ray, Chanel Avenant, Janet P. Hapgood (2018). **Inflammation and HIV-1 infection are modulated by relative levels and cross-talk between the progesterone and the glucocorticoid receptors**.

Statement by the candidate: The MDA-PR-B+ promoter-reporter assay data shown were conducted by the candidate which includes cell culture maintenance, the experimental procedure as well as statistical analyses. The present author compiled the poster and presented the findings.

17th International Congress on Hormonal Steroids and Hormones & Cancer – Cape Town, South Africa – Nov 2018

Kim Enfield, Chanel Avenant, Janet P. Hapgood (2018). **The regulation of the progesterone receptor isoforms by progestins and the glucocorticoid receptor.**

Statement by the candidate: All data shown were conducted by the candidate which includes cell culture maintenance, conducting the promoter-reporter assays, western blotting and statistical analyses. The present author compiled the poster and presented the findings.

Appendix D

Research articles

Biochemical and Biophysical Research Communications xxx (xxxx) xxx

Contents lists available at ScienceDirect

Biochemical and Biophysical Research Communications

journal homepage: www.elsevier.com/locate/ybbrc

Characterisation of progestins used in hormonal contraception and progesterone via the progesterone receptor

Kim Enfield [a, 1], Meghan Cartwright [b, 1], Renate Louw-du Toit [b], Chanel Avenant [a], Donita Africander [b], Janet P. Hapgood [a, c, *]

[a] Department of Molecular and Cell Biology, University of Cape Town, Private Bag X3, Rondebosch, Cape Town, 7700, South Africa
[b] Department of Biochemistry, Stellenbosch University, Private Bag X1, Matieland, 7602, South Africa
[c] Institute of Infectious Disease and Molecular Medicine, University of Cape Town, South Africa

ARTICLE INFO

Article history:
Received 4 September 2020
Accepted 15 September 2020
Available online xxx

Keywords:
Progestins
Progesterone
Progesterone receptor
Dose-response
Potency
Efficacy

ABSTRACT

Different progestogens are widely used in hormonal therapy and mediate their therapeutic actions via the progesterone receptor (PR). Little published data exist on their relative efficacies and potencies via the PR, while those available may be confounded by off-target receptors, different methodologies and model systems. We performed dose-response analysis to investigate the efficacies and potencies for transcription of progesterone and several progestins widely used in contraception via the B isoform of human PR (PR-B). We compared responses using three different cell lines and two different transient transfection conditions. Results show that *in vitro* biological responses via PR-B for the select progestogens can vary significantly in biocharacter, rank order and absolute values for efficacies and potencies, depending on the cell line and transfection condition. Progestogen rank orders for published relative binding affinities are mostly different to those for relative efficacies and potencies. These *in vitro* differences suggest that rank orders and absolute values of the efficacies and potencies of the progestogens are likely to vary *in vivo* in a cell-specific and progestogen-specific manner, and cannot easily be extrapolated from *in vitro* data, as is usually the practice. While obtaining such data *in vivo* is not possible, these *in vitro* data show proof of concept for likely significant cell- and progestogen-specific PR-B effects.

1. Introduction

Synthetic progestogens (progestins) are used for hormonal therapy to mimic the actions of progesterone (P_4), by binding to and activating the progesterone receptor (PR), with the B isoform of the PR (PR-B) being the predominant and most transcriptionally active isoform [1]. However, some progestins are associated with side-effects such as increased risk of breast cancer, cardiovascular disease and HIV-1 acquisition [2].

Development of therapeutic progestins requires determination of affinities, efficacies (maximal response a progestin can elicit) and potencies (EC_{50}; the concentration that can elicit half the maximal response) for transcriptional regulation in cell line models expressing the PR, or potential off-target steroid receptors (SRs). This provides important information predictive of clinical relevance and side-effects [1,3]. The PR regulates transcription of specific target genes via multiple mechanisms including direct binding to progesterone response elements (PREs) in the promoter region of these genes or tethering to various DNA-bound transcription factors [4]. To determine potencies and efficacies for transcription via a particular receptor, dose-response analysis is usually performed using promoter-reporter constructs in cell lines overexpressing that receptor, where the promoter contains a SR binding site such as a PRE, ideally in a cell line deficient in competing receptors [5,6]. While the physiological relevance of such models could be

Abbreviations: AR, Androgen receptor; ETG, Etonogestrel; GR, Glucocorticoid receptor; LNG, Levonorgestrel; MPA, Medroxyprogesterone Acetate; NET, Norethindrone/Norethisterone; P_4, Progesterone; PR, Progesterone receptor; PRE, Progesterone response element; R5020, Promegestone; RBA, Relative binding affinity.

* Corresponding author. Department of Molecular and Cell Biology, University of Cape Town, Private Bag X3, Rondebosch, Cape Town, 7700, South Africa.
E-mail addresses: enfkim001@myuct.ac.za (K. Enfield), meghanc@sun.ac.za (M. Cartwright), renate@sun.ac.za (R.L.-d. Toit), avncha002@gmail.com (C. Avenant), drho@sun.ac.za (D. Africander), janet.hapgood@uct.ac.za (J.P. Hapgood).

[1] These authors contributed equally.

https://doi.org/10.1016/j.bbrc.2020.09.058
0006-291X/

disputed, they do yield direct evidence of relative receptor-specific effects of different progestins when performed in parallel experiments, which is almost impossible to otherwise obtain. Although preclinical animal and clinical models are more physiologically relevant, they have several limitations, including confounding factors due to species- and gene-specific effects, metabolism and off-target SR effects.

As it is thought that the off-target biological activity of progestins via SRs other than the PR are associated with side-effects [1,7], we have previously determined the efficacies and potencies of progestins via the glucocorticoid receptor (GR) [8], androgen receptor (AR) [9,27], mineralocorticoid [10] and estrogen receptors [9] in HEK293 or COS-1 cells with overexpressed SRs. Similar published studies assessing the relative efficacies and potencies of different progestins via the PR are surprisingly limited, and only a few [5,6,11–14] have investigated multiple progestins in parallel in the same model system. Notably, potencies reported for the PR and determined using *in vitro* models show a wide range of values between studies for progestins widely used in contraception in sub-Saharan Africa (Table 1).

This study thus aimed to directly compare the transcriptional activities of the selected progestins medroxyprogesterone acetate (MPA), norethisterone (NET), levonorgestrel (LNG) and etonogestrel (ETG), relative to each other, P_4 and the PR-specific synthetic agonist promegestone (R5020) via exogenously expressed human PR-B in COS-1 cells. As different model systems are often used when studying the transcriptional activity of progestins, we also sought to determine whether cell line and transfection conditions could be confounding factors influencing reported efficacies and potencies.

2. Materials and methods

2.1. Cell lines and materials

COS-1 monkey kidney and U2OS human bone osteosarcoma cells obtained from the ATCC (USA), and the MDA-MB-231 human breast adenocarcinoma cells received from Adrienne Edkins (Rhodes University, RSA), were maintained as previously described [22]. Only mycoplasma-negative cells were used for experiments. P_4, MPA, NET, LNG and ETG were purchased from Sigma-Aldrich, RSA, and R5020 from PerkinElmer Life and Analytical Science, RSA. The human PR-B (pSG5-hPR-B) expression vector [23] and the pTAT-2xPRE-E1b-luciferase [24] construct were received from Eric Kalkhoven (University Medical Centre Utrecht, The Netherlands) and Guido Jenster (Erasmus University of Rotterdam, Netherlands), respectively. The pSG5 empty vector [25] was obtained from Gunnar Mellgren (University of Bergen, Norway).

Table 1
Progestins widely used in contraception in sub-Saharan Africa and investigated in this study.

Parent structure[a]	Progestogen	Structure	Published potencies (pM) for human PR[b]
-	Progesterone (P_4)	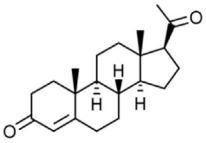	98[#], 400[#], 580[*] 800[#], 1000 – 5810[*]
P_4	Promegestone (R5020)	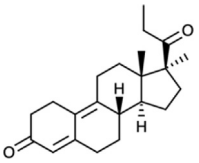	2.23[#], 60.5[§], 120[#], 5000[*]
	Medroxyprogesterone acetate (MPA)	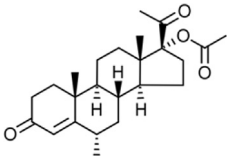	50[*], 100[*], 120[#], 150[*]
Testosterone	Norethisterone (NET)	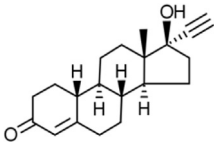	53[#], 380[*], 400 –1550[*]
	Levonorgestrel (LNG)	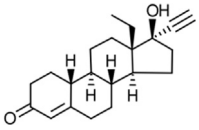	5.8[#], 169[*],190[*], 342[*]
	Etonogestrel (ETG)	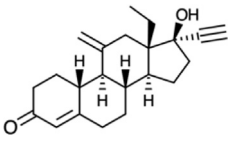	30[*], 257[*]

[a][1]; [b] [5,6,19–21,11–18] [*] PR isoform not specified. [#]PR-B. [§]PR-A.

2.2. Reporter assays

Promoter-reporter assays were performed essentially as previously described [9], with a few modifications. Briefly, COS-1 or MDA-MB-231 cells were seeded at a density of 2×10^6 cells, while U2OS cells were seeded at 1.5×10^6 cells into 10 cm dishes. Cells were transiently transfected, using XtremeGene HP (Roche Molecular Biochemicals), as follows: Transfection condition #1: 900 ng of the pSG5 empty vector or pSG5-hPR-B and 9000 ng of the pTAT-2xPRE-E1b-luciferase construct; Transfection condition #2: 3500 ng pSG5 or pSG5-hPR-B and 1410 ng pTAT-2xPRE-E1b-luciferase. The following day, the transfected cells were reseeded into 96-well plates at a density of 1×10^4 cells per well and subsequently treated with vehicle (0.1% EtOH) or increasing concentrations of the test compounds for 24 h in either serum-free medium (COS-1 and U2OS), or medium containing charcoal-stripped fetal calf serum (FCS) (MDA-MB-231). Luciferase activity was measured and normalized as previously described [9].

2.3. Immunoblotting

Protein samples were prepared as previously described [26] and 20 μg separated on a 10% SDS-polyacrylamide gel before transfer to nitrocellulose membranes (Amersham) and blocking in 10% fat-free milk powder. Membranes were probed with anti-PR (PGR-312-L-CE, Leica Biosystems, UK) or anti-glyceraldehyde-3-phosphate dehydrogenase (GAPDH; 0411, Santa Cruz Biotechnology, USA) (loading control) followed with the HRP-conjugated secondary goat anti-mouse antibody (Santa Cruz Biotechnology, USA). Proteins were visualised using enhanced chemiluminescence (Bio-Rad Laboratories, Inc. USA) and a MyECL Imager (Pierce Thermo Scientific Inc. USA), and expression levels quantified using ImageJ (Version 1.49).

2.4. Data and statistical analysis

Graph Pad Prism® software version 7 was used for data analysis. Non-linear regression and sigmoidal dose-response were used with the slope set to one. One- or two-way ANOVA (analysis of variance) and the Bonferroni (compares all pairs of columns) post-test were used for statistical analysis when multiple ligands were tested in parallel, while unpaired *t*-tests were used when ligands were not tested in parallel. The error bars represent the standard error of the mean (SEM) of at least three independent experiments, each performed in triplicate.

3. Results

3.1. Some progestogens have different efficacies and potencies via PR-B

To compare the efficacies and potencies of select progestogens, promoter-reporter and dose-response analyses were performed in COS-1 cells exogenously expressing human PR-B (Fig. 1). This cell line was selected due to negligible endogenous expression of SRs [3]. Relative to the R5020 response in PR-B transfected cells, negligible transactivation by all the progestogens was observed in the absence of transfected PR-B (Fig. 1A). In PR-B-transfected cells, all progestogens except MPA were full agonists for transactivation (Fig. 1B and C). MPA was significantly less efficacious than all progestogens investigated except P_4 (Fig. 1C), suggesting it is a partial agonist relative to R5020, NET, ETG and LNG. Interestingly, although MPA displayed a similar potency to NET, it was significantly more potent than all the other progestogens investigated, while P_4 was the least potent ligand (Fig. 1D).

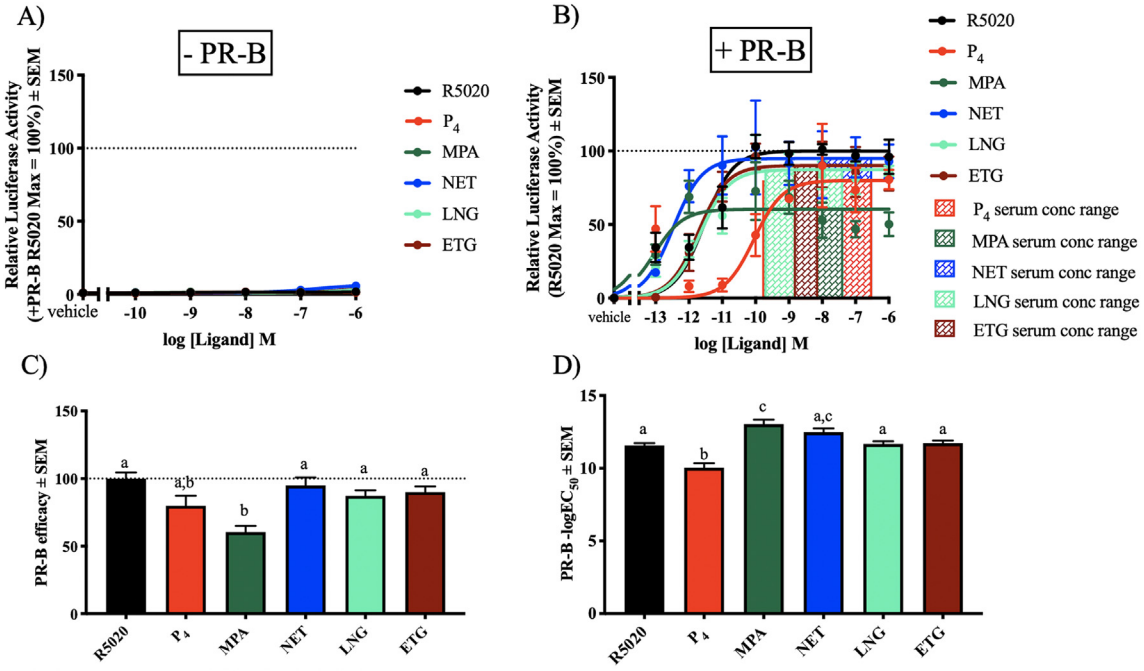

Fig. 1. Some progestogens display different efficacies and potencies via PR-B. COS-1 cells transiently transfected with (A) 900 ng pSG5-empty vector or (B–D) pSG5-hPR-B expression vector and 9000 ng pTAT-2xPRE-E1b luciferase reporter (transfection condition #1), were treated with 0.1% EtOH (vehicle) or increasing concentrations of each ligand for 24 h. Luciferase activity was measured and normalized to protein concentration. (A–B) Relative luciferase activity is shown with PR-B R5020 (maximal response) set as 100% and all other response relative to this. The shaded bars in B indicate the reported serum concentrations of progestogens in women. (C) Efficacy and (D) -logEC_{50} values ± SEM of the ligands via PR-B were plotted and analysed using one-way ANOVA with a Bonferroni post-test. Different letters denote statistically significant differences while the same letters do not.

3.2. Relative and absolute efficacies and potencies are cell-specific

To investigate whether the efficacies and potencies of the progestogens via human PR-B are influenced by the model system, we also performed experiments in the MDA-MB-231 breast cancer (Fig. 2A) and U2OS bone osteosarcoma (Fig. 2B) cell lines. These cell lines do not express endogenous PR, while low endogenous GR or AR levels are sometimes detectable [28,29]. However, we observed negligible reporter transactivation in the absence of exogenous PR-B (Supplementary Fig. 1). When the efficacies of the progestogens via PR-B were compared between the cell lines, the only statistically significant differences were seen with P_4, MPA and ETG (Fig. 2C). Both ETG and MPA were significantly more efficacious in U2OS cells compared to MDA-MB-231 cells, with MPA also being more efficacious compared to the COS-1 cells, while P_4 was significantly less efficacious in U2OS cells compared to MDA-MB-231 cells (Fig. 2C). The efficacy and potency rank orders were not conserved between cell lines (Supplementary Fig. 2). A greater number of statistically significant differences was observed for potencies compared to efficacies across the three cell lines (Fig. 2D). All the progestogens investigated via PR-B in the three cell lines had potency and efficacy values falling within the serum concentration range found in contraceptive users (Figs. 1B, 2A-B, Supplementary Table 2). Although all cell lines were transfected with 900 ng PR-B (transfection condition #1), the MDA-MB-231 cells expressed much less PR-B compared to both COS-1 and U2OS cells, while U2OS cells expressed the most PR-B (Supplementary Fig. 3G).

3.3. Relative and absolute efficacies and potencies are mostly not significantly affected by transfection conditions

Next, we investigated whether the efficacies and potencies of the progestogens via PR-B are influenced by the transfection conditions. When comparing the first (Fig. 1B–D) to the second (Fig. 3A–C) transfection condition, very few significant differences were detected. Only NET displayed a significantly lower efficacy via condition 2 (Fig. 3B), while only MPA was more potent via condition 1 (Fig. 3C). The progestogen responses via PR-B using condition 2 were also investigated in MDA-MB-231 and U2OS cells (Supplementary Figs. 3A–B). No significant differences in efficacy were observed in

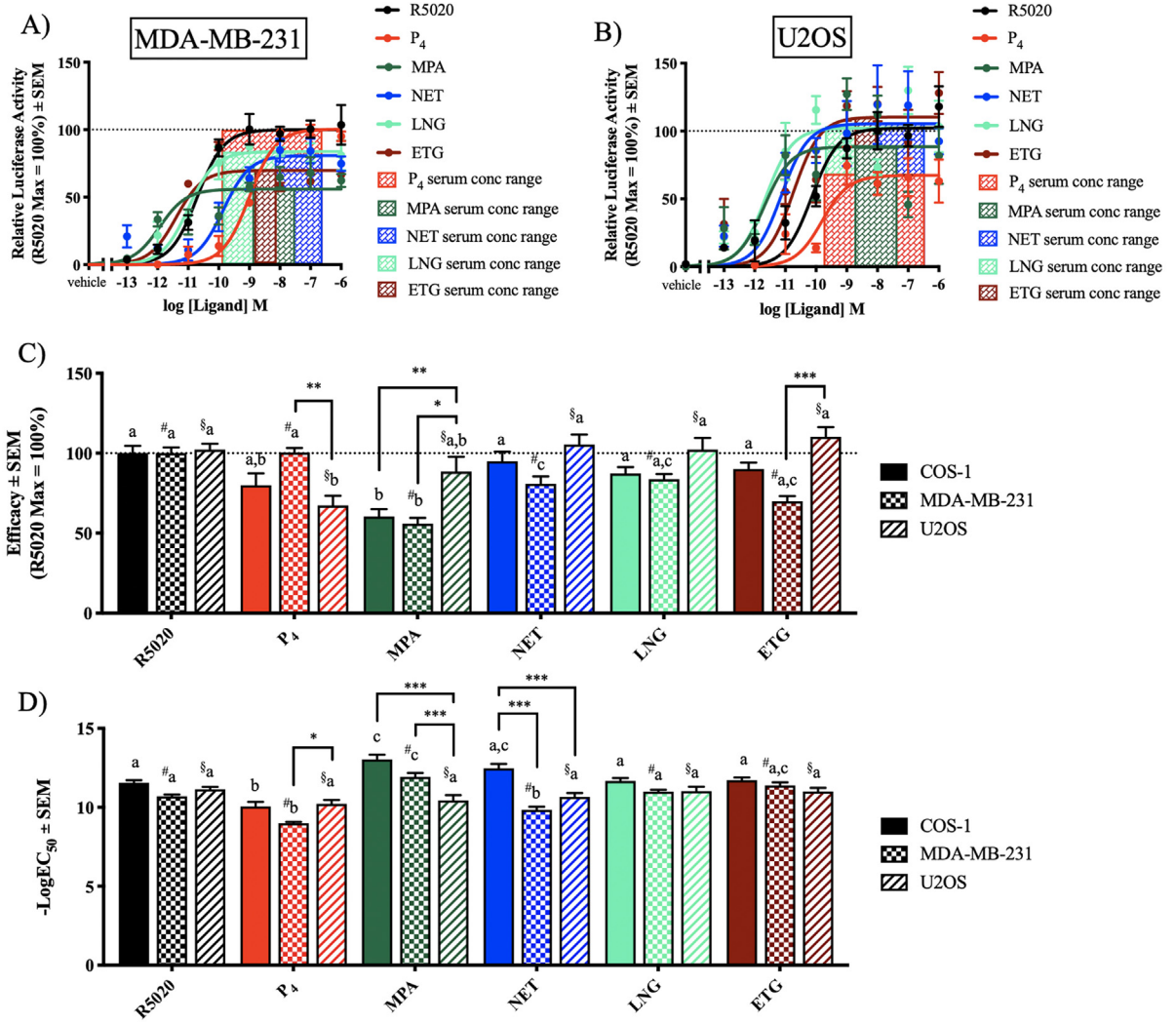

Fig. 2. Progestogen efficacies and potencies via PR-B are cell line-specific. (A) MDA-MB-231 and (B) U2OS cells were transfected and treated as for Fig. 1B–D, while results were analysed as in Fig. 1A and B. (C) The bar graph shows the efficacies ± SEM for the COS-1 (Fig. 1), MDA-MB-231 and U2OS cell-lines, while (D) shows the -logEC50 values ± SEM. Relative efficacies and -logEC_{50} were analysed using unpaired *t*-tests with *, **, *** denoting $p < 0.05$, 0.01 and 0.001, respectively. One-way ANOVA with a Bonferroni post-test was performed to determine statistical differences within each cell line (COS-1, no symbol, MDA-MB-231 # and U2OS §) where different letters denote statistically significant differences while the same letters do not.

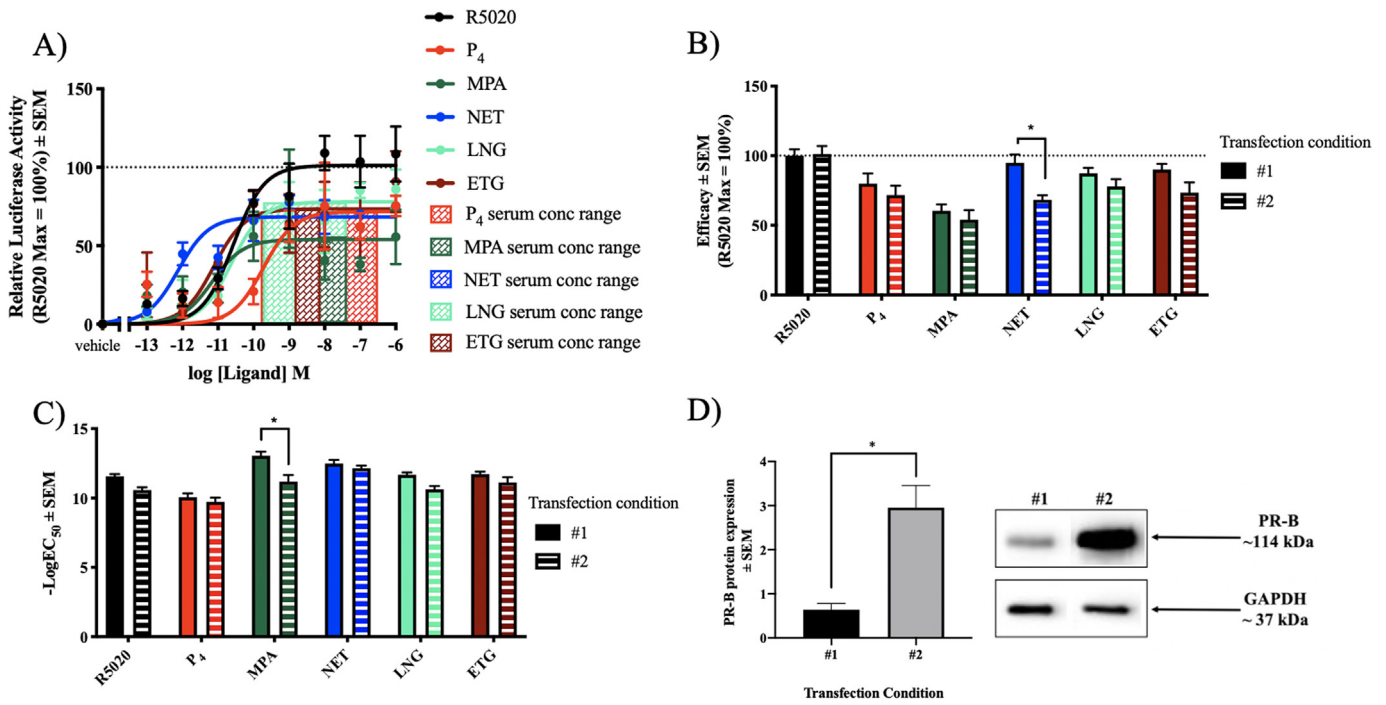

Fig. 3. Progestogen efficacies and potencies via PR-B are minimally influenced by transfection conditions. COS-1 cells, transiently transfected as for Fig. 1 (transfection condition #1) or 3500 ng pSG5-hPR-B expression vector and 1410 ng pTAT-2xPRE-E1b-luciferase (transfection condition #2), were treated with the 0.1% EtOH (vehicle) or increasing concentrations of each ligand for 24 h. Luciferase activity was measured and normalized to the protein concentration. (A) Relative luciferase activity is shown with R5020 set as 100% and all other responses relative to this. (B) Efficacy and (C) -logEC_{50} values ± SEM of the ligands via PR-B using transfection condition #1 vs #2 were plotted. (D) Total protein was harvested and a representative Western blot of the PR-B expression levels between the two different transfection conditions is shown. Two-way ANOVA with a Bonferroni post-test (B and C) and unpaired *t*-tests (D) were performed to determine statistical differences * denoting $p < 0.05$.

MDA-MB-231 and U2OS cells (Supplementary Figs. 3C–D), while similar to COS-1 cells, MPA was more potent via condition 1 in the MDA-MB-231 cells, however more potent via condition 2 in the U2OS cells (Supplementary Figs. 3E–F). NET was more potent via condition 2 in the MDA-MB-231 cells (Supplementary Fig. 3E). Interestingly, about 4-fold more PR-B was expressed under condition 2 compared to condition 1 in COS-1 cells (Fig. 3D). A similar increase in PR-B expression under condition 2 was observed for MDA-MB-231 cells, while the increase for U2OS cells was negligible (Supplementary Fig. 3G).

4. Discussion

Our study is the first to determine efficacies and potencies of these progestogens in parallel within the same model system. We show that all progestogens, except MPA, are full agonists for transactivation via human PR-B in the COS-1 cell line. While MPA displays similar potency to NET, it is significantly more potent than R5020, LNG, ETG and P_4. Only two studies have previously investigated the potencies of P_4, NET, LNG and ETG in parallel [13,14], one of which included MPA [14], via the human PR. Our results are not directly comparable since Bain and co-workers performed experiments in U2OS cells stably expressing multiple copies of the PRE and did not specify the PR isoform or include R5020 and MPA [13], while the study by Bray and co-workers included MPA and was conducted in T47D cells expressing both PR isoforms [14]. The absolute EC_{50} values for PR-B (Supplementary Table 1) are lower than those reported in both studies [13,14]. However, in agreement with our study, P_4 is the least potent progestogen and the rank order is very similar to that determined for PR-B in the U2OS cells. Other studies obtained similar potencies with overexpressed PR-B for R5020 in HeLa cells [16] and P_4 and LNG in HEK293 cells [6], to those we obtained for those progestins in COS-1 cells, while other studies have reported greater potencies for P_4 [5,12]. In terms of MPA and NET, much lower potencies were obtained for human PR-B in some other studies [5,6] compared to our study. Clearly the absolute and relative values obtained for progestogen potencies in different studies are highly dependent on the model system used. Thus, while data are consistent across studies, differences in absolute and relative progestogen potencies between studies could be due to multiple factors, including differences in cell type, promoter-reporter constructs, expression levels of the PR, method of dose-response analysis or the PR isoform(s) investigated.

Given these apparent discrepancies, we investigated whether efficacies and potencies of the progestogens for human PR-B are sensitive to the model system used. We found that MPA acts as a full agonist only in the U2OS cells, but a partial agonist in the other 2 cell lines, while most other progestogens are full agonists in all 3 cell lines. We show that relative potencies of the progestogens are more sensitive than efficacies to the cell line model system used. A possible explanation could be differential metabolism [22], either to decrease the effective concentration of select progestogens, and/or production of a metabolite that is active via the PR. Different cell lines could express different types and/or expression levels of co-regulators which may play a role in PR-B-mediated transcriptional regulation, as different ligands may cause differential recruitment of coregulators [30], and are sensitive to which progestogen is bound to the PR. Indeed, it has been shown that the ratio of coactivators and corepressors could modulate the inhibitory or stimulatory effects of the PR antagonist, RU486 [31]. All the cell line models used contain the downstream factors necessary to support PR-mediated transcription as evident from the potent responses. It is possible that some *in vivo* cofactors in cells that express endogenous PR are not present in some or all of our cell line

models which may result in different relative potencies and efficacies *in vivo*. When investigating the effects of changing both PR-B levels and DNA reporter template levels in all three cell lines, our results show that both efficacies and potencies of most progestogens are not significantly affected by the change in transient transfection conditions. However, the biocharacter of NET changes from being a full to a partial agonist, suggesting that NET in complex with PR-B is particularly sensitive to changing the concentrations and/or ratio of PR-B to DNA template.

In summary, our results show that biological responses via the PR for different progestogens *in vitro* can vary in rank order, biocharacter, and absolute values for efficacies and potencies, depending mainly on the cell line and to only a limited extent on transient transfection conditions. One of the key findings of our work is that it is difficult to establish statistically significant differences by dose-response analysis for efficacy and potency even *in vitro*, when multiple ligands are investigated in parallel. Thus caution should be used when drawing conclusions about differences between ligands without any statistical analysis of significance of difference. We established that significant differences are detected in our assays between the efficacies and potencies of several progestogens. Moreover, we show that the rank order for progestogen efficacies and potencies sometimes but not always correlate with rank order for relative binding affinities for PR-B (Supplementary Table 2 and Supplementary Fig. 4), confirming that affinity is not proportional to biological activity [8]. While steroid efficacy and potency are affected by affinity for the receptor, they are also affected by precise conformation induced by the steroid, as well as cell-specific cofactors and SR expression levels [32,33]. Our results suggest several of these factors may play a role in the progestogen-specific and cell-specific efficacies and potencies of the progestins via the PR-B.

The physiological significance of our results is to suggest that rank order and absolute values for efficacy and potency, and even biocharacter, of progestogens are likely to vary in different cells and tissues *in vivo* and cannot easily be predicted from *in vitro* dose-response assays or receptor binding affinities. Nevertheless, the *in vitro* results show valuable proof of concept effects and present viable strategies to further directly investigate mechanisms of such effects. Our findings showing that the EC_{50} values of the progestogens are well below the reported serum levels found in women using contraceptives containing these progestogens (Supplementary Table 2). Although this suggests that these progestogens are likely to elicit similar effects *in vivo*, we show that absolute potency values change depending on assay conditions, suggesting that these may vary *in vivo* in a cell-specific manner. Further studies to understand mechanisms of progestogens *in vitro* on endogenous genes via PR-B, as well as clinical studies investigating specific biological responses to progestogens, would allow a more comprehensive understanding of the benefit/side-effect profiles of these clinically-significant steroids, and facilitate choice and dose of progestin for use in hormonal therapy.

Declaration of competing interest

The authors declare that they have no known competing financial interests or personal relationships that could have appeared to influence the work reported in this paper.

Please note that all *Biochemical and Biophysical Research Communications* authors are required to report the following potential conflicts of interest with each submission. If applicable to your manuscript, please provide the necessary declaration in the box above.

(1) All third-party financial support for the work in the submitted manuscript.
(2) All financial relationships with any entities that could be viewed as relevant to the general area of the submitted manuscript.
(3) All sources of revenue with relevance to the submitted work who made payments to you, or to your institution on your behalf, in the 36 months prior to submission.
(4) Any other interactions with the sponsor of outside of the submitted work should also be reported. (5) Any relevant patents or copyrights (planned, pending, or issued).
(6) Any other relationships or affiliations that may be perceived by readers to have influenced, or give the appearance of potentially influencing, what you wrote in the submitted work. As a general guideline, it is usually better to disclose a relationship than not.

Acknowledgements

This work was supported by the Eunice Kennedy Shriver National Institute of Child Health & Human Development [R01HD083026]. We thank John Woodland for intellectual contributions.

Appendix A. Supplementary data

Supplementary data to this article can be found online at https://doi.org/10.1016/j.bbrc.2020.09.058.

References

[1] F. Stanczyk, J. Hapgood, S. Winer, et al., Progestogens used in postmenopausal hormone therapy: differences in their pharmacological properties, intracellular actions, and clinical effects, Endocr. Rev. 34 (2013) 171–208, https://doi.org/10.1210/er.2012.
[2] J. Hapgood, C. Kaushic, Z. Hel, Hormonal contraception and HIV-1 acquisition: biological mechanisms, Endocr. Rev. 39 (2018) 36–78, https://doi.org/10.1210/er.2017-00103.
[3] D. Africander, N. Verhoog, J. Hapgood, Molecular mechanisms of steroid receptor-mediated actions by synthetic progestins used in HRT and contraception, Steroids 76 (2011) 636–652, https://doi.org/10.1016/j.steroids.2011.03.001.
[4] C. Proietti, M. Cenciarini, P. Elizalde, Revisiting progesterone receptor (PR) actions in breast cancer: insights into PR repressive functions, Steroids 133 (2018) 75–81, https://doi.org/10.1016/j.steroids.2017.12.015.
[5] S. Sasagawa, Y. Shimizu, H. Kami, et al., Dienogest is a selective progesterone receptor agonist in transactivation analysis with potent oral endometrial activity due to its efficient pharmacokinetic profile, Steroids 73 (2008) 222–231, https://doi.org/10.1016/j.steroids.2007.10.003.
[6] N. Kumar, J. Fagart, P. Liere, et al., Nestorone® as a novel progestin for nonoral contraception: structure-activity relationships and brain metabolism studies, Endocrinology 158 (2017) 170–182, https://doi.org/10.1210/en.2016-1426.
[7] N. Moore, T. Hickey, L. Butler, et al., Multiple nuclear receptor signaling pathways mediate the actions of synthetic progestins in target cells, Mol. Cell. Endocrinol. 357 (2012) 60–70, https://doi.org/10.1016/j.mce.2011.09.019.
[8] K. Ronacher, K. Hadley, C. Avenant, et al., Ligand-selective transactivation and transrepression via the glucocorticoid receptor: role of cofactor interaction, Mol. Cell. Endocrinol. 299 (2009) 219–231, https://doi.org/10.1016/j.mce.2008.10.008.
[9] R. Louw-du Toit, M. Perkins, J. Hapgood, et al., Comparing the androgenic and estrogenic properties of progestins used in contraception and hormone therapy, Biochem. Biophys. Res. Commun. 491 (2017) 140–146, https://doi.org/10.1016/j.bbrc.2017.07.063.
[10] R. Louw-du Toit, J. Hapgood, D. Africander, A direct comparison of the transcriptional activities of progestins used in contraception and menopausal hormone therapy via the mineralocorticoid receptor, Biochem. Biophys. Res. Commun. 526 (2020) 466–471, https://doi.org/10.1016/j.bbrc.2020.03.100.
[11] B. Attardi, J. Burgenson, S. Hild, et al., CDB-4124 and its putative monodemethylated metabolite , CDB-4453 , are potent antiprogestins with reduced antiglucocorticoid activity : in vitro comparison to mifepristone and CDB-2914, Mol. Cell. Endocrinol. 188 (2002) 111–123.
[12] B. Attardi, S. Koduri, S. Hild, Relative progestational and androgenic activity of four progestins used for male hormonal contraception assessed in vitro in relation to their ability to suppress LH secretion in the castrate male rat, Mol.

Cell. Endocrinol. 328 (2010) 16–21, https://doi.org/10.1016/j.mce.2010.06.010.
[13] P. Bain, A. Kumar, Y. Ogino, et al., Nortestosterone-derived synthetic progestogens do not activate the progestogen receptor of Murray-Darling rainbowfish (Melanotaenia fluviatilis) but are potent agonists of androgen receptors alpha and beta, Aquat. Toxicol. 163 (2015) 97–101, https://doi.org/10.1016/j.aquatox.2015.03.021.
[14] J. Bray, S. Jelinsky, R. Ghatge, et al., Quantitative analysis of gene regulation by seven clinically relevant progestins suggests a highly similar mechanism of action through progesterone receptors in T47D breast cancer cells, J. Steroid Biochem. Mol. Biol. 97 (2005) 328–341, https://doi.org/10.1016/j.jsbmb.2005.06.032.
[15] C. Lim, C. Baumann, H. Htunt, et al., Differential localization and activity of the A- and B-forms of the human progesterone receptor using green fluorescent protein chimeras, Mol. Endocrinol. 13 (1999) 366–375, https://doi.org/10.1210/mend.13.3.0247.
[16] H. Abdel-Hafiz, M. Dudevoir, K. Horwitz, Mechanisms underlying the control of progesterone receptor transcriptional activity by SUMOylation, J. Biol. Chem. 284 (2009) 9099–9108, https://doi.org/10.1074/jbc.M805226200.
[17] A. Escande, N. Servant, F. Rabenoelina, et al., Regulation of activities of steroid hormone receptors by tibolone and its primary metabolites, J. Steroid Biochem. Mol. Biol. 116 (2009) 8–14, https://doi.org/10.1016/j.jsbmb.2009.03.008.
[18] C. Tegley, L. Zhi, K. Marschke, et al., 5-Benzylidene 1,2-dihydrochromeno[3,4-F]Quinolines, a novel class of nonsteroidal human progesterone receptor agonists, J. Med. Chem. 41 (1998) 4354–4359, https://doi.org/10.1021/jm980366a.
[19] R. Austin, B. Maschera, A. Walker, et al., Mometasone furoate is a less specific glucocorticoid than fluticasone propionate, Eur. Respir. J. 20 (2002) 1386–1392, https://doi.org/10.1183/09031936.02.02472001.
[20] Z. Zhang, A. Olland, Y. Zhu, et al., Molecular and pharmacological properties of a potent and selective novel nonsteroidal progesterone receptor agonist tanaproget, J. Biol. Chem. 280 (2005) 28468–28475, https://doi.org/10.1074/jbc.M504144200.
[21] K. Madauss, S. Deng, R. Austin, et al., Progesterone receptor ligand binding pocket flexibility: crystal structures of the norethindrone and mometasone furoate complexes, J. Med. Chem. 47 (2004) 3381–3387, https://doi.org/10.1021/jm030640n.
[22] S. Skosana, J. Woodland, M. Cartwright, et al., Differential metabolism of clinically-relevant progestogens in cell lines and tissue: implications for biological mechanisms, J. Steroid Biochem. Mol. Biol. 189 (2019) 145–153, https://doi.org/10.1016/j.jsbmb.2019.02.010.
[23] P. Kastner, M. Bocquel, B. Turcotte, et al., Transient expression of human and chicken progesterone receptors does not support alternative translational initiation from a single mRNA as the mechanism generating two receptor isoforms, J. Biol. Chem. 265 (1990) 12163–12167.
[24] G. Jenster, T. Spencer, M. Burcin, et al., Steroid receptor induction of gene transcription: a two-step model, Proc. Natl. Acad. Sci. Unit. States Am. 94 (1997) 7879–7884, https://doi.org/10.1073/pnas.94.15.7879.
[25] S. Green, I. Issemann, E. Sheer, A versatile in vivo and in vitro eukaryotic expression vector for protein engineering, Nucleic Acids Res. 16 (1988) 369, https://doi.org/10.1093/nar/16.1.369.
[26] R. Louw-du Toit, J. Hapgood, D. Africander, Medroxyprogesterone acetate differentially regulates interleukin (IL)-12 and IL-10 in a human ectocervical epithelial cell line in a glucocorticoid receptor (GR)-dependent manner, J. Biol. Chem. 289 (2014) 31136–31149, https://doi.org/10.1074/jbc.M114.587311.
[27] D. Africander, K. Storbeck, J. Hapgood, A comparative study of the androgenic properties of progesterone and the progestins, medroxyprogesterone acetate (MPA) and norethisterone acetate (NET-A), J. Steroid Biochem. Mol. Biol. 143 (2014) 404–415, https://doi.org/10.1016/j.jsbmb.2014.05.007.
[28] K. Horwitz, D. Zava, A. Thilagar, et al., Steroid receptor analyses of nine human breast cancer cell lines, Canc. Res. 38 (1978) 2434–2437.
[29] K. Hadley, An Investigation into the Role of Acetylation and Ligand-dependent Nuclear Localisation in Glucocorticoid Receptor Transcriptional regulation, in: Doctor of Philosophy Doctoral Thesis, University of Cape Town, 2010. http://hdl.handle.net/11427/10607.
[30] K. Scarpin, J. Graham, P. Mote, et al., Progesterone action in human tissues: regulation by progesterone receptor (PR) isoform expression, nuclear positioning and coregulator expression, Nucl. Recept. Signal. 7 (2009) e009, https://doi.org/10.1621/nrs.07009.
[31] Z. Liu, D. Auboeuf, J. Wong, et al., Coactivator/corepressor ratios modulate PR-mediated transcription by the selective receptor modulator RU486, Proc. Natl. Acad. Sci. Unit. States Am. 99 (2002) 7940–7944, https://doi.org/10.1016/j.purol.2010.08.008.
[32] S. Simons, C. Chow, The road less travelled: new views of steroid receptor action from the path of dose-response curves, Mol. Cell. Endocrinol. 348 (2012) 373–382, https://doi.org/10.1038/mp.2011.182.
[33] S. Simons, Glucocorticoid receptor co-factors as therapeutic targets, Curr. Opin. Pharmacol. 10 (2010) 613–619, https://doi.org/10.1038/mp.2011.182.

Journal of Steroid Biochemistry and Molecular Biology 189 (2019) 145–153

Contents lists available at ScienceDirect

Journal of Steroid Biochemistry and Molecular Biology

journal homepage: www.elsevier.com/locate/jsbmb

Differential metabolism of clinically-relevant progestogens in cell lines and tissue: Implications for biological mechanisms

Salndave B. Skosana[a], John G. Woodland[a], Meghan Cartwright[b], Kim Enfield[a], Maleshigo Komane[a], Renate Louw-du Toit[b], Zephne van der Spuy[c], Chanel Avenant[a], Donita Africander[b], Karl-Heinz Storbeck[b], Janet P. Hapgood[a,d,*]

[a] Department of Molecular and Cell Biology, University of Cape Town, South Africa
[b] Department of Biochemistry, Stellenbosch University, South Africa
[c] Department of Obstetrics and Gynaecology, University of Cape Town, Groote Schuur Hospital, Cape Town, South Africa
[d] Institute of Infectious Disease and Molecular Medicine, University of Cape Town, South Africa

ARTICLE INFO

Keywords:
Contraceptives
Metabolism
Progesterone
Progestins
Steroids
UHPSFC-MS/MS

ABSTRACT

Steroid hormones regulate a variety of physiological processes, including reproductive function, and are widely used in hormonal therapy. Synthetic progestogens, or progestins, were designed to mimic progesterone (P_4) for use in contraception and hormonal replacement therapy in women. Medroxyprogesterone acetate (MPA) and norethisterone (NET) are the most widely used injectable contraceptives in the developing world, while other progestins such as levonorgestrel (LNG), etonogestrel (ETG) and nestorone (NES) are used in or being developed for other forms of contraception. As concerns remain about the most appropriate choice of progestin and dosage, and the associated side-effects, the mechanisms and biological effects of progestins are frequently investigated in various *in vitro* mammalian cell line and tissue models. However, whether progestogens are differentially metabolised in different cell types *in vivo* or *in vitro* is unknown. For nine mammalian cell lines commonly used to investigate progestogen mechanisms of action, we developed and validated an ultra-high performance supercritical fluid chromatography-tandem mass spectrometry (UHPSFC-MS/MS) protocol for simultaneously quantifying the metabolism of the above-mentioned steroids. We show for the first time that, while 50–100% of P_4 was metabolised within 24 h in all cell lines, the metabolism of the progestins is progestin- and cell line-specific. We also show that MPA and NET are significantly metabolised in human cervical tissue, but to a lesser extent than P_4. Taken together, our findings suggest that differential progestogen metabolism may play a role in cell-specific therapeutic and side-effects. Relative affinities for binding to steroid receptors as well as potencies, efficacies and biocharacters for transcriptional activity of progestins, relative to P_4, are most frequently determined using some of the cell lines investigated. Our results, however, suggest that differential metabolism of progestins and P_4 may confound these results. In particular, metabolism may under-estimate the receptor-mediated intrinsic *in vitro* binding and dose-response values and predicted endogenous physiological effects of P_4.

1. Introduction

Choice of hormonal contraception and hormone replacement therapy (HRT) in women is an important public health issue, especially regarding possible side-effects relevant to cancer, metabolic disorders, cardiovascular complications, bone mineral density and susceptibility to infectious diseases [1,2,3]. Synthetic steroids are commonly utilised in contraceptive treatments and HRT. These synthetic steroids, known as progestins or synthetic progestogens, are intended to mimic the actions of the endogenous hormone P_4 [1–3] and are classified into two groups. The first class of progestins, which includes medroxyprogesterone acetate (MPA) and nestorone (NES), is structurally related to P_4, while the second class is structurally related to testosterone (T), and includes norethisterone (NET), etonogestrel (ETG) and levonorgestrel (LNG) [2,3]. Injectable progestins, which are especially popular in the developing world as contraceptives due to their discreet

Abbreviations: DEX, dexamethasone; ETG, etonogestrel; LNG, levonorgestrel; MPA, medroxyprogesterone acetate; NES, nestorone; NET, norethisterone; P_4, progesterone; PR, progesterone receptor; T, testosterone

* Corresponding author at: Department of Molecular and Cell Biology, University of Cape Town, South Africa.
E-mail address: Janet.Hapgood@uct.ac.za (J.P. Hapgood).

https://doi.org/10.1016/j.jsbmb.2019.02.010
Received 20 December 2018; Received in revised form 22 February 2019; Accepted 24 February 2019
Available online 26 February 2019
0960-0760/

nature, include MPA and NET, the latter administered in its enanthate form (NET-EN) [2,3]. Other progestins such as LNG and ETG are widely used in combined oral contraceptives and implants and, together with NES, are currently being investigated for use intravaginally or in multipurpose prevention technologies [3].

Progestin research relies extensively on model systems using well-established laboratory cell lines [2–6] or *in vitro* experiments with primary cells, tissue or tissue extracts [7–12]. In such experiments, specific concentrations of the steroids are used and these concentrations are assumed to remain constant over the incubation period. Differences in activity between steroids is thought to be due to their different biocharacters, and metabolism is not taken into account. Differential metabolism may confound the results of concentration-dependent experiments such as dose-response analyses and binding studies [2–4]. It is well established that progestins act intracellularly via binding to and activating the progesterone receptor (PR) [2,3], which is a ligand-activated transcription factor. Evidence is emerging that some of the side-effects of progestins may occur by off-target effects via binding to and activating steroid receptors other than the PR [3,5]. However, very little is known about the metabolism of progestins; in particular, whether this metabolism is cell-specific, which metabolites are produced, what the role is of metabolites and whether metabolism may confound interpretation of the results when investigating relative biological activities.

The aim of this work was therefore to investigate the metabolism of P_4 and selected progestins in nine commonly used laboratory cell lines, and to validate select findings in endocervical tissue. To this end, we developed and validated an ultra-high-performance supercritical fluid chromatography-tandem mass spectrometry (UHPSFC-MS/MS) method for the separation and quantification of these progestogens in the nanomolar range, as detected in the serum of women. We included the synthetic glucocorticoid dexamethasone (DEX) in our panel of steroids, since the activity of progestins is often investigated in parallel with DEX, given the established glucocorticoid activity of MPA [10,13,14]. Results showed that P_4 was substantially metabolised in all cells lines and the endocervical tissue after 24 h, while cell line- and steroid-specific metabolism were observed for the different progestins.

2. Materials and methods

2.1. Steroids and solvents

LNG was obtained from the United Stated Pharmacopoeia (USP, Rockville, MD, USA) and Sigma-Aldrich (South Africa). P_4, MPA, NES, DEX, NET, ETG, T, UHPLC-grade methanol, absolute ethanol, formic acid and methyl *tert*-butyl ether (MTBE) were all purchased from Sigma-Aldrich (South Africa).

2.2. Cell lines and endocervical tissue

Human embryonic kidney cells (HEK293T), human epithelial cervical cancer cells (HeLa), human endocervical cells (END-1), human bone osteosarcoma epithelial cells (U2OS) and monkey kidney fibroblast cells (COS-1) were purchased from American Type Culture Collection (ATCC, USA). Human cervical cells (TZM-bl) were procured from the NIH AIDS Reagent Program, Division of AIDS, NIAID, NIH, from Dr John C. Kappes, Dr Xiaoyun Wu and Tranzyme Inc. (ARP, NIH, USA). The human MDA-MB-231 breast cancer cell line was originally acquired from ATCC, but was received from Prof Adrienne Edkins at Rhodes University, South Africa, while Prof Ana Soto at Tufts University, Boston, USA provided the human MCF-7 BUS breast cancer cells. The human T47D breast cancer cell line was donated by Prof Iqbal Parker at the University of Cape Town, South Africa.

Endocervical tissue was obtained after informed consent from HIV-1 negative, post-menopausal women undergoing hysterectomies for benign reasons. Ethical permission was obtained from the Human Research Ethics Committee (University of Cape Town) for the duration of this study (HREC 258/2017). Fresh tissue was supplied from two sites in the Western Cape, South Africa; namely, Groote Schuur and Tygerberg Hospitals.

2.3. Cell line culture

HEK293T, HeLa, U2OS, TZM-bl, T47D and COS-1 were all cultured in Dulbecco's modified Eagle's medium (DMEM) (Sigma-Aldrich, South Africa) supplemented with 1 mM sodium pyruvate (Sigma-Aldrich, South Africa), 44 mM sodium bicarbonate (Sigma-Aldrich, South Africa), 10% (v/v) fetal bovine serum (FBS) (Thermo Scientific, South Africa), 100 IU/mL penicillin and 100 µg/mL streptomycin (Sigma-Aldrich, South Africa). Culture medium for MDA-MB-231 cells was as described above, with the addition of 2 mM L-glutamine (Sigma-Aldrich, South Africa). Culture medium for MCF-7 BUS cells was as described above, except that 5% heat-inactivated FBS was used. END-1 cells were maintained in keratinocyte serum-free (KSF) medium (Sigma-Aldrich, South Africa) supplemented with the provided keratinocyte growth supplement, 100 IU/mL penicillin and 100 µg/mL streptomycin (Gibco Invitrogen). Cells were maintained at 37°C in a water-jacketed incubator (90% humidity and 5% CO_2). All cells were routinely tested and found to be mycoplasma-free.

2.4. Cervical tissue experiments

Cervical tissue was processed as previously described by Fletcher et al. (i.e. between one to three hours post-operation) [15]. Excess underlying stromal tissue was removed from the epithelial layer of the endocervical tissue. The epithelial layer was then diced into 3 mm^3 explant pieces that were randomly placed into separate wells of 96-well round-bottomed plates. Non-polarised explants were cultured in 200 µL Roswell Park Memorial Institute medium (RPMI) (Lonza, Switzerland) supplemented with 10% (v/v) charcoal stripped FBS (Thermo Scientific, USA), 2 mM L-glutamine (Sigma-Aldrich, South Africa), 10 µg/mL Fungizone (Sigma-Aldrich, South Africa), 10 U/mL interleukin-2, 100 IU/mL penicillin and 100 mg/mL streptomycin (Sigma-Aldrich, South Africa). Cervical tissue explants were incubated in quadruplicate with steroids in RPMI and incubated at 37°C in a water-jacketed incubator (90% humidity and 5% CO_2) for 24 h.

2.5. Cell line and tissue incubations with steroids

Cells were seeded at 5×10^4 cells per well (T47D, MCF-7 BUS, MDA-MB-231) or 1×10^5 cells per well (END-1, U2OS, TZM-bl, HEK293T, COS-1 and HeLa) in full phenol red-containing media in a 24-well Greiner Bio-One CELLSTAR tissue culture plate. Tissue was processed and plated as described above. Following a 24-hour incubation period, T47D, MCF-7 BUS and MDA-MB-231 cell media was replaced with phenol red-free media. For analysis of extent of metabolism, the cells and no-cell controls were washed with pre-warmed media then treated with 100 nM steroid or vehicle (0.1% v/v ethanol) in serum-free media. The U2OS, TZM-bl, HEK293T, COS-1, END-1 and HeLa cells were treated in phenol red-containing DMEM, while T47D, MCF-7 BUS and MDA-MB-231 cells were treated in phenol red-free DMEM. Upon treatment, 500 µL of the steroid- and vehicle-containing media was aliquoted into a glass tube and stored at −20°C; this served as the T_0 control. After 24 h, 500 µL aliquots of media were removed from the cells (or no-cell control) and transferred into clean glass tubes and stored at −20°C prior to extraction

2.6. Preparation of standards and samples

Individual stock solutions of the seven steroids (P_4, MPA, NES, NET, LNG, ETG and DEX) plus internal standard T were prepared in absolute ethanol (1 mg/mL) and stored at −20°C until use. These individual

stock solutions were later used to prepare two standard master mixes (1 000 ng/mL and 1 ng/mL) containing all of the above-mentioned steroids in ethanol. These standard master mixes were subsequently used to prepare standards (1 mL, 0.01–100 ng/mL) by the addition of the appropriate volume of the standard master mix to either (i) DMEM containing 1% penicillin-streptomycin and 10% FBS ("supplemented DMEM"), (ii) DMEM without penicillin-streptomycin or FBS ("unsupplemented DMEM"), (iii) KSF without penicillin-streptomycin or FBS, (iv) RPMI 1640 without penicillin-streptomycin or FBS or (v) 50% methanol (no matrix). Samples used for method validation (1 mL) were prepared by spiking the matrix with the appropriate volume of the master mixes. 100 µL of internal standard prepared in distilled water to a final concentration of 1 ng/mL was added to all samples and standards.

2.7. Steroid extractions

Samples and standards were extracted using a 1:3 ratio of sample to MTBE (v/v). The samples were shaken at 1 000 rpm for 15 min before being placed at −80°C for an hour to allow the aqueous phase to freeze. The MTBE layer containing steroids was transferred to a pyrolyzed glass test tube and the MTBE was evaporated at room temperature in a fume hood overnight, or under a stream of nitrogen gas. Samples were subsequently reconstituted in 150 µL 50% methanol and stored at −20°C prior to analysis.

2.8. Instruments and chromatographic conditions for UHPSFC-MS/MS

Steroids were separated using an Acquity Ultra High Performance Convergence Chromatography (UPC^2) system (Waters Corporation, Milford, USA) with an Acquity UPC^2 Ethylene Bridged Hybrid (BEH) column (3 mm × 100 mm, 1.7 µm particle size). The mobile phase consisted of liquid CO_2 (Mobile phase A) and methanol [Mobile phase B (MPB)]. A 2.5-minute gradient inlet method was used to separate the steroids using a constant flow rate of 1.9 mL/min according to the following protocol: 4% MPB from 0 to 1 min; 10% MPB from 1 to 1.5 min; 25% MPB from 1.5 to 2.5 min and back to 4% MPB at 2.5 min for re-equilibration.

The column temperature and automated back pressure regulator were set to 60°C and 1700 pounds-force per square inch (psi), respectively. The injection volume was 2.0 µL. Quantitative mass spectrometric detection was carried out using a Xevo TQ-S triple quadrupole mass spectrometer (Waters, Milford, USA). A make-up pump fed 1% formic acid in methanol into the mixer preceding the MS line at a constant flow rate of 0.2 mL/min. All steroids were analysed in multiple reaction monitoring (MRM) mode using an electrospray probe in the positive ionisation mode (ESI+). The following settings were used: capillary voltage of 3.8 kV, desolvation temperature 350°C, desolvation gas 900 L/h and cone gas 150 L/h. MRM transitions are included in Supporting Table 1. Data collection and analysis were performed using MassLynx 4.1 (Waters Corporation).

2.9. UHPSFC-MS/MS method validation

Standard curves were generated for each steroid metabolite using standards prepared in either of the four matrices listed above or 50% methanol (no matrix), and included the following concentrations: 0, 0.01, 0.1, 0.25, 0.5, 1.0, 5.0, 10, 25, 50 and 100 ng/mL. The limit of detection (LOD) for each steroid was defined as the lowest concentration at which a signal-to-noise (S/N) ratio greater than three was measured for the quantifier ion. The lower limit of quantification (LLOQ) for each steroid was defined as the lowest concentration for each steroid at which: a S/N ratio greater than ten was measured for the quantifier ion; a S/N ratio greater than three was measured for the qualifier ion; an acceptable precision [% relative standard deviation (% RSD) < 20] could be measured. The upper limit of quantification (ULOQ) was defined as the maximum concentration at which the % RSD values did not exceed 20. Precision was defined as the % RSD from the average calculated concentrations following the repeated injection (n = 6) of a simple sample. Accuracy was defined as the % RSD from the analysis of independent replicate samples (n = 6).

2.10. Statistical analysis

Results were analysed using GraphPad Prism 7 from GraphPad Software, Inc. (La Jolla, California, USA). Data are expressed as mean ± SEM. To evaluate whether the metabolism of a steroid within a cell line/tissue was statistically significant, a paired *t*-test was performed to compare results in the absence and presence of cells. Statistical significance is denoted by the relevant p-value. Multiple paired *t*-tests were used to compare the metabolism of the seven steroids within a cell line to each other, and to compare the metabolism of a specific steroid across different cell lines. (ANOVA was not used since these experiments were not all performed in parallel.) Where statistical significance was determined, it is denoted by *, **, ***, or **** to indicate $p < 0.05$, $p < 0.01$, $p < 0.001$, or $p < 0.0001$, respectively.

3. Results

3.1. Validation and performance of UHPSFC-MS/MS method

A UHPSFC-MS/MS method was developed for the quantification of six clinically-relevant, commercially-available progestogens and DEX. Their chemical structures are depicted in Fig. 1. Molecular ion species, MRM mass transitions and retention time for each steroid are given in Supporting Table 1. Comprehensive method validation was performed, the results of which are listed in Table 1.

As most of the cell lines were treated with unsupplemented DMEM, accuracy and precision were determined only for this medium at a minimum of three concentrations within the calibration range of each steroid as shown in Table 1, i.e. 1, 10 and 100 ng/mL. Acceptable % RSDs were obtained for all concentrations for both accuracy and precision, which were less than 20 at concentrations of 1, 10 and 100 ng/mL. Accuracy at low concentrations ranged from 11 to 18% at 1 ng/mL, 11–18.9% at 10 ng/mL and 8–17% at 100 ng/mL. Precision at low concentrations ranged from 14–19% at 1 ng/mL, 4–16% at 10 ng/mL and 9–19% at 100 ng/mL. LLOQs ranged from 0.01 ng/mL for P_4 to 5.00 ng/mL for LNG, ETG and DEX, allowing for the quantification of steroids at levels at the low nanomolar range. For each of unsupplemented DMEM, KSF and RMPI media, the ULOQ was 100 ng/mL (the highest concentration measured), while ULOQ in supplemented DMEM was 50 ng/mL.

3.2. Effects of adsorption and hydrophobicity

Following the development and validation of the UHPSFC-MS/MS method we first considered the potential effects of adsorption of the steroids to the cell culture plates, before measuring the metabolism of the steroids. To do this we assessed the differences in steroid concentration between the T_0 and media from no-cell control plate incubations for all the steroids in the different experiments (Supporting Fig. 1). There was 0%–40% adsorption of the steroids to the cell culture plates across experiments (Fig. 2 and Supporting Fig. 1). We further investigated whether there was a correlation between hydrophobicity and adsorption of steroids. Results showed a positive correlation suggesting that the adsorption of steroids to the cell culture plates increases with increasing hydrophobicity (Fig. 2). We investigated whether retention of the steroids occurred within the cell pellets. We found that this was negligible (Supporting Fig. 2) and hence was not taken into account when calculating percentage metabolism. Based on these results, metabolism (Section 3.3–3.5) was calculated relative to a no-cell control parallel incubation in cell culture plates and hence was

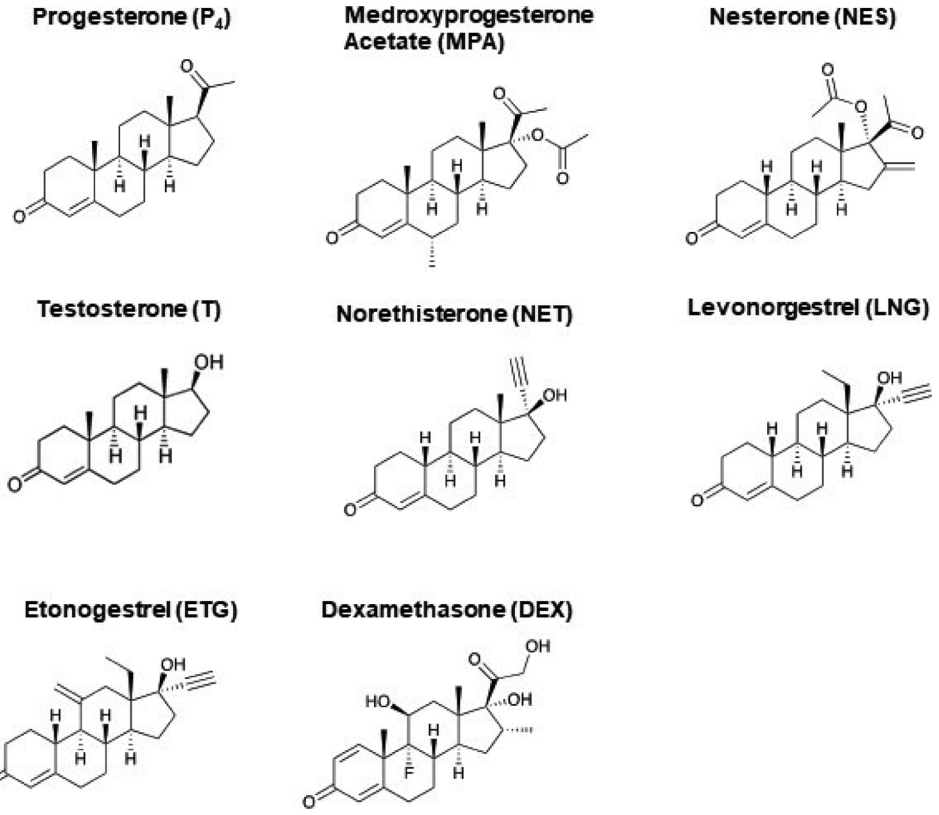

Fig. 1. The chemical structures of the seven commercially-available steroids described in this work. MPA and NES are structurally related to P_4 while NET, LNG and ETG are structurally related to T. DEX is a synthetic glucocorticoid.

independent of adsorption to the cell culture plates.

3.3. Differential metabolism of steroids between cell lines

Next, we incubated nine common laboratory cell lines, along with a parallel plate without any cells ("no-cell control"), with 100 nM of each steroid for 24 h. We subsequently measured the concentration of steroid present in the cell and no-cell supernatants. The percentage metabolism of each individual steroid in a cell line was calculated as the difference between the steroid remaining in the absence (no-cell) and presence of cells. When percentage metabolism of a ligand was less than zero, it was represented as zero. It should be noted that steroid incubations were performed in the absence of serum for 24 h as is frequently done for experiments in cell lines incubated with steroids [16–18]. It is possible that the presence of serum may affect metabolism.

When comparing metabolism effects, it was noted that the error bars were in general much greater for some cells than for others, as well as between some progestins for a particular cell line. Assessment of no-cell samples indicates that this reflects variations in technical error during experiments. Only differences that were found to be statistically significant are highlighted and discussed below. It should, however, be noted that there may be other differences that are significant, but beyond the statistical power of the experiments. The most striking result was that P_4 was extensively metabolised by all the cell lines, although the extent of metabolism varied from 50 to 97%, showing some cell line-specific effects (Figs. 3 and 4). Although the metabolism of the progestins and DEX was also cell line-specific, it ranged from 0 to 50%, with the rank order for most to least metabolised steroid different for each cell line. These did not appear to be related to the anatomical source or type of cell line, as shown in Fig. 4. However, some trends were apparent (Figs. 3 and 4). Of the cervical cell lines, HeLa exhibited a higher percentage of significant metabolism for most progestogens than observed in TZM-bl and END-1 cells, except for NET and ETG where END-1 cells exhibited more metabolism. The T47D cell line

Table 1
Comprehensive method validation data: r^2, LOD (ng/mL and nM), LLOQ (ng/mL and nM), accuracy (% RSD, n = 6) and precision (% RSD, n = 6). LOD, LLOQ, accuracy and precision are shown for unsupplemented DMEM only. (-) indicates that the concentration is below the LLOQ for that steroid and is therefore not included.

Steroid	r^2 (Unsupplemented DMEM)	LOD, ng/mL (nM)	LLOQ, ng/mL (nM)	Accuracy % RSD, 1 ng/mL	Accuracy % RSD, 10 ng/mL	Accuracy % RSD, 100 ng/mL	Precision % RSD, 1 ng/mL	Precision % RSD, 10 ng/mL	Precision % RSD, 100 ng/mL
P_4	0.9928	0.01 (0.03)	0.01 (0.03)	18.2	12.6	8.3	16.9	9.5	9.5
MPA	0.9939	0.5 (1.3)	1 (2.6)	10.9	11.1	9.7	14.0	6.7	9.3
NES	0.9955	0.5 (1.3)	1 (2.7)	16.5	18.9	16.9	19.0	16.1	18.8
NET	0.9951	0.5 (1.7)	1 (3.3)	14.3	11.5	9.8	14.1	4.4	9.7
LNG	0.9739	0.01 (0.03)	5 (16.0)	–	4.7	11.2	–	7.4	9.7
ETG	0.9960	1 (3.18)	5 (15.4)	–	13.1	8.0	–	10.9	8.7
DEX	0.9951	5 (12.7)	5 (12.7)	–	12.8	16.9	–	12.5	11.8

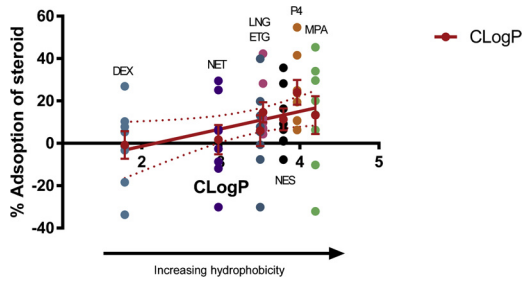

Fig. 2. Predicted steroid hydrophobicity correlates with adsorption. Regression analysis was performed to determine whether there was a correlation between the adsorption and hydrophobicity of the seven clinically-relevant steroids. The percentage adsorption of each steroid to the tissue culture plates was determined from the difference between the time-zero (T_0) measurement and its corresponding no-cell control. CLogP values were predicted using ChemDraw Professional Version 16.0.1.4 (PerkinElmer Informatics, Inc.). Non-linear regression using GraphPad Prism Version 7 (GraphPad Software, Inc.) revealed a correlation with $r^2 = 0.5394$.

exhibited the highest significant metabolism within the breast cancer cell lines, except for NES where MCF-7 BUS showed greater significant metabolism. END-1, T47D, MCF-7 BUS and COS-1 cells were the most metabolically diverse cells in the panel, with all four of these cell lines displaying significant metabolism of P_4 and ETG; and three of these four cell lines showing metabolism of DEX (Fig. 3). Interestingly, COS^{-1} cells displayed a similar high degree of significant metabolism for both P_4 (60%) and DEX (53%). These cell lines were followed by U2OS cells, which significantly metabolised three steroids. TZM-bl and MDA-MB-231 cells had significant metabolism of P_4 and one other steroid, namely, MPA and ETG respectively. HeLa and HEK293 T cells displayed the lowest metabolic activity of progestogens with significant metabolism observed only for P_4 (Fig. 3). Taken together, there was no significant difference in the overall metabolism of the progestins structurally related to P_4 (MPA and NES) compared to those steroids structurally related to T (NET, LNG and ETG) (Fig. 4). There was an average of four times more metabolism observed for P_4 than for the other steroids.

3.4. Differential metabolism of steroids within cell lines

Upon comparison of the metabolism of each steroid within each cell line, it was observed that, apart from P_4, all steroids were metabolised in a cell-specific manner (Fig. 3 and Supporting Fig. 3). T47D, END-1 and HeLa cells had the highest percentage metabolism of P_4 with over 90% metabolism in all three cell lines. HEK293 T and COS^{-1} cells displayed the least metabolism of P_4 with only 50% and 60% metabolism, respectively. P_4 demonstrated the greatest differences in metabolism compared to other steroids within each cell line (Fig. 4 and Supporting Fig. 3).

ETG was the second most metabolised steroid, with significant metabolism in five cell lines ranging between 14% and 43% (Figs. 3 and 4). HeLa cells showed a high percentage of metabolism of ETG with 28% metabolism; this, however, was not significant (Fig. 4). MPA and DEX were significantly metabolised in three cell lines each. Significant metabolism of MPA was observed in U2OS, TZM-bl and T47D cells, ranging between 19% and 55% (Fig. 3). Significant metabolism of DEX was observed in END-1, MCF-7 BUS and COS^{-1} cells with metabolism ranging from 8% and 52%. As shown in Fig. 4, metabolism of DEX in HeLa, T47D and U2OS cells, although not significant, ranged from 21% to 37%. TZM-bl, HEK293 T and MDA-MB-231 cells exhibited less than 10% metabolism of DEX. NET and NES were significantly metabolised only in two cell lines each (Fig. 3). NET was significantly metabolised only in U2OS and MCF-7 BUS cells (Fig. 3). NES was metabolised in END-1 and MCF-7 BUS cell lines by 9% and 40%, respectively (Fig. 4). There was 41% metabolism of NES in COS^{-1} cells, and between 0% and 20% in the remaining cell lines; however, these effects were not statistically significant (Supporting Fig. 3). LNG was significantly metabolised only in COS^{-1} cells with 23% metabolism which was comparable to the metabolism in T47D and HeLa cells which exhibited 22% and 20% metabolism, respectively. However, these latter effects were not statistically significant. The metabolism of LNG in the remaining six cell lines was less than 10% (Supporting Fig. 3).

3.5. Metabolism in endocervical tissue

To determine if the metabolism observed in cell lines would be similar in a more physiologically-relevant system, we investigated the metabolism of three progestogens in post-menopausal endocervical tissue explants following a 24-hour incubation. P_4 was investigated due to the high rate of metabolism in all cell lines, whilst MPA and NET were chosen as representative of progestins structurally related to P_4 and T, respectively.

P_4 was completely metabolised in the endocervical tissue explants after 24 h (Fig. 5). The results for P_4, but not MPA and NET, are comparable to those observed in the three cervical cell lines (Fig. 3). There was between approximately 87% and 96% metabolism of P_4 in the cervical cell lines, which is similar to the 100% metabolism in tissue (Fig. 5). As depicted in Fig. 5, 38% of MPA was metabolised in tissue. This is different from the pattern observed in cervical cell lines in which TZM-bl cells exhibited significant, but less, metabolism of MPA, (Fig. 3) while no significant metabolism was observed in the other cervical cell lines. While NET was not significantly metabolised in the cervical cell lines, endocervical tissue metabolised 43% of available NET.

4. Discussion

Previous research into progestogen metabolism has been limited and has typically focused on measuring the serum or urine concentrations of progestogens and/or their metabolites in a clinical setting [19–26]. In this work we investigated, for the first time, the cell- and steroid-specific metabolism of a range of clinically-relevant steroids using *in vitro* cell line models. These cell line models are widely used to investigate the biocharacter and mechanisms of action of these steroids, which themselves are commonly used in hormonal therapy and steroid receptor-based studies. We developed and validated a UHPSFC-MS/MS method of measuring the concentration of seven steroids in cell culture media, which allowed for the determination of the metabolism of these steroids by these cell lines. Our experimental design corrected for adsorption (up to 40%) of the steroids to the cell culture plates, where we found a positive correlation between adsorption and increasing hydrophobicity. The extent of metabolism could be measured from analysing the medium (supernatant) alone, since we found no significant retention of parent steroid in the cell pellets.

We found that individual progestins and DEX are differentially metabolised within the same cell line, and amongst different cell lines. For example, over 24 h, some progestins are not significantly metabolised in a particular cell type (< 20%), while others display a high degree of metabolism (20–50%) in the same cell type. A particular progestin can be metabolised to a vastly different degree in different cell lines (e.g. MPA metabolised by 55% in T47D and less than 10% metabolism in HEK293 T and MDA-MB-231 cells). We detected no correlation between extent of metabolism and whether progestins were structurally related to P_4 or T.

Taken together, these results may have important physiological and pharmacological implications. Progestins used in hormonal contraception and HRT are known to exert several side-effects, such as effects on bone mineral density, metabolism, cardiovascular effects and reproductive cancers [2–4,6]. Progestins also exert their contraceptive effects at several levels at different target tissues. If these *in vitro* effects of metabolism are translated *in vivo*, this suggests that different progestins may exert very different side-effects and may be more or less

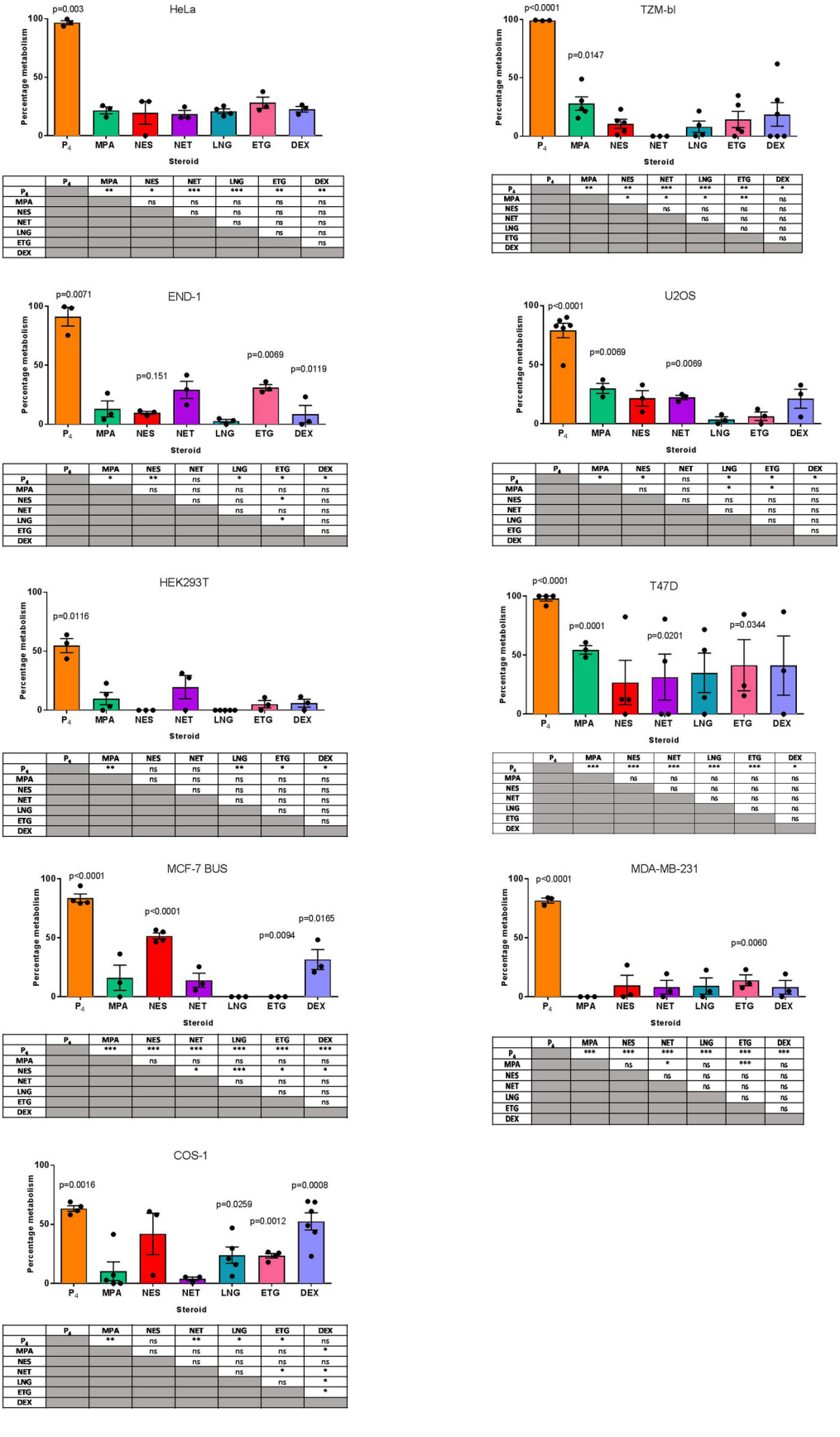

Fig. 3. Differential metabolism of seven clinically-relevant steroids following incubation at 100 nM for 24 h in nine different cell lines. Medium containing the steroids was added to a 12-well plate, containing no cells, as a negative control for metabolism. Steroids were extracted and analysed by UHPSFC-MS/MS. The amount of steroid present in the medium after incubation with the cells was expressed as a % relative to the amount of progestin in the negative control for metabolism, which was set as 100%. These data show the mean ± SEM of a minimum of three independent biological repeats. Statistical analysis via paired *t*-tests was performed on each steroid and statistically significant differences relative to its no cell control are indicated by the p-value above bar. To quantify whether the relative metabolism of two steroids within a cell line was significantly different, multiple *t*-tests were performed between steroids. Significant differences in tables below the histograms are indicated by asterisks where *, **, ***, **** represent $p < 0.05$, $p < 0.01$, $p < 0.001$ and $p < 0.0001$, respectively.

efficacious for contraception due not only to their inherent biocharacters, potencies and efficacies, but also due to differential metabolism in different target cells and tissues. This metabolism could both selectively lower their effective concentrations at the target cells in a cell-specific manner and may, also result in different metabolites with different off-target effects. The tissue findings are particularly

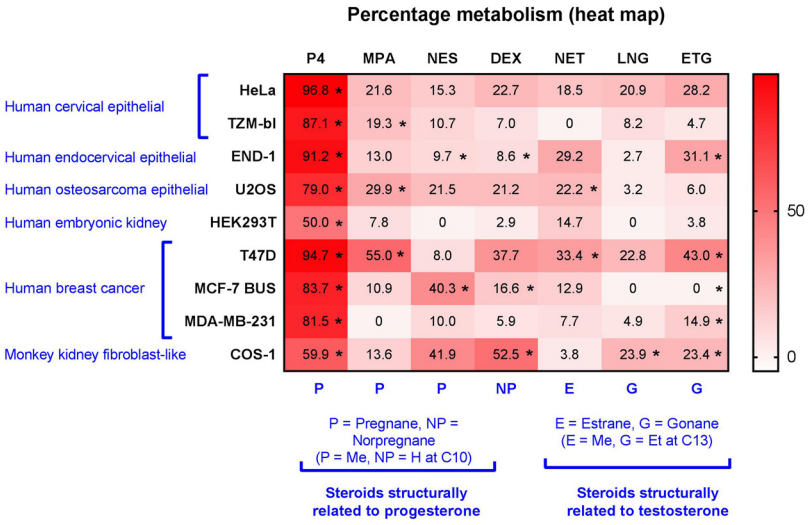

Fig. 4. Heat map summarising differential metabolism of seven clinically-relevant steroids. Data are from Fig. 3 and cell lines and steroids are grouped according to anatomical and structural similarities, respectively. Pregnanes (P) have a methyl group at C10 position, while norpregnanes (NP) have a hydrogen group at C10; estranes (E) have a methyl group at C13, while gonanes (G) have an ethyl group at C13. Data are represented as % metabolism relative to the no-cell control which was set to 100%. Statistical significance is indicated by asterisks.

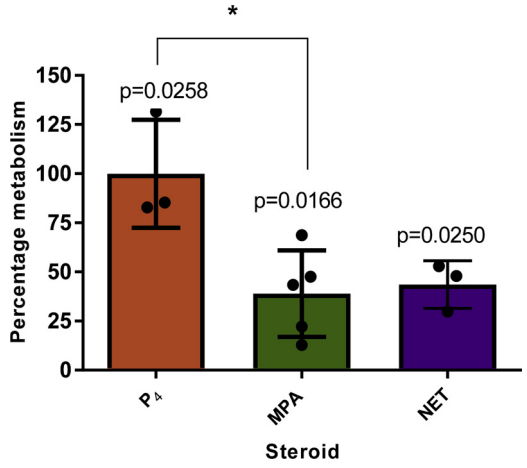

Fig. 5. Differential metabolism of three clinically-relevant progestogens in post-menopausal endocervical tissue. Tissue explants were incubated with 100 nM progestogens for 24 h. The supernatant was removed and extracted before quantification via UHPSFC-MS/MS, as described in methods. Results were normalised to the progestogen concentration detected in a corresponding no-tissue control experiment to account for adsorption loss. The data show the mean ± SEM of three to five independent biological repeats. Statistical analysis via paired *t*-tests was performed comparing the progestogen concentration in the supernatant of the tissue condition to the no-tissue control; significant results are indicated by the p-value above the bar. To determine whether the relative metabolism of the progestogens was significantly different, an unpaired *t*-test with Welch's correction was performed. Statistical significance indicated with * represents $p < 0.05$.

interesting since they suggest that doses and types of progestins used for intravaginal delivery need to be carefully considered, taking into account that the progestins may be significantly metabolised in the tissues. The results also suggest that different cell types contain different steroid metabolising enzymes which discriminate between the progestins, despite some of their structures being similar. Although, the identification of the enzymes that metabolise DEX and the progestins in our models was beyond the scope of the present study, it would be an interesting avenue to explore in future studies.

Our results with P_4 showing the rapid and substantial metabolism of this steroid in all the cells lines and in the cervical tissue, are particularly interesting. These results suggest that enzymes that metabolise P_4 are widely expressed in most cell types, including the female genital tract, bones and breast tissue, and that its rapid turnover may be a mechanism required physiologically to fine-control PR responses to endogenous P_4. Our results are consistent with those of Arici et al. who reported 90% metabolism of P_4 in isolated primary endometrial stromal and gland cells after 24 h [27]. However, it should be noted that only one time point was assessed and that the temporal dynamics of P_4 metabolism may differ between cell lines. Moreover, the metabolism of P_4 appears to be independent of PR expression since a similar extent of metabolism was seen in all three breast cancer cell lines even though T47D and MCF-7 BUS cells are PR-positive whilst MDA-MB-231 cells are PR-negative [28]. Several researchers have reported that 20α-(*S*)-hydroxyprogesterone is a major metabolite of P_4 via the actions of AKR1C1 [28–30]. Whether AKRIC1 or its isozymes are involved in metabolism of P_4 in our model systems remains to be investigated.

Wiebe and Lewis found that breast cancer cell lines express higher levels of SRD5A1 and lower levels of AKR1C enzymes [31]. Therefore, breast cancer cells have a higher conversion of P_4 to 5α-pregnane metabolites as opposed to other systemic cells and tissues. This has major implications, as 5α-pregnanes modify the growth of tumour cells within breast tissue. This highlights the importance of examining the metabolism of steroids, as some metabolites are active and may be a confounding factor in receptor-based studies comparing P_4 -activity to other progestins [28,32,33]. HEK293 T (human embryonic kidney cells) and COS-1 cells (monkey kidney cells) had the lowest metabolism of P_4, which may mean that kidneys have lower turnover of P_4.

An important implication of our findings is that the detected differential and rapid metabolism of P_4, progestins and DEX may confound the interpretation of results when investigating mechanisms of action and biological responses via steroid receptors using *in vitro* and pre-clinical models. This would be particularly relevant to the determination of relative binding affinities and potencies (EC_{50} values), which are highly relevant to drug efficacy, specificity and design. We have previously proposed that the determination of progestogen binding affinities and potencies via a specific receptor are dependent on a number of factors, including metabolism of the progestogen [4]. Several researchers have investigated binding affinities of one or more progestogens and/or DEX in COS-1 cells or cytosols prepared from MCF-7 cells [16–18,34,35] or in cytosols prepared from tissue [11,12]. Given that COS-1 cells show high metabolism of P_4 and DEX relative to progestins such as MPA and NET, which show no metabolism in these cells, the reported relative binding affinities may be underestimated for P_4 and DEX [16–18]. If metabolising activity is retained in cytosols, our results suggest that relative binding affinities for NET, but not LNG or ETG, from MCF-7 cytosols [34,35] may also be underestimated. Similarly, potencies (EC_{50}) and/or efficacies (maximal activities) have been reported for transcriptional activity using one or more progestogens and/or DEX in either COS-1, T47D, MCF-7 BUS, END-1, or HEK293 cell lines

investigated in this study [11,16–18,36–39,40], or in primary cell models [8,9]. The reported potencies and efficacies may also be underestimated, particularly for P_4, compared to some progestins, and to different degrees, depending on the cell model. For example, the relative potency of P_4 via the androgen receptor (AR) and PR in HEK293 T cells may be greater than that reported relative to LNG or NES [39], while the potency of P_4 and DEX may be greater than that reported for other progestins in COS-1 cells for a particular receptor such as the PR, androgen, glucocorticoid and mineralocorticoid receptors [16–18,39]. Potentially further complicating the interpretation, are different metabolites of these steroids produced in different cells that may also confound the results. Clearly, further investigation into the steroid- and cell-specific effects of metabolism of these clinically-relevant compounds, and the biological activities of their metabolites, is urgently required.

Funding

This work was supported by the Eunice Kennedy Shriver National Institute of Child Health & Human Development [R01HD83026] and the South African Medical Research Council.

Declarations of interest

None.

Acknowledgements

We would like to acknowledge Dr Marietjie Stander, Mr Malcolm Taylor, Mr Erick Van Schalkwyk and Mr Jonathan Quanson for their assistance with the UHPSFC-MS/MS. The authors thank the following people for consenting suitable patients and providing cervical tissue: Shane Moore, Lynn Keck, Anne Hoffman and Tony Wu at Groote Schuur Hospital; Hennie Botha, Rudolf Boshoff, and the registrars at Tygerberg Hospital.

Appendix A. Supplementary data

Supplementary material related to this article can be found, in the online version, at doi:https://doi.org/10.1016/j.jsbmb.2019.02.010.

References

[1] T.A. Shchelkunova, I.A. Morozov, Molecular basis and tissue specificity of the progestin effect, Molekulyarnaya Biologiya 49 (2015) 728–748.
[2] D. Africander, N. Verhoog, J.P. Hapgood, Molecular mechanisms of steroid receptor-mediated actions by synthetic progestins used in HRT and contraception, Steroids 76 (2011) 636–652.
[3] F.Z. Stanczyk, J.P. Hapgood, S. Winer, D.R. Mishell Jr, Progestogens used in postmenopausal hormone therapy: differences in their pharmacological properties, intracellular actions, and clinical effects, Endocr. Rev. 34 (2013) 171–208.
[4] J.P. Hapgood, D. Africander, R. Louw, R.M. Ray, J.M. Rohwer, Potency of progestogens used in hormonal therapy: toward understanding differential actions, J. Steroid Biochem. Mol. Biol. 142 (2014) 39–47, https://doi.org/10.1016/j.jsbmb.2013.08.001.
[5] R. Louw-du Toit, M.S. Perkins, J.P. Hapgood, D. Africander, Comparing the androgenic and estrogenic properties of progestins used in contraception and hormone therapy, Biochem. Biophys. Res. Commun. 491 (2017) 140–146, https://doi.org/10.1016/j.bbrc.2017.07.063.
[6] J.P. Hapgood, D. Koubovec, A. Louw, D. Africander, Not all progestins are the same: implications for usage, Trends Pharmacol. Sci. 25 (2004) 554–557.
[7] J.P. Hapgood, R.M. Ray, Y. Govender, C. Avenant, M. Tomasicchio, Differential glucocorticoid receptor-mediated effects on immunomodulatory gene expression by progestin contraceptives: implications for HIV-1 pathogenesis, Am. J. Reprod. Immunol. 71 (2014) 505–512.
[8] L. Kleynhans, N. Du Plessis, G.F. Black, A.G. Loxton, M. Kidd, P.D. van Helden, G. Walzl, K. Ronacher, Medroxyprogesterone acetate alters mycobacterium bovis BCG-induced cytokine production in peripheral blood mononuclear cells of contraceptive users, PLoS One 6 (2011) e24639, , https://doi.org/10.1371/journal.pone.0024639.
[9] J.B. Engler, N. Kursawe, M.E. Solano, K. Patas, S. Wehrmann, N. Heckmann, F. Luhder, H.M. Reichardt, P.C. Arck, S.M. Gold, M.A. Friese, Glucocorticoid receptor in T cells mediates protection from autoimmunity in pregnancy, Proc. Natl. Acad. Sci. U. S. A. 114 (2017) E181–E190.
[10] M. Maritz, R.M. Ray, A.J. Bick, M. Tomasicchio, J.G. Woodland, Y. Govender, Z. van der Spuy, C. Avenant, J.P. Hapgood, Increased CCR5 Levels Result in Increased R5-HIV Replication by Medroxyprogesterone Acetate, Unlike Norethisterone, via the Glucocorticoid Receptor, AIDS Res. Hum. Retroviruses 34 (2018) Abstract no. OA12.03.
[11] U. Fuhrmann, E.P. Slater, K.H. Fritzemeier, Characterization of the novel progestin gestodene by receptor binding studies and transactivation assays, Contraception 51 (1995) 45–52.
[12] A. Kasid, K. Buckshee, V. Hingorani, K.R. Laumas, Interaction of progestins with steroid receptors in human uterus, Biochem. J. 176 (1978) 531–539.
[13] Y. Govender, C. Avenant, N.J.D. Verhoog, R.M. Ray, N.J. Grantham, et al., The injectable-only contraceptive medroxyprogesterone acetate, unlike norethisterone acetate and progesterone, regulates inflammatory genes in endocervical cells via the glucocorticoid receptor, PLoS One 9 (2014) e96497, , https://doi.org/10.1371/journal.pone.0096497.
[14] R. Louw-du Toit, J.P. Hapgood, D. Africander, Medroxyprogesterone acetate differentially regulates interleukin (IL)-12 and IL-10 in a human ectocervical epithelial cell line in a glucocorticoid receptor (GR)-dependent manner, J. Biol. Chem. 289 (2017) 31136–31149, https://doi.org/10.1074/jbc.M114.587311.
[15] P. Fletcher, Y. Kiselyeva, G. Wallace, J. Romano, G. Griffin, L. Margolis, R. Shatock, The nonnucleoside reverse transcriptase inhibitor UC-781 inhibits human immunodeficiency virus type 1 infection of human cervical tissue and dissemination by migratory cells, J. Virol. 79 (2005) 11179–11186.
[16] K. Ronacher, K. Hadley, C. Avenant, E. Stringer, S.S. Simons Jr, A. Louw, J.P. Hapgood, Ligand-selective transactivation and transrepression via the glucocorticoid receptor: role of cofactor interaction, Mol. Cell. Endocrinol. 299 (2009) 219–223.
[17] D. Africander, R. Louw, J.P. Hapgood, Investigating the anti-mineralocorticoid properties of synthetic progestins used in hormone therapy, Biochem. Biophys. Res. Commun. 433 (2013) 305–310.
[18] D.J. Africander, K.H. Storbeck, J.P. Hapgood, A comparative study of the androgenic properties of progesterone and the progestins, medroxyprogesterone acetate (MPA) and norethisterone acetate (NET-A), J. Steroid Biochem. Mol. Biol. 143 (2014) 404–415;
M.C. Chu, G.S. Nakhuda, X. Zhang, F.Z. Stanczyk, R.A. Lobo, Formation of ethinyl estradiol in women during treatment with norethindrone acetate, J. Clin. Endocrinol. Metab. 92 (2007) 2205–2207.
[19] A.B. Edelman, G. Cherala, F.Z. Stanczyk, Metabolism and pharmacokinetics of contraceptive steroids in obese women: a review, Contraception 82 (2010) 314–323.
[20] M.L. Helmreich, R.A. Huseby, Identification of a 6,21-dihydroxylated metabolite of medroxyprogesterone acetate in human urine, J. Clin. Endocrinol. Metab. 22 (1962) 018–1032.
[21] J. Huber, Pharmacokinetics of Implanon, Contraception 58 (1998) 85S–90S.
[22] P.V. Prasad, M. Bashir, R. Sitruk-Ware, N. Kumar, Single-dose pharmacokinetics of nestorone, a potential female-contraceptive, Steroids 75 (2010) 252–264.
[23] P. Ravinder, V. Shatrugna, K. Madhavan, B. Sivakumar, Pharmacokinetics of orally administered norethisterone enanthate in rabbit, monkey, and women, Contraception 55 (1997) 373–379.
[24] M. Hümpel, H. Wendt, G. Pommerenke, C. Weiβ, U. Speck, Investigations of pharmacokinetics of levonorgestrel to specific consideration of a possible first-pass effect in women, Contraception 17 (1978) 207–220.
[25] S. Jeppsson, S. Gershagen, E.D. Johansson, G. Rannevik, Plasma levels of medroxyprogesterone acetate (MPA), sex-hormone binding globulin, gonadal steroids, gonadotrophins and prolactin in women during long-term use of depo-MPA (Depo-Provera) as a contraceptive agent, Acta Endocrinol. (Copenh) 99 (1982) 339–343.
[26] A. Arici, P.B. Marshburn, P.C. MacDonald, R.A. Dombrowsk, Progesterone metabolism in adipose cells, Steroids 64 (1999) 530–534.
[27] J.P. Wiebe, G. Zhang, I. Welch, H.T. Cadieux-Pitre, Progesterone metabolites regulate induction, growth, and suppression of estrogen- and progesterone receptor-negative human breast cell tumors, Breast Cancer Res. 15 (2013) R38.
[28] M. Sinreih, M. Anko, S. Zukunft, J. Adamski, Rizner, Important roles of the AKR1C2 and SRD5A1 enzymes in progesterone metabolism in endometrial cancer model cell lines, Chem. Biol. Interact. 234 (2015) 297–308, https://doi.org/10.1016/j.cbi.2014.11.012.
[29] T.L. Rizner, T.M. Penning, Role of aldo–keto reductase family 1 (AKR1) enzymes in human steroid metabolism, Steroids 79 (2014) 49–63.
[30] J. Lewis, M. Wiebe, J.G. Heathcote, Expression of progesterone metabolizing enzyme genes (AKR1C1, AKR1C2, AKR1C3, SRD5A1, SRD5A2) is altered in human breast carcinoma, BMC Cancer 4.27 (2004), https://doi.org/10.1186/1471-2407-4-27.
[31] V.C. Lin, R. Jin, P. Tan, S. Aw, C. Woon, B. Bay, Progesterone induces cellular differentiation in MDA-MB-231 breast Cancer cells transfected with progesterone receptor complementary DNA, Am. J. Pathol. 162 (6) (2003).
[32] S. Diederich, B. Hanke, W. Oelkers, V. Bahr, Metabolism of dexamethasone in the human kidney:nicotinamide adenine dinucleotide-dependent 11b-Reduction, J. Clin. Endocrinol. Metab. 82 (1997) 1598–1602.
[33] W.G. Schoonen, G.H. Deckers, M.E. de Gooijer, R. de Ries, H.J. Kloosterboer, Hormonal properties of norethisterone, 7alpha-methyl-norethisterone and their derivatives, J. Steroid Biochem. Mol. Biol. 74 (2000) 213–222.
[34] G.H. Deckers, W.G. Schoonen, H.J. Kloosterboer, Influence of the substitution of 11-methylene, delta(15), and/or 18-methyl groups in norethisterone on receptor binding, transactivation assays and biological activities in animals, J. Steroid Biochem. Mol. Biol. 74 (2000) 83–92.

[35] Y. Govender, C. Avenant, N.J. Verhoog, R.M. Ray, N.J. Grantham, D. Africander, J.P. Hapgood, The injectable-only contraceptive medroxyprogesterone acetate, unlike norethisterone acetate and progesterone, regulates inflammatory genes in endocervical cells via the glucocorticoid receptor, PLoS One 9 (2014) e96497.

[36] N. Kumar, J. Fagart, P. Liere, S.J. Mitchell, A.R. Knibb, I. Petit-Topin, M. Rame, M. El-Etr, M. Schumacher, J.J. Lambert, M.E. Rafestin-Oblin, R. Sitruk-Ware, Nestorone(R) as a novel progestin for nonoral contraception: structure-activity relationships and brain metabolism studies, Endocrinology 158 (2017) 170–182.

[37] G. Viswanath, S. Halder, G. Divya, C.B. Majumder, P. Roy, Detection of potential (anti)progestagenic endocrine disruptors using a recombinant human progesterone receptor binding and transactivation assay, Mol. Cell. Endocrinol. 295 (2008) 1–9.

[38] S. Sasagawa, Y. Shimizu, H. Kami, T. Takeuchi, S. Mita, K. Imada, S. Kato, K. Mizuguchi, Dienogest is a selective progesterone receptor agonist in transactivation analysis with potent oral endometrial activity due to its efficient pharmacokinetic profile, Steroids 73 (2008) 222–231.

[39] A. Courtin, L. Communal, M. Vilasco, D. Cimino, N. Mourra, M. de Bortoli, D. Taverna, A.-M. Faussat, M. Chaouat, P. Forgez, A. Gompel, Glucocorticoid receptor activity discriminates between progesterone and medroxyprogesterone acetate effects in breast cells, Breast Cancer Res. Treat. 131 (2012) 49–63, https://doi.org/10.1007/s10549-011-1394-5.

Biochemical and Biophysical Research Communications xxx (xxxx) xxx

Contents lists available at ScienceDirect

Biochemical and Biophysical Research Communications

journal homepage: www.elsevier.com/locate/ybbrc

Maraviroc, tenofovir disoproxil fumarate and dapivirine, activate progesterone receptor B in the absence progestogens

Kim Enfield [a], Sigcinile Dlamini [a], Chanel Avenant [a], Michael Kuipa [a], Janet P. Hapgood [a, b, *]

[a] Department of Molecular and Cell Biology, University of Cape Town, Private Bag X3, Rondebosch 7701, South Africa
[b] Institute of Infectious Disease and Molecular Medicine, University of Cape Town, Private Bag X3, Rondebosch 7701, South Africa

ARTICLE INFO

Article history:
Received 18 September 2020
Accepted 24 September 2020
Available online xxx

Keywords:
Antiretroviral drugs
Progesterone receptor
Progestins
Ligand-independent activation

ABSTRACT

Antiretroviral therapy has slowed the HIV/AIDS pandemic and is currently being used as a prophylactic measure for individuals at high risk of infection. However, concerns over adverse effects of long-term use need to be explored. We hypothesize that this may occur, at least in part, through off-target effects via select steroid receptors (SRs) that broadly regulate multiple physiological processes. We investigated the effects of maraviroc (MVC), tenofovir disoproxil fumarate (TDF), and dapivirine (DPV) on progesterone receptor B (PR-B) transcriptional activity. We found that MVC and TDF activate PR-B transcription in the absence of progestogens on a PR-regulated promoter reporter construct and on endogenous PR-regulated genes. MVC and TDF exhibited no direct binding to PR-B; however, increased PR-B phosphorylation was detected with TDF but not MVC. DPV transactivated *gilz* and *ptgs2* in the absence of progestogens and exhibited PR-B binding while showing no effects on phosphorylation, suggesting that it may activate PR-B through a direct mechanism. Our study shows that potential off-target immunomodulatory effects of MVC, TDF and DPV occur *in vitro* and these are most likely mediated by different mechanisms of PR-B activation.

1. Introduction

Combination antiretroviral therapy (cART) has significantly reduced HIV-1 mortality worldwide [1]. However, patients receiving cART have an increased risk of mortality from a variety of complications, including cardiovascular disease, renal failure, bone disease and cancer [2]. Although the role of cART is unclear in the development of these complications, since HIV itself contributes to them, this does raise concerns that antiretroviral drugs (ARVs) may contribute to this increased risk of mortality due to off-target effects [3,4]. Additionally, many people taking ARVs are also taking other drugs, such as contraceptives in HIV-1-positive women of reproductive age [5] raising the issue of potential drug-drug interactions. Whether ARVs exert off-target effects via steroid receptors (SRs) in the absence or presence of contraceptives is important in understanding possible side-effects.

Our previous study showed that the ARV, tenofovir disoproxil fumarate (TDF), induces progestogen-independent activation of a reporter gene *in vitro* via the progesterone receptor B (PR-B), unlike dapivirine (DPV) [6]. That TDF can modulate PR-B activity suggests that off-target effects of some ARVs may occur via SRs [7]. Through its action as a ligand-activated transcription factor, the PR regulates many female reproductive processes, including mammary gland development, proliferation, ovulation, pregnancy, as well as inflammation [8]. Synthetic progestogens or progestins designed to target the PR are used in hormonal contraceptives and these include norethisterone (NET) and levonorgestrel (LNG) [9,10]. It is well established that hormonal contraceptives cross-talk with SRs other than the PR [9]; however, whether ARVs cross-talk with the PR is relatively unexplored.

TDF, which is used for both cART and pre-exposure prophylaxis (PrEP), has adverse off-target effects on renal function and bone mineral density [11,12]. Due to concern over toxicity of long-term TDF use, other ARVs are being considered for cART and PrEP. DPV is the most clinically advanced PrEP candidate in development for intravaginal delivery [13]. Maraviroc (MVC) is another ARV used in cART and currently being investigated for PrEP [14]. MVC is a potent

* Corresponding author. Department of Molecular and Cell Biology, University of Cape Town, Private Bag X3, Rondebosch 7701, South Africa, .
E-mail addresses: enfkim001@myuct.ac.za (K. Enfield), gcina.dlamini@uct.ac.za (S. Dlamini), chanel.avenant@uct.ac.za (C. Avenant), kpxmic002@myuct.ac.za (M. Kuipa), janet.hapgood@uct.ac.za (J.P. Hapgood).

https://doi.org/10.1016/j.bbrc.2020.09.107
0006-291X/

C–C chemokine receptor type 5 (CCR5) antagonist that prevents the interaction of HIV-1 gp120 with human CCR5 [15], the principal co-receptor of CCR5-tropic HIV-1. Serious adverse off-target side-effects have not been identified thus far for DPV and MVC [16,17], while in recent years MVC has been investigated *in vitro* for its positive off-target effects on tumour reduction in metastatic cancers [18,19]. However, several studies have shown that MVC has both anti-inflammatory [20,21] and pro-inflammatory effects [22]. Whether the PR is involved in mediating any of these off-target effects of ARVs is unknown and requires investigation.

2. Materials and methods

2.1. Compounds and plasmids

Promegestone (R5020), norethisterone (NET) and levonorgestrel (LNG) were obtained from Sigma-Aldrich, RSA. Maraviroc (MVC), tenofovir disoproxil fumarate (TDF) and dapivirine (DPV) were obtained from the AIDS Research and Reference Reagent Program, Division of AIDS, NIAID, NIH (USA) and Selleck Chemicals (USA). All progestins and ARVs were made up to a stock concentration of 10 mM in absolute ethanol or dimethyl sulfoxide (DMSO, Sigma Aldrich, RSA), respectively. [^{3}H]-Progesterone (50 Ci/mmol) (AEC-Amersham, RSA) was used as a final concentration of 40 nM diluted in serum-free, phenol red-free media. The pTAT-2xPRE-E1b-luciferase plasmid, driven by the E1b promoter and containing two copies of the rat progesterone response element (PRE), was obtained from Erasmus University of Rotterdam [23]. The human PR-B expression vector, pSG5hPR-B, was obtained as a gift from the University of Stellenbosch [24]. pcDNA 3.1 (empty vector used as a negative control) was obtained from Invitrogen, RSA.

2.2. Cell culture

Human breast cancer MDA-MB-231 PR-B+ cells, engineered to express the human (h)PR (Prof. Valerie Lin (Nanyang Technological University, Singapore) were cultured as previously described [25]. Human osteosarcoma U2OS cells (ATCC) were cultured as previously described [25]. Cells were routinely checked for mycoplasma and only mycoplasma-negative cells were used. Ligands or vehicle controls were added to cells in phenol red-free Dulbecco's Modified Eagle Medium (DMEM, Sigma Aldrich, RSA) containing 7.5% charcoal-stripped fetal calf serum (Separations, RSA) to give the final concentrations indicated in the figures, such that all incubation mixtures contained 0.1% (vol/vol) EtOH and 0.1% (vol/vol) DMSO (Sigma Aldrich, RSA).

2.3. Reporter assays

Promoter-reporter assays were performed as previously described [6], with a few modifications. Briefly, MDA-MB-231-PR-B+ cells were seeded into 10 cm dishes at a density of 2×10^6 cells. After 24 h, the cells were transiently transfected with 9 μg pTAT-2xPRE-E1b-luciferase using XtremeGene9 (Roche, RSA) as per the manufacturer's instructions. After 24 h, transfected cells were reseeded into 96-well plates at a density of 1×10^4 cells per well and treated with increasing concentrations of LNG in the presence of vehicle (DMSO) or 1 μM ARV for 24 h.

2.4. RNA extraction, cDNA synthesis and quantitative real-time PCR

This was carried out as previously described [6], with a few modifications. Briefly, MDA-MB-231-PR-B+ cells were seeded at a density of 2.5×10^5 cells per well in 6-well plates. After 24 h, cells were treated with progestins or ARVs for 24 h, harvested in 800 μL TriReagent® (Sigma-Aldrich, RSA) and processed for RNA according to the manufacturer's instructions. 250 ng RNA was reverse-transcribed using the High-Capacity cDNA Reverse Transcription Kit (Applied Biosystems, RSA), according to the manufacturer's instructions. Real-time quantitative reverse transcription PCR (qRT-PCR) was performed using the FastStart Essential DNA Green Master kit (Roche, RSA) on a RotorGene 3000 (Qiagen, Netherlands)

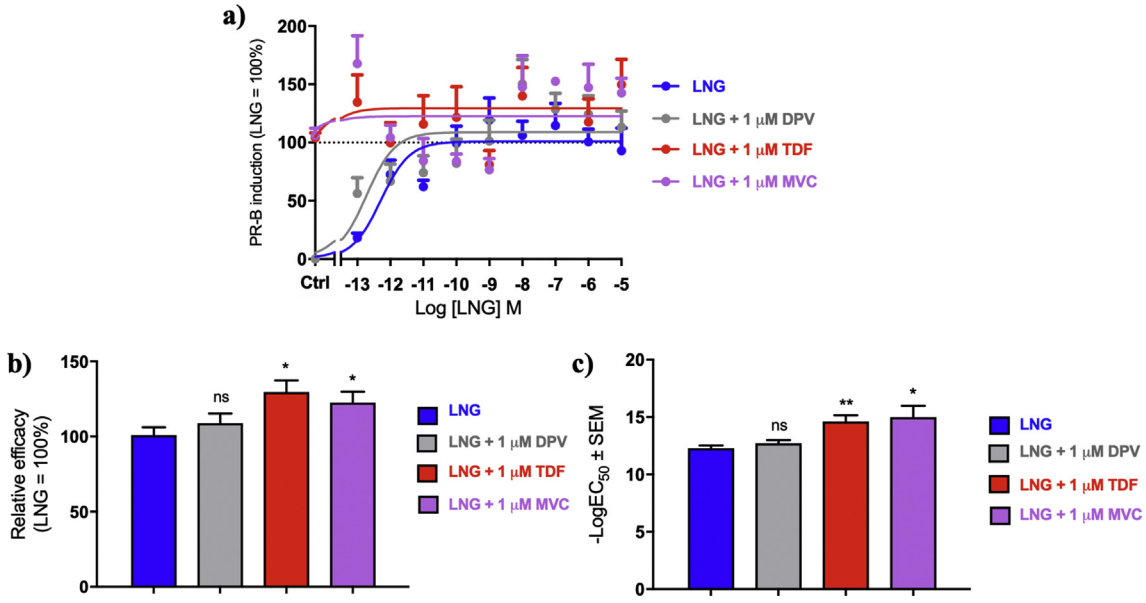

Fig. 1. MVC activates PR-B in the absence of LNG and increases LNG efficacy. MDA-MB-231 cells were treated with control (ctrl, 0.1% ethanol + 0.1% DMSO for LNG only, or 0.1% ethanol + 1 μM ARV for the combination treatments) or increasing concentrations of LNG alone or in combination with 1 μM ARV for 24 h. Thereafter, Luciferase and Bradford assays were performed. a) The % induction of PR-B activity of each condition relative to LNG = 100%. b) Shows the -logEC_{50} (M) values and c) shows efficacy as % maximal response. Data are plotted as means ± SEM for each condition. Data were analysed using unpaired t-tests relative to vehicle only where * and ** indicate p-value <0.05 and < 0.01 respectively, while ns indicates no significant difference. Data shown are pooled results of four independent experiments, each performed in triplicate. The previously reported TDF and DPV curves [6] are here shown with the MVC curve for comparative purposes, where these were done in parallel.

qRT-PCR machine, according to the manufacturer's instructions. The expression of the glucocorticoid-induced leucine zipper (*gilz)* gene and the prostaglandin-endoperoxide synthase 2 (*ptgs2)* gene were investigated. Validated *gilz* primers were purchased from Qiagen, RSA. Primers for*ptgs2* have previously been reported [26]. Glyceraldehyde 3-phosphate dehydrogenase (*gapdh)* was used as the reference gene as previously reported [27].

2.5. Whole cell binding

Competitive whole cell binding assays were performed in U2OS cells as previously described [28], with a few modifications. Briefly, U2OS cells were seeded into 24-well plates at a density of 5×10^4 cells per well. Twenty-four hours later, the cells were transiently transfected with 250 ng pSG5hPR-B or pcDNA 3.1 vector using Xtreme-Gene9. The following day, the cells were washed and incubated for 3 h with 40 nM [^{3}H]-Progesterone (50 Ci/mmol) (PerkinElmer Life and Analytical Science, RSA) in the presence of 0.1% ethanol or 10 μM unlabelled competitor compound in antibiotic-free, phenol red-free and serum-free media. Total binding ([^{3}H]-Progesterone only) was determined by scintillation counting and expressed as 100%. Specific bound [^{3}H]-Progesterone was calculated as the difference between

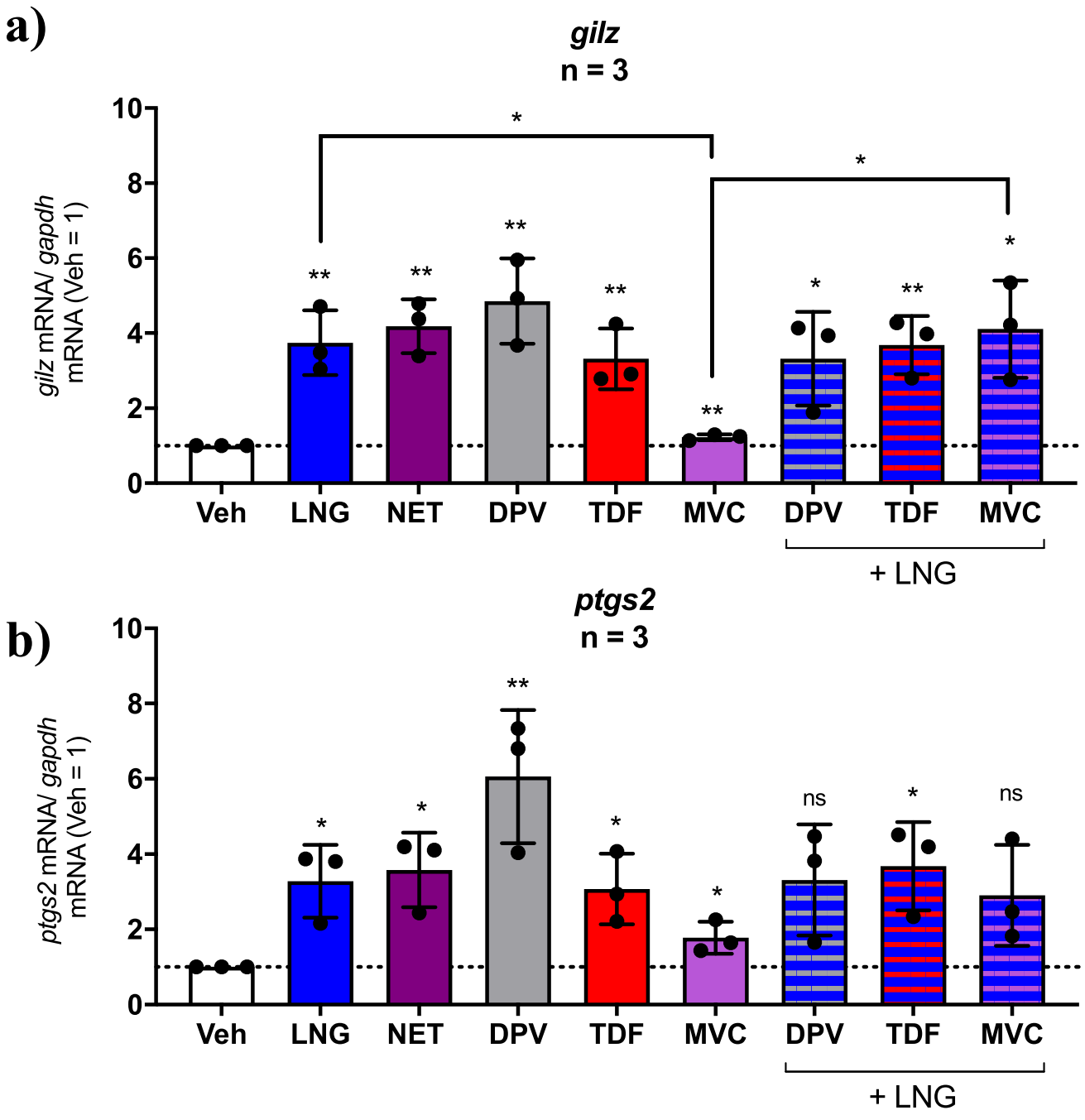

Fig. 2. Two PR-regulated genes are induced by DPV, TDF and MVC alone and in combination with LNG. MDA-MB-231 cells were treated with 100 nM progestin, 1 μM ARV alone or in combination with 100 nM LNG or vehicle (0.1% ethanol and 0.1% DMSO) for 24 h. Relative mRNA levels of *gilz* (a) and *ptgs2* (b) were normalized to *gapdh* mRNA levels. Relative expression was determined by normalising to veh = 1. Relative fold-induction was analysed using unpaired t-tests with * and ** denoting p-value <0.05 and < 0.01 respectively, while ns indicates no significant difference. Data are shown as mean ± SEM from three pooled independent experiments.

total and non-specific binding ([^{3}H]-Progesterone plus 10 μM unlabelled competitor) and expressed as a relative % of total binding. All values were normalized against total protein concentration as determined by the Bradford assay [29].

2.6. Western blot and protein quantification

Western blotting was carried out as previously described [30]. The primary antibodies for hPR (NCL-L-PGR-312, Leica Biosystems, USA), phospho-hPR (Ser294) (MA1414, ThermoFisher Scientific, RSA) and GAPDH (0411 sc-47724 Santa Cruz Biotechnology, Inc, USA) were diluted 1:1000, 1:100 and 1:4000, respectively. Membranes were washed and incubated for 1 h with the secondary goat-*anti*-mouse (sc-2313, Santa Cruz Biotechnology, Inc, USA) antibody (1:5000). Thereafter, the membranes were washed again and incubated with Pierce ECL-chemiluminescent western blotting substrate (Thermo Scientific, USA). Proteins were visualized by autoradiography using Amersham Hyperfilm™ MP high performance autoradiography film (AEC-Amersham, RSA). For consecutive detection steps, membranes were stripped as previously described [30]. Densitometric quantification of film was carried out using ImageJ™ Software (NIH, USA).

2.7. Data analysis

Results were analysed using GraphPad Prism (version 7) software from GraphPad Software Inc. (La Jolla California, USA). For dose-response curves, the receptor agonists were used as reference ligands and their maximal response was set to 100%. Dose-response curves were fitted with a non-linear regression model using "log agonist vs response", with a fixed Hill slope of one. All other curves were then plotted relative to the best-fit maximal value of the reference ligand. All data were assessed for normality and a parametric one-way ANOVA or a non-parametric Kruskal Wallis test were performed accordingly. Thereafter, unpaired t-tests were used to assess statistical significance. Data were plotted as mean ± SEM on histograms.

3. Results

3.1. MVC activates PR-B in the absence of a progestogen and significantly increases LNG efficacy

We have previously shown that TDF, unlike DPV, activates PR-B in the absence of a progestogen [6]. We next wished to investigate whether MVC could activate PR-B. Dose-response promoter-reporter assays were used to investigate the effect of MVC on efficacies (maximal response) and potencies (logEC_{50} values) of PR-B transcriptional activity in the absence and presence of increasing concentrations of LNG in MDA-MB-231 PR-B+ stably-expressing cells. As expected, LNG acted as an agonist (Fig. 1a). MVC induced PR-B activity, reaching 100% maximal response similar to that of the highest LNG concentration, both in the absence and in the presence of low doses of LNG (Fig. 1a). MVC significantly increased the potency (Fig. 1b and Supplementary Table 1) and efficacy (Fig. 1c and Supplementary Table 1) of LNG via PR-B. As previously reported TDF, unlike DPV, also activates the PR-B [6] (Fig. 1).

3.2. MVC, TDF and DPV transactivate endogenous PR-regulated genes

PR-B activity of MVC, TDF and DPV was next investigated for the first time on the endogenously expressed PR-regulated genes *gilz* and *ptgs2*. DPV and TDF treatment alone were able to induce *gilz* and *ptgs2* mRNA expression to similar extents as PR-B-saturating concentrations of LNG and NET (Fig. 2a and b and Supplementary Table 2). MVC alone was also able to partially induce both *gilz* and *ptgs2* mRNA expression, but to a lesser degree (1.23- and 1.78-fold, respectively) (Fig. 2a and b and Supplementary Table 2). Although both TDF and MVC induced a slight but significant increase in LNG efficacy in the reporter assays (Fig. 1c), none of the ARVs significantly increased the efficacy of LNG on either of the endogenous genes (Fig. 2a and b and Supplementary Table 2).

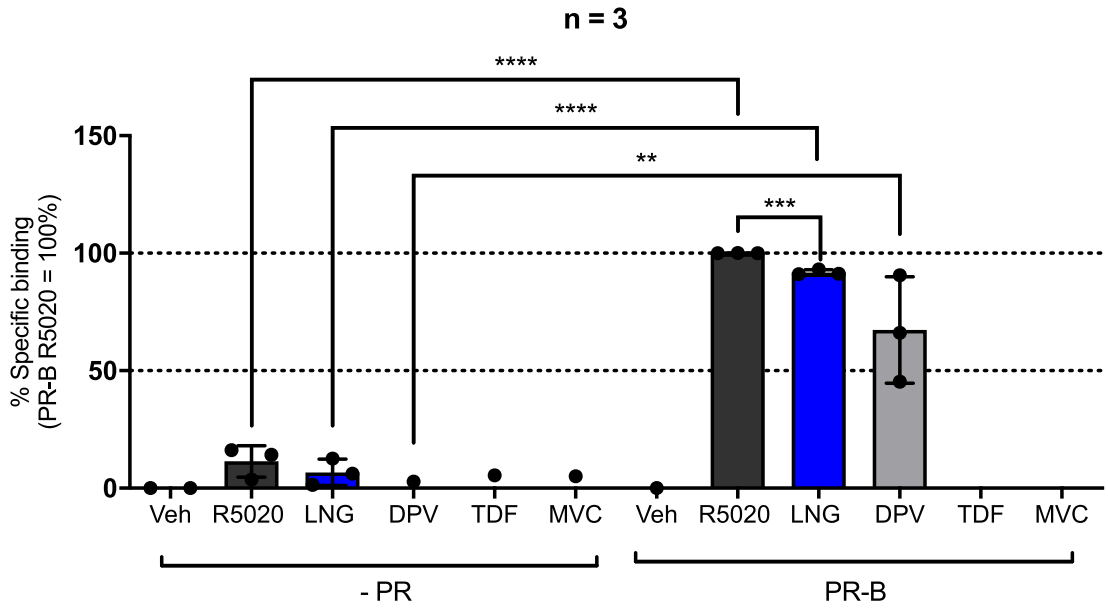

Fig. 3. R5020, LNG and DPV exhibit competition with progesterone binding to PR-B. Specific binding was observed after a 3-h incubation in the presence of 40 nM [^{3}H]-Progesterone. R5020 and LNG were tested at 1 μM and DPV, TDF and MVC were tested at 10 μM. Specific binding was analysed using unpaired t-tests with *** and **** denoting p-value <0.001 and < 0.0001, respectively. Mean ± SEM data is calculated based on three pooled independent experiments where each condition consisted of three technical repeats.

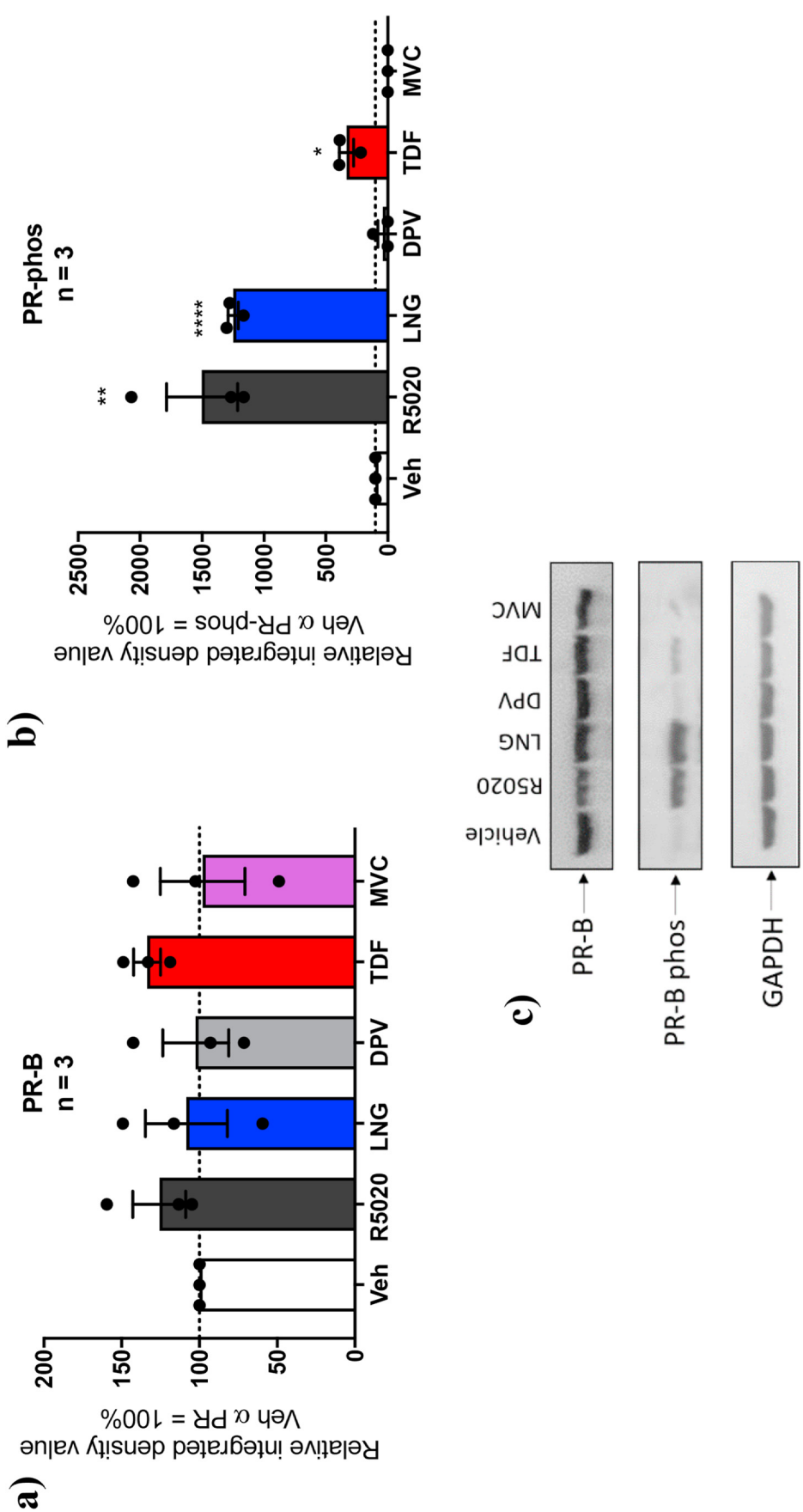

Fig. 4. PR-B phosphorylation is induced by R5020, LNG and TDF. MDA-MB-231 cells were treated with 100 nM R5020, LNG or 1 μM ARV or vehicle (0.1% DMSO and 0.1% ethanol) for 3 h. Thereafter, the cells were harvested, and a Western blot was performed. a) Shows total PR-B protein levels relative to veh = 100%. b) Shows percentage phosphorylation for PR-B relative to veh = 100%. c) A representative Western blot is shown, indicating signals for total PR-B, phosphorylated PR-B and the housekeeping protein, GAPDH. Relative protein levels were quantified using ImageJ software and analysed using unpaired t-tests with *, ** and **** denoting p-value <0.05, <0.01 and < 0.0001, respectively. Mean ± SEM data is calculated based on three pooled independent experiments.

3.3. DPV, unlike TDF and MVC, competes with progestogen for binding to PR-B

Having shown that MVC, TDF and DPV induce expression of endogenous PR-regulated genes, we next investigated whether these ARVs bind to PR-B by performing whole cell competitive binding assays. Maximal specific binding to PR-B of the agonists R5020 and LNG was significantly higher in the presence than in the absence of PR-B, although some background binding was observed in the absence of PR-B (Fig. 3 and Supplementary Table 3). In the presence of PR-B, MVC and TDF did not exhibit any competition for binding of radiolabelled progesterone. Surprisingly, DPV exhibited approximately 70% maximal binding to PR-B compared to R5020, with no significant difference detected in competitive binding between LNG and DPV (Fig. 3 and Supplementary Table 3).

3.4. PR agonists and TDF increase PR-B phosphorylation

Whether MVC, TDF and DPV affect PR-B protein expression levels and PR-B phosphorylation was also investigated. There were no significant differences in total PR-B protein expression levels for all treatments investigated (Fig. 4a and c). However, TDF along with R5020 and LNG, significantly increased PR-B protein phosphorylation levels at residue Ser294, while DPV and MVC did not exhibit detectable effects on this residue under these conditions (Fig. 4b and c).

4. Discussion

Few studies have investigated the effect of ARVs on activation of steroid receptors [7]. We show for the first time that MVC activates PR-B in the absence of progestogens *in vitro*, as shown previously by us for TDF on reporter genes [6]. This effect of MVC was similar to the progestogen-only maximal response on reporter assays. MVC induction of the endogenous *gilz* and ptgs2 genes was also observed, albeit to a lesser extent. The *gilz* gene plays a role in regulating the anti-inflammatory immune response [31], and is widely known for being induced by glucocorticoids via binding of the glucocorticoid receptor (GR) [31] to glucocorticoid response elements in the *gilz* promoter, as well as by progestins via the PR [32]. Several lines of evidence suggest that the effects we observe are due to the PR and not the GR. Though the cells used in the study do express the GR (Supplementary Fig. 1), we and others have shown that LNG, NET [33,34] and the ARVs used in this study (Supplementary Fig. 2) do not activate the GR.

Our study is the first to offer insight into the possible mechanisms of PR-B activation by TDF and MVC. Our results suggest different mechanisms may be involved for these ARVs (Supplementary Table 4). TDF may activate the PR indirectly, for example via activation of a mitogen-activated protein kinase (MAPK), resulting in PR phosphorylation at Ser294, since MAPKs are implicated in activation of PR-B by phosphorylation at this residue [35]. Further investigation into the mechanism by which MVC activates PR-B is required, including investigating the regulation of PR co-activators such as SRC-1 or p300 [36] as well as other PR phosphorylation sites.

DPV may activate the PR via a different mechanism, involving binding to PR-B resulting in transactivation of PR-regulated genes (Supplementary Table 4). This result is consistent with *in silico* molecular docking in our previous study that showed that DPV has some binding affinity potential for the PR, albeit low [6]. However, DPV did not exhibit transcriptional activity via the PR-B in the reporter assays, but did to a similar extent as the progestogens alone, for both endogenous genes investigated. This intriguing result is consistent with a different mechanism for activation of gene expression by DPV versus MVC. Possible reasons for the strikingly different results on reporter versus endogenous genes for DPV may include that native chromatin structure is required for the effects of DPV. Alternatively, or additionally, specific promoter elements/architecture may be required that are absent in the pTAT-2xPRE-E1b promoter but present in the *gilz* promoter, and/or a particular ratio of components of the signalling pathway may be required.

Taken together, our results provide proof of concept that MVC, TDF and DPV do exhibit context-specific off-target biological effects on PR-B activation, via different mechanisms. Further studies are required to dissect these mechanisms. Our results suggest that off-target effects on the PR-B by these ARVs may have important physiological implications for PR-mediated responses, although their physiological relevance is as yet unknown. The *in vitro* results suggest that these ARVs could induce PR-like responses in the absence of progestogens, and/or increase the efficacy of progestogens *in vivo*. Whether such effects are observed in clinical studies is unknown, but our results suggest a need for monitoring of clinical data for this possibility. For example, since the *ptgs2* gene plays a role in regulating the ovulatory inflammation required for successful ovulation in women [37], the presence of these ARVs may affect ovulation via PR-B. Similarly, the effects we obtained on the *gilz* gene suggest that ARVs could increase anti-inflammatory responses in PR-expressing tissues. Other i*n vitro* studies have shown that TDF [38] and MVC [39] induce apoptosis in breast cancer cells, a process known to be regulated by the PR [40]. However, our results showing that MVC, TDF and DPV had no effect on LNG efficacy on transactivation of the endogenous genes investigated are encouraging as they may indicate that simultaneous use of these ARVs with LNG will not impact on the biological effects of LNG *in vivo*.

Acknowledgements

This work was supported by the Eunice Kennedy Shriver National Institute of Child Health & Human Development [R01HD083026] to JH. We thank all members of the Hapgood laboratory for intellectual discussions.

Declaration of competing interest

The authors declare that they have no known competing financial interests or personal relationships that could have appeared to influence the work reported in this paper.

Appendix A. Supplementary data

Supplementary data to this article can be found online at https://doi.org/10.1016/j.bbrc.2020.09.107.

References

[1] T.D. Frank, A. Carter, D. Jahagirdar, et al., Global, regional, and national incidence, prevalence, and mortality of HIV, 1980–2017, and forecasts to 2030, for 195 countries and territories: A systematic analysis for the Global Burden of Diseases, Injuries, and Risk Factors Study 2017, Lancet HIV 6 (2019) e831–e859, https://doi.org/10.1016/S2352-3018(19)30196-1.
[2] S.G. Deeks, HIV infection, inflammation, immunosenescence, and aging, Annu. Rev. Med. 62 (2011) 141–155, https://doi.org/10.1146/annurev-med-042909-093756.
[3] N. Obel, H.F. Thomsen, G. Kronborg, et al., Ischemic heart disease in HIV-infected and HIV-uninfected individuals: A population-based cohort study, Clin. Infect. Dis. 44 (2007) 1625–1631, https://doi.org/10.1086/518285.
[4] A.C. Pettit, M.J. Giganti, S.M. Ingle, et al., Increased non-AIDS mortality among persons with AIDS-defining events after antiretroviral therapy initiation, J. Int. AIDS Soc. 21 (2018), e25031, https://doi.org/10.1002/jia2.25031.
[5] Who, Implementation Tool: Providing Contraceptive Services in the Context of HIV Treatment Programmes: HIV Treatment and Reproductive Health, World Health Organization, 2019.
[6] S. Dlamini, M. Kuipa, K. Enfield, et al., Reciprocal modulation of antiretroviral drug and steroid receptor function in vitro, Antimicrob. Agents Chemother. 64

(2019), https://doi.org/10.1128/AAC.01890-19.
[7] J. Svard, F. Blanco, D. Nevin, et al., Differential interactions of antiretroviral agents with LXR, ER and GR nuclear receptors: potential contributing factors to adverse events, Br. J. Pharmacol. 171 (2014) 480–497, https://doi.org/10.1111/bph.12480.
[8] S.L. Grimm, S.M. Hartig, D.P. Edwards, Progesterone receptor signaling mechanisms, J. Mol. Biol. 428 (2016) 3831–3849, https://doi.org/10.1016/j.jmb.2016.06.020.
[9] D. Africander, N. Verhoog, J.P. Hapgood, Molecular mechanisms of steroid receptor-mediated actions by synthetic progestins used in HRT and contraception, Steroids 76 (2011) 636–652, https://doi.org/10.1016/j.steroids.2011.03.001.
[10] F.Z. Stanczyk, J.P. Hapgood, S. Winer, et al., Progestogens used in postmenopausal hormone therapy: differences in their pharmacological properties, intracellular actions, and clinical effects, Endocr. Rev. 34 (2012) 171–208, https://doi.org/10.1210/er.2012-1008.
[11] I.F. Grigsby, L. Pham, L.M. Mansky, et al., Tenofovir-associated bone density loss, Therapeut. Clin. Risk Manag. 6 (2010) 41, https://doi.org/10.2147/TCRM.S8836.
[12] M. Horberg, B. Tang, W. Towner, et al., Impact of tenofovir on renal function in HIV-infected, antiretroviral-naive patients, J. Acquir. Immune Defic. Syndr. 53 (2010) 62–69, https://doi.org/10.1097/QAI.0b013e3181be6be2.
[13] D.J. Murphy, C.F. McCoy, P. Boyd, et al., Drug stability and product performance characteristics of a dapivirine-releasing vaginal ring under simulated real-world conditions, Int. J. Pharm. 565 (2019) 351–357, https://doi.org/10.1016/j.ijpharm.2019.05.027.
[14] R.M. Gulick, T.J. Wilkin, Y.Q. Chen, et al., Safety and tolerability of maraviroc-containing regimens to prevent HIV infection in women: a phase 2 randomized trial, Ann. Intern. Med. 167 (2017) 384–393, https://doi.org/10.7326/M17-0520.
[15] P. Dorr, M. Westby, S. Dobbs, et al., Maraviroc (UK-427,857), a potent, orally bioavailable, and selective small-molecule inhibitor of chemokine receptor CCR5 with broad-spectrum anti-human immunodeficiency virus type 1 activity, Antimicrob. Agents Chemother. 49 (2005) 4721–4732, https://doi.org/10.1128/Aac.49.11.4721-4732.2005.
[16] J.M. Baeten, T. Palanee-Phillips, E.R. Brown, et al., Use of a vaginal ring containing dapivirine for HIV-1 prevention in women, N. Engl. J. Med. 375 (2016) 2121–2132, https://doi.org/10.1056/NEJMoa1506110.
[17] J. Weehuizen, A. Wensing, T. Mudrikova, et al., Efficacy and safety of long-term maraviroc use in a heterogeneous group of HIV-infected patients: A retrospective cohort study, Int. J. Antimicrob. Agents 54 (2019) 215–222, https://doi.org/10.1016/j.ijantimicag.2019.02.018.
[18] E. Halvorsen, M. Hamilton, A. Young, et al., Maraviroc decreases CCL8-mediated migration of CCR5+ regulatory T cells and reduces metastatic tumor growth in the lungs, OncoImmunology 5 (2016), e1150398, https://doi.org/10.1080/2162402X.2016.1150398.
[19] Y. Tanabe, S. Sasaki, N. Mukaida, et al., Blockade of the chemokine receptor, CCR5, reduces the growth of orthotopically injected colon cancer cells via limiting cancerassociated fibroblast accumulation, Oncotarget 7 (2016) 48335, https://doi.org/10.1080/2162402X.2016.1150398.
[20] H. Arberas, A. Guardo, M. Bargallo, et al., In vitro effects of the CCR5 inhibitor maraviroc on human T cell function, J. Antimicrob. Chemother. 68 (2013) 577–586, https://doi.org/10.1093/jac/dks432.
[21] J. Díaz-Delfín, P. Domingo, M. Giralt, et al., Maraviroc reduces cytokine expression and secretion in human adipose cells without altering adipogenic differentiation, Cytokine 61 (2013) 808–815, https://doi.org/10.1016/j.cyto.2012.12.013.
[22] N. Madrid-Elena, M.L. García-Bermejo, S. Serrano-Villar, et al., Maraviroc is associated with latent HIV-1 reactivation through NF-κB activation in resting CD4+ T cells from HIV-infected individuals on suppressive antiretroviral therapy, J. Virol. (2018), https://doi.org/10.1128/JVI.01931-17. JVI. 01931-01917.
[23] G. Jenster, T.E. Spencer, M.M. Burcin, et al., Steroid receptor induction of gene transcription: A two-step model, Proc. Natl. Acad. Sci. U. S. A 94 (1997) 7879–7884, https://doi.org/10.1073/pnas.94.15.7879.
[24] P. Kastner, M.-T. Bocquel, B. Turcotte, et al., Transient expression of human and chicken progesterone receptors does not support alternative translational initiation from a single mRNA as the mechanism generating two receptor isoforms, J. Biol. Chem. 265 (1990) 12163–12167.
[25] S.B. Skosana, J.G. Woodland, M. Cartwright, et al., Differential metabolism of clinically-relevant progestogens in cell lines and tissue: implications for biological mechanisms, J. Steroid Biochem. Mol. Biol. 189 (2019) 145–153, https://doi.org/10.1016/j.jsbmb.2019.02.010.
[26] A. Billich, F. Bornancin, D. Mechtcheriakova, et al., Basal and induced sphingosine kinase 1 activity in A549 carcinoma cells: Function in cell survival and IL-1β and TNF-α induced production of inflammatory mediators, Cell. Signal. 17 (2005) 1203–1217, https://doi.org/10.1016/j.cellsig.2004.12.005.
[27] N.J. Verhoog, A. Du Toit, C. Avenant, et al., Glucocorticoid-independent repression of tumor necrosis factor (TNF) α-stimulated interleukin (IL)-6 expression by the glucocorticoid receptor a potential mechanism for protection against an excessive inflammatory response, J. Biol. Chem. 286 (2011) 19297–19310, https://doi.org/10.1074/jbc.M110.193672.
[28] D.J. Africander, K.H. Storbeck, J.P. Hapgood, A comparative study of the androgenic properties of progesterone and the progestins, medroxyprogesterone acetate (MPA) and norethisterone acetate (NET-A), J. Steroid Biochem. Mol. Biol. 143 (2014) 404–415, https://doi.org/10.1016/j.jsbmb.2014.05.007.
[29] M.M. Bradford, A rapid and sensitive method for the quantitation of microgram quantities of protein utilizing the principle of protein-dye binding, Anal. Biochem. 72 (1976) 248–254, https://doi.org/10.1016/0003-2697(76)90527-3.
[30] A. Kotitschke, H. Sadie-Van Gijsen, C. Avenant, et al., Genomic and non-genomic cross talk between the gonadotropin-releasing hormone receptor and glucocorticoid receptor signaling pathways, Mol. Endocrinol. 23 (2009) 1726–1745, https://doi.org/10.1210/me.2008-0462.
[31] S. Ronchetti, G. Migliorati, C. Riccardi, GILZ as a mediator of the anti-inflammatory effects of glucocorticoids, Front. Endocrinol. 6 (2015) 170, https://doi.org/10.3389/fendo.2015.00170.
[32] Y. Govender, C. Avenant, N.J. Verhoog, et al., The injectable-only contraceptive medroxyprogesterone acetate, unlike norethisterone acetate and progesterone, regulates inflammatory genes in endocervical cells via the glucocorticoid receptor, PloS One 9 (2014), e96497, https://doi.org/10.1371/journal.pone.0096497.
[33] K. Ronacher, K. Hadley, C. Avenant, et al., Ligand-selective transactivation and transrepression via the glucocorticoid receptor: role of cofactor interaction, Mol. Cell. Endocrinol. 299 (2009) 219–231, https://doi.org/10.1016/j.mce.2008.10.008.
[34] R. Sitruk-Ware, Reprint of pharmacological profile of progestins, Maturitas 61 (2008) 151–157, https://doi.org/10.1016/j.maturitas.2008.11.011.
[35] L.S. Treviño, N.L. Weigel, Phosphorylation: A fundamental regulator of steroid receptor action, Trends Endocrinol. Metab. 24 (2013) 515–524, https://doi.org/10.1016/j.maturitas.2008.11.011.
[36] Z. Liu, J. Wong, S.Y. Tsai, et al., Sequential recruitment of steroid receptor coactivator-1 (SRC-1) and p300 enhances progesterone receptor-dependent initiation and reinitiation of transcription from chromatin, Proc. Natl. Acad. Sci. U. S. A 98 (2001) 12426–12431, https://doi.org/10.1073/pnas.231474798.
[37] C.J. Park, P.-C. Lin, S. Zhou, et al., Progesterone receptor serves the ovary as a trigger of ovulation and a terminator of inflammation, Cell Rep. 31 (2020) 107496, https://doi.org/10.1016/j.celrep.2020.03.060.
[38] K. Thabethe, G. Adefolaju, M. Hosie, An in vitro study of the effects of emtricitabine, tenofovir disoproxil fumarate and efavirenz on a breast cancer cell line, MCF-7, J. Basic. Appl. Sci. Res. 3 (2013) 444–452.
[39] A. Pervaiz, M. Zepp, S. Mahmood, et al., CCR5 blockage by maraviroc: a potential therapeutic option for metastatic breast cancer, Cell. Oncol. 42 (2019) 93–106, https://doi.org/10.1007/s13402-018-0415-3.
[40] S.M. Quirk, R.G. Cowan, R.M. Harman, Progesterone receptor and the cell cycle modulate apoptosis in granulosa cells, Endocrinology 145 (2004) 5033–5043, https://doi.org/10.1210/en.2004-0140.

AMERICAN SOCIETY FOR MICROBIOLOGY | Antimicrobial Agents and Chemotherapy®

ANTIVIRAL AGENTS

Reciprocal Modulation of Antiretroviral Drug and Steroid Receptor Function *In Vitro*

Sigcinile Dlamini,[a] Michael Kuipa,[a] Kim Enfield,[a] Salndave Skosana,[a] John G. Woodland,[a] Johnson Mosoko Moliki,[a] Alexis J. Bick,[a] Zephne van der Spuy,[b] Michelle F. Maritz,[a]* Chanel Avenant,[a] Janet P. Hapgood[a,c]

[a]Department of Molecular and Cell Biology, University of Cape Town, Cape Town, South Africa
[b]Department of Obstetrics and Gynaecology, University of Cape Town, Groote Schuur Hospital, Cape Town, South Africa
[c]Institute of Infectious Disease and Molecular Medicine, University of Cape Town, Cape Town, South Africa

ABSTRACT Millions of women are exposed simultaneously to antiretroviral drugs (ARVs) and progestin-based hormonal contraceptives. Yet the reciprocal modulation by ARVs and progestins of their intracellular functions is relatively unexplored. We investigated the effects of tenofovir disoproxil fumarate (TDF) and dapivirine (DPV), alone and in the presence of select steroids and progestins, on cell viability, steroid-regulated immunomodulatory gene expression, activation of steroid receptors, and anti-HIV-1 activity *in vitro*. Both TDF and DPV modulated the transcriptional efficacy of a glucocorticoid agonist via the glucocorticoid receptor (GR) in the U2OS cell line. In TZM-bl cells, DPV induced the expression of the proinflammatory interleukin 8 (IL-8) gene while TDF significantly increased medroxyprogesterone acetate (MPA)-induced expression of the anti-inflammatory glucocorticoid-induced leucine zipper (GILZ) gene. However, peripheral blood mononuclear cell (PBMC) and ectocervical explant tissue viability and gene expression results, along with TZM-bl HIV-1 infection data, are reassuring and suggest that TDF and DPV, in combination with dexamethasone (DEX) or MPA, do not reciprocally modulate key biological effects in primary cells and tissue. We show for the first time that TDF induces progestogen-independent activation of the progesterone receptor (PR) in a cell line. The ability of TDF and DPV to influence GR and PR activity suggests that their use may be associated with steroid receptor-mediated off-target effects. This, together with cell line and individual donor gene expression responses in the primary models, raises concerns that reciprocal modulation may cause side effects in a cell- and donor-specific manner *in vivo*.

KEYWORDS ARV, HIV-1, cell viability, dapivirine, gene expression, inflammation, progesterone receptor, progestin, steroid receptor, tenofovir disoproxil fumarate

Women in sub-Saharan Africa are disproportionately affected by human immunodeficiency virus type 1 (HIV-1) and face a high risk of unintended pregnancy and sexually transmitted infections (1). As a result, millions of HIV-1-positive women are concurrently taking oral antiretroviral drugs (ARVs) and progestogen-containing hormonal contraceptives. Multipurpose prevention technologies (MPTs) are in development to safely and effectively protect healthy women against HIV-1 and unwanted pregnancy. Understanding the relationship between ARVs and hormonal contraceptives is therefore essential for insight on potential short- and long-term side effects associated with their simultaneous use. Adverse effects associated with the use of ARVs and hormonal contraceptives include bone density loss, kidney and liver toxicity, cardiovascular damage, lactic acidosis, and effects on immune function (2, 3). However, studies on the reciprocal modulation of ARV and synthetic progestogen (progestin) intracellular activity are limited. We hypothesize that progestins may affect the efficacy

Citation Dlamini S, Kuipa M, Enfield K, Skosana S, Woodland JG, Moliki JM, Bick AJ, van der Spuy Z, Maritz MF, Avenant C, Hapgood JP. 2020. Reciprocal modulation of antiretroviral drug and steroid receptor function *in vitro*. Antimicrob Agents Chemother 64:e01890-19. https://doi.org/10.1128/AAC.01890-19.

Address correspondence to Janet P. Hapgood, janet.hapgood@uct.ac.za.

* Present address: Michelle F. Maritz, Futures Industries Institute, ARC Centre of Excellence in Convergent Bio-Nano Science, University of South Australia, Adelaide, Australia.

Received 18 September 2019
Returned for modification 14 October 2019
Accepted 23 October 2019

Accepted manuscript posted online 28 October 2019
Published 20 December 2019

of ARVs and that ARVs may modulate steroid receptor activity in the absence and presence of steroids, which may impact the efficacy and side effects of these drugs.

Tenofovir disoproxil fumarate (TDF), the prodrug form of tenofovir (TFV), is a nucleotide reverse transcriptase inhibitor, widely used in combination with other ARVs in the HIV-1 treatment regimen (4). Currently, TDF is approved as an oral preexposure prophylaxis (PrEP) method in combination with emtricitabine (FTC) for the prevention of HIV-1 infection in healthy individuals. It has been shown in phase I clinical trials to be safe and well tolerated as an intravaginal ring in sexually abstinent women; however, a recent phase I trial assessing the safety and pharmacokinetics of a 90-day TDF intravaginal ring in sexually active women found that the ring causes ulcerations and increases inflammatory markers in women using the ring compared to those in women receiving a placebo (5, 6). Dapivirine (DPV), a nonnucleoside reverse transcriptase inhibitor, is the most clinically advanced microbicide targeted for intravaginal delivery. In 2016, two phase III clinical trials found that a 30-day DPV intravaginal ring reduced the risk of HIV infection by approximately 30%, and modeling data from follow-up open-label extension studies have suggested a greater risk reduction of approximately 50% overall for women using the ring over a 1-year period (7–9). The DPV ring is now under regulatory review for use in developing countries with high HIV incidence.

The most commonly used progestin in sub-Saharan Africa is the 3-monthly injectable contraceptive medroxyprogesterone acetate (MPA), referred to as Depo-Provera or depot MPA intramuscular (DMPA-IM) (10). Levonorgestrel (LNG), widely used in the region as a contraceptive in different formulations and with different delivery methods, is also a leading candidate for the development of dual ARV–progestin MPTs. These progestins are synthetic steroid ligands that elicit intracellular responses by binding to and activating steroid receptors (11). The primary targets for progestins are the progesterone receptors (PR-A and PR-B); however, some progestins, such as MPA, are also known to cross talk with other steroid receptors, such as the glucocorticoid receptor (GR) and the androgen receptor (AR) (12). Through their actions as ligand-activated transcription factors, steroid receptors can activate or repress transcription to influence multiple processes in cells and tissues (13). MPA is a known full-to-partial GR agonist and induces immunomodulatory effects and increased HIV infection via GR-mediated mechanisms *in vitro* (13–15). Clinical epidemiological studies also suggest that DMPA-IM increases the risk of HIV-1 over that with no contraception (16) or an LNG implant (17).

Several clinical and pharmacokinetic studies have evaluated the effects of simultaneous use of some ARVs and progestins on pregnancy, HIV-1 acquisition or disease progression, and changes in serum drug concentrations. To date, efavirenz (EFV) is the only ARV shown to decrease contraceptive efficacy by influencing the metabolism of progestins in women, resulting in a decrease in progestin levels (18, 19). A study evaluating the effects of hormonal contraceptives on ARV efficacy showed that DMPA-IM, LNG, and combined oral contraceptives have no detectable effect on the efficacy of combined antiretroviral therapy containing nonnucleoside reverse transcriptase inhibitors other than DPV or protease inhibitors (20). Limited *in vitro* studies have shown that TDF and DPV have immunomodulatory effects (21–23), and this may indicate the involvement of steroid receptors such as the GR, a known immune regulator. A recent *in vitro* study showed that MPA, but not LNG or norethisterone (NET), is able to inhibit the anti-HIV-1 activities of TFV and tenofovir alafenamide in blood and tissue $CD4^+$ T cells, most likely by lowering intracellular concentrations of TFV diphosphate (24). These clinical and *in vitro* studies suggest that drug-drug interactions do occur *in vivo*.

Potential off-target effects and drug-drug interactions of ARVs and progestins are likely to be dose dependent. The progestins and ARVs used for PrEP and MPTs exhibit a wide range of concentrations in the vagina and in serum or plasma (Table 1). Additional *in vivo* studies are required to investigate drug-drug interactions, as are *in vitro* studies to identify and predict as yet unidentified off-target effects and their dose dependency.

TABLE 1 Intravaginal and plasma or serum concentrations of ARV and progestin candidates for MPTs

Product[a]	Concentration(s)				Reference(s)
	Released in product	In cervicovaginal fluid (μM)	In cervical tissue (μM)	In plasma or serum (nM)	
ARVs					
TFV gel	1% (vol/vol) gel[b]	41–34,000	0.7–4,800	11.83[c]	79, 80[d]
TDF ring	365 mg[e]	88–236	9–30	1.2–5.2	5[d]
TDF (HAART)	300 mg[h]	ND[f]	ND	1,100–1,140	81[d]
TDF–FTC oral PrEP	300 mg[h] TDF, 200 mg[h] FTC	ND	79[c]	77–87	82[g]
DPV ring	25 mg[e]	17[c]	2–21	0.7–0.89	7,[d] 9,[d] 54[g]
Progestins					
DMPA-IM (injectable)	150 mg[e]	ND	ND	21[c]	57,[g] 83,[g] 84[d]
ETG–EE ring (NuvaRing)	120 μg[h] ETG, 15 μg[h] EE	ND	0.002[c] (ETG), 0.0004 (EE)	3.7[c] (ETG), 0.05[c] (EE)	85[g]
LNG-releasing IUS (Mirena)	30 μg[h]; 52 mg[e]	100–370	2.5[c]	0.2,[c] 0.97[c]	34, 86[d]
LNG (implant, oral pill)	150 mg[e] (implant); 1.5 mg[h] (oral pill)	ND	ND	0.3–28	87,[g] 88,[d] 89[g]
NES–EE ring	150 μg[h] NES, 15 μg[h] EE	ND	ND	0.3[c]	90[g]
MPTs					
DPV + LNG ring	200 mg[e] DPV, 320 mg[e] LNG	ND	ND	2.1[c] (DPV), 5.1[c] (LNG)	91[d]
TFV + LNG ring	8–10 mg[h] TFV, 20 μg[h] LNG	34–3,484 (TFV), ND (LNG)	6.9–2,865 (TFV), ND (LNG)	8[c] (TFV), 0.9–1.6 (LNG)	92[d]

[a]HAART, highly active antiretroviral therapy; ETG, etonogestrel; EE, ethinyl estradiol; IUS, intrauterine system; NES, Nestorone.
[b]Pericoitally applied.
[c]Mean concentration.
[d]Concentrations in plasma.
[e]Single dose.
[f]ND, not determined.
[g]Concentrations in serum.
[h]Daily dose.

In the present study, we evaluated the abilities of select steroid ligands and ARVs to reciprocally modulate their respective intracellular functions, namely, the regulation of gene expression via activation of steroid receptors by steroid ligands and the inhibition of HIV-1 infection by TDF and DPV. Dose-dependent effects of TDF and DPV on GR, PR, and AR activity in the absence and presence of receptor agonists in *in vitro* cell line, peripheral blood mononuclear cell (PBMC), and ectocervical tissue explant models were investigated, and the effects of MPA, LNG, and other receptor-specific agonists on the dose-dependent inhibition of HIV-1 infection by TDF and DPV were investigated in the TZM-bl reporter cell line.

RESULTS

The concentration ranges of the ARVs used in this study were selected to reflect those that have been measured intravaginally and in blood previously (Table 1). The steroid concentrations chosen were intended to fully saturate possible cognate steroid receptors or, for dose-response analysis, to span the pharmacologically relevant concentrations of steroids (13, 25, 26). Steroid stimulation times of 24 or 48 h were used, since these have been previously established to elicit inflammatory gene responses in the models used in the study.

Effects of ARVs and steroids on cell and tissue viability. We used 3-(4,5-dimethylthiazol-2-yl)-2,5-diphenyltetrazolium bromide (MTT) assays to investigate whether ARVs affect cell or tissue viability. In TZM-bl cells, concentrations of TDF ranging from 0.01 to 100 μM and concentrations of DPV ranging from 0.01 to 1 μM did not affect cell viability (Fig. 1A and B). However, 10 and 100 μM DPV significantly reduced cell viability (Fig. 1A and B). In PBMCs, only a 100 μM concentration of either ARV significantly reduced cell viability (Fig. 1C and D). A 5% concentration of dimethyl sulfoxide (DMSO) was used as a positive control for cytotoxicity in TZM-bl cells (Fig. 1A

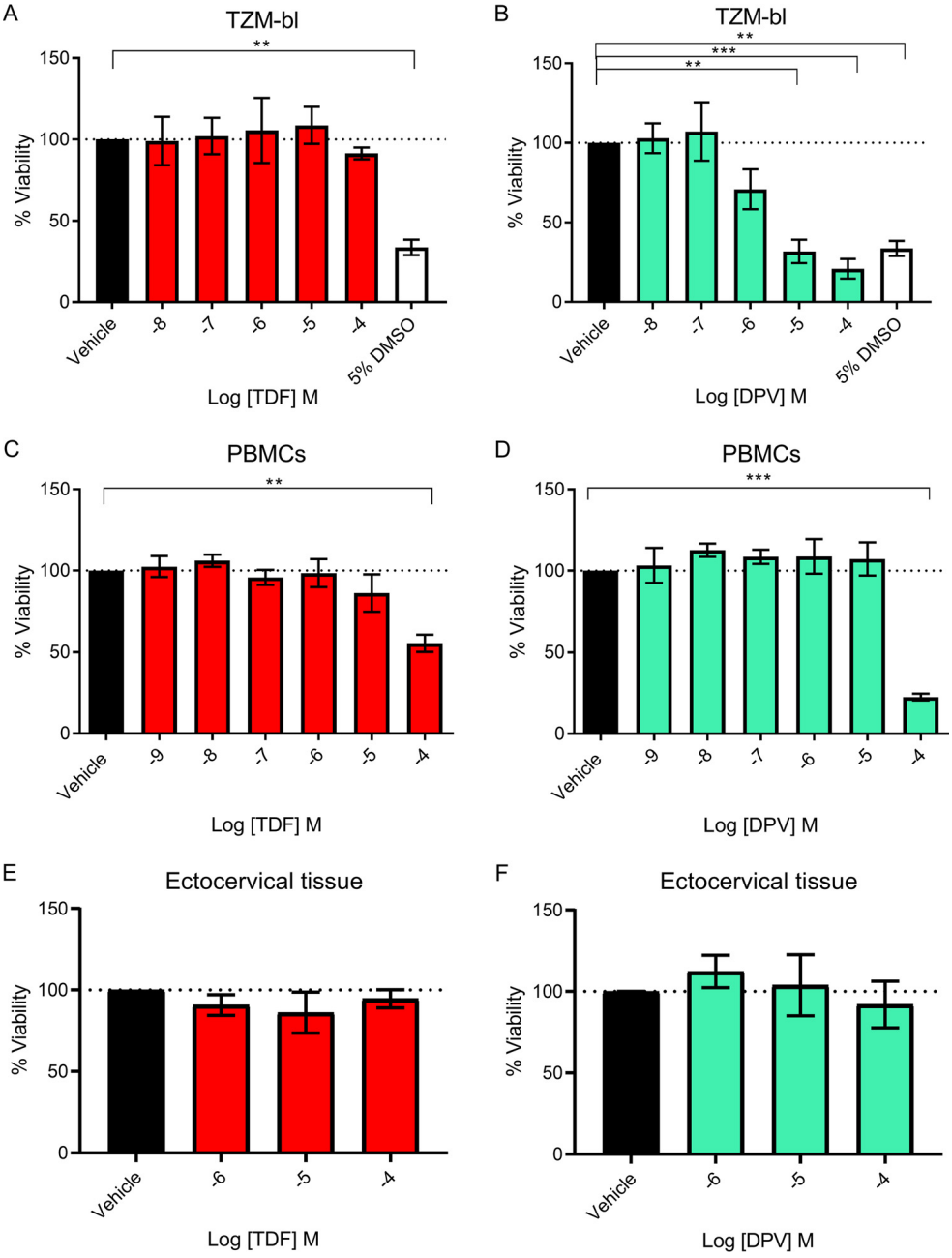

FIG 1 Effects of ARVs on the viability of TZM-bl cells, PBMCs, and cervical explant tissues. TZM-bl cells (A and B), PBMCs (C and D), and ectocervical explant tissues (E and F) were treated with different concentrations of TDF and DPV, ranging from 10^{-10} M to 10^{-4} M, in triplicate, for 24 h, and DMSO (0.1%, vol/vol) was used as the vehicle control. A 5% concentration of DMSO was used as the positive control in TZM-bl cells and PBMCs (data not shown). Cells were treated with MTT reagent for 2 h, and after solubilization, the absorbance was read at 595 nm. Cell viability was normalized to that for the vehicle control, which was set to 100%. Graphs show pooled results of three independent experiments for TZM-bl cells (A and B), data from four PBMC donors, with experiments for each condition carried out in triplicate and results represented as means ± standard deviations (C and D), or pooled results from four cervical explant donors (E and F). Statistical analysis was carried out using one-way ANOVA, followed by Tukey's multiple-comparison posttest. Statistical significance in the comparison of the vehicle control to ARV treatment is indicated by asterisks (**, $P < 0.01$; ***, $P < 0.001$).

and B), and a range of 5 to 20% DMSO was used in PBMCs (data not shown). The viability of ectocervical explant tissues appeared unaffected by TDF and DPV concentrations ranging from 1 to 100 μM (Fig. 1E and F). Cell viability with ARVs was not altered by the presence of 100 nM steroids (dexamethasone [DEX] or MPA), alone or in combination with 1 μM ARV, in TZM-bl cells. However, in PBMCs, the presence of

100 nM DEX significantly reduced cell viability by approximately 30% (see Fig. S1A and B in the supplemental material). We next performed gene expression analysis in the various models using only ARV concentrations shown not to reduce viability in the cell/tissue models, in order to avoid confounding the interpretation of the data. Given the slight reduction in cell viability by 100 nM DEX in PBMCs, all the PBMC gene expression results were normalized for cell viability and interpreted with due caution.

ARV modulation of endogenous steroid-regulated inflammatory genes. To examine the ability of ARVs to modulate endogenous immunomodulatory genes, the relative mRNA expression of the established (27–29) steroid-regulated anti-inflammatory glucocorticoid-induced leucine zipper (GILZ) gene and of two proinflammatory genes, encoding interleukin 6 (IL-6) and IL-8, was assessed in TZM-bl cells, PBMCs, and tissue explants. These genes were chosen as model GR-regulated genes. GILZ has been shown previously to be upregulated in several model systems by glucocorticoids via a mechanism involving binding of the GR to glucocorticoid response elements in the promoter (30). IL-6 has been shown previously to be downregulated in several model systems by glucocorticoids and other steroids via a mechanism involving tethering of the steroid receptor to other transcription factors, such as NF-κB, recruited to the promoters (31), while effects on IL-8 are reportedly variable (32, 33). Cells and tissues were stimulated with 1 μM DPV or 10 μM TDF in the absence and presence of 100 nM DEX or MPA. In all three model systems, DEX and/or MPA was found to increase GILZ mRNA levels and to repress IL-6 mRNA levels, as expected, while no statistically significant effects were observed for IL-8. The results are summarized in Table S1 in the supplemental material.

In TZM-bl cells, neither TDF (up to 10 μM) nor DPV (up to 100 nM) affected GILZ mRNA levels on their own (see Fig.S2A and S3A and B in the supplemental material). However, TDF, more than DPV, increased the efficacy of MPA-induced GILZ expression in MPA dose-response analysis, although these effects were not statistically significant (Fig. 2A and B). TDF dose-response analysis (1 to 100 μM TDF) in the presence of 100 nM MPA revealed that TDF at 10 and 100 μM significantly increased MPA-induced GILZ expression by approximately 1.5- and 2-fold, respectively (Fig. S2A), but had no significant effect on the MPA responses of IL-6 and IL-8 in TZM-bl cells (Fig. S2B and C). Unlike TDF, DPV alone significantly induced IL-8 mRNA expression by 11-fold, and appeared to induce IL-6 mRNA expression by 10-fold, in TZM-bl cells (Fig. 2C and D). DEX and MPA significantly repressed IL-6 expression by 10-fold and 5-fold, respectively, and appeared to induce IL-8 expression by 3.4-fold and 3.5-fold, respectively (Fig. 2C and D). Costimulation with TDF did not appear to alter these DEX or MPA responses (Fig. 2C and D). However, costimulation with DPV inhibited DEX and MPA repression and returned IL-6 expression to basal levels (Fig. 2C). Interestingly, for IL-8 expression, the effect of the combination of DPV with DEX or MPA appeared to be steroid specific. DEX in combination with DPV did not alter DPV-induced IL-8 expression; however, the combination of MPA and DPV resulted in a significant 1.6-fold potentiation of the DPV-induced IL-8 response (Fig. 2D). Lower doses of TDF and DPV, in the range of 0.1 to 100 nM, had no significant effect on GILZ, IL-6, or IL-8 mRNA levels, either in the absence or in the presence of MPA (Fig. S3).

Results in PBMCs are shown for pooled effects on 13 donors (Fig. 3), as well as for subgroups of donors, in order to illustrate more clearly the diversity and frequency of donor-specific effects (see Fig.S4 to S6 in the supplemental material). In PBMCs, TDF and DPV had no detectable effect on GILZ mRNA levels for the majority of donors (Fig. 3A; also Fig. S4A). As expected, DEX treatment significantly induced GILZ mRNA expression by 8-fold, as for TZM-bl cells, but this induction remained unchanged in the presence of ARVs, in contrast to the response in TZM-bl cells. As expected, DEX also significantly repressed IL-6 mRNA levels by about 3-fold, and this repression was not influenced by combination with ARVs (Fig. 3B). DEX alone and in combination with ARVs had no detectable effect on IL-8 mRNA levels (Fig. 3C). In the majority of donors, DPV and TDF showed no detectable significant effects on IL-6 and IL-8 mRNA expression (Fig. 3B and C; also Fig.S5B and S6B). The PBMC responses in donor samples

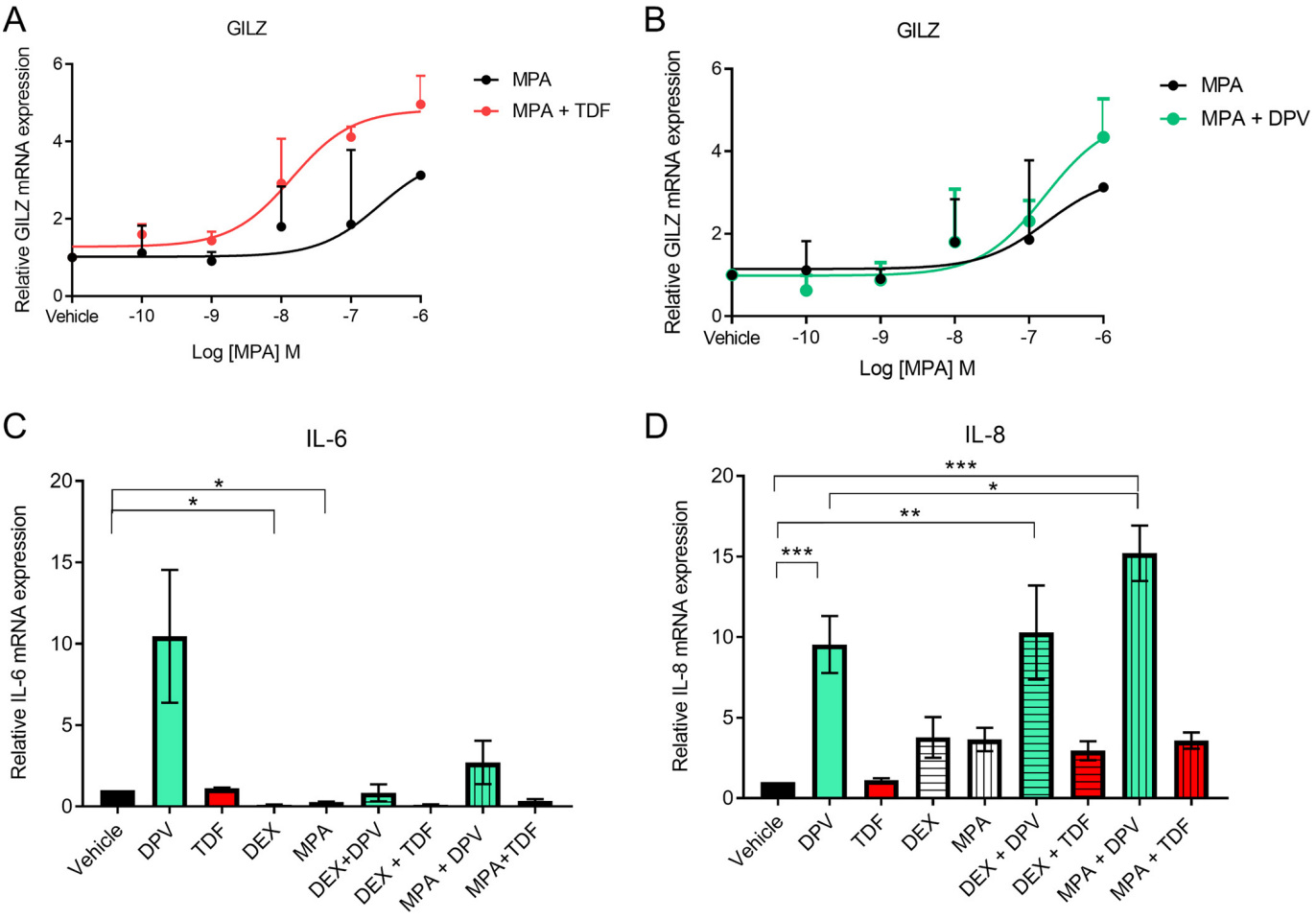

FIG 2 Effects of TDF and DPV on inflammatory gene mRNA levels in human cervical TZM-bl cells. Gene expression was evaluated after 24 h of stimulation with the indicated concentrations of ARVs and steroids. GILZ mRNA expression with increasing doses of MPA in the absence and presence of 10 μM TDF (A) or 1 μM DPV (B). IL-6 (C) and IL-8 (D) mRNA expression in the presence of 100 nM DEX or MPA, 1 μM TDF or DPV, or combinations thereof. EtOH plus DMSO (0.1% [vol/vol] for each) was used as the vehicle control. RNA was isolated, and cDNA was synthesized. Then mRNA expression levels were determined by qRT-PCR and were normalized to GAPDH mRNA expression levels. The relative fold change in expression was determined by setting the value for the vehicle control to 1. Pooled results of three or more independent experiments are shown and are represented as means ± SEM. Panels A and B were assessed for statistical significance using two-way ANOVA with Tukey's multiple-comparison posttest for comparison of the curves, although no statistical significance was obtained. For panels C and D, statistical significance was assessed with a nonparametric Kruskal-Wallis test, with Dunn's multiple-comparison posttest for comparison of the conditions. Statistical significance is indicated by asterisks (*, $P < 0.05$; **, $P < 0.01$; ***, $P < 0.001$).

showed a high degree of variability. Subgroup analysis did, however, reveal donor-specific effects, with some donors exhibiting at least 2-fold upregulation (as for IL-6 and IL-8 in TZM-bl cells) or downregulation in the mRNA levels of some genes in response to ARVs (Fig.S5 and S6).

Experiments in explant tissue were performed with DPV and not TDF, due to the limited availability of fresh tissue. Most of the results were very similar to those obtained in PBMCs (Fig. 4A to C). DPV alone appeared to have no effect on GILZ mRNA (Fig. 4A). As observed in PBMCs and TZM-bl cells, DEX significantly induced GILZ mRNA by 8-fold, and MPA appeared to increase GILZ mRNA by 2.4-fold (Fig. 4A). MPA or DEX alone appeared to repress IL-6 by approximately 1.5- or 2-fold, respectively (Fig. 4B), but had no effect on IL-8 (Fig. 4C), as observed in PBMCs and TZM-bl cells. DPV did not appear to modulate the DEX or MPA responses for any of the genes (Fig. 4A to C). As with PBMCs, there was high donor-specific variability in responses, making it difficult to establish significance for small effects. While DPV alone appeared to have no effect on any of the three genes for the pooled samples, it appeared to have a proinflammatory effect on IL-6 and IL-8 for some of the donor samples (Fig. 4B and C), as for some PBMC donor samples and for TZM-bl cells.

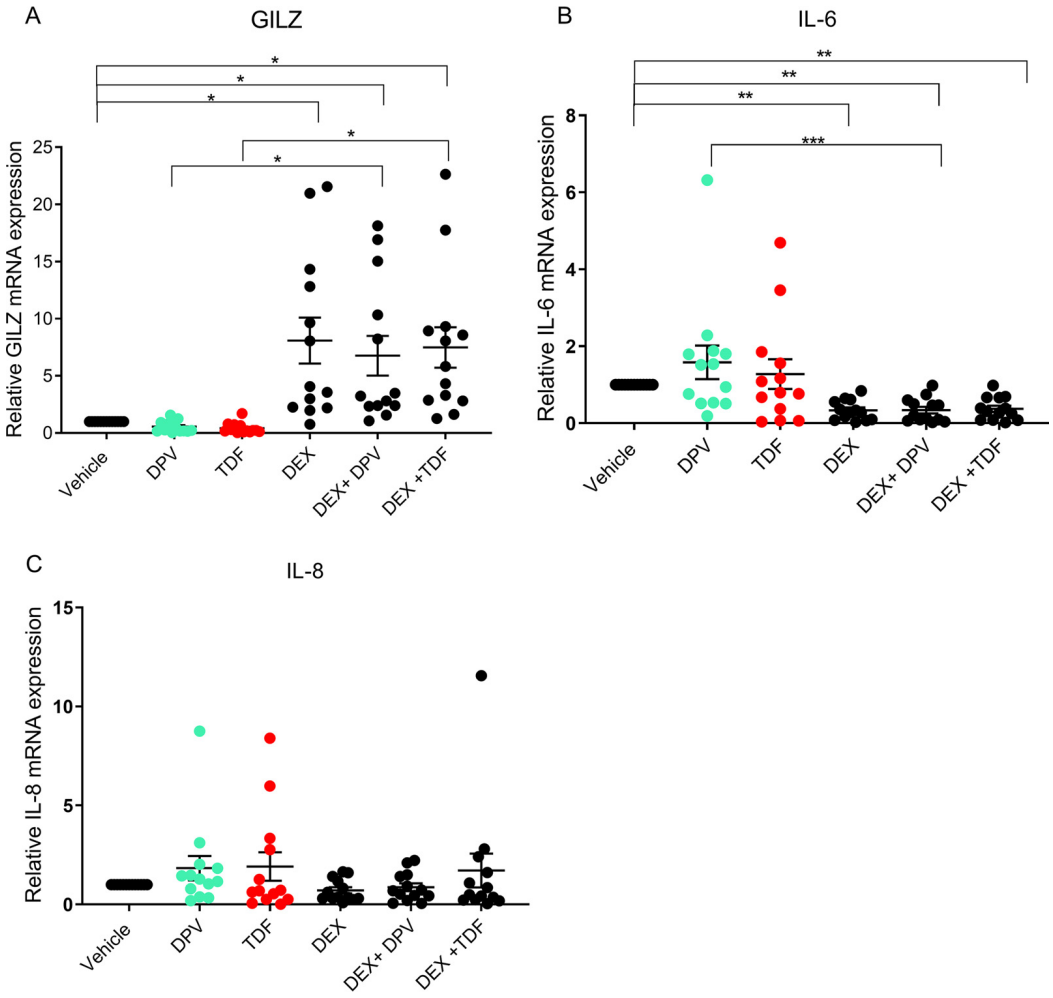

FIG 3 Immunomodulatory effects of ARVs in PBMCs. Nonactivated PBMCs were stimulated with TDF and DPV at 1 μM in the absence and presence of 100 nM DEX, or with the vehicle control (EtOH plus DMSO, each at 0.1% [vol/vol]) for 48 h. RNA was isolated from PBMCs, and thereafter cDNA was synthesized. Relative changes in GILZ (A), IL-6 (B), and IL-8 (C) mRNA expression levels were determined by qRT-PCR and were normalized to GAPDH mRNA expression levels. The relative fold change in expression was determined by setting the value for the vehicle control to 1. Pooled results of 13 patients are shown for each condition (with experiments carried out in triplicate) and are represented as means ± SEM. A Kruskal-Wallis test was performed with Dunn's multiple-comparison posttest to determine significant differences between treatments. Statistical significance is indicated by asterisks (*, $P < 0.05$; **, $P < 0.01$; ***, $P < 0.001$).

ARV effects on steroid receptor transcriptional activity. We next investigated the effects of ARVs on the efficacy and potency of the transcriptional effects of GR, PR-B, and AR agonists by using promoter-reporter assays. Western blotting showed that steroid receptors were successfully exogenously expressed in U2OS cells (see Fig. S7 in the supplemental material). Assessment of the *in vitro* toxicity of TDF and DPV in U2OS cells by use of the MTT cell viability assay showed that concentrations as high as 1 μM for either ARV were not deleterious, while 10 μM DPV but not TDF resulted in a loss of viability (see Fig. S8).

TDF (1 μM) significantly increased the efficacy of DEX transcriptional activity via the GR by 33%. DPV had a similar effect, which approached significance ($P = 0.0531$), increasing DEX transcriptional activity by 25% (Fig. 5A and B; see also Table S2 in the supplemental material). These increases were similar to the effects of both TDF and DPV on MPA in TZM-bl cells (Fig. 2A and B; also Fig. S2A). The potency of DEX was not significantly altered in the presence of either ARV (Table S2). Neither ARV appeared to have a significant effect on the efficacy and potency of the synthetic AR agonist mibolerone (MIB) (Fig. 5C and D; see also Table S3). Surprisingly, 1 μM TDF, unlike DPV, significantly increased PR-B-mediated transcriptional activity alone and in the presence

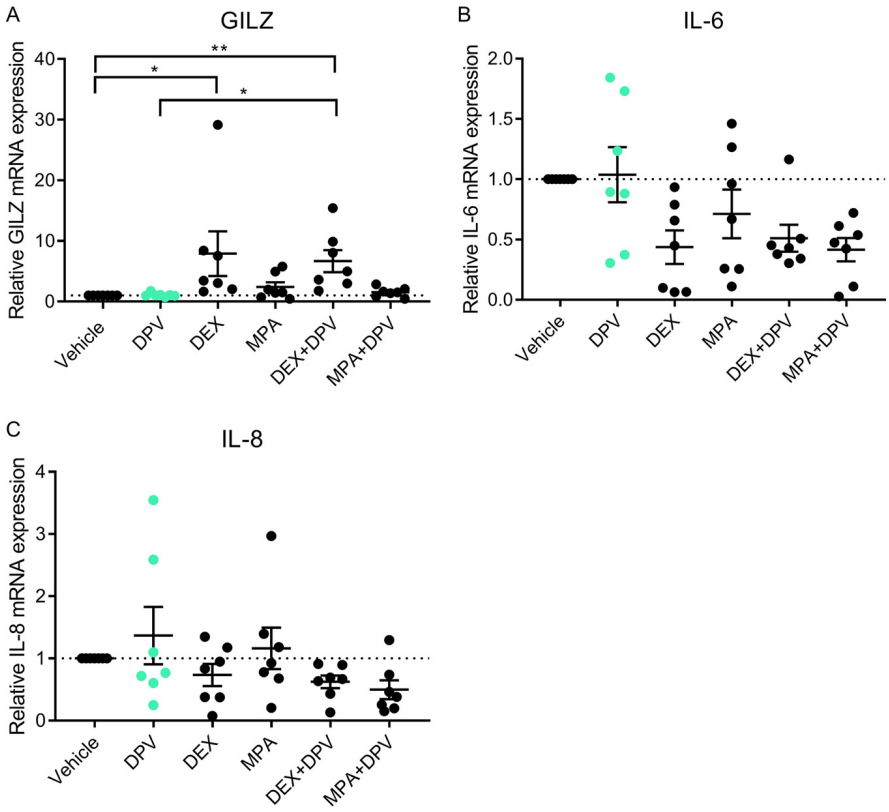

FIG 4 Immunomodulatory effects of ARVs in ectocervical explant tissue. Ectocervical explants were stimulated with 1 μM DPV or 100 nM DEX or MPA, or combinations thereof, as indicated. RNA was isolated, and thereafter, cDNA was synthesized. Relative changes in GILZ (A), IL-6 (B), and IL-8 (C) mRNA expression levels were determined by qRT-PCR and were normalized to GAPDH mRNA expression levels. The relative fold change in expression was determined by setting the value for the vehicle control to 1. Pooled results of matched incubations performed on seven donors are shown (with each condition tested in triplicate) and are represented as means ± SEM. A Kruskal-Wallis test was performed with Dunn's multiple-comparison posttest to determine significant differences between treatments. Statistical significance is indicated by asterisks (*, $P < 0.05$; **, $P < 0.01$).

of low concentrations of LNG (0.0001 nM to 0.001 nM) (Fig. 5E). At higher concentrations of LNG, TDF did not significantly affect the efficacy of LNG via the PR. DPV also had no effect on the transcriptional efficacy and potency of LNG via the PR (Fig. 5F; see also Table S4). The potencies and efficacies for each of the dose-response curves in Fig. 5 are detailed in Tables S2 to S4.

Following the observation that TDF transactivated PR-B in a progestogen-independent manner, the dose dependency of this response was similarly assessed using a promoter-reporter assay in U2OS cells. The cells were stimulated with increasing concentrations of TDF, ranging from 1 nM to 1 μM, in the absence or presence of 100 nM progesterone (P_4). TDF had a 50% effective concentration (EC_{50}) of 599 ± 33 nM for PR-B, and the potency of TDF was significantly decreased in the presence of 100 nM P_4 (Fig. 6; see also Table S5 in the supplemental material). Agonist-independent effects of TDF and DPV at concentrations ranging from 100 nM to 10 μM via the AR and GR were also assessed, but no significant induction of these receptors was observed in the absence of receptor agonists (see Fig. S9).

Similarly, the induction of PR-B transcriptional activity by TDF was investigated in the MDA-MB-231 cell line, which stably and constitutively expresses PR-B (Fig. 7; see also Table S6 in the supplemental material). As expected, 1 μM TDF activated PR-B in the absence of LNG (Fig. 7) and significantly increased the transcriptional efficacy of LNG in these cells (Table S6). As shown in U2OS cells, DPV did not influence the transcriptional efficacy or potency of LNG in MDA-MB-231 cells.

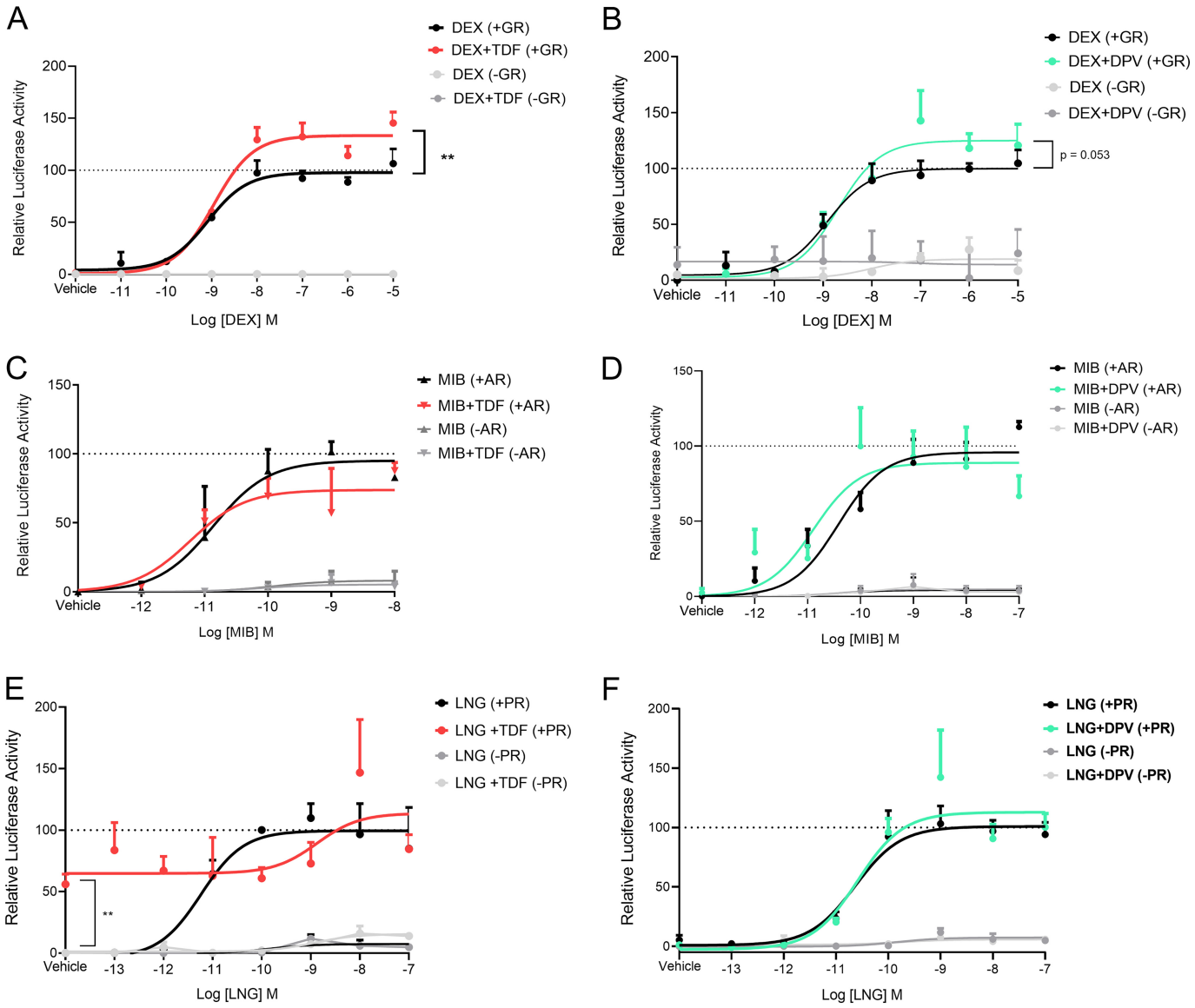

FIG 5 Effects of TDF and DPV on the transcriptional efficacies and potencies of GR, PR-B, and AR in the presence of their agonists. U2OS cells were seeded onto 10-cm^2 plates at a density of 1.5×10^5 and were incubated for 24 h. Thereafter, cells were transiently transfected for 24 h with pTAT-GRE-LUC and pcDNA-3 (empty vector) or the receptor expression vector pSV-hAR, pcDNA3-hGR-WT, or pSG5-PRB. Cells were reseeded onto 96-well plates at densities of 1×10^4/well for GR and AR and 5×10^4/well for PR-B. The cells were then treated with increasing concentrations of the receptor agonist MIB, DEX, or LNG in the absence or presence of 1 μM TDF or DPV. EtOH plus DMSO (0.1% [vol/vol] for each) was used as the vehicle control, and cells were incubated for 24 h. Cells were lysed, and the luciferase activity was measured for GR (A and B), AR (C and D), and PR-B (E and F). Luciferase activity was normalized to the protein content per well as determined by the Bradford assay. Furthermore, luciferase activity was normalized to the plateau value of the reference ligand (DEX, MIB, or LNG), which was set to 100%, in order to obtain the relative fold induction. Pooled results from three or more independent experiments are shown, and data are represented as means ± SEM. Unpaired *t* tests were used to determine the statistical significances of efficacies and potencies. **, $P < 0.01$.

The data observed in the current study reveal that TDF, but not DPV, significantly affects the function of the steroid receptors GR and PR, while neither TDF nor DPV has a significant effect on the AR. These differential activities may result from direct interaction between the ARVs and the steroid receptors. To investigate this, *in silico* molecular docking was employed to assess whether TDF and DPV exhibited an affinity for the ligand-binding pockets of either the GR, PR-B, or the AR (for the latter receptor, two structures were evaluated.) To validate these calculations, binding affinities were first predicted for the crystallized agonist in complex with the receptor ligand-binding domain of each receptor. Following these test simulations, the results suggested that TDF had low affinity for the ligand-binding pockets of all three steroid receptors, in contrast to the receptor agonists (see Table S7 in the supplemental material). DPV

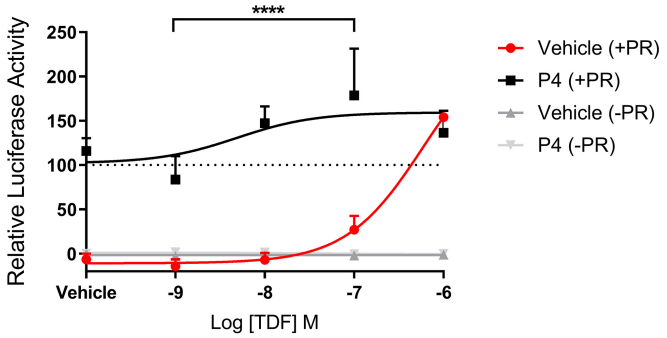

FIG 6 Dose-dependent effects of TDF on ligand-independent PR-B activation. U2OS cells were seeded and incubated for 24 h. Thereafter, cells were transiently transfected for 24 h with pTAT-GRE-LUC and pcDNA-3 (empty vector) or pSG5-PRB. Cells were then reseeded and were treated with various concentrations of TDF (10^{-9} M to 10^{-6} M) in the absence or presence of 100 nM P_4 for 24 h. Cells were lysed, and luciferase activity was measured. Luciferase activity was normalized to the protein content per well as determined by the Bradford assay and to the vehicle control (0.1% EtOH, 0.1% DMSO) in order to obtain the normalized relative fold induction. Pooled results from three independent experiments are shown, and data are represented as means ± SEM. Unpaired *t* tests were used to determine the statistical significances of efficacies and potencies. ****, $P < 0.0001$.

exhibited some binding affinity for the PR and GR, although this was not reflected in transcriptional activity: DPV had no significant effect on GR or PR activity on its own. Mono- and dianionic charged states of TFV were also evaluated, and these species exhibited negligible affinity for the ligand-binding domains of the three receptors.

Modulation of ARV efficacy by steroids. The effects of steroid ligands on the efficacies and potencies of ARVs for inhibition of HIV-1 replication were assessed using HIV-1 infection assays in TZM-bl cells. Ligands that bind to either the GR (DEX), the AR (MIB, LNG), or both the AR and GR (MPA) were chosen (25, 26, 29, 34). DEX and MPA alone appeared to increase the level of HIV-1 infection, as reported previously (15), although in this experiment, the effect was not statistically significant (Fig. 8). We found that 100 nM DEX, MPA, or LNG and 0.01 nM MIB did not significantly affect the efficacy or potency of TDF or DPV for the inhibition of HIV-1 infection (Fig. 8).

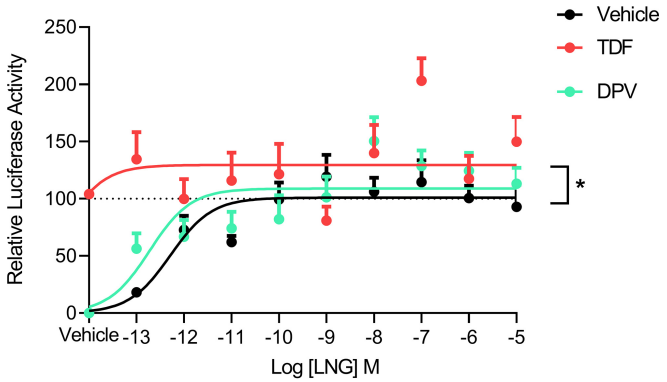

FIG 7 Effects of ARVs on endogenous PR activity in the presence of LNG in MDA-MB-231 cells. MDA-MB-231 cells stably transfected with PR-B were transiently transfected with 9 μg pTAT-GRE-LUC and thereafter were reseeded onto 96-well plates at a density of 1×10^4/well. Cells were treated with increasing concentrations of LNG in the absence or presence of 1 μM TDF or DPV for 24 h. EtOH plus DMSO (0.1% [vol/vol] for each) was used as the vehicle control, and cells were incubated for 24 h. Cells were lysed, and the luciferase activity was measured for the PR. Luciferase activity was normalized to the protein content per well as determined by a Bradford assay. Furthermore, luciferase activity was normalized to the plateau of the reference ligand LNG, which was set to 100%, in order to obtain the relative fold induction. Pooled results from four independent experiments are shown, and data are represented as means ± SEM. Unpaired *t* tests were used to determine the statistical significances of efficacies and potencies. *, $P < 0.05$.

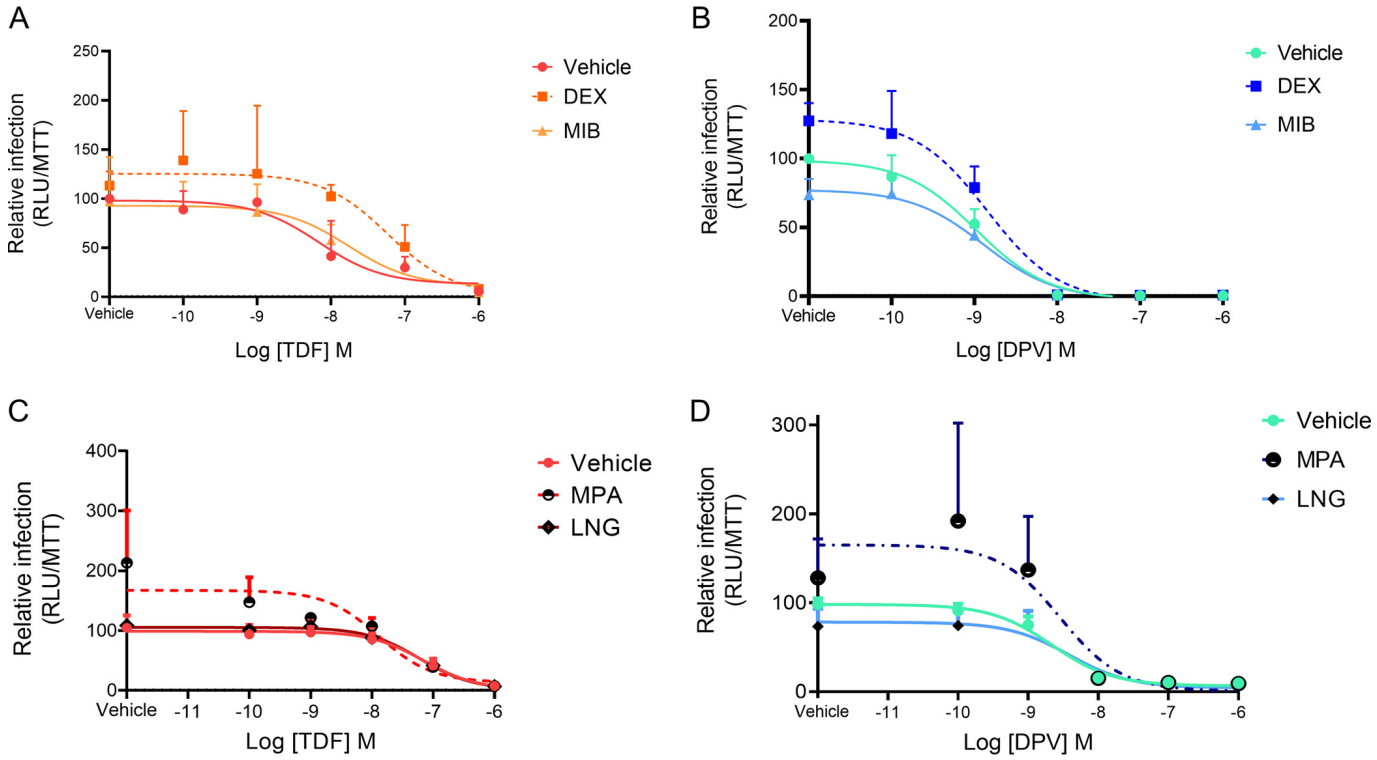

FIG 8 Inhibition of HIV-1 infection by TDF and DPV in the absence and presence of steroid receptor agonists. TZM-bl cells were exposed to increasing concentrations of TDF or DPV in the absence or presence of 100 nM DEX or 0.01 nM MIB (A and B), or in the absence or presence of 100 nM MPA or LNG (C and D), for 24 h prior to exposure to HIV-$1_{BaL\text{-}Renilla}$ in the presence of the compounds for 48 h. EtOH plus DMSO (0.1% [vol/vol] for each) was used as the vehicle control. HIV-1 infection was determined by measuring HIV-1 long terminal repeat activity, as expressed by relative luciferase units (RLU), using the Bright-Glo system (Promega), and these values were normalized to the corresponding MTT absorbance readings (RLU/MTT). Pooled results from four independent experiments are shown, where each condition was tested in triplicate, and data are represented as means ± SEM.

DISCUSSION

In the present study, we evaluated the abilities of TDF and DPV to reciprocally modulate their respective intracellular functions alone and together with steroid ligands.

In TZM-bl cells, PBMCs, and explant tissue, DEX or MPA alone exhibited anti-inflammatory effects by upregulation of GILZ and downregulation of IL-6 mRNA. These results provide confidence that the detection of expected steroid-induced changes in gene expression in these models was reproducible. Differential regulation of select immune function genes by TDF and DPV in the absence and presence of steroid ligands was observed in TZM-bl cells. However, no effects were detected for the genes assessed in pooled data from PBMCs and explant tissue. In TZM-bl cells, DPV induced proinflammatory effects on the IL-6 and IL-8 genes, unlike TDF. High concentrations of TDF and DPV were found to increase the efficacy of MPA-induced effects on GILZ in TZM-bl cells. Similar effects were observed for DEX-induced efficacy with a promoter-reporter plasmid in U2OS cells. DPV effects on the IL-6 and IL-8 genes were modulated by DEX or MPA in TZM-bl cells, and this was not seen for TDF. DEX and MPA inhibited the DPV-induced proinflammatory response of the IL-6 gene. MPA also enhanced the proinflammatory effect of DPV on IL-8 in TZM-bl cells, an effect not observed for DEX. In contrast, the results in PBMCs and explants are reassuring in that they suggest, if they occur *in vivo*, that there is very little reciprocal modulation of immunomodulatory gene expression for these ARVs and clinically relevant steroids. However, the cell line results provide proof of concept that reciprocal modulation could occur in some cells, including both ARV- and steroid-specific effects, but their physiological relevance is unclear.

The results for both PBMCs and explants show a high degree of interindividual donor variability, as reported previously (35, 36). Some of the individual donor re-

sponses that we observed in the primary models correspond to effects observed in TZM-bl cells and raise the possibility that for some donors, ARVs may have both proinflammatory and anti-inflammatory effects, and some reciprocal modulation between these ARVs and steroids could occur.

These donor-specific effects on gene expression in primary models may be reflected in the various responses of patients to ARV treatment, the underlying factors for which may include patient genotype, age, levels of endogenous hormones and other drugs, nutrition, and disease state (37–39). About 60% of the explant tissue donors were positive for herpes simplex virus 1 (HSV-1), and their ages ranged from 31 to 56 years, factors that may contribute to the various responses observed. Female donors of PBMCs were negative for some infections, including HIV-1 and syphilis, but were not tested for all possible infections or HSV-1 infection, and thus, it is not known whether other underlying infections influenced the immune gene responses to ARVs.

The immunomodulatory effects that we observed with TDF (0.1 nM to 100 μM) and DPV (0.1 to 1 μM) in TZM-bl cells in the present study occurred at physiologically relevant ARV doses (for TDF, 1.2 nM to 79 μM; for DPV, 0.7 nM to 21 μM) (Table 1). We did not detect responses of select genes *in vitro* in PBMCs with 1 μM TDF or DPV, concentrations greater than those detected (0.7 to 5 nM) in the sera of patients, suggesting that these ARVs alone are unlikely to have systemic immunomodulatory effects *in vivo*. However, it is possible that effects on PBMCs may be observed at lower ARV concentrations. We also did not detect responses of select genes *in vitro* in ectocervical tissue with 1 μM DPV alone, suggesting that inflammatory effects do not occur at this concentration. However, such effects may occur at higher concentrations in the female genital tract (FGT), as measured for the DPV vaginal ring (Table 1). *In vivo* clinical data for the DPV vaginal ring suggest that this is unlikely, since no serious adverse effects of the ring indicating excessive inflammation in the genital tracts of women who used it were detected in phase II and III clinical trials (9, 40). Phase I clinical trials of the TDF vaginal ring in sexually abstinent women reported previously that it was safe, with minimal adverse events (5). However, a recent phase I clinical trial showed that women using the TDF ring had higher expression of cytokines and chemokines, including IL-6 and IL-8, than women using a placebo ring (6). Further experiments are required to investigate immunomodulatory effects of high doses of DPV and TDF in FGT tissue models.

Our data in TZM-bl cells contribute to the limited *in vitro* studies that show that ARVs influence immune function independently of their HIV-1-inhibitory action. The immunomodulatory effects of TDF in human PBMCs have been described previously. After infection with live bacteria, followed by stimulation with Toll-like receptor (TLR) or tumor necrosis factor alpha (TNF-α), TDF at doses ranging from 12.5 to 50 μM decreased the expression of the proinflammatory cytokine IL-8 and the anti-inflammatory cytokine IL-10 and increased the expression of the proinflammatory cytokine IL-12 (41). TFV at a concentration of 3.5 mM has been shown to upregulate the expression of macrophage inflammatory protein 3α (MIP-3α), IL-8, and TNF-α in macrophages derived from blood monocytes, as well as in primary epithelial cells derived from the endometria and ectocervices of healthy women (21, 22). However, these reports (21, 22, 41) used much higher concentrations of these ARVs than are detected systemically. Additionally, in human genital epithelial cells, DPV at concentrations of $\geq$10 μM was shown to produce small increases in IL-8 secretion (23), in agreement with our findings in TZM-bl cells. Our results further suggest that side effects of TDF and DPV due to loss of cell viability are unlikely to occur at concentrations up to 10 μM for both ARVs in PBMCs and 100 μM in ectocervical tissue, although this is likely to be cell and tissue specific.

To our knowledge, this is the first study to investigate the effects of ARVs on GR, PR, and AR transcriptional activity in the presence of their respective agonists. Svard et al. reported previously that a panel of ARVs, including TFV and EFV, bind to the liver X receptor (LXR) and the estrogen receptor (ER) (42). In the study by Svard et al., ARVs predicted to bind to the GR were not able to bind *in vitro* or to induce GR transcriptional activity (42). Our results show that TDF and DPV alone do not affect the transcriptional

activity of the GR (Fig. S9 in the supplemental material). We show for the first time that TDF and DPV increase the transcriptional efficacy of the GR agonist DEX in U2OS cells and that TDF significantly activates the PR in a ligand-independent manner. In contrast, TDF and DPV had no effect on the potency or efficacy of the AR agonist MIB.

These *in vitro* ARV effects on GR and PR activity are potentially important if they are translated *in vivo*. For the ubiquitously expressed GR, our results suggest that *in vivo*, TDF and DPV may potentiate the effects of GR ligands at times, such as when cortisol levels are high or during glucocorticoid therapy. This may be relevant for several GR-regulated physiological processes, including metabolism, bone mineral density (BMD), and cardiovascular and immune function (43). BMD loss is a known side effect of TFV use in HIV-1-positive patients and in HIV-1-negative PrEP users (44, 45). Several *in vitro* studies have implicated TDF in decreasing BMD (46, 47). Activation of the GR has also been implicated in decreasing BMD (48, 49). Whether the GR is involved in any of the above effects of TDF is unknown. Since the progestin MPA is a potent partial-to-full agonist of the GR (50), HIV-1-positive women using DMPA-IM for contraception and taking TDF or DPV may exhibit increased GR activity leading to increased side effects, such as loss of BMD or immunosuppression, and/or increased beneficial effects of other GR-regulated physiological functions.

A novel finding of this study is that TDF, but not DPV, significantly activates the transcriptional activity of PR-B in the absence of a progestogen and increases the efficacy of PR-B in the presence of the progestogen LNG. This has important implications that may be relevant to PR-regulated physiological processes, including reproduction, reproductive tissue cancers (51), immune function, and bone density. TDF and TFV have not been shown previously to affect reproductive functions (52, 53). BMD is regulated by both estrogen and P_4 (54–56). A dose-dependent relationship with BMD loss has also been shown for adolescent girls receiving high-dose DMPA-IM (150 mg) compared to the lower-dose subcutaneous DMPA (DMPA-SC) (104 mg) (54–58). These studies suggest that high concentrations of PR ligands such as MPA and LNG may create a hypoestrogenic environment and reduce BMD. Our results suggest a possible link between TDF use, the PR and/or the GR, and BMD loss. Since TDF used as an intravaginal ring for PrEP is set to deliver concentrations as high as 30 μM to the FGT (6), where the GR and PR are abundantly expressed (unpublished data; also reference 59), our results suggest that side effects with TDF and/or DPV via the GR or PR in the FGT may be highly relevant. PBMCs have also been shown to express GR mRNA and protein (60, 61), and some studies (60) but not others (61) show that they express detectable PR. This suggests that side effects with TDF and/or DPV via the GR or PR may also be highly relevant in a systemic context.

The mechanisms whereby TDF but not DPV affects PR-B function remain to be determined and were beyond the scope of the present study. Our *in silico* docking data suggest that this is not likely to be due to direct binding of TDF to the PR-B ligand-binding pocket. The finding that TDF alone does not cause similar activation of the GR or AR suggests that the mechanism is specific to PR-B signaling and is unlikely to involve general components of the transcriptional machinery. A mechanism involving a direct effect on PR-B, other than binding to the ligand-binding pocket, or an indirect effect, such as an effect on a protein that interacts specifically with PR-B, may be involved. Further studies on the transactivation and transrepression of endogenous genes and more-detailed mechanistic studies may provide further insights.

An encouraging finding of our study was that neither MPA nor LNG affected the potency or efficacy of TDF or DPV in the inhibition of HIV-$1_{BaL\text{-}Renilla}$ replication in TZM-bl cells. We have also shown previously that this is the case for MPA and maraviroc (15), suggesting that these progestins, when used for contraception, are unlikely to affect the efficacy of these ARVs for HIV-1 inhibition in women. This is consistent with previous clinical studies showing that MPA does not affect ARV efficacy (20, 62). In contrast, a recent *in vitro* study showed that MPA, but not LNG or NET, inhibited the anti-HIV-1 activity of TFV in blood and endometrial $CD4^+$ T cells, most likely via lowering of the intracellular TFV diphosphate levels (24). This suggests that the influ-

ence of MPA on ARV efficacy and potency may differ depending on the cell type. A previous clinical study has also shown that TDF levels are lowered in pregnant HIV-negative women, also suggesting that changes in hormones during pregnancy may influence ARV efficacy (63). Previous clinical studies have not shown any interactions of LNG with ARVs, and hence, LNG may be the more suitable choice for use as a hormonal contraceptive in MPTs (64, 65).

Our study had several limitations, including the limited donor size of PBMC and explant models, which affected the statistical power of the study as well as our ability to fully characterize the effects of both ARVs and the progestins on inflammatory gene expression. Furthermore, our gene expression analysis was restricted to three genes and models, and we may have observed different results for others. Since we did not investigate the effects of >1 μM concentrations of TDF and DPV in PBMCs, or >1 μM concentrations of DPV in genital tract tissue, it is possible that effects do occur *in vitro* under those conditions. Furthermore, we cannot draw any conclusions about *in vitro* effects in other genital tract compartments. The use of a transactivation model only of steroid receptor transcriptional activity is also a limiting factor, since steroid receptor activity also occurs via a transrepression model, and the effect of ARVs on transrepression is unknown. The physiological relevance of the TZM-bl cell results remains to be explored *in vivo*. Nevertheless, our findings provide novel insights into the mechanisms and reciprocal modulation of activities with combinatorial usage of ARVs and GR, AR, and PR ligands, which may have important implications *in vivo*. Our PBMC and explant gene expression results and HIV-1 infection data are largely reassuring in showing that TDF and DPV, in combination with DEX or MPA, do not reciprocally modulate key biological effects, and thus, these ARVs would be suitable for combination with MPA in MPTs. However, the TZM-bl gene expression data, individual gene expression responses for some donors in the primary models, and the effects of the ARVs on GR and PR function *in vitro* raise concerns that some negative effects could occur in a cell- and donor-specific manner *in vivo*. Further experiments are required to evaluate the dose- and time-dependent effects of ARVs and steroid receptor ligands *in vitro* and their physiological relevance *in vivo*.

MATERIALS AND METHODS

Ethics. Ethical approval to conduct this study was granted by the Human Research Ethics Committee of the Faculty of Health Sciences of the University of Cape Town, Cape Town, South Africa (approval no. HREC 210/2011).

Test compounds. The ARVs TDF and DPV were purchased from the AIDS Research and Reference Reagent Program, Division of AIDS, NIAID, NIH (USA), and Selleck Chemicals (USA), respectively. The ARVs were made up to a stock concentration of 10^{-1} M in DMSO (Sigma-Aldrich, South Africa). DMSO was chosen as the solvent due to its high maximal solubility of approximately 10^{-1} M for both TDF and DPV (66, 67). Stock concentrations of ARVs were serially diluted 1:10 with DMSO from 10^{-2} M to 10^{-7} M. The steroids used in the study included the progestins MPA and LNG, as well as the synthetic GR and AR agonists DEX and MIB, respectively. These were obtained from Sigma-Aldrich (South Africa), except for MIB, which was obtained from Perkin-Elmer (USA). Stock concentrations of steroids ranged from 10^{-3} M to 10^{-6} M in ethanol (EtOH). Ligands or a control vehicle was added to cells to give the final concentrations indicated in the figures, such that all incubation mixtures contained 0.1% (vol/vol) EtOH and 0.1% (vol/vol) DMSO. The use of EtOH and DMSO as the vehicle at these low final concentrations is common practice in the literature and was not toxic to the cells (25, 41, 68).

Cell culture. Human cervical indicator TZM-bl cells (NIH AIDS Reagent Program, Division of AIDS, NIAID, NIH) were used for the HIV-1 inhibition assays. U2OS human osteosarcoma cells were used for the luciferase reporter assays because they are deficient in endogenous steroid receptors (American Type Culture Collection [ATCC], USA). MDA-MB-231 cells stably transfected with PR-B were a kind gift from Valerie Lin (Nanyang Technological University, Singapore) and were also used for luciferase reporter assays. HEK293T human embryonic kidney cells (ATCC, USA) were used to generate infectious molecular clones. All cells, except the MDA-MB-231 breast cancer cells, were grown in 75-cm^2 flasks in full Dulbecco's modified Eagle's medium (DMEM) (Sigma-Aldrich, South Africa) supplemented with 1 mM sodium pyruvate (Sigma-Aldrich, South Africa), 44 mM sodium bicarbonate (Sigma-Aldrich, South Africa), 10% (vol/vol) fetal calf serum (FCS) (Thermo Scientific, South Africa), 100 IU/ml penicillin, and 100 mg/ml streptomycin (Sigma-Aldrich, South Africa). MDA-MB-231 cells were cultured in full DMEM supplemented with 7.5% (vol/vol) FCS (Thermo Scientific, South Africa) and 100 mg/ml neomycin (Sigma-Aldrich, South Africa). For experimental incubations with MDA-MB-231 cells, phenol red-free full DMEM supplemented with 5% charcoal-stripped (c-s) FCS was used. Cells were maintained at 37°C in a water-jacketed incubator (at 90% humidity under 5% CO_2).

Cell viability. Cell viability was determined using the 3-(4,5-dimethylthiazol-2-yl)-2,5-diphenyltetrazolium bromide (MTT) assay (Sigma-Aldrich, South Africa) according to the manufacturer's instructions and was

measured on a spectrophotometer (Thermo Scientific, USA) at 595 nm. DMSO was used as the positive control for cytotoxicity at concentrations ranging from 5 to 20% (69, 70).

PBMC isolation. Whole blood from anonymous healthy female donors who were negative for HIV-1, syphilis, and hepatitis B and C was obtained from the Western Cape Blood Service (South Africa) after written informed consent. PBMCs were isolated using Histopaque-1077 Hybri-Max (Sigma-Aldrich, South Africa) density centrifugation with Leucosep tubes (Greiner Bio-One, Germany) according to the manufacturer's instructions. PBMCs were isolated as described previously (15). Cells were incubated overnight and thereafter were pelleted and washed twice by centrifugation at 250 × *g* in 1× phosphate-buffered saline (PBS) supplemented with 1% (vol/vol) c-s FCS.

Cervical tissue explants. Cervical tissue was obtained from seven HIV-1-negative premenopausal women, with normal Pap smears and undergoing hysterectomies for benign reasons, after informed consent. Anonymized fresh tissue was supplied from two sites in the Western Cape, South Africa, namely, Groote Schuur Hospital and Tygerberg Hospital. The majority of the samples were positive for HSV-1 and negative for HSV-2. Cervical tissue was processed as described previously (14) between 1 and 3 h postoperation.

Stimulation with compounds, RNA isolation, and quantitative reverse transcription-PCR (qRT-PCR). TZM-bl cells were seeded at a concentration of 1×10^5/ml in 12-well plates in full DMEM. After 24 h, cells were stimulated with ARVs or steroids for 24 h and thereafter were harvested in 400 μl Tri Reagent (Sigma-Aldrich, South Africa). PBMCs were seeded into 5-ml Falcon tubes (Becton Dickinson Scientific, South Africa) at a density of 2 million cells in 2 ml full RPMI medium. Subsequently, PBMCs were stimulated with ARVs and steroids for 48 h and thereafter were pelleted by centrifugation at 250 × *g* for 5 min and harvested in 400 μl Tri Reagent (Sigma-Aldrich, South Africa). TZM-bl cells and PBMCs were then processed for RNA according to the manufacturer's instructions. Cervical tissue explants were stimulated in triplicate or quadruplicate with steroid ligands and ARVs in full RPMI medium and were incubated at 37°C in a water-jacketed incubator (at 90% humidity under 5% CO_2) for 48 h. For RNA isolation, cervical explants were harvested in 800 μl QIAzol in 2-ml cryovial tubes (Nunc, Germany) and were subsequently homogenized using a hand-held homogenizer (TissueRuptor; Qiagen, The Netherlands) with disposable probes (TissueRuptor probes; Qiagen, The Netherlands). Cervical explant tissue RNA was thereafter isolated using the RNeasy Microarray Tissue minikit (Qiagen, The Netherlands) according to the manufacturer's instructions. The times chosen for incubation of compounds in the different models were based on previous experiments in our laboratory showing that robust changes in gene expression occurred at these time points. Whether different effects occurred after different times was not investigated.

RNA (250 ng) was reverse transcribed using the High-Capacity cDNA Reverse Transcription kit (Applied Biosystems, South Africa) according to the manufacturer's instructions. Real-time qRT-PCR was performed using the FastStart Essential DNA Green Master kit (Roche) on a Rotor-Gene 3000 (Qiagen, The Netherlands) qRT-PCR machine according to the manufacturer's instructions. The genes investigated were the anti-inflammatory GILZ gene and the proinflammatory IL-8 and IL-6 genes. A validated GILZ primer set was purchased from Qiagen South Africa. The IL-6 and IL-8 primers have been reported previously (71). Glyceraldehyde-3-phosphate dehydrogenase (GAPDH) was used as the reference gene as reported previously (32). The IL-8 and GAPDH primers were used at a concentration of 500 nM, while IL-6 primers were used at 250 nM. The qRT-PCR profiles for IL-6, IL-8, and GAPDH were established by Verhoog et al. (32).

Virus propagation and TZM-bl infection assay. Initial viral stocks were prepared as described previously (15). TZM-bl cells were seeded at a concentration of 5×10^4/ml in a 96-well flat-bottom culture plate in full DMEM. The following day, the TZM-bl cells were stimulated either with progestin or its vehicle control (0.1% [vol/vol] EtOH) or with ARV or its vehicle control (0.1% [vol/vol] DMSO), or with both, for 24 h in triplicate. Cells were then infected with 20 IU/ml HIV-$1_{BaL\text{-}Renilla}$ and were harvested 48 h later with Bright-Glo luciferase lysis buffer (Promega, USA). Luminescence was determined on a luminometer (Modulus Microplate reader; Promega, USA) in which relative light units (RLU) were measured for each well. Cell viability was measured using the MTT assay by measuring absorbance at 595 nm on a spectrophotometer (Thermo Scientific, USA). Luciferase readings were normalized to MTT values (RLU/MTT). Dose-response data were analyzed relative to the maximal response generated by the vehicle (set to 100%), and a nonlinear regression model was employed with the Hill slope set to unity. Fifty percent infective concentrations (IC_{50}) were compared using an unpaired, two-tailed *t* test.

Plasmids and transfection. U2OS cells were transfected with either the GR (72), the AR (73), or the PR (74) reporter system, each containing the steroid receptor plasmid, a luciferase reporter gene plasmid (pTAT-GRE-LUC [75]) containing the receptor response elements, and an empty vector (pCDNA3; Invitrogen, UK) that was used as the negative control for the steroid receptor plasmid. To ensure consistent transfection efficiency, cells were transfected in a 10-cm^2 dish (Greiner Bio-One International) at a density of 1.5×10^6 using the X-tremeGENE 9 reagent (Roche, South Africa) according to the manufacturer's recommendations. Thereafter, the cells were trypsinized, replated into 96-well plates, and stimulated with compounds for 24 h. The transfection conditions for each receptor were as follows: for the human GR (hGR), 10 μg pcDNA3-hGR plus 3.75 μg pTAT-GRE-LUC; for the human AR (hAR), 2.5 μg pSV-hAR plus 1.88 μg pTAT-GRE-LUC; and for human PR-B (hPR-B), 3.5 μg pSG5-hPR-B plus 1.41 μg pTAT-GRE-LUC. MDA-MB-231 cells, which are stably transfected with PR-B, were transfected with 9 μg pTAT-GRE-LUC only.

Luciferase reporter assay. U2OS cells were incubated with the respective ARVs and/or steroid treatments for 24 h. Thereafter, the cells were washed with ice-cold PBS and were harvested in 25 μl reporter lysis buffer (Promega, Madison, WI, USA). The luciferase activity for each condition was detected in the presence

of the substrate luciferin (Promega, Madison, WI, USA) using a Modulus Microplate luminometer and was normalized to the total protein concentration as determined by the Bradford assay (76).

Western blotting. To confirm steroid receptor transfection, Western blot analysis was performed, essentially as described previously (77), with lysates of U2OS cells bulk transfected with GR, PR, or AR expression vectors or the empty vector pCDNA3 in luciferase reporter assays. Positive controls for each receptor were prepared from COS-1 cells seeded in 12-well plates at a density of 1×10^5/ml and, after 24 h, transfected with 1 μg GR, PR, or AR expression vectors. Transfected U2OS cells were seeded in 12-well plates at a density of 1×10^5/ml. The next day, cells were washed once in PBS, lysed with 50 μl 2× SDS sample buffer (5× SDS sample buffer is 100 mM Tris [pH 6.8], 5% [vol/vol] SDS, 20% [vol/vol] glycerol, 5% [vol/vol] β-mercaptoethanol, and 0.1% [wt/vol] bromophenol blue), and then boiled at 100°C for 10 min. The following antibodies were used: anti-AR (441; catalog no. sc-7305; Santa Cruz Biotechnology) at 1:1,000, anti-GR (G-5; sc-393232; Santa Cruz Biotechnology) at 1:5,000, anti-PR (NCL-L-PGR-312; Leica Biosystems) at 1:1,000, and anti-GAPDH (0411; sc-47724; Santa Cruz Biotechnology) at 1:15,000. A goat anti-rabbit secondary antibody (sc-2313; Santa Cruz Biotechnology) was used for the anti-AR antibody at a 1:10,000 dilution, and an anti-mouse secondary antibody [mouse IgG(κ) light chain binding protein conjugated to horseradish peroxidase (m-IgGκ BP-HRP; sc-516102; Santa Cruz Biotechnology)] was used for the antibodies to GR, PR, and GAPDH and was added at a 1:5,000 dilution.

***In silico* molecular docking.** All computational predictions were carried out using desktop workstations running the Scientific Linux 7.4 operating system (OS) using the Glide utility included in the Schrödinger suite, release 2017-3. The Protein Data Bank entries of the steroid receptors (1E3G, 1XQ3, 3D90, 4UDC) were prepared using the Maestro PrepWizard. Structures were completed with the addition of bond orders and missing side chains. Nonbound waters were removed, and where applicable, the B chains of dimerized structures were removed. Automated optimization protocols were then run to refine the structures. Glide docking grids of default length, centered on the native ligands, were created. Docking simulations were performed iteratively using the Glide SP setting until a plausible docking pose was found. Binding energies were calculated using the Prime molecular mechanics generalized Born surface area (MM-GBSA) minimization and the binding energy calculation package provided with the Schrödinger suite. MM-GBSA calculations were performed using the variable dielectric generalized Born solvent model. The minimization was performed with flexibility tolerated for all protein atoms within a 10 Å radius of the ligand.

Data analysis. Results were analyzed using GraphPad Prism (version 7) software from GraphPad Software Inc. (La Jolla, CA, USA). For dose-response curves, the receptor agonists were used as reference ligands, and their values were set to 100%. Dose-response curves were fit with a nonlinear regression model using "log(agonist) versus response," with a fixed Hill slope of 1, to obtain the best-fit maximal responses. All other curves were then plotted relative to the best-fit maximal value of the reference ligand. All the data were tested for normality, and parametric or nonparametric tests were performed accordingly (78). Unpaired *t* tests were performed to compare the EC_{50} values and maximal responses of dose-response curves from different treatments. For experiments that had one condition or two different conditions, parametric one-way analysis of variance (ANOVA) or two-way ANOVA was performed with a Tukey multiple-comparison posttest (comparing all groups to the vehicle control), or a nonparametric Kruskal-Wallis test was performed with Dunn's multiple-comparison posttest. Data were plotted as means ± standard errors of the means (SEM) on histograms; the number of replicates per condition and the number of independent biological repeats are given in each figure legend.

SUPPLEMENTAL MATERIAL

Supplemental material is available online only.

SUPPLEMENTAL FILE 1, PDF file, 0.4 MB.

ACKNOWLEDGMENTS

This work was supported by the Eunice Kennedy Shriver National Institute of Child Health and Human Development (grant R01HD83026, to J.P.H.). Bursaries or fellowships were funded by the Harry Crossley Research Foundation (S.D., S.S.), the University of Cape Town (S.D., S.S., K.E., M.K.), the Poliomyelitis Research Foundation (K.E., M.K.), the Claude Leon Foundation (M.F.M.), and the National Research Foundation of South Africa (S.S., K.E., M.K., J.G.W.). The funders had no role in the study design, data collection, or interpretation of the data from the study.

We thank the following people for finding suitable consenting patients and providing cervical tissue: Shane Moore, Lynn Keck, Anne Hoffman, and Tony Wu at Groote Schuur Hospital and Hennie Botha, Rudolf Boshoff, and the registrars at Tygerberg Hospital. Finally, we thank all the members of the Hapgood laboratory for intellectual discussions.

S.D., M.K., and K.E. performed about 25%, 20%, and 15% of the experiments, respectively. S.S., J.G.W., J.M.M., A.J.B., and M.F.M. each contributed 8% of the experiments performed. All the authors contributed to the design and planning of experiments, the analysis and interpretation of data, and the writing of the paper. J.P.H.

conceived the project and directed the research. M.F.M. and C.A. played significant roles in the cosupervision of S.D. and M.K. and of S.S. and K.E., respectively. J.P.H. and S.D. wrote most of the paper, with significant contributions by M.K. and J.G.W.

REFERENCES

1. UNAIDS. 16 July 2019. Global AIDS update 2019—communities at the centre. UNAIDS, Geneva, Switzerland. https://www.unaids.org/sites/default/files/media_asset/2019-global-AIDS-update_en.pdf.
2. Carr A, Cooper DA. 2000. Adverse effects of antiretroviral therapy. Lancet 356:1423–1430. https://doi.org/10.1016/S0140-6736(00)02854-3.
3. Jacobstein R, Polis CB. 2014. Progestin-only contraception: injectables and implants. Best Pract Res Clin Obstet Gynaecol 28:795–806. https://doi.org/10.1016/j.bpobgyn.2014.05.003.
4. Meintjes G, Moorhouse MA, Carmona S, Davies N, Dlamini S, van Vuuren C, Manzini T, Mathe M, Moosa Y, Nash J, Nel J, Pakade Y, Woods J, Van Zyl G, Conradie F, Venter F. 2017. Adult antiretroviral therapy guidelines 2017. South Afr J HIV Med 18:776. https://doi.org/10.4102/sajhivmed.v18i1.776.
5. Keller MJ, Mesquita PM, Marzinke MA, Teller R, Espinoza L, Atrio JM, Lo Y, Frank B, Srinivasan S, Fredricks DN, Rabe L, Anderson PL, Hendrix CW, Kiser PF, Herold BC. 2016. A phase 1 randomized placebo-controlled safety and pharmacokinetic trial of a tenofovir disoproxil fumarate vaginal ring. AIDS 30:743–751. https://doi.org/10.1097/QAD.0000000000000979.
6. Keller MJ, Wood L, Billingsley JM, Ray LL, Goymer J, Sinclair S, McGinn AP, Marzinke MA, Frank B, Srinivasan S, Liu C, Atrio JM, Espinoza L, Mugo N, Spiegel HML, Anderson PL, Fredricks DN, Hendrix CW, Marrazzo J, Bosinger SE, Herold BC. 2019. Tenofovir disoproxil fumarate intravaginal ring for HIV pre-exposure prophylaxis in sexually active women: a phase 1, single-blind, randomised, controlled trial. Lancet HIV 6:e498–e508. https://doi.org/10.1016/S2352-3018(19)30145-6.
7. Baeten JM, Palanee-Phillips T, Brown ER, Schwartz K, Soto-Torres LE, Govender V, Mgodi NM, Matovu Kiweewa F, Nair G, Mhlanga F, Siva S, Bekker L-G, Jeenarain N, Gaffoor Z, Martinson F, Makanani B, Pather A, Naidoo L, Husnik M, Richardson BA, Parikh UM, Mellors JW, Marzinke MA, Hendrix CW, van der Straten A, Ramjee G, Chirenje ZM, Nakabiito C, Taha TE, Jones J, Mayo A, Scheckter R, Berthiaume J, Livant E, Jacobson C, Ndase P, White R, Patterson K, Germuga D, Galaska B, Bunge K, Singh D, Szydlo DW, Montgomery ET, Mensch BS, Torjesen K, Grossman CI, Chakhtoura N, Nel A, Rosenberg Z, McGowan I, Hillier S. 2016. Use of a vaginal ring containing dapivirine for HIV-1 prevention in women. N Engl J Med 375:2121–2132. https://doi.org/10.1056/NEJMoa1506110.
8. International Partnership for Microbicides. 2019. A long-acting ring to help women protect themselves against HIV. International Partnership for Microbicides, Silver Spring, MD.
9. Nel A, van Niekerk N, Kapiga S, Bekker L-G, Gama C, Gill K, Kamali A, Kotze P, Louw C, Mabude Z, Miti N, Kusemererwa S, Tempelman H, Carstens H, Devlin B, Isaacs M, Malherbe M, Mans W, Nuttall J, Russell M, Ntshele S, Smit M, Solai L, Spence P, Steytler J, Windle K, Borremans M, Resseler S, Van Roey J, Parys W, Vangeneugden T, Van Baelen B, Rosenberg Z. 2016. Safety and efficacy of a dapivirine vaginal ring for HIV prevention in women. N Engl J Med 375:2133–2143. https://doi.org/10.1056/NEJMoa1602046.
10. United Nations Department of Economic and Social Affairs, Population Division. 2019. World contraceptive use 2019. https://www.un.org/en/development/desa/population/publications/dataset/contraception/wcu2019.asp.
11. Stanczyk FZ, Hapgood JP, Winer S, Mishell DR, Jr. 2013. Progestogens used in postmenopausal hormone therapy: differences in their pharmacological properties, intracellular actions, and clinical effects. Endocr Rev 34:171–208. https://doi.org/10.1210/er.2012-1008.
12. Africander D, Verhoog N, Hapgood JP. 2011. Molecular mechanisms of steroid receptor-mediated actions by synthetic progestins used in HRT and contraception. Steroids 76:636–652. https://doi.org/10.1016/j.steroids.2011.03.001.
13. Hapgood JP, Kaushic C, Hel Z. 2018. Hormonal contraception and HIV-1 acquisition: biological mechanisms. Endocr Rev 39:36–78. https://doi.org/10.1210/er.2017-00103.
14. Ray RM, Maritz MF, Avenant C, Tomasicchio M, Dlamini S, van der Spuy Z, Hapgood JP. 2019. The contraceptive medroxyprogesterone acetate, unlike norethisterone, directly increases R5 HIV-1 infection in human cervical explant tissue at physiologically relevant concentrations. Sci Rep 9:4334. https://doi.org/10.1038/s41598-019-40756-7.
15. Maritz MF, Ray RM, Bick AJ, Tomasicchio M, Woodland JG, Govender Y, Avenant C, Hapgood JP. 2018. Medroxyprogesterone acetate, unlike norethisterone, increases HIV-1 replication in human peripheral blood mononuclear cells and an indicator cell line, via mechanisms involving the glucocorticoid receptor, increased CD4/CD8 ratios and CCR5 levels. PLoS One 13:e0196043. https://doi.org/10.1371/journal.pone.0196043.
16. Polis CB, Curtis KM, Hannaford PC, Phillips SJ, Chipato T, Kiarie JN, Westreich DJ, Steyn PS. 2016. An updated systematic review of epidemiological evidence on hormonal contraceptive methods and HIV acquisition in women. AIDS 30:2665–2683. https://doi.org/10.1097/QAD.0000000000001228.
17. Evidence for Contraceptive Options and HIV Outcomes (ECHO) Trial Consortium. 2019. HIV incidence among women using intramuscular depot medroxyprogesterone acetate, a copper intrauterine device, or a levonorgestrel implant for contraception: a randomised, multicentre, open-label trial. Lancet 394:303–313. https://doi.org/10.1016/S0140-6736(19)31288-7.
18. Chappell CA, Lamorde M, Nakalema S, Chen BA, Mackline H, Riddler SA, Cohn SE, Darin KM, Achilles SL, Scarsi KK. 2017. Efavirenz decreases etonogestrel exposure: a pharmacokinetic evaluation of implantable contraception with antiretroviral therapy. AIDS (London, England) 31:1965–1972. https://doi.org/10.1097/QAD.0000000000001591.
19. Trivedi S, Zia Y, Tang J, Lameck C, Tegha G, Kourtis A. 2018. Medroxyprogesterone acetate (MPA) concentrations among HIV-infected depot MPA (DMPA) users receiving tenofovir antiretroviral therapy (art) in Lilongwe, Malawi. Contraception 98:367. https://doi.org/10.1016/j.contraception.2018.07.117.
20. Cohn S, Park JG, Watts D, Stek A, Hitti J, Clax P, Yu S, Lertora J. 2007. Depo-medroxyprogesterone in women on antiretroviral therapy: effective contraception and lack of clinically significant interactions. Clin Pharmacol Ther 81:222–227. https://doi.org/10.1038/sj.clpt.6100040.
21. Biswas N, Rodriguez-Garcia M, Crist SG, Shen Z, Bodwell JE, Fahey JV, Wira CR. 2013. Effect of tenofovir on nucleotidases and cytokines in HIV-1 target cells. PLoS One 8:e78814. https://doi.org/10.1371/journal.pone.0078814.
22. Biswas N, Rodriguez-Garcia M, Shen Z, Crist SG, Bodwell JE, Fahey JV, Wira CR. 2014. Effects of tenofovir on cytokines and nucleotidases in HIV-1 target cells and the mucosal tissue environment in the female reproductive tract. Antimicrob Agents Chemother 58:6444–6453. https://doi.org/10.1128/AAC.03270-14.
23. Gali Y, Delezay O, Brouwers J, Addad N, Augustijns P, Bourlet T, Hamzeh-Cognasse H, Arien KK, Pozzetto B, Vanham G. 2010. *In vitro* evaluation of viability, integrity, and inflammation in genital epithelia upon exposure to pharmaceutical excipients and candidate microbicides. Antimicrob Agents Chemother 54:5105–5114. https://doi.org/10.1128/AAC.00456-10.
24. Shen Z, Rodriguez-Garcia M, Patel MV, Bodwell J, Kashuba ADM, Wira CR. 2017. Hormonal contraceptives differentially suppress TFV and TAF inhibition of HIV infection and TFV-DP in blood and genital tract $CD4^+$ T cells. Sci Rep 7:17697. https://doi.org/10.1038/s41598-017-18078-3.
25. Africander DJ, Storbeck KH, Hapgood JP. 2014. A comparative study of the androgenic properties of progesterone and the progestins, medroxyprogesterone acetate (MPA) and norethisterone acetate (NET-A). J Steroid Biochem Mol Biol 143:404–415. https://doi.org/10.1016/j.jsbmb.2014.05.007.
26. Hapgood JP, Africander D, Louw R, Ray RM, Rohwer JM. 2014. Potency of progestogens used in hormonal therapy: toward understanding differential actions. J Steroid Biochem Mol Biol 142:39–47. https://doi.org/10.1016/j.jsbmb.2013.08.001.
27. Africander D, Louw R, Verhoog N, Noeth D, Hapgood JP. 2011. Differential regulation of endogenous pro-inflammatory cytokine genes by medroxyprogesterone acetate and norethisterone acetate in cell lines of the female genital tract. Contraception 84:423–435. https://doi.org/10.1016/j.contraception.2011.06.006.

28. Govender Y, Avenant C, Verhoog NJ, Ray RM, Grantham NJ, Africander D, Hapgood JP. 2014. The injectable-only contraceptive medroxyprogesterone acetate, unlike norethisterone acetate and progesterone, regulates inflammatory genes in endocervical cells via the glucocorticoid receptor. PLoS One 9:e96497. https://doi.org/10.1371/journal.pone.0096497.
29. Hapgood JP, Ray RM, Govender Y, Avenant C, Tomasicchio M. 2014. Differential glucocorticoid receptor-mediated effects on immunomodulatory gene expression by progestin contraceptives: implications for HIV-1 pathogenesis. Am J Reprod Immunol 71:505–512. https://doi.org/10.1111/aji.12214.
30. Ayroldi E, Riccardi C. 2009. Glucocorticoid-induced leucine zipper (GILZ): a new important mediator of glucocorticoid action. FASEB J 23:3649–3658. https://doi.org/10.1096/fj.09-134684.
31. Coutinho AE, Chapman KE. 2011. The anti-inflammatory and immunosuppressive effects of glucocorticoids, recent developments and mechanistic insights. Mol Cell Endocrinol 335:2–13. https://doi.org/10.1016/j.mce.2010.04.005.
32. Verhoog NJ, Du Toit A, Avenant C, Hapgood JP. 2011. Glucocorticoid-independent repression of tumor necrosis factor (TNF) α-stimulated interleukin (IL)-6 expression by the glucocorticoid receptor: a potential mechanism for protection against an excessive inflammatory response. J Biol Chem 286:19297–19310. https://doi.org/10.1074/jbc.M110.193672.
33. Fukakusa M, Bergeron C, Tulic MK, Fiset P-O, Al Dewachi O, Laviolette M, Hamid Q, Chakir J. 2005. Oral corticosteroids decrease eosinophil and CC chemokine expression but increase neutrophil, IL-8, and IFN-γ–inducible protein 10 expression in asthmatic airway mucosa. J Allergy Clin Immunol 115:280–286. https://doi.org/10.1016/j.jaci.2004.10.036.
34. Nilsson CG, Haukkamaa M, Vierola H, Luukkainen T. 1982. Tissue concentrations of levonorgestrel in women using a levonorgestrel-releasing IUD. Clin Endocrinol (Oxf) 17:529–536. https://doi.org/10.1111/j.1365-2265.1982.tb01625.x.
35. Hillyer P, Mordelet E, Flynn G, Male D. 2003. Chemokines, chemokine receptors and adhesion molecules on different human endothelia: discriminating the tissue-specific functions that affect leucocyte migration. Clin Exp Immunol 134:431–441. https://doi.org/10.1111/j.1365-2249.2003.02323.x.
36. Whitney AR, Diehn M, Popper SJ, Alizadeh AA, Boldrick JC, Relman DA, Brown PO. 2003. Individuality and variation in gene expression patterns in human blood. Proc Natl Acad Sci U S A 100:1896–1901. https://doi.org/10.1073/pnas.252784499.
37. Brodin P, Davis MM. 2017. Human immune system variation. Nat Rev Immunol 17:21–29. https://doi.org/10.1038/nri.2016.125.
38. Smetnev AS, Golitsyn SP, Levin ER, Sokolov SF, Koltunova MI. 1988. Study of the comparative anti-arrhythmic effectiveness of allapinin, ethacizine and mexitil in patients with ventricular disorders of cardiac rhythm. Ter Arkh 60:34–38. (In Russian.)
39. Smith JM, Flexner C. 2017. The challenge of polypharmacy in an aging population and implications for future antiretroviral therapy development. AIDS 31:S173–S184. https://doi.org/10.1097/QAD.0000000000001401.
40. Nel A, Smythe S, Young K, Malcolm K, McCoy C, Rosenberg Z, Romano J. 2009. Safety and pharmacokinetics of dapivirine delivery from matrix and reservoir intravaginal rings to HIV-negative women. J Acquir Immune Defic Syndr 51:416–423. https://doi.org/10.1097/qai.0b013e3181acb536.
41. Melchjorsen J, Risør MW, Søgaard OS, O'Loughlin KL, Chow S, Paludan SR, Ellermann-Eriksen S, Hedley DW, Minderman H, Østergaard L, Tolstrup M. 2011. Tenofovir selectively regulates production of inflammatory cytokines and shifts the IL-12/IL-10 balance in human primary cells. J Acquir Immune Defic Syndr 57:265–275. https://doi.org/10.1097/QAI.0b013e3182185276.
42. Svard J, Blanco F, Nevin D, Fayne D, Mulcahy F, Hennessy M, Spiers JP. 2014. Differential interactions of antiretroviral agents with LXR, ER and GR nuclear receptors: potential contributing factors to adverse events. Br J Pharmacol 171:480–497. https://doi.org/10.1111/bph.12480.
43. Caplan A, Fett N, Rosenbach M, Werth VP, Micheletti RG. 2017. Prevention and management of glucocorticoid-induced side effects: a comprehensive review. A review of glucocorticoid pharmacology and bone health. J Am Acad Dermatol 76:1–9. https://doi.org/10.1016/j.jaad.2016.01.062.
44. Grigsby IF, Pham L, Mansky LM, Gopalakrishnan R, Mansky KC. 2010. Tenofovir-associated bone density loss. Ther Clin Risk Manag 6:41–47.
45. Kasonde M, Niska RW, Rose C, Henderson FL, Segolodi TM, Turner K, Smith DK, Thigpen MC, Paxton LA. 2014. Bone mineral density changes among HIV-uninfected young adults in a randomised trial of pre-exposure prophylaxis with tenofovir-emtricitabine or placebo in Botswana. PLoS One 9:e90111. https://doi.org/10.1371/journal.pone.0090111.
46. Barbieri AM, Chiodini I, Ragni E, Colaianni G, Gadda F, Locatelli M, Lampertico P, Spada A, Eller-Vainicher C. 2018. Suppressive effects of tenofovir disoproxil fumarate, an antiretroviral prodrug, on mineralization and type II and type III sodium-dependent phosphate transporters expression in primary human osteoblasts. J Cell Biochem 119:4855–4866. https://doi.org/10.1002/jcb.26696.
47. Grant PM, Cotter AG. 2016. Tenofovir and bone health. Curr Opin HIV AIDS 11:326–332. https://doi.org/10.1097/COH.0000000000000248.
48. Canalis E, Mazziotti G, Giustina A, Bilezikian J. 2007. Glucocorticoid-induced osteoporosis: pathophysiology and therapy. Osteoporos Int 18:1319–1328. https://doi.org/10.1007/s00198-007-0394-0.
49. Rauch A, Seitz S, Baschant U, Schilling AF, Illing A, Stride B, Kirilov M, Mandic V, Takacz A, Schmidt-Ullrich R, Ostermay S, Schinke T, Spanbroek R, Zaiss MM, Angel PE, Lerner UH, David J-P, Reichardt HM, Amling M, Schütz G, Tuckermann JP. 2010. Glucocorticoids suppress bone formation by attenuating osteoblast differentiation via the monomeric glucocorticoid receptor. Cell Metab 11:517–531. https://doi.org/10.1016/j.cmet.2010.05.005.
50. Ronacher K, Hadley K, Avenant C, Stubsrud E, Simons SS, Jr, Louw A, Hapgood JP. 2009. Ligand-selective transactivation and transrepression via the glucocorticoid receptor: role of cofactor interaction. Mol Cell Endocrinol 299:219–231. https://doi.org/10.1016/j.mce.2008.10.008.
51. Diep CH, Daniel AR, Mauro LJ, Knutson TP, Lange CA. 2015. Progesterone action in breast, uterine, and ovarian cancers. J Mol Endocrinol 54:R31–R53. https://doi.org/10.1530/JME-14-0252.
52. Heffron R, Mugo N, Hong T, Celum C, Marzinke MA, Ngure K, Asiimwe S, Katabira E, Bukusi EA, Odoyo J, Tindimwebwa E, Bulya N, Baeten JM. 2018. Pregnancy outcomes and infant growth among babies with in-utero exposure to tenofovir-based preexposure prophylaxis for HIV prevention. AIDS 32:1707–1713. https://doi.org/10.1097/QAD.0000000000001867.
53. Were EO, Heffron R, Mugo NR, Celum C, Mujugira A, Bukusi EA, Baeten JM. 2014. Pre-exposure prophylaxis (PrEP) does not affect the fertility of HIV-1 uninfected men. AIDS 28:1977–1982. https://doi.org/10.1097/QAD.0000000000000313.
54. Clarke BL, Khosla S. 2010. Female reproductive system and bone. Arch Biochem Biophys 503:118–128. https://doi.org/10.1016/j.abb.2010.07.006.
55. Schmidmayr M, Magdolen U, Tübel J, Kiechle M, Burgkart R, Seifert-Klauss V. 2008. Progesterone enhances differentiation of primary human osteoblasts in long-term cultures: the influence of concentration and cyclicity of progesterone on proliferation and differentiation of human osteoblasts *in vitro*. Geburtshilfe Frauenheilkd 68:722–728. (In German.). https://doi.org/10.1055/s-2008-1038711.
56. Seifert-Klauss V, Prior JC. 2010. Progesterone and bone: actions promoting bone health in women. J Osteoporos 2010:845180. https://doi.org/10.4061/2010/845180.
57. Bonny AE, Lange HL, Manos BE, Gothard MD, Rogers LK. 2016. Evidence of a dose-response relationship between medroxyprogesterone acetate and bone mineral density loss in adolescents. J Pediatr Adolesc Gynecol 29:159. https://doi.org/10.1016/j.jpag.2016.01.003.
58. Lange HL, Manos BE, Gothard MD, Rogers LK, Bonny AE. 2017. Bone mineral density and weight changes in adolescents randomized to 3 doses of depot medroxyprogesterone acetate. J Pediatr Adolesc Gynecol 30:169–175. https://doi.org/10.1016/j.jpag.2016.10.011.
59. Ray RM. 2015. Ph.D. thesis. Differential effects of progestogens on HIV-1 replication and host gene expression in primary PBMCs and cervical tissue explants. University of Cape Town, Cape Town, South Africa.
60. Cabrera-Muñoz E, Fuentes-Romero LL, Zamora-Chávez J, Camacho-Arroyo I, Soto-Ramírez LE. 2012. Effects of progesterone on the content of CCR5 and CXCR4 coreceptors in PBMCs of seropositive and exposed but uninfected Mexican women to HIV-1. J Steroid Biochem Mol Biol 132:66–72. https://doi.org/10.1016/j.jsbmb.2012.02.001.
61. Tomasicchio M, Avenant C, Du Toit A, Ray RM, Hapgood JP. 2013. The progestin-only contraceptive medroxyprogesterone acetate, but not norethisterone acetate, enhances HIV-1 Vpr-mediated apoptosis in human $CD4^+$ T cells through the glucocorticoid receptor. PLoS One 8:e62895. https://doi.org/10.1371/journal.pone.0062895.
62. Heffron R, Mugo N, Were E, Kiarie J, Bukusi EA, Mujugira A, Frenkel LM, Donnell D, Ronald A, Celum C, Baeten JM; Partners PrEP Study Team. 2014. Preexposure prophylaxis is efficacious for HIV-1 prevention among women using depot medroxyprogesterone acetate for contraception. AIDS 28:2771–2776. https://doi.org/10.1097/QAD.0000000000000493.

63. Pyra M, Anderson PL, Hendrix CW, Heffron R, Mugwanya K, Haberer JE, Thomas KK, Celum C, Donnell D, Marzinke MA, Bukusi EA, Mugo NR, Asiimwe S, Katabira E, Baeten JM. 2018. Tenofovir and tenofovir-diphosphate concentrations during pregnancy among HIV-uninfected women using oral preexposure prophylaxis. AIDS 32:1891–1898. https://doi.org/10.1097/QAD.0000000000001922.
64. Todd CS, Deese J, Wang M, Hubacher D, Steiner MJ, Otunga S, Van Damme L, FEM-PrEP Study Group. 2015. Sino-implant (II) continuation and effect of concomitant tenofovir disoproxil fumarate-emtricitabine use on plasma levonorgestrel concentrations among women in Bondo, Kenya. Contraception 91:248–252. https://doi.org/10.1016/j.contraception.2014.10.008.
65. Tseng A, Hills-Nieminen C. 2013. Drug interactions between antiretrovirals and hormonal contraceptives. Expert Opin Drug Metab Toxicol 9:559–572. https://doi.org/10.1517/17425255.2013.772579.
66. Selleck. 2013. Dapivirine (TMC120). https://www.selleckchem.com/products/dapivirine.html.
67. Selleck. 2019. Tenofovir disoproxil fumarate. https://www.selleckchem.com/datasheet/Tenofovir-Disoproxil-Fumarate-S140002-DataSheet.html.
68. Timm M, Saaby L, Moesby L, Hansen EW. 2013. Considerations regarding use of solvents in *in vitro* cell based assays. Cytotechnology 65:887–894. https://doi.org/10.1007/s10616-012-9530-6.
69. Da Violante G, Zerrouk N, Richard I, Provot G, Chaumeil JC, Arnaud P. 2002. Evaluation of the cytotoxicity effect of dimethyl sulfoxide (DMSO) on Caco2/TC7 colon tumor cell cultures. Biol Pharm Bull 25:1600–1603. https://doi.org/10.1248/bpb.25.1600.
70. Forman S, Kás J, Fini F, Steinberg M, Ruml T. 1999. The effect of different solvents on the ATP/ADP content and growth properties of HeLa cells. J Biochem Mol Toxicol 13:11–15. https://doi.org/10.1002/(SICI)1099-0461(1999)13:1<11::AID-JBT2>3.0.CO;2-R.
71. Wolf K, Schulz C, Riegger G, Pfeifer M. 2002. Tumour necrosis factor-α induced CD70 and interleukin-7R mRNA expression in BEAS-2B cells. Eur Respir J 20:369–375. https://doi.org/10.1183/09031936.02.00303602.
72. Ray DW, Suen CS, Brass A, Soden J, White A. 1999. Structure/function of the human glucocorticoid receptor: tyrosine 735 is important for transactivation. Mol Endocrinol 13:1855–1863. https://doi.org/10.1210/mend.13.11.0376.
73. Brinkmann AO, Blok LJ, de Ruiter PE, Doesburg P, Steketee K, Berrevoets CA, Trapman J. 1999. Mechanisms of androgen receptor activation and function. J Steroid Biochem Mol Biol 69:307–313. https://doi.org/10.1016/s0960-0760(99)00049-7.
74. Kastner P, Bocquel MT, Turcotte B, Garnier JM, Horwitz KB, Chambon P, Gronemeyer H. 1990. Transient expression of human and chicken progesterone receptors does not support alternative translational initiation from a single mRNA as the mechanism generating two receptor isoforms. J Biol Chem 265:12163–12167.
75. Sui X, Su L, Chu J. 1999. Expression of *bcl-2* gene in the evolution of chronic myelogenous leukemia to blast crisis and its implication. Zhonghua Xue Ye Xue Za Zhi 20:27–29. (In Chinese.)
76. Bradford MM. 1976. A rapid and sensitive method for the quantitation of microgram quantities of protein utilizing the principle of protein-dye binding. Anal Biochem 72:248–254. https://doi.org/10.1006/abio.1976.9999.
77. Avenant C, Kotitschke A, Hapgood JP. 2010. Glucocorticoid receptor phosphorylation modulates transcription efficacy through GRIP-1 recruitment. Biochemistry 49:972–985. https://doi.org/10.1021/bi901956s.
78. Dzikiti LN, Girdler-Brown B. 2017. Parametric hypothesis tests for the difference between two population means. Strengthen Health Syst 2:40–46.
79. Marrazzo JM, Ramjee G, Richardson BA, Gomez K, Mgodi N, Nair G, Palanee T, Nakabiito C, van der Straten A, Noguchi L, Hendrix CW, Dai JY, Ganesh S, Mkhize B, Taljaard M, Parikh UM, Piper J, Mâsse B, Grossman C, Rooney J, Schwartz JL, Watts H, Marzinke MA, Hillier SL, McGowan IM, Chirenje ZM. 2015. Tenofovir-based preexposure prophylaxis for HIV infection among African women. N Engl J Med 372:509–518. https://doi.org/10.1056/NEJMoa1402269.
80. Schwartz JL, Rountree W, Kashuba AD, Brache V, Creinin MD, Poindexter A, Kearney BP. 2011. A multi-compartment, single and multiple dose pharmacokinetic study of the vaginal candidate microbicide 1% tenofovir gel. PLoS One 6:e25974. https://doi.org/10.1371/journal.pone.0025974.
81. Fung HB, Stone EA, Piacenti FJ. 2002. Tenofovir disoproxil fumarate: a nucleotide reverse transcriptase inhibitor for the treatment of HIV infection. Clin Ther 24:1515–1548. https://doi.org/10.1016/s0149-2918(02)80058-3.
82. Hendrix CW, Andrade A, Bumpus NN, Kashuba AD, Marzinke MA, Moore A, Anderson PL, Bushman LR, Fuchs EJ, Wiggins I, Radebaugh C, Prince HA, Bakshi RP, Wang R, Richardson P, Shieh E, McKinstry L, Li X, Donnell D, Elharrar V, Mayer KH, Patterson KB. 2016. Dose frequency ranging pharmacokinetic study of tenofovir-emtricitabine after directly observed dosing in healthy volunteers to establish adherence benchmarks (HPTN 066). AIDS Res Hum Retroviruses 32:32–43. https://doi.org/10.1089/AID.2015.0182.
83. Fotherby K, Koetsawang S, Mathrubutham M. 1980. Pharmacokinetic study of different doses of Depo Provera. Contraception 22:527–536. https://doi.org/10.1016/0010-7824(80)90105-5.
84. Nanda K, Callahan R, Taylor D, Wang M, Agot K, Jenkins D, Van Damme L, Dorflinger L, FEM-PrEP Study Group. 2016. Medroxyprogesterone acetate levels among Kenyan women using depot medroxyprogesterone acetate in the FEM-PrEP trial. Contraception 94:40–47. https://doi.org/10.1016/j.contraception.2016.03.003.
85. Roumen FJ, Dieben TO. 2006. Comparison of uterine concentrations of ethinyl estradiol and etonogestrel after use of a contraceptive vaginal ring and an oral contraceptive. Fertil Steril 85:57–62. https://doi.org/10.1016/j.fertnstert.2005.06.040.
86. Buckner LR, Drobnis EZ, Augustine MS, Rogers LK, Akers J, Mott PD, Hope TJ, Quayle AJ, Schust DJ. 2019. Cervical and systemic concentrations of long acting hormonal contraceptive (LARC) progestins depend on delivery method: implications for the study of HIV transmission. PLoS One 14:e0214152. https://doi.org/10.1371/journal.pone.0214152.
87. Hidalgo MM, Hidalgo-Regina C, Bahamondes MV, Monteiro I, Petta CA, Bahamondes L. 2009. Serum levonorgestrel levels and endometrial thickness during extended use of the levonorgestrel-releasing intrauterine system. Contraception 80:84–89. https://doi.org/10.1016/j.contraception.2009.01.004.
88. Licea-Perez H, Wang S, Bowen CL, Yang E. 2007. A semi-automated 96-well plate method for the simultaneous determination of oral contraceptives concentrations in human plasma using ultra performance liquid chromatography coupled with tandem mass spectrometry. J Chromatogr B Analyt Technol Biomed Life Sci 852:69–76. https://doi.org/10.1016/j.jchromb.2006.12.052.
89. Sivin I, Lähteenmäki P, Ranta S, Darney P, Klaisle C, Wan L, Mishell DR, Lacarra M, Viegas OA, Bilhareus P, Koetsawang S, Piya-Anant M, Diaz S, Pavez M, Alvarez F, Brache V, LaGuardia K, Nash H, Stern J. 1997. Levonorgestrel concentrations during use of levonorgestrel rod (LNG ROD) implants. Contraception 55:81–85. https://doi.org/10.1016/s0010-7824(96)00276-4.
90. Sivin I, Mishell DR, Alvarez F, Brache V, Elomaa K, Lähteenmäki P, Massai R, Miranda P, Croxatto H, Dean C, Small M, Nash H, Jackanicz TM. 2005. Contraceptive vaginal rings releasing Nestorone and ethinylestradiol: a 1-year dose-finding trial. Contraception 71:122–129. https://doi.org/10.1016/j.contraception.2004.08.010.
91. Achilles SL, Hendrix CW, Poloyac SM, Hoesley CJ, Peda M, Gundacker H, Mensch BS, Marzinke MA, Devlin B, Nel AM, Piper JM, Johnson S, Chen BA, on behalf of the MTN-030/IPM 041 Protocol Team. 2018. Safety and pharmacokinetics of dapirivine and levonorgestrel vaginal rings for multipurpose prevention of HIV and pregnancy, abstr OA12.02LB. HIV Research for Prevention (HIVR4P). 22 to 25 October 2018, Madrid, Spain.
92. Thurman AR, Schwartz JL, Brache V, Clark MR, McCormick T, Chandra N, Marzinke MA, Stanczyk FZ, Dezzutti CS, Hillier SL, Herold BC, Fichorova R, Asin SN, Rollenhagen C, Weiner D, Kiser P, Doncel GF. 2018. Randomized, placebo controlled phase I trial of safety, pharmacokinetics, pharmacodynamics and acceptability of tenofovir and tenofovir plus levonorgestrel vaginal rings in women. PLoS One 13:e0199778. https://doi.org/10.1371/journal.pone.0199778.